

DISS. ETH NO. 27475

**Study of the physiological impact of early life
trauma from multiomics to reproductive biology**

A thesis submitted to attain the degree of
DOCTOR OF SCIENCES of ETH ZURICH
(Dr. sc. ETH Zurich)

presented by
Martin Roszkowski

MSc – University of Zurich, Switzerland
born on 04.02.1987
citizen of Baden AG

accepted on the recommendation of

Prof. Isabelle Mansuy, examiner
Prof. Johannes Bohacek, co-examiner
Dr. Johannes vom Berg, co-examiner

2021

Abstract of the doctoral thesis

In many species, environmental factors and life experiences can change the phenotypic traits of exposed individuals and their progeny. Traumatic stress is a type of environmental experience that can modify behavior, cognition and physiological functions such as metabolism, in mammals. Many of the effects of traumatic stress can be transmitted to subsequent generations even when individuals from these generations are not exposed to any traumatic stressor. Such environmentally-induced effects are an important mode of trait transmission across generation, which involve factors in the germline other than the genetic code. In rodents, where most of the work on epigenetic inheritance is conducted, the limited amount of sperm per male poses constraints on downstream analyses. The challenge, therefore, is the possibility to analyze DNA and RNA, and produce offspring from the sperm of a single male.

To solve these challenges, we established an experimental strategy called OmniSperm that enabled simultaneous multiomic analyses and artificial insemination with a single-male sperm sample. To enable this, we improved the sperm collection method increasing the yield from a single male mouse from around 5 million sperm cells to 40 million sperm cells. We applied this approach to profile the DNA methylome and transcriptome of a father's sperm and related them to the transcriptome of the offspring generated from the same sperm. We also validate the method using a mouse model of transgenerational transmission of early life trauma, demonstrating the method's capability to examine the transcriptome dynamics between sperm and the resulting embryos. Although our data sets limited us to correlative comparisons, we were able to relate a potential interplay between DNA methylation at regulatory regions and their resulting transcriptome. In particular, we identified a potential trauma-induced dysregulation of transcription factors, that may drive changes in the developing embryo, such as Clock (circadian TF) and the trans-acting TFs (Sp) 1, 2 and 3. These transcription factors are important mediators of selective gene activation in spermatogenesis and were shown to be essential for mouse development.

During the development of OmniSperm, we identified the extraction of high-quality RNA from sperm to be a particularly challenging step in investigating molecular mechanisms of epigenetic inheritance. Guanidinium thiocyanate-phenol-chloroform (AGPC) is a widely used and efficient method to obtain pure RNA from most tissues and cells. However, we found that it was not efficient in lysing sperm cells because they are resistant to chaotropic lysis solutions containing guanidinium thiocyanate such as Buffer RLT+ and Trizol. We showed that disulfide bonds play an important role in conveying chemical resistance of sperm cells. These lysis issues were overcome by using tris(2-carboxyethyl)phosphine (TCEP) as an efficient lysis enhancer of AGPC solutions that can retain reducing activity even at acidic pH. Trizol supplemented with TCEP allows the complete and rapid lysis of sperm cells, increasing RNA yield by 100-fold and resulting in RNA with optimal quality for reverse transcription and polymerase chain reaction.

In parallel to investigating the effects of early life trauma on the male germ line, we also studied the immediate and long-term impact on metabolism and various tissues in the mothers, their young pups and adult offspring. Mothers milk is the main source of nutrients for infants and has been shown to modulate offspring's development, physiology and behaviour. We examined the impact of traumatic stress on the mother's milk and the offspring's physiology. The collection of mouse milk is challenging and typically yielded only little milk. Therefore, we first established a new method, wherein mammary glands were excised and the milk retrieved through centrifugation. We found altered miRNAs in mammary gland milk and partially digested milk collected from pups' stomachs. Similarly, metabolomics analysis of maternal milk showed widespread dysregulation of milk macronutrients and metabolites. We compared the altered metabolite networks and identified enriched pathways for AGE-RAGE signaling, and protein digestion and absorption. These changes were validated by targeted amino acid analysis and found evidence trauma-induced metabolome and miRNA expression changes in the dams and their offspring, with potential metabolic and immunological consequences for the developing pups.

Finally, we investigated whether bones were affected by early life trauma. Bone pathology was previously reported to occur frequently in stressed individuals and a comprehensive examination of mechanisms linking life stress, depression and disturbed bone homeostasis was missing. In a translational study, mice exposed to early life trauma were found to exhibit altered gene expression, higher innervation density in bones and increased catabolic bone turnover. Depressive study participants which experienced childhood neglect also showed disturbed bone homeostasis and their bone density was reduced.

In summary, the work in this thesis investigated the immediate and long-term consequences of early life trauma on various tissues in mice. Methods were improved or new ones established to provide sufficient starting material for multiple types of molecular analyses.

Zusammenfassung der Doktorarbeit

Umweltfaktoren und Lebensereignisse können in zahlreichen Spezies zu phänotypischen Veränderungen in den betroffenen Individuen und deren Nachkommen führen. Traumatischer Stress ist eine Art von Umweltfaktor welcher in Säugetieren das Verhalten und physiologische Funktionen, wie zum Beispiel den Metabolismus, verändern kann. Die Folgen von traumatischem Stress können auch an die nachfolgende Generation vererbt werden. Dazu müssen die Nachkommen selbst nicht direkt dem traumatischen Stress ausgesetzt gewesen sein. Solche durch die Umwelt ausgelösten Vererbungseffekte sind ein wichtiger Modus, um bestimmte Merkmale an die nachfolgende Generation zu vererben, ohne dabei das genetische Erbgut an sich zu verändern. Diese Form der epigenetischen Vererbung wird vor allem in Nagetieren wie z.B. Mäusen untersucht. Allerdings ist die Untersuchung von epigenetischer Vererbung in Mäusen schwierig, weil nur wenige Spermienzellen eingesammelt werden können. Eine zu lösende Herausforderung war deshalb genügend Spermienzellen von einer männlichen Maus einzusammeln, um einerseits Nachkommen zu zeugen und andererseits molekulare Analysen an der Desoxyribonukleinsäure (DNA) sowie der Ribonukleinsäure (RNA) durchzuführen.

Um diese Einschränkungen zu lösen, haben wir eine neue experimentelle Strategie namens OmniSperm etabliert. Diese erlaubt mehrere Omics-analysen sowie künstliche Insemination mit einer Spermienprobe von einem einzelnen Männchen durchzuführen. Wir haben dazu die Art und Weise der Spermieneinsammlung verbessert. Dadurch konnten wir die Anzahl gesammelter Spermien von 5 Million auf 40 Millionen pro Maus verbessern. Wir verwenden die OmniSperm Strategie um in den Spermien die DNA-Methylierung und deren Transkriptom (die Gesamtheit aller RNAs) zu untersuchen. Ferner konnten wir diese Eigenschaften dann auch direkt mit den resultierenden Embryonen vergleichen, weil die Embryonen von den gleichen Spermien gezeugt wurden. Diesen Ansatz haben wir validiert mittels eines etablierten Models der transgenerationalen Vererbung der Effekte von traumatischem Stress. Obwohl unsere Datensätze nur Korrelationen erlauben, konnten wir potenzielle Interaktionen erkennen zwischen der veränderten DNA-Methylierung und regulatorischen Regionen der DNA, sowie dem daraus resultierenden Transkriptom. Wir identifizierten Veränderungen von Transkriptionsfaktoren (TF), welche durch das Trauma ausgelöst wurden, und die vermutlichen Veränderungen im sich entwickelnden Embryo

hervorrufen können, wie zum Beispiel: Clock (ein zirkadianischer TF) und die in trans agierenden TF (Sp) 1, 2 und 3. Diese Transkriptionsfaktoren sind wichtige Modulatoren von gezielter Geneaktivierung in der Produktion von Spermien und essenziell für die Entwicklung von Mäusen.

Während der Entwicklung von der OmniSperm Strategie waren wir mit einer weiteren Herausforderung konfrontiert: Die Extraktion von RNAs aus Mausspermien war anders als erwartet nicht effektiv. Die typische RNA-Extraktionsmethode verwendet eine Mischung von Phenol, Chloroform und Guanidiniumthiocyanat (engl. Abk. AGPC) um Zellen aufzubrechen und anschliessend reine RNA von guter Qualität zu extrahieren. Allerdings stellte sich heraus, dass die Spermienzellen nicht effektiv aufgebrochen werden können durch AGPC und sie auch anderen chaotropischen Lyse-Puffern wie z.B. «Buffer RLT+» oder «Trizol» widerstehen. Wir konnten zeigen, dass die Disulfidbrücken eine wichtige Rolle bei dieser Art der chemischen Widerstandsfähigkeit der Spermienzellen spielen. Die Lyse konnten unter Zugabe von tris(2-carboxyethyl)phosphine (TCEP) deutlich verbessert werden, weil TCEP auch bei niedrigem pH wirkt. Eine Mischung aus Trizol und TCEP löste Spermienzellen rasch und komplett auf. Dies erhöhte die Menge an RNA um das Hundertfache, welche anschliessend für Reverse Transkription und Polymerase-Kettenreaktion verwendet werden konnte.

Parallel zu unseren Untersuchungen in der Keimbahn von Männchen haben wir auch die Langzeitfolgen für den Metabolismus und diverse Gewebe der Mutter, deren junge und erwachsene Nachkommen näher untersucht. Die Milch der Mütter ist die Hauptquelle von Nährstoffen für Säuglinge und frühere Untersuchungen haben gezeigt, dass die Milch die Entwicklung, Physiologie und das Verhalten von Nachkommen beeinflussen kann. Wir untersuchten die Effekte von traumatischem Stress auf die Milch von Mäusen und deren Nachkommen. Wir stellten fest, dass das Einsammeln von Mausmilch mit bisherigen Methoden schwierig war und typischerweise nur wenig Milch resultierte. Wir haben deshalb einen anderen Ansatz etabliert, bei dem das Brustgewebe entfernt und die Milch anschliessend mittels Zentrifugation eingesammelt werden konnte. Wir beobachteten, dass in der mütterlichen Milch und der Milch aus den Mägen der Jungtiere mehrere regulatorische Micro-RNAs (miRNA) aufgrund des traumatischen Stresses verändert waren. Ferner wurden die Metaboliten der Milch analysiert und es zeigte sich, dass zahlreiche Makronährstoffe und Metaboliten verändert waren. Wir verglichen die veränderten Metaboliten Netzwerke mit bereits publizierten Daten aus dem Blut der Jungtiere und identifizierten biochemische

Reaktionswege für die Signalkaskade «AGE-RAGE» sowie Proteinverdauung und Proteinabsorption. Diese Veränderungen konnten wir mittels gezielter Analyse von Aminosäuren im Blut der Jungtiere bestätigen. Die Veränderungen der miRNAs und Metaboliten in der mütterlichen Milch sowie dem Blut der Nachkommen deuteten auf mögliche Konsequenzen für den entwickelnden Organismus hin.

Zuletzt untersuchten wir ob traumatischer Stress sich auf die Knochen auswirkt. Diverse Knochenpathologien treten häufiger in chronisch gestressten Individuen auf. Allerdings fehlte bisher eine umfassende Untersuchung, die Stress und Depression mit einer veränderten Knochenhomöostase in Verbindung bringen. In unserem Studienansatz untersuchten wir, wie sich traumatischer Stress im frühkindlichen Alter auswirken kann. Wir fanden veränderte Genexpression und höhere Nervendichte in den Knochen, sowie eine erhöhte Rate der Knochenerneuerung. Bei depressiven Studienteilnehmer, welche als Kinder vernachlässigt wurden, fanden wir ebenfalls Anzeichen für eine gestörte Knochenhomöostase und geringere Knochendichte.

Zusammenfassen, haben wir in dieser Doktorarbeit die unmittelbaren und lebenslangen Konsequenzen von frühkindlichem, traumatischem Stress in verschiedenen Organen, Geweben und Zellen untersucht und dabei zahlreiche Veränderungen festgestellt. Mehrere Methoden wurden entweder verbessert oder neu etabliert, um genügend Material für mehrere Arten von molekularen Analysen durchführen zu können.

Table of contents

1. Introduction - Transgenerational Epigenetics of Traumatic Stress.....	13
1.1. Abstract	14
1.2. Introduction	15
1.2.1. Traumatic stress.....	16
1.2.2. Epigenetic mechanisms relevant to the effects of traumatic stress on the brain	18
1.3. Transgenerational inheritance of traumatic stress	21
1.3.1. Animal models.....	21
1.3.2. Human studies	27
1.4. Mechanisms of inter- and trans-generational inheritance	29
1.4.1. Epigenetic mechanisms in the germ-line	29
1.4.2. Induction of epigenetic mechanisms in the germ-line by traumatic stress	29
1.4.3. How are these effects passed to the offspring?	30
1.4.4. Persistence of epigenetic marks related to trauma across generations	31
1.4.5. Potential of anti-stress therapies to prevent transmission of the effects of traumatic stress.....	31
1.5. Transgenerational inheritance of traumatic stress from an evolutionary point	32
1.6. Conclusions and Outlook.....	33
1.7. References.....	34

2. OmniSperm: Multiomic analyses of sperm and offspring production from a single male	43
2.1. Abstract	44
2.2. Introduction, results and discussion.....	44
2.3. Materials and Methods.....	51
2.3.1. Animals	51
2.3.2. Model of postnatal trauma.....	51
2.3.3. Sperm collection.....	52
2.3.4. Somatic cell lysis treatment and sperm lysis.....	52
2.3.5. DNA extraction	53
2.3.6. RNA extraction	53
2.3.7. Whole genome bisulfite sequencing	53
2.3.8. Sperm RNA sequencing.....	54
2.3.9. Embryo RNA sequencing.....	54
2.3.10. Epididymosome collection and characterization.....	55
2.3.11. Artificial insemination	56
2.3.12. Embryo collection.....	56
2.3.13. Data, statistics and visualization.....	57
2.4. Conflict of Interest.....	57
2.5. Authors and Contributions	57
2.6. Funding	57
2.7. Acknowledgments.....	58
2.8. Data Availability Statement.....	58
2.9. References.....	58
2.10. Supplementary Figures.....	60

3. High efficiency RNA extraction from sperm cells using guanidinium thiocyanate supplemented with tris(2-carboxyethyl)phosphine.....	72
3.1. Abstract	73
3.2. Introduction	74
3.3. Results	75
3.3.1. Mouse sperm cells are resistant to AGPC RNA extraction.....	75
3.3.2. Examining sperm lysis properties and reduction of disulfide bonds	78
3.3.3. TCEP enhances AGPC lysis.....	81
3.4. Discussion	84
3.5. Materials and Methods.....	87
3.5.1. Animals	87
3.5.2. Mouse sperm collection	87
3.5.3. Cell lysis	87
3.5.4. RNA extraction	88
3.5.5. RNA quantification and characterization	88
3.5.6. Quantification of disulfide bond reduction	89
3.5.7. Data, statistics and visualization	89
3.6. Conflict of Interest.....	90
3.7. Author Contributions	90
3.8. Funding	90
3.9. Acknowledgments.....	90
3.10. Data Availability Statement.....	90
3.11. Abbreviations	90
3.12. References.....	91

4. Chronic postnatal stress dysregulates maternal milk composition and alters offspring's early life physiology.....	95
4.1. Abstract	96
4.2. Introduction	97
4.3. Results	99
4.3.1. Chronic postnatal stress dysregulates early life development and maternal milk macronutrients	99
4.3.2. Chronic postnatal stress increased miRNAs in maternal milk and digested milk from pups.....	102
4.3.3. Maternal milk macronutrients and metabolites are dysregulated by chronic postnatal stress	104
4.3.4. Chronic postnatal stress dysregulates physiologically important metabolites and networks in maternal milk and offspring blood.....	106
4.3.5. Dysregulated metabolite networks and amino acid imbalances in maternal milk and pup serum.....	108
4.4. Discussion	110
4.5. Materials and Methods.....	112
4.5.1. Animals	112
4.5.2. Chronic postnatal stress, body weight and temperature measurements	112
4.5.3. Milk collection.....	112
4.5.4. Metabolite quantification and enrichment analysis	114
4.5.5. Targeted amino acid analysis	115
4.5.6. miRNA expression analysis	115
4.5.7. Data, statistics and visualization	115
4.6. Conflict of Interest.....	116

4.7. Authors and Contributions	116
4.8. Funding	116
4.9. Acknowledgments.....	116
4.10. Data Availability Statement.....	116
4.11. References.....	117
4.12. Supplementary Figures.....	121
4.13. Supplementary Tables	126

5. Effects of Early Life Stress on Bone Homeostasis in Mice and Humans....	158
5.1. Abstract	159
5.2. Introduction	160
5.3. Results	162
5.3.1. Mouse Study – Bone Innervation and Neuronal Mediators	162
5.3.2. Mouse Study – Bone Metabolic Parameters.....	166
5.3.3. Mouse Study – Bone Microarchitecture	167
5.3.4. Human Study - Descriptive Results	168
5.3.5. Human Study - Bone Metabolic Parameters.....	168
5.3.6. Human Study - Bone Mineral Density	168
5.4. Discussion	172
5.5. Materials and Methods.....	176
5.5.1. Mouse Study – Animal Model	176
5.5.2. Mouse Study - Collection of Serum Samples.....	177
5.5.3. Mouse Study - Collection of Bone Samples.....	177
5.5.4. Mouse Study - Histomorphometry of Neuronal Markers.....	178
5.5.5. Mouse Study - qPCR for Gene Expression in Bone Samples	178

5.5.6. Mouse Study - ELISA of Serum Samples	179
5.5.7. Mouse Study - μ CT of Bone Samples.....	179
5.5.8. Human Study – Participants.....	179
5.5.9. Human Study – Study Procedure.....	180
5.5.10. Human Study – Psychometric Measures.....	180
5.5.11. Human Study – Serum Bone Marker Measurement.....	181
5.5.12. Human Study – DXA Measurement.....	181
5.5.13. Statistical Analysis	182
5.6. Author Contributions	182
5.7. Funding	183
5.8. Abbreviations	183
5.9. References.....	185
6. Discussion and outlook	194
6.1. References.....	204
7. Acknowledgments	209

Appendix – CV of Martin Roszkowski

Book Chapter

1. Introduction - Transgenerational Epigenetics of Traumatic Stress

Ali Jawaid^{1,†}, Martin Roszkowski^{1,†}, Isabelle M. Mansuy¹

[†] Shared first authorship: Martin Roszkowski prepared the illustration and wrote the book chapter.

¹ Laboratory of Neuroepigenetics, Brain Research Institute of the University of Zurich and Institute for Neuroscience of the ETH Zurich, Zurich, Switzerland

This chapter has been published in the book “Neuroepigenetics and Mental Illness” in:
Progress in Molecular Biology and Translational Science



Publication date: 1.3.2018

DOI: 10.1016/bs.pmbts.2018.03.003

1.1. Abstract

Traumatic stress is a type of environmental experience that can modify behavior, cognition and physiological functions such as metabolism, in mammals. Many of the effects of traumatic stress can be transmitted to subsequent generations even when individuals from these generations are not exposed to any traumatic stressor. This book chapter discusses the concept of epigenetic/non-genomic inheritance of such traits involving the germ-line in mammals. It includes a comprehensive review of animal and human studies on inter- and trans-generational inheritance of the effects of traumatic stress, some of the epigenetic changes in the germ-line currently known to be associated with traumatic stress, and possible mechanisms for their induction and maintenance during development and adulthood. We also describe some experimental interventions that attempted to prevent the transmission of these effects, and consider the evolutionary importance of trans-generational inheritance and future outlook of the field.

1.2. Introduction

Environmental experiences can have a long-lasting impact on cognition and behavior of an individual. Cognitive and behavioral effects usually involve dynamic changes in gene expression and cellular signaling pathways in the brain. These molecular changes are complex and largely brought about by epigenetic or non-genetic mechanisms such as DNA methylation, histone posttranslational modifications (HPTMs) and non-coding RNAs (ncRNAs). Emerging evidence suggests that environment-induced epigenetic changes can persist for a long time and some of these changes can also be transmitted to subsequent generations even when if individuals from these generations are not exposed to the initial environmental stimulus (reviewed in [1]).

Traumatic stress is one such environmental factor, which has trans-generational effects in mammals. Traumatic experiences, both in early and late life, are major risk factors for behavioral dysfunctions and mental disorders. Importantly, there is increasing evidence for inter- and trans-generational cycles of behavioral adaptation in response to traumatic stress, which are largely mediated by epigenetic mechanisms. In most scenarios, stressful experiences negatively affect behaviors across generations and constitute heritable risk factors for neuropsychiatric disorders (reviewed in [2]). For example, early life traumatic stress leads to a multitude of behavioral abnormalities including pro-depressive behaviors across two generations of offspring in mice [3]. However, there is also evidence for transmission of positive functional adaptations and in the involvement of some brain pathways in these adaptations in the offspring of traumatized mice that allow behavioral flexibility and improved goal-directed behavior [4].

This chapter discusses the epigenetic mechanisms important for brain functions in the context of susceptibility to traumatic stress and its consequences. Current evidence for inter- and trans-generational inheritance of the effects of traumatic stress in animals and humans is reviewed and some of the potential underlying molecular mechanisms described. The evolutionary importance of transgenerational epigenetic inheritance, its potential clinical implications, and future outlook are also briefly discussed.

1.2.1. Traumatic stress

In a medical or biological context, stress is a physical, mental or emotional factor that can be acute or chronic, and causes body and/or mental tension. Stress can be induced in response to external (environmental or psychological) or internal (physical illness or injury) stimuli. It typically leads to a fight or flight response, which involves broad activation of neurological and endocrinological processes. Acute stress is a strong psychological response to a novel and unpredictable threatening event. When exposure to such events is repetitive and strong enough to induce a persistent response, generally over a month in humans and more than a week in mice, it becomes chronic (reviewed in [5,6]). Traumatic stress is a particular type of stress involving an acute or chronic reaction to shocking and emotionally overwhelming situations generally involving a threat to physical or personal integrity. Clinically, in humans, it exists in the form of acute stress disorder (ASD), which can be classified as post-traumatic stress disorder (PTSD) when persisting for more than a month. Both ASD and PTSD are characterized by intrusion symptoms involving recurrent memories, dreams, or flash backs of the traumatic event, dissociative symptoms including traumatic amnesia, avoidance symptoms, hyper arousal and negative mood according to Diagnostic and Statistical Manual of Mental Disorders 5th edition (DSM V).[7] An important trigger of traumatic stress is early childhood trauma, which involves traumatic events in childhood, such as physical or sexual abuse, deprived parental care, natural disasters, or forced displacement. Similarly, experiencing of witnessing traumatic events during adult-hood, such as military combat, physical or sexual abuse, disease, physical injury, etc. can lead to chronic traumatic stress in many individuals (reviewed in [8]).

Long-term traumatic stress can lead to marked changes of brain functions, in particular mental health. Human studies suggest that PTSD is often co-morbid with depression and anxiety [9] and is associated with a greater prevalence and incidence of dementia [10]. This could be partially attributed to a decrease in hippocampal volume observed in individuals with PTSD [11]. Beyond the brain, traumatic stress over prolonged periods also leads to harmful effects on other body functions. PTSD is a risk factor for cardiovascular and cerebrovascular diseases, gastrointestinal dysfunctions, rheumatoid arthritis, and cancer [12].

At the molecular level, traumatic stress alters the integrity of the hypothalamic-pituitary-adrenal (HPA) axis. An important endocrinological circuit in HPA axis involves the release of corticotropin releasing hormone (CRH) from the hypothalamus, which stimulates

the release of adrenocorticotropic hormone (ACTH) from the pituitary. ACTH, in turn, induces the release of cortisol (CORT) from adrenal glands. Importantly, cortisol inhibits the release of ACTH as a physiological negative feedback, whereas, ACTH has a similar negative feedback on the release of CRH (reviewed in [8]). PTSD patients have gross alterations in the HPA axis, including a sustained release of CRH, blunted negative feed-back of ACTH on CRH release, and hypercortisolism [13]. On the contrary, some other studies suggest a role for hypocortisolism in development of PTSD and other stress related bodily disorders after traumatic stress [14,15]. This is combined with altered responses of hippocampal and amygdala, brain regions providing critical input to the HPA axis [16].

Importantly, the effects of traumatic stress on the brain are pleiotropic and mediated by complex signaling pathways besides HPA axis. Notably, traumatic stress affects the expression and functioning of mineralocorticoids, which are implicated in the regulation of basal HPA axis activity, traumatic memories, and stress resilience (reviewed in [17]). Traumatic stress can also dysregulate the balance between oxytocin and arginine vasopressin (avp), which have a critical role in the regulation of social and emotional responses, ranging from parenting to partner preference and stress-reactivity (reviewed in [18]). Similarly, noradrenergic system and catecholamines are thought to underlie the development of PTSD after trauma exposure (reviewed in [19]), and serotonergic signaling in the susceptibility to and long-term effects of traumatic stress [20,21].

The effects of traumatic stress on the brain are more profound during certain periods of life. The brain is particularly sensitive to environmental stimuli during prenatal, early postnatal and pubertal periods due to higher plasticity of the brain, increased neurogenesis, relative immaturity of the stress-responsive circuitry and neuroendocrine dynamics [22,23]. Animal studies have reflected that there are sensitive periods for transgenerational transmission of environmental effects as well [24]. In the next section, we briefly review the epigenetic mechanisms that are relevant to the effects of traumatic stress on the brain and are of potential importance in the transgenerational epigenetic inheritance of the effects of traumatic stress.

1.2.2. Epigenetic mechanisms relevant to the effects of traumatic stress on the brain

DNA methylation, which in mammals most commonly occurs at cytosine-guanine dinucleotides (CpG), has traditionally been viewed as a fairly stable epigenetic mark mostly responsible for gene silencing (reviewed in [25,26]). Silencing takes place by direct inhibition of the binding of transcription factors, or by recruitment of methyl-CpG binding proteins (MBPs) and associated repressive chromatin-remodeling components [27]. However, CpG methylation is also present at the promoter and coding region of actively transcribed genes, where it can associate with transcriptional activity [28]. Recent evidence has shown that in many cells including post-mitotic cells like adult neurons, DNA methylation is dynamically regulated and CpGs can be actively methylated and demethylated [29,30]. DNA demethylation involves a succession of biochemical steps implicating several enzymes. During this process, 5-methylcytosine (5-mC) is successively oxidized into 5-hydroxymethylcytosine (5-hmC), 5-formylcytosine (5-fC) and 5-carboxylcytosine (5-cAC) by ten-eleven translocation (TET) proteins. 5-fC and 5-cAC can ultimately be removed and repaired by terminal deoxycytidyl transferases (TdTs) generating an unmodified cytosine [31]. In contrast to 5-fC and 5-cAC, 5-hmC is enriched in the adult brain, especially in the hippocampus, cortex and cerebellum [32–34]. The high abundance of 5-hmC in the brain and its stability [35] suggest that this modification is not just a transient by-product of 5-mC metabolism but also serves as an epigenetic mark thought to play an important role in brain processes.

Importantly, traumatic stress leads to long-term changes in global, as well as, locus-specific DNA methylation (reviewed in [36]) making it a candidate epigenetic mechanism underlying long-term effects of traumatic stress. Mice subjected to an acute stress paradigm involving forced swim in cold water demonstrate altered methylation of several immediate early genes in the dentate gyrus and the subsequent behavioral response [37]. Further, DNA methylation is a critical regulator of fear memory, which signifies its importance in long-term consequences of traumatic stress in the brain [38].

Histone modifications - Covalent post-translation modifications of histone proteins are other important epigenetic marks that primarily involve acetylation, methylation, phosphorylation, ubiquitination, and SUMOylation (reviewed in [39]). These modifications control the accessibility of the chromatin to the transcriptional machinery, in a sequence and

activity-dependent manner [40]. Generally, acetylation and phosphorylation, occurring on lysine (K) and serine (S), threonine (T) or tyrosine (Y) residues respectively, are associated with transcriptional activation [39]. In contrast, histone methylation on lysine residues is associated with both actively transcribed and silenced genes [40–42]. Similarly, histone ubiquitination is associated with both transcriptional silencing and activation depending on whether it occurs on H2A or H2B respectively [43]. Finally, histone SUMOylation, which requires addition of small-ubiquitin like modifier (SUMO) to histones, negatively regulates gene transcription in the brain, often in association with other epigenetic regulators [44,45].

Importantly, several HPTMs are affected by both acute and chronic stress [46,47]. Key stress-induced cascades, such as corticosterone and glutamate signaling may contribute to the regulation of HPTMs to modulate gene expression and behavior [48]. Pre-clinical studies suggesting the use of histone deacetylase (HDAC) inhibitors in trauma therapy and anxiety treatment provide further support for a role of histone regulation during and after traumatic stress (reviewed in [49]).

Non-coding RNAs - Epigenetic regulation of gene expression can also be achieved by ncRNAs like microRNAs (miRNAs). MiRNAs are 20-22 nucleotide long RNAs that act by degradation of mRNA targets or translational repression (reviewed in [50]). MiRNA biogenesis involves a succession of cellular steps regulated by the RNase Drosha and its partner DeGeorge syndrome critical region 8 (DGCR8) in the nucleus, followed by further processing by another RNase Dicer and its partner TAR RNA binding protein (TRBP) in the cytoplasm. Once formed, miRNAs associate with Argonaute proteins in the cytoplasm to form the RNA-induced silencing complex (RISC). RNA-binding proteins can additionally modulate the efficiency of the microprocessor, Dicer or RISC (reviewed in [50]). Many miRNAs and components of miRNA biogenesis machinery are highly expressed in the brain, mostly in a region-specific manner. Importantly, miRNAs have been implicated in the susceptibility of the brain to trauma and in the effects of trauma exposure [51,52]. A number of studies on PTSD patients highlight a potential involvement of miRNAs as mediators and/ or moderators of the effects of traumatic stress (reviewed in [53]).

While other ncRNAs such as lncRNA and piRNAs have a demonstrated role in various molecular pathways, their contribution to the effects of traumatic stress has been less well studied. Similar to miRNAs, lncRNAs are widely abundant in the brain [54] and in some cases,

they share the miRNA biogenesis machinery [55]. LncRNAs can interfere and compete with the functions of miRNAs. They can also influence mRNA stability and splicing, and transcriptional regulation (reviewed in [56]). The lncRNA Gomafu was recently shown to be down regulated after fear conditioning, providing a lncRNA candidate possibly involved in traumatic stress [57]. piRNAs are mainly known for their role in genomic defense against mobile elements in the germ line [58]. However, they may have a similar role in the CNS by restricting the activity of mobile elements in the developing and mature brain [59]. Novel insight in the role of piRNAs in the epigenetic regulation of memory also points to their potential functions in traumatic stress [60].

RNA modifications - Most RNAs carry a large variety of chemical modifications such as 1-methyladenosine (m^1A), 1-methylguanosine (m^1G), N^6 -methyladenosine (m^6A), 5-methylcytidine (m^5C) or pseudouridine (Ψ) methylation [61,62]. Although the role of such modifications in RNA is less well understood than in DNA, their main effect is to alter the binding affinity for the complementary strand and modify the structure of the folded RNA [63]. This in turn can drastically alter the binding affinity of RNA to other RNAs, and to RNA binding proteins, thus influencing RNA stability and sub-cellular localization [64,65]. Currently, little is known about the potential role of the epitranscriptome in traumatic stress. Recent findings showed that the RNA demethylase FTO is affected by contextual fear conditioning [66]. It is therefore very likely that the epitranscriptome contributes to the epigenetic effects of traumatic stress.

Most epigenetic mechanisms have so far been studied individually, but a combination of different epigenetic mechanisms is likely responsible for the effects of traumatic stress at the molecular level. Thus, it is important to take into account the complex interplay of the combined cellular machinery that shapes and regulates the epigenome. Although there is currently no study providing such integrated view of the epigenome and epitranscriptome after traumatic stress, developmental studies have examined HPTMs in the context of DNA methylation and showed that they can guide *de novo* methylation [67].

1.3. Transgenerational inheritance of traumatic stress

A growing body of evidence suggests that the effects of traumatic stress can be transmitted to subsequent generations, even when these generations are not exposed to the initial traumatic event. When these effects are transferred from parents to the direct offspring, it is termed as intergenerational inheritance while transmission to at least two generations of offspring is transgenerational [2]. In this chapter, we will review evidence for both inter- and trans-generational effects of traumatic stress, which are both important although transgenerational inheritance is more relevant from an evolutionary point of view [68]. The chapter will focus on the inheritance of the effects of postnatal trauma and their transmission to subsequent generations [1]. The effects of prenatal stress will be discussed only briefly as evidence is still sparse and the mediating mechanisms have been less well studied [69,70].

Effects of postnatal traumatic stress can be transmitted to the offspring independently of the germline, and in this case, involve social transmission and acquisition of behavioral or physiological patterns from parent to offspring. True inheritance of the effects of traumatic stress involves transmission through germ cells and implicates epigenetic mechanisms [1]. In rodents, traumatic stress has been shown to affect behavior, cognitive functioning, and metabolism of subsequent generations through complex and yet not fully understood epigenetic mechanisms. Similar effects exist in humans, although mechanistic explanations are even more limited. This section summarizes pertinent evidence in support of inter- and trans-generational inheritance of traumatic stress in animals and humans, and results are summarized in Tables 1 and 2.

1.3.1. Animal models

Recent animal studies have reported inter- and trans-generational effects of traumatic stress using rodents and other species. Observations in birds and reptiles are interesting to consider because these animals are precocial (relatively mature at birth), unlike rodents which are relatively immature [71]. Animal studies on transgenerational inheritance typically use the nomenclature adapted from studies of genetic inheritance in which the offspring produced from the first genetic cross is labeled as (filial 1) F1 and subsequent generations involving breeding of affected F1 to naïve breeders or affected F1 are F2, F3, etc. (Fig. 1).

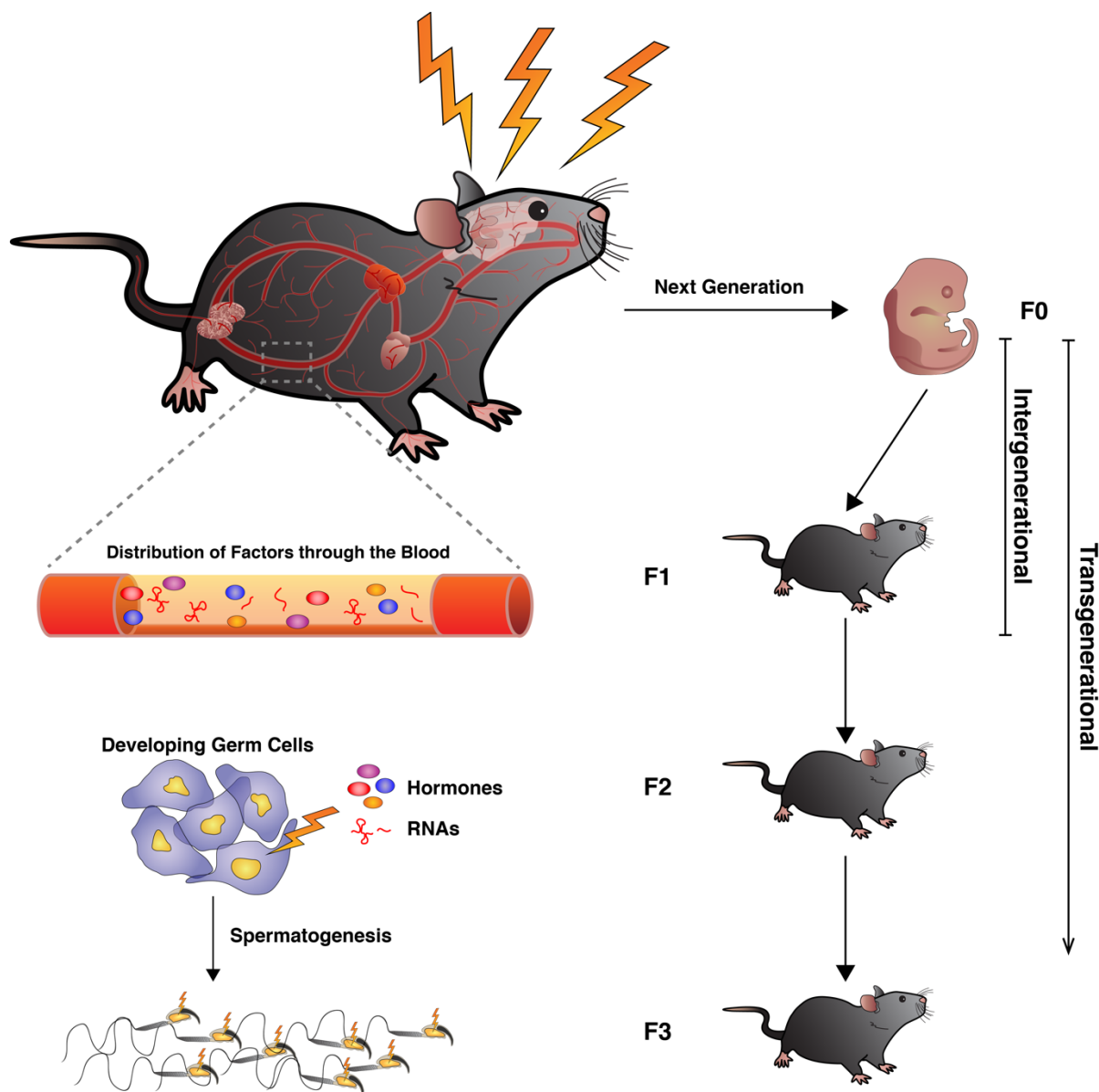


Figure 1: Potential mechanisms of induction and persistence of transgenerational effects of traumatic stress. Traumatic stress may alter circulating factors (hormones, cytokines, and/or circulating ncRNAs) in trauma-exposed animals. These changes have the potential to affect the epigenome of the developing sperm. This could be either through direct uptake of circulating ncRNAs by developing gametes, or through the effect of circulating cytokines and hormones on enzymes regulating DNA methylation, HPTMs or ncRNAs. These changes may serve as vectors of transmission of the effects of traumatic stress to the next generation. Similar or related mechanisms may then be responsible for persistence of transgenerational phenotypes across generations.

Rodent studies on inter- and trans-generational effects of traumatic stress have provided important mechanistic insight about how these effects can be transmitted across generations. These models have used different paradigms including interrupted or impaired maternal care, maternal separation or fear conditioning [8]. Babb et al. used chronic social stress during lactation to impair maternal care in a cohort of mice (F0). The deprived male offspring (F1) was then mated with naïve females to produce an F2 generation, which had decreased social behaviors during puberty and adulthood. The behavioral anomalies were accompanied by alterations in corticosterone and oxytocin in both F2 females and males and prolactin in F2 females only [72]. Similarly, a study on mice with impaired maternal care (F1) due to post partum depression (PPD), induced by pre-pregnancy chronic stress exposure in the form of daily restraint and night time illumination, in mothers (F0) showed transgenerational inheritance of depressive behaviors and altered mTOR-Akt signaling in the F2 offsprings [73].

Unpredictable maternal separation combined with unpredictable maternal stress (MSUS) is a solid model of transgenerational inheritance in mice, and one of the rare to affect several successive generations. This model uses a combination of daily unpredictable separation of newborn pups (F1) from their mother (F0), with unpredictable stress exposure of mothers (F0) during separation [3]. These repetitive and unpredictable traumatic experiences during postnatal day 1-14 alter behavior of the offspring in up to three generations. F2 and F3 MSUS mice show depressive-like behaviors, which are not due to any alteration in maternal care as they persist after cross fostering [3]. Further, F2 and F3 mice have altered behavioral response to aversive environment, more risk-taking behaviors and impaired social recognition memory [3,74]. Hippocampus-dependent spatial memory and synaptic plasticity are also affected in F1 and F2 animals and molecular pathways related to learning and memory are altered [75]. Further, both F1 and F2 MSUS mice have disrupted functional connectivity of brain serotonergic pathways, including limbic circuits implicated in mood disorders [76]. Interestingly, MSUS also confers some adaptive advantages to the offspring, especially increased behavioral flexibility and improved goal-directed behaviors [4]. The transgenerational effects of MSUS are not only limited to the brain, but also affect glucose and insulin metabolism. MSUS F2 generation have a faster glucose clearance on the glucose tolerance test (GTT) despite lower level of fasting insulin. They also weigh less than controls despite a higher dietary intake [74].

Besides early life adversity, traumatic stressors during postnatal or adult life also have transmissible behavioral effects. Chronic stress involving social instability and disrupted social hierarchy from postnatal day 27 to 76 enhances anxiety and induces social deficits in mice in up to three generations [77]. Chronic social defeat can also induce depressive behaviors in female and male offspring (F1) of stressed male mice (F0) [78]. Some of these effects could be transmitted by *in vitro* fertilization (IVF), suggesting their dependence on germ cells. Odor fear conditioning in mice (F0) was reported to induce behavioral sensitivity to an odor in F2 and F3 offspring, and be accompanied by changes in the olfactory system in the brain of F2 and F3 that could be recapitulated by IVF [79]. These results overall suggest that the effects of traumatic stress can be passed to subsequent generations in rodents.

Non-rodent studies - In domesticated chickens (*Gallus gallus*), gene expression and feeding behavior are altered in the offspring (F1) of animals exposed to unpredictable food access [80]. While the study did not focus on behavioral or molecular aspects of traumatic stress, it was the first to suggest intergenerational inheritance in response to stress in birds. Another study using chronic stress by intermittent social isolation for the first three months of life showed that male offspring (F1) of stressed chickens (F0) have altered expression of over 40 genes in the brain. However, there was no difference in fear-related behavior in the F1 offspring of stressed versus unstressed F0 [81]. A more recent study from the same group exposed chickens (F0) to a stress paradigm involving food frustration, physical restraint and social isolation on alternating days for a total of 6 days during early life, early puberty or late puberty. Behavioral and hormonal assessment of the progeny (F1) showed a heightened corticosterone response to acute restraint stress in F1 offspring of chickens exposed to stress (F0) during puberty. Similarly, F1 offspring of F0 exposed to stress during late puberty and early life had higher body weight at hatching and at one month of age respectively [82]. Finally, a recent study on eastern fence lizards (*Sceloporus undulatus*) showed that ancestral exposure to stress (in the form of predator invasion for many generations) showed a more robust corticosterone response to restraint and ACTH injection. These results indicate that ancestral stress exposure can re-program the offspring HPA axis [83].

Table 1: Studies on Inter- and Transgenerational Inheritance of the Effects of Traumatic Stress in Animals

Species	Acute or Chronic Traumatic Stress	Early Life or Adult Stress	Main Effects(s)	Mechanism of Inter/Transgenerational Inheritance	Generations Affected	Author, Year
Domesticated chickens <i>(Gallus gallus)</i>	Chronic social isolation	Early	Altered gene expression in the offspring brain	Not tested	Two	Goerlich, 2012
	Chronic food frustration, physical restrain, social isolation	Early, puberty, adult	Increased CORT, higher body weight in the offspring	Not tested	Two	Ericson, 2016
Mice (<i>Mus musculus</i>)	Chronic (impaired maternal care)	Early	Decreased social behaviors, and alterations in cortisol, and oxytocin in the offspring	Not tested	Two	Babb, 2014
	Chronic (impaired maternal care)	Early	Pro-depressive behaviors, and altered mTOR-Akt signaling in the offspring	Not tested	Two	Wu, 2016
	Chronic (impaired maternal care)	Early	Pro-depressive behaviors, decreased social anxiety, and decreased social recognition memory in the offspring	Not tested	Three	Franklin, 2010
	Chronic (impaired maternal care)	Early	Pro-depressive behaviors and altered glucose metabolism in the offspring	Sperm RNA as vector of transgenerational inheritance	Three	Gapp, 2014

Continued

Table 1: Studies on Inter- and Transgenerational Inheritance of the Effects of Traumatic Stress in Animals - Continued

Species	Acute or Chronic Traumatic Stress	Early Life or Adult Stress	Main Effects(s)	Mechanism of Inter/Transgenerational Inheritance	Generations Affected	Author, Year
Mice (<i>Mus musculus</i>)	Chronic (impaired maternal care)	Early	Impaired spatial memory, and synaptic plasticity in the offspring	Not tested	Two	Bohacek, 2015
	Chronic (impaired maternal care)	Early	Improved goal-directed behavior in the offspring	Changes in sperm mineralocorticoid receptor	Two	Gapp, 2014
	Chronic (impaired maternal care)	Early	Changes in serotonergic circuitry in the brain of the offspring	Not tested	Two	Razoux, 2017
	Chronic (impaired maternal care)	Early	Brain metabolic alterations in the offspring	Not tested	Two	Gapp, 2017
	Chronic social defeat	Adult	Pro-depressive behaviors in the offspring	Not tested, however germline transmission of effect was confirmed by <i>in vitro</i> fertilization	Three	Saavedra-Rodriguez, 2013
	Acute odor fear conditioning	Adult	Behavioral sensitivity to odor in the offspring	Olfactory pathways, germline transmission of effect was confirmed by <i>in vitro</i> fertilization	Three	Dias, 2013

1.3.2. Human studies

Literature about the inheritance of the effects of traumatic stress in humans has slowly accumulated in the past decade (Table 2). However, it remains thin and studies in humans also generally lack clear ‘cause and effect’ association, mechanistic explanations or germ-line assessment, which are admittedly less tractable in humans than in animals. Like in animals, parental care seems to be a strong determinant of transgenerational inheritance of the effects of traumatic stress in humans. A recent study in Germany showed that low maternal bonding in mothers and high level of paternal stress are associated with a clinical diagnosis of borderline personality disorder (BPD) in the offspring [84]. Similarly, based on a large Swedish population-based cohort, a study showed that parental death during ‘slow growth period’ (time before the start of puberty, generally 9-12 years of age for boys) in boys leads to prematurity and low birth weight in their offspring [85]. Evidence from small-scale studies from the 60s and 70s, indicates signs of psychopathology in children of Holocaust survivors [86]. More recently, trauma exposure in holocaust survivors was shown to induce neuropsychiatric changes in their children and be associated with alterations in some epigenetic marks, in particular DNA methylation in FK506 binding protein 5 gene [87]. The children of holocaust survivors had increased susceptibility to PTSD, primarily women survivors [88,89], which could be related to low cortisol level [90]. Increased anxiety symptoms have also been reported in children of individuals who developed hyper-arousal related to genocide exposure in Cambodia [91] and increased depression and anxiety in children of genocide exposed people in Rwanda [92].

Intergenerational inheritance of behavioral dysfunctions has also been reported in families subjected to forced displacement or immigration. A study on adult descendants of individuals exposed to forced displacement with or without PTSD showed implicit avoidance of displacement-related stimuli in relation to PTSD [93]. The effects of traumatic stress have also been suggested to be transmitted to the offspring in Latin American immigrants [94] and increased depressive and somatization symptoms in the offspring of immigrants exposed to torture and forced displacement was reported in a Swedish study [95]. Emerging evidence further shows intergenerational inheritance in relation to combat trauma. The descendants of World War II or Vietnam war veterans exhibit various psychological impairments [96], violence and hostility behaviors, which positively correlated with the intensity and duration of exposure to combat trauma in their parents [97]. Further, veterans of the Serbian-Bosnian

conflict with PTSD have children with increased developmental, behavioral and emotional problems [98,99]. Finally, a very recent study on offspring of Finnish evacuees during World War II showed a two times increased risk of psychiatric hospitalization in women whose mothers were evacuated compared to those whose mothers were not evacuated [100].

In conclusion, although less studied from a mechanistic point of view, inter- and possibly trans-generational inheritance of the effects of traumatic stress is supported by empirical evidence in humans.

Table 2: Studies on Intergenerational Inheritance of the Effects of Traumatic Stress in Humans

Acute or chronic traumatic stress	Early or late life stress	Main Effects(s)	Author, Year
Chronic (low maternal bonding)	Early	Increased risk of BPD in the offspring	Infurna, 2016
Chronic (paternal death)	Early	Prematurity and low birth weight in the offspring	Vägerö, 2017
Chronic (Holocaust survivors)		Increased psychopathology, increased susceptibility to PTSD, and low cortisol levels in the offspring	Yehuda, 1998 Yehuda, 2000 Yehuda, 2008
Chronic (genocide exposure in Cambodia)		Increased anxiety in the offspring	Field, 2013
Chronic (genocide exposure in Rwanda)		Increased anxiety and depression in the offspring	Rieder, 2013
Chronic (combat exposure during Vietnam war)		Increased hostility in the offspring	Glenn, 2002
Chronic (combat exposure during Bosnia-Serbia war)		Increased emotional and developmental problems in the offspring. Increased social and behavioral problems in the offspring	Klaric, 2008 Coric, 2016
Chronic (World War II in Finland)		Increase psychiatric hospitalizations in women whose mothers were evacuated	Santavirta, 2018
Chronic (immigrants exposed to torture and forced displacement)		Increased depressive and somatization symptoms in the offspring	Daud, 2005

1.4. Mechanisms of inter- and trans-generational inheritance

Inheritance across generations can occur through both matrilineal and patrilineal lineages [1]. Mechanistically, evidence for transmission through males is characteristically dominant, and will therefore be described here. Four major questions are addressed 1) Which epigenetic mechanisms serve as vectors of inheritance in the context of traumatic stress, 2) How does traumatic stress induce these epigenetic changes in the germline, 3) How epigenetic changes induced in the germ-line are transmitted to the offspring, and 4) How do these effects persist across generations.

1.4.1. Epigenetic mechanisms in the germ-line

Like somatic cells, germ cells also have DNA modifications, HPTMs and ncRNAs. In sperm, DNA can be differentially methylated by environmental factors at different loci. Traumatic stress induced by MSUS in mice induces hypomethylation at promoter CpGs of corticotropin-releasing factor 2 (*Crfr2*) and protein kinase C gamma (*Prkcg*), and hypermethylation at the promoter of methyl CpG-binding protein 2 (*Mecp2*) and *Nr3c2* (the gene encoding for mineralocorticoid receptor (MR)). Similar alterations in DNA methylation are also observed in the brain of the offspring [3,75]. Environmental stressors can also modulate HPTMs and related proteins such as Polycomb repressive complex 2 (PRC2) for instance in *D. melanogaster* and *C. elegans* [101,102]. In rodents, the contribution of histones to transgenerational inheritance is more limited since most histones (95-99%) are replaced by protamines in sperm [1]. ncRNAs have also been implicated in the effects of traumatic stress across generations, in this case with some causal evidence. MSUS was shown to alter the ncRNA content in sperm, in particular miRNAs and piRNAs [74,103,104]. Injection of sperm RNAs from MSUS-exposed males into wild-type fertilized oocytes could recapitulate behavioral and metabolic impairments in the resulting mice and in their progeny, providing strong evidence for a direct link between sperm RNA and transmission of symptoms [74]. It was suggested that 9 miRNAs, shown to be upregulated in sperm by adult paternal stress may recapitulate corticosterone level alteration, but further effects have not been addressed, limiting conclusions of this study [103].

1.4.2. Induction of epigenetic mechanisms in the germ-line by traumatic stress

While changes in the germ-line epigenome have been proposed as vectors of transgenerational inheritance of the effects of traumatic stress, how traumatic stress affects the

germ-line epigenome remains unknown. Circulating factors may be involved, as they can access germ cells and other tissues like the brain and possibly mediate the effects of traumatic stress. Interestingly, just like the brain, germ cells are in a immunologically privileged tissue protected by the blood-testis barrier. To access germ cells in adult gonads, circulating factors, therefore, need to be lipid soluble and easily transportable such as hormones, cytokines or circulating RNAs (Figure 1). These factors may be released by stress pathways and act via receptors like adrenergic receptors[105], MR [106], gonadotropin-releasing hormone (GnRH) receptor [107], arginine vasopressin receptors [108], which are present on sperm cells. Hormonal treatment has indeed been shown to change sperm ncRNA content [109]. Cytokines make other important circulating factors to consider as they can cross the blood-testis and blood-brain barrier, and are even implicated in the regulation of the barrier [110]. Cytokine receptors are also present on sperm [107].

Circulating RNAs could also be carriers of the impact of traumatic stress to germ cells. In mammals, circulating RNAs are mainly transported in extracellular vesicles called exosomes. Exosomes enriched in ncRNAs are generated from parent cells, and can cross blood-testes or blood-brain barrier to affect cells behind the barrier. The developing sperm can acquire ncRNAs from prostasomes and epidydimosomes, two specialized types of exosomes, during maturation [111]. It is possible that the ncRNA content of such exosomes could be altered e.g. from distal somatic cells, and then alter the ncRNA content of sperm. Evidence from *C.elegans* shows that extracellular dsRNA can reach the developing embryo through vesicles, and cause gene silencing in the progeny. These results suggest a possible mechanism for the transmission of experience-dependent effects between generations [112].

1.4.3. How are these effects passed to the offspring?

Another important question to address is how the effects of traumatic stress are passed from the germ-line to the brain of the offspring. One possibility is that changes induced by traumatic stress in germ cells are maintained during development and escape reprogramming to be passed to all three embryonic layers. Evidence in the MSUS model shows that similar epigenetic alterations affect the brain and sperm of trauma-exposed mice (F1) and the brain and sperm of their offspring (F2) [74,75]. Alternately, epigenetic modifications in germ cells may in turn regulate the mechanisms controlling brain development. For instance, beta catenin, which regulates neuronal differentiation in embryonic stem cells [113], is regulated by miR-

375, a microRNA altered in the sperm of trauma-exposed mice [74]. Parallel investigations on germ cells of trauma-exposed animals, as well as, the developing embryo, post-natal offspring brain and adult offspring brain, are likely to reveal valuable clues about the mechanisms underlying the persistence of the transgenerational effects of traumatic stress.

1.4.4. Persistence of epigenetic marks related to trauma across generations

It is currently not known how persistent epigenetic modifications induced by trauma are in brain and sperm. However, it has been observed that while the offspring of traumatized individuals exhibit similar behavioral symptoms, some epigenetic changes are not present in this offspring e.g. miRNAs in sperm. It is possible that initial changes directly induced by trauma are transferred to other epigenetic marks to be perpetuated, consistent with evidence of strong cross-talks between epigenetic mechanisms e.g. miRNAs regulating DNA methyl transferases (DNMTs) [114], or Methyl CPG binding protein 2 (MeCP2) regulating miRNAs biogenesis [115]. It could also be that epigenetic changes induced by traumatic stress in germ cells are somehow transformed into genomic changes in subsequent generations due to decreased genomic stability, and lead to copy number variations (CNV). Exposure of the endocrine disruptor vinclozolin was shown to increase CNVs in the F3 generation [116], suggesting that it could also be the case after traumatic stress. Future studies on transgenerational inheritance of traumatic stress may benefit from whole germline genome, epigenome, as well as, RNA sequencing to ascertain how epigenetic marks of traumatic stress persist across generations.

1.4.5. Potential of anti-stress therapies to prevent transmission of the effects of traumatic stress

While traumatic stress may lead to inherited effects in the offspring, transmission may be prevented by behavioral paradigms or pharmacological manipulations of trauma-exposed animals. Environmental enrichment (EE) of fathers for instance, was shown to prevent the transmission of the effects of traumatic stress and reverse epigenetic alterations, in particular DNA methylation alterations in the hippocampus, in the offspring [117]. In Ras-GRF knock out mice, 2 weeks of EE at postnatal 15 day EE could correct long term potentiation (LTP) deficits and fear memory impairment, and even enhanced LTP in the offspring of control mice [118]. EE can also reverse increased anxiety-like behaviors and prevent against seizures in a genetic absence epilepsy rat from Strasbourg (GAERS) model of absence seizures, an effect

transmitted across generation [119]. It is however important to note that while EE has shown potential to prevent the transmission of effects of traumatic stress or other behaviors, it has shown only limited effects on anxiety- and depression-related behaviors when used alone. A recent study involving parental EE failed to improve anxiety or depression-related behaviors and did not normalize serum corticosterone levels post-stress in the offspring [104].

Not surprisingly, oxytocin (OXT) and vasopressin (AVP) have shown potential to reverse the effects of chronic social stress (CSS) in mice. F2 female offspring of dams exposed to CSS have increased repetitive/perseverative and anxiety behaviors and deficits in social behavior. Treatment of F1 dams with OXT following CSS prevented transmission of repetitive and anxiety behaviors in F2 offspring, whereas intranasal AVP treatment in F1 dams showed positive effects on behavior deficits and anxiety. Interferon gamma (IFN-gamma) was proposed as a mediator of these effects [120].

1.5. Transgenerational inheritance of traumatic stress from an evolutionary point of view

The evolutionary significance of transgenerational epigenetic inheritance is an extremely interesting aspect that challenges the Darwinian view of evolution [121]. With respect to the effects of traumatic stress, one can question whether their transmission has any evolutionary benefit, since most of these effects are negative. However, these effects may help the offspring better cope in certain conditions, as shown for instance in MSUS mice which have better behavioral flexibility, in hostile environments [3]. However; most of the effects are maladaptive in normal and insult-free conditions suggesting that this could provide a way of ‘epigenetic natural selection’ in which selection is driven by an organism’s ability to adapt to a changing environment rather than survive the environmental adversity based on innate abilities. Epigenetic inheritance may also contribute to genome evolution since DNA methylation can lead to the formation of epialleles and then to genomic changes [121]. For example, increased CNVs in response to changes in methylation could be a means through which epigenetic inheritance could contribute to evolution [116]. The emerging role of RNAs in transgenerational epigenetic inheritance could be a supplement to the RNA theory of evolution (reviewed in [122]). Therefore, cumulative evidence and theoretical hypotheses do suggest that transgenerational epigenetic inheritance may play a role in evolution. In the context of traumatic stress, it may allow an evolutionary advantage under certain hostile

conditions. Expansion of the transgenerational studies on the effects of traumatic stress to more than 2-3 generations; delineating transgenerational studies based on how well the animals coped with trauma; and exposure of offspring to both hostile and non-hostile conditions might be important considerations to assess the evolutionary importance of transgenerational inheritance of traumatic stress.

1.6. Conclusions and Outlook

The evidence that effects of traumatic stress can be passed to subsequent generations has accumulated in the past years. The epigenetic mechanisms serving as vectors of such transmission and factors responsible for their induction in germ cells are under study. However, a number of questions and challenges remain in this field. First, it is important to have more comprehensive analyses of transmitted phenotypes. Considering that chronic stress can have wide physiological consequences, it is important to determine if the cardiovascular, immunological, gastrointestinal system, and endocrine systems are also affected in any model of trauma. It is also important to delineate the transgenerational effects in individuals in addition to large cohorts. Increasing evidence from human studies suggest that only a fraction of individuals develop PTSD after exposure to trauma while a few individuals become more resilient; a phenomenon described as post-traumatic growth (PTG) [123]. It is possible that a transgenerational phenotype is different in trauma-susceptible versus resilient animals/individuals. Third, it is also important to identify the factors responsible for induction of epigenetic modification in the germline and the signaling pathways sensitive to such factors. More direct evidence for the relevance of epigenetic modifications, is also needed, using for instance gene-editing tools such as CRISPR-Cas (reviewed in [124]). The epigenetic machinery in germ and/or embryonic cells may be edited to determine the role of some of its components in transmission. Finally, it is important that accessible biological fluids such as saliva, blood, and semen be analyzed in traumatized human populations and in their offspring to assess if mechanisms of transmission identified in animal models are relevant for humans. This step is also likely to provide valuable information to screen populations with parental trauma for phenotypic atypicalities. In the future, one could envision translation of research on transgenerational epigenetic inheritance to the bed-side. A clinical world offering ‘epigenetic counseling’, ‘epigenetic prophylaxis’ or ‘epigenetic therapy’ in populations exposed to traumatic stress and/or their offsprings might eventually become reality.

1.7. References

1. Bohacek, J.; Mansuy, I.M. Molecular insights into transgenerational non-genetic inheritance of acquired behaviours. *Nat. Rev. Genet.* **2015**, *16*, 641–652, doi:10.1038/nrg3964.
2. Klengel, T.; Dias, B.G.; Ressler, K.J. Models of Intergenerational and Transgenerational Transmission of Risk for Psychopathology in Mice. *Neuropsychopharmacology* **2016**, *41*, 219–231, doi:10.1038/npp.2015.249.
3. Franklin, T.B.; Russig, H.; Weiss, I.C.; Gräff, J.; Linder, N.; Michalon, A.; Vizi, S.; Mansuy, I.M. Epigenetic transmission of the impact of early stress across generations. *Biol. Psychiatry* **2010**, *68*, 408–15, doi:10.1016/j.biopsych.2010.05.036.
4. Gapp, K.; Soldado-Magraner, S.; Alvarez-Sánchez, M.; Bohacek, J.; Vernaz, G.; Shu, H.; Franklin, T.B.; Wolfer, D.; Mansuy, I.M. Early life stress in fathers improves behavioural flexibility in their offspring. *Nat. Commun.* **2014**, *5*, 5466, doi:10.1038/ncomms6466.
5. Schneiderman, N.; Ironson, G.; Siegel, S.D. Stress and Health: Psychological, Behavioral, and Biological Determinants. *Annu. Rev. Clin. Psychol.* **2005**, *1*, 607–628, doi:10.1146/annurev.clinpsy.1.102803.144141.
6. Beery, A.K.; Kaufer, D. Stress, social behavior, and resilience: Insights from rodents. *Neurobiol. Stress* **2015**, *1*, 116–127.
7. Association, A.P. *Diagnostic and Statistical Manual of Mental Disorders (5th ed.)*; 5th ed.; American Psychiatric Association: Washington, DC, 2013; ISBN 978-0-89042-554-1.
8. Lupien, S.J.; McEwen, B.S.; Gunnar, M.R.; Heim, C. Effects of stress throughout the lifespan on the brain, behaviour and cognition. *Nat. Rev. Neurosci.* **2009**, *10*, 434–445, doi:10.1038/nrn2639.
9. Ginzburg, K.; Ein-Dor, T.; Solomon, Z. Comorbidity of posttraumatic stress disorder, anxiety and depression: A 20-year longitudinal study of war veterans. *J. Affect. Disord.* **2010**, *123*, 249–257, doi:10.1016/j.jad.2009.08.006.
10. Qureshi, S.U.; Kimbrell, T.; Pyne, J.M.; Magruder, K.M.; Hudson, T.J.; Petersen, N.J.; Yu, H.J.; Schulz, P.E.; Kunik, M.E. Greater prevalence and incidence of dementia in older veterans with posttraumatic stress disorder. *J. Am. Geriatr. Soc.* **2010**, *58*, 1627–1633, doi:10.1111/j.1532-5415.2010.02977.x.
11. Childress, J.E.; McDowell, E.J.; Dalai, V.V.K.; Bogale, S.R.; Ramamurthy, C.; Jawaid, A.; Kunik, M.E.; Qureshi, S.U.; Schulz, P.E. Hippocampal volumes in patients with chronic combat-related posttraumatic stress disorder: A systematic review. *J. Neuropsychiatry Clin. Neurosci.* **2013**, *25*, 170, doi:10.1176/appi.neuropsych.12010003.
12. Qureshi, S.U.; Pyne, J.M.; Magruder, K.M.; Schulz, P.E.; Kunik, M.E. The link between post-traumatic stress disorder and physical comorbidities: A systematic review. *Psychiatr. Q.* **2009**, *80*, 87–97, doi:10.1007/s11126-009-9096-4.
13. de Kloet, C.S.; Vermetten, E.; Geuze, E.; Kavelaars, A.; Heijnen, C.J.; Westenberg, H.G.M. Assessment of HPA-axis function in posttraumatic stress disorder: Pharmacological and non-pharmacological challenge tests, a review. *J. Psychiatr. Res.* **2006**, *40*, 550–567.
14. Heim, C.; Ehlert, U.; Hellhammer, D.H. The potential role of hypocortisolism in the pathophysiology of stress-related bodily disorders. *Psychoneuroendocrinology* **2000**, *25*, 1–35, doi:10.1016/S0306-4530(99)00035-9.

15. Rohleder, N.; Joksimovic, L.; Wolf, J.M.; Kirschbaum, C. Hypocortisolism and increased glucocorticoid sensitivity of pro-Inflammatory cytokine production in Bosnian war refugees with posttraumatic stress disorder. *Biol. Psychiatry* **2004**, *55*, 745–751, doi:10.1016/j.biopsych.2003.11.018.
16. Sherin, J.E.; Nemeroff, C.B. Post-traumatic stress disorder: The neurobiological impact of psychological trauma. *Dialogues Clin. Neurosci.* **2011**, *13*, 263–278.
17. ter Heegde, F.; De Rijk, R.H.; Vinkers, C.H. The brain mineralocorticoid receptor and stress resilience. *Psychoneuroendocrinology* **2015**, *52*, 92–110.
18. Neumann, I.D.; Landgraf, R. Balance of brain oxytocin and vasopressin: Implications for anxiety, depression, and social behaviors. *Trends Neurosci.* **2012**, *35*, 649–659.
19. Hendrickson, R.C.; Raskind, M.A. Noradrenergic dysregulation in the pathophysiology of PTSD. *Exp. Neurol.* **2016**, *284*, 181–195.
20. Lee, H.J.; Lee, M.S.; Kang, R.H.; Kim, H.; Kim, S.D.; Kee, B.S.; Kim, Y.H.; Kim, Y.K.; Kim, J.B.; Yeon, B.K.; et al. Influence of the serotonin transporter promoter gene polymorphism on susceptibility to posttraumatic stress disorder. *Depress. Anxiety* **2005**, *21*, 135–139, doi:10.1002/da.20064.
21. Bryant, R.A.; Felmingham, K.L.; Falconer, E.M.; Pe Benito, L.; Dobson-Stone, C.; Pierce, K.D.; Schofield, P.R. Preliminary Evidence of the Short Allele of the Serotonin Transporter Gene Predicting Poor Response to Cognitive Behavior Therapy in Posttraumatic Stress Disorder. *Biol. Psychiatry* **2010**, *67*, 1217–1219, doi:10.1016/j.biopsych.2010.03.016.
22. Fuhrmann, D.; Knoll, L.J.; Blakemore, S.J. Adolescence as a Sensitive Period of Brain Development. *Trends Cogn. Sci.* **2015**, *19*, 558–566.
23. Hensch, T.K. Critical period plasticity in local cortical circuits. *Nat. Rev. Neurosci.* **2005**, *6*, 877–888, doi:10.1038/nrn1787.
24. Gapp, K.; von Ziegler, L.; Tweedie-Cullen, R.Y.; Mansuy, I.M. Early life epigenetic programming and transmission of stress-induced traits in mammals: How and when can environmental factors influence traits and their transgenerational inheritance? *BioEssays* **2014**, *36*, 491–502, doi:10.1002/bies.201300116.
25. Bird, A. DNA methylation patterns and epigenetic memory. *Genes Dev.* **2002**, *16*, 6–21, doi:10.1101/gad.947102.
26. Klose, R.J.; Bird, A.P. Genomic DNA methylation: the mark and its mediators. *Trends Biochem. Sci.* **2006**, *31*, 89–97, doi:10.1016/j.tibs.2005.12.008.
27. Jones, P.L.; Veenstra, G.J.C.; Wade, P.A.; Vermaak, D.; Kass, S.U.; Landsberger, N.; Strouboulis, J.; Wolffe, A.P. Methylated DNA and MeCP2 recruit histone deacetylase to repress transcription. *Nat. Genet.* **1998**, *19*, 187–191.
28. Bahar Halpern, K.; Vana, T.; Walker, M.D. Paradoxical role of DNA methylation in activation of FoxA2 gene expression during endoderm development. *J. Biol. Chem.* **2014**, *289*, 23882–92, doi:10.1074/jbc.M114.573469.
29. Tognini, P.; Napoli, D.; Tola, J.; Silingardi, D.; Della Ragione, F.; D’Esposito, M.; Pizzorusso, T. Experience-dependent DNA methylation regulates plasticity in the developing visual cortex. *Nat. Neurosci.* **2015**, *18*, 956–958, doi:10.1038/nn.4026.
30. Rudenko, A.; Dawlaty, M.; Seo, J.; Cheng, A.; Meng, J.; Le, T.; Faull, K.; Jaenisch, R.; Tsai, L.H. Tet1 is critical for neuronal activity-regulated gene expression and memory extinction. *Neuron* **2013**, *79*, 1109–

- 1122, doi:10.1016/j.neuron.2013.08.003.
31. Kohli, R.M.; Zhang, Y. TET enzymes, TDG and the dynamics of DNA demethylation. *Nature* **2013**, *502*, 472–9, doi:10.1038/nature12750.
32. Globisch, D.; Münzel, M.; Müller, M.; Michalakis, S.; Wagner, M.; Koch, S.; Brückl, T.; Biel, M.; Carell, T. Tissue Distribution of 5-Hydroxymethylcytosine and Search for Active Demethylation Intermediates. *PLoS One* **2010**, *5*, e15367, doi:10.1371/journal.pone.0015367.
33. Münzel, M.; Globisch, D.; Brückl, T.; Wagner, M.; Welzmiller, V.; Michalakis, S.; Müller, M.; Biel, M.; Carell, T. Quantification of the sixth DNA base hydroxymethylcytosine in the brain. *Angew. Chem. Int. Ed. Engl.* **2010**, *49*, 5375–7, doi:10.1002/anie.201002033.
34. Song, C.-X.; Szulwach, K.E.; Fu, Y.; Dai, Q.; Yi, C.; Li, X.; Li, Y.; Chen, C.-H.; Zhang, W.; Jian, X.; et al. Selective chemical labeling reveals the genome-wide distribution of 5-hydroxymethylcytosine. *Nat. Biotechnol.* **2011**, *29*, 68–72, doi:10.1038/nbt.1732.
35. Bachman, M.; Uribe-Lewis, S.; Yang, X.; Williams, M.; Murrell, A.; Balasubramanian, S. 5-Hydroxymethylcytosine is a predominantly stable DNA modification. *Nat Chem* **2014**, *6*, 1049–1055, doi:10.1038/nchem.2064.
36. Jawahar, M.C.; Murgatroyd, C.; Harrison, E.L.; Baune, B.T. Epigenetic alterations following early postnatal stress: a review on novel aetiological mechanisms of common psychiatric disorders. *Clin. Epigenetics* **2015**, *7*, 122, doi:10.1186/s13148-015-0156-3.
37. Saunderson, E.A.; Spiers, H.; Mifsud, K.R.; Gutierrez-Mecinas, M.; Trollope, A.F.; Shaikh, A.; Mill, J.; Reul, J.M.H.M. Stress-induced gene expression and behavior are controlled by DNA methylation and methyl donor availability in the dentate gyrus. *Proc. Natl. Acad. Sci.* **2016**, *113*, 4830–4835, doi:10.1073/pnas.1524857113.
38. Zovkic, I.B.; Sweatt, J.D. Epigenetic Mechanisms in Learned Fear: Implications for PTSD. *Neuropsychopharmacology* **2013**, *38*, 77–93, doi:10.1038/npp.2012.79.
39. Bannister, A.J.; Kouzarides, T. Regulation of chromatin by histone modifications. *Cell Res.* **2011**, *21*, 381–95, doi:10.1038/cr.2011.22.
40. Li, B.; Carey, M.; Workman, J.L. The Role of Chromatin during Transcription. *Cell* **2007**, *128*, 707–719, doi:10.1016/j.cell.2007.01.015.
41. Peters, A.H.; Schübeler, D. Methylation of histones: playing memory with DNA. *Curr. Opin. Cell Biol.* **2005**, *17*, 230–238, doi:10.1016/j.ceb.2005.02.006.
42. Klose, R.J.; Zhang, Y. Regulation of histone methylation by demethylimation and demethylation. *Nat. Rev. Mol. Cell Biol.* **2007**, *8*, 307–318, doi:10.1038/nrm2143.
43. Cao, J.; Yan, Q. Histone ubiquitination and deubiquitination in transcription, DNA damage response, and cancer. *Front. Oncol.* **2012**, *2*, 26, doi:10.3389/fonc.2012.00026.
44. Cheng, J.; Huang, M.; Zhu, Y.; Xin, Y.-J.; Zhao, Y.-K.; Huang, J.; Yu, J.-X.; Zhou, W.-H.; Qiu, Z. SUMOylation of MeCP2 is essential for transcriptional repression and hippocampal synapse development. *J. Neurochem.* **2014**, *128*, 798–806, doi:10.1111/jnc.12523.
45. Stielow, C.; Stielow, B.; Finkernagel, F.; Scharfe, M.; Jarek, M.; Suske, G. SUMOylation of the polycomb group protein L3MBTL2 facilitates repression of its target genes. *Nucleic Acids Res.* **2014**, *42*, 3044–58, doi:10.1093/nar/gkt1317.

46. Reed, B.; Fang, N.; Mayer-Blackwell, B.; Chen, S.; Yuferov, V.; Zhou, Y.; Kreek, M.J. Chromatin alterations in response to forced swimming underlie increased prodynorphin transcription. *Neuroscience* **2012**, *220*, 109–118, doi:10.1016/j.neuroscience.2012.06.006.
47. Hunter, R.G.; McCarthy, K.J.; Milne, T.A.; Pfaff, D.W.; McEwen, B.S. Regulation of hippocampal H3 histone methylation by acute and chronic stress. *Proc. Natl. Acad. Sci.* **2009**, *106*, 20912–20917, doi:10.1073/pnas.0911143106.
48. Reul, J.M.H.M. Making memories of stressful events: A journey along epigenetic, gene transcription, and signaling pathways. *Front. Psychiatry* **2014**, *5*, 1–11, doi:10.3389/fpsyg.2014.00005.
49. Whittle, N.; Singewald, N. HDAC inhibitors as cognitive enhancers in fear, anxiety and trauma therapy: where do we stand? *Biochem. Soc. Trans.* **2014**, *42*, 569–581, doi:10.1042/BST20130233.
50. Ha, M.; Kim, V.N. Regulation of microRNA biogenesis. *Nat. Rev. Mol. Cell Biol.* **2014**, *15*, 509–24, doi:10.1038/nrm3838.
51. Mannironi, C.; Camon, J.; De Vito, F.; Biundo, A.; De Stefano, M.E.; Persiconi, I.; Bozzoni, I.; Fragapane, P.; Mele, A.; Presutti, C. Acute Stress Alters Amygdala microRNA miR-135a and miR-124 Expression: Inferences for Corticosteroid Dependent Stress Response. *PLoS One* **2013**, *8*, 1–11, doi:10.1371/journal.pone.0073385.
52. Pan-Vazquez, A.; Rye, N.; Ameri, M.; McSparron, B.; Smallwood, G.; Bickerdyke, J.; Rathbone, A.; Dajas-Bailador, F.; Toledo-Rodriguez, M. Impact of voluntary exercise and housing conditions on hippocampal glucocorticoid receptor, miR-124 and anxiety. *Mol. Brain* **2015**, *8*, 40, doi:10.1186/s13041-015-0128-8.
53. Snijders, C.; de Nijs, L.; Baker, D.G.; Hauger, R.L.; van den Hove, D.; Kenis, G.; Nievergelt, C.M.; Boks, M.P.; Vermetten, E.; Gage, F.H.; et al. MicroRNAs in Post-traumatic Stress Disorder. In *Current Topics in Behavioral Neurosciences*; Springer, Berlin, Heidelberg, 2017; pp. 1–24.
54. Mercer, T.R.; Dinger, M.E.; Sunkin, S.M.; Mehler, M.F.; Mattick, J.S. Specific expression of long noncoding RNAs in the mouse brain. *Proc. Natl. Acad. Sci. U. S. A.* **2007**, *105*, 716–721, doi:10.1073/pnas.0706729105.
55. Quinn, J.J.; Chang, H.Y. Unique features of long non-coding RNA biogenesis and function. *Nat. Rev. Genet.* **2016**, *17*, 47–62, doi:10.1038/nrg.2015.10.
56. Kung, J.T.Y.; Colognori, D.; Lee, J.T. Long noncoding RNAs: Past, present, and future. *Genetics* **2013**, *193*, 651–669, doi:10.1534/genetics.112.146704.
57. Spadaro, P. a.; Flavell, C.R.; Widagdo, J.; Ratnu, V.S.; Troup, M.; Ragan, C.; Mattick, J.S.; Bredy, T.W. Long noncoding RNA-directed epigenetic regulation of gene expression is associated with anxiety-like behavior in mice. *Biol. Psychiatry* **2015**, *1*–12, doi:10.1016/j.biopsych.2015.02.004.
58. Aravin, A.A.; Sachidanandam, R.; Bourc’his, D.; Schaefer, C.; Pezic, D.; Toth, K.F.; Bestor, T.; Hannon, G.J. A piRNA pathway primed by individual transposons is linked to de novo DNA methylation in mice. *Mol. Cell* **2008**, *31*, 785–99, doi:10.1016/j.molcel.2008.09.003.
59. Rajan, K.S.; Ramasamy, S. Retrotransposons and piRNA: The missing link in central nervous system. *Neurochem. Int.* **2014**, doi:10.1016/j.neuint.2014.05.017.
60. Landry, C.D.; Kandel, E.R.; Rajasethupathy, P. New mechanisms in memory storage: piRNAs and epigenetics. *Trends Neurosci.* **2013**, *36*, 535–42, doi:10.1016/j.tins.2013.05.004.

61. Harcourt, E.M.; Ketrys, A.M.; Kool, E.T. Chemical and structural effects of base modifications in messenger RNA. *Nature* **2017**, *541*, 339–346, doi:10.1038/nature21351.
62. Basanta-Sanchez, M.; Temple, S.; Ansari, S.A.; D’Amico, A.; Agris, P.F. Attomole quantification and global profile of RNA modifications: Epitranscriptome of human neural stem cells. *Nucleic Acids Res.* **2015**, *44*, 1–10, doi:10.1093/nar/gkv971.
63. Lewis, C.J.T.; Pan, T.; Kalsotra, A. RNA modifications and structures cooperate to guide RNA–protein interactions. *Nat. Rev. Mol. Cell Biol.* **2017**, *18*, 202–210, doi:10.1038/nrm.2016.163.
64. Zhao, B.S.; Roundtree, I.A.; He, C. Post-transcriptional gene regulation by mRNA modifications. *Nat. Rev. Mol. Cell Biol.* **2016**, *18*, 31–42, doi:10.1038/nrm.2016.132.
65. Liu, N.; Pan, T. N6-methyladenosine?encoded epitranscriptomics. *Nat. Struct. Mol. Biol.* **2016**, *23*, 98–102, doi:10.1038/nsmb.3162.
66. Walters Mercaldo, V., Gillon, C.J., Yip, M., Neve, R.L., Boyce, F.M., Frankland, P.W., Josselyn, J.A., B.J. The Role of the RNA Demethylase FTO (Fat Mass and Obesity-Associated) and mRNA Methylation in Hippocampal Memory Formation. *Neuropsychopharmacology* **2017**, In Press, 1–9, doi:10.1038/npp.2017.31.
67. Ambrosi, C.; Manzo, M.; Baubec, T. Dynamics and Context-Dependent Roles of DNA Methylation. *J. Mol. Biol.* **2017**, *429*, 1459–1475, doi:10.1016/j.jmb.2017.02.008.
68. Burggren, W. Epigenetic Inheritance and Its Role in Evolutionary Biology: Re-Evaluation and New Perspectives. *Biology (Basel)*. **2016**, *5*, 24, doi:10.3390/biology5020024.
69. Ward, I.D.; Zucchi, F.C.R.; Robbins, J.C.; Falkenberg, E.A.; Olson, D.M.; Benzies, K.; Metz, G.A. Transgenerational programming of maternal behaviour by prenatal stress. *BMC Pregnancy Childbirth* **2013**, *13*, S9, doi:10.1186/1471-2393-13-S1-S9.
70. Weber-Stadlbauer, U.; Richetto, J.; Labouesse, M.A.; Bohacek, J.; Mansuy, I.M.; Meyer, U. Transgenerational transmission and modification of pathological traits induced by prenatal immune activation. *Mol. Psychiatry* **2017**, *22*, 102–112, doi:10.1038/mp.2016.41.
71. Scheiber, I.B.R.; Weiß, B.M.; Kingma, S.A.; Komdeur, J. The importance of the altricial – precocial spectrum for social complexity in mammals and birds – a review. *Front. Zool.* **2017**, *14*, 3, doi:10.1186/s12983-016-0185-6.
72. Babb, J.A.; Carini, L.M.; Spears, S.L.; Nephew, B.C. Transgenerational effects of social stress on social behavior, corticosterone, oxytocin, and prolactin in rats. *Horm. Behav.* **2014**, *65*, 386–393, doi:10.1016/j.yhbeh.2014.03.005.
73. Wu, R.; Zhang, H.; Xue, W.; Zou, Z.; Lu, C.; Xia, B.; Wang, W.; Chen, G. Transgenerational impairment of hippocampal Akt-mTOR signaling and behavioral deficits in the offspring of mice that experience postpartum depression-like illness . *Prog.Neuro-psychopharmacol.Biol.Psychiatry* **2016**, *73*, 11–18, doi:10.1016/j.pnpbp.2016.09.008.
74. Gapp, K.; Jawaid, A.; Sarkies, P.; Bohacek, J.; Pelczar, P.; Prados, J.; Farinelli, L.; Miska, E.; Mansuy, I.M. Implication of sperm RNAs in transgenerational inheritance of the effects of early trauma in mice. *Nat. Neurosci.* **2014**, *17*, 667–669, doi:10.1038/nn.3695.
75. Bohacek, J.; Farinelli, M.; Mirante, O.; Steiner, G.; Gapp, K.; Coiret, G.; Ebeling, M.; Durán-Pacheco, G.; Iniguez, A.L.; Manuella, F.; et al. Pathological brain plasticity and cognition in the offspring of males

- subjected to postnatal traumatic stress. *Mol. Psychiatry* **2015**, *20*, 621–631, doi:10.1038/mp.2014.80.
76. Razoux, F.; Russig, H.; Mueggler, T.; Baltes, C.; Dikaiou, K.; Rudin, M.; Mansuy, I.M. Transgenerational disruption of functional 5-HT1AR-induced connectivity in the adult mouse brain by traumatic stress in early life. *Mol. Psychiatry* **2017**, *22*, 519–526, doi:10.1038/mp.2016.146.
77. Saavedra-Rodríguez, L.; Feig, L.A. Chronic social instability induces anxiety and defective social interactions across generations. *Biol. Psychiatry* **2013**, *73*, 44–53, doi:10.1016/j.biopsych.2012.06.035.
78. Dietz, D.M.; Laplant, Q.; Watts, E.L.; Hodes, G.E.; Russo, S.J.; Feng, J.; Oosting, R.S.; Vialou, V.; Nestler, E.J. Paternal transmission of stress-induced pathologies. *Biol. Psychiatry* **2011**, *70*, 408–414, doi:10.1016/j.biopsych.2011.05.005.
79. Dias, B.G.; Ressler, K.J. Parental olfactory experience influences behavior and neural structure in subsequent generations. *Nat. Neurosci.* **2013**, *17*, 89–96, doi:10.1038/nn.3594.
80. Nätt, D. Stress and the Offspring: Adaptive Transgenerational Effects of Unpredictability on Behaviour and Gene Expression in Chickens (*Gallus gallus*). *Sci. Technol.* **2008**.
81. Goerlich, V.C.; Nätt, D.; Elfwing, M.; Macdonald, B.; Jensen, P. Transgenerational effects of early experience on behavioral, hormonal and gene expression responses to acute stress in the precocial chicken. *Horm. Behav.* **2012**, *61*, 711–718, doi:10.1016/j.yhbeh.2012.03.006.
82. Ericsson, M.; Henriksen, R.; Bélteky, J.; Sundman, A.-S.; Shionoya, K.; Jensen, P. Long-Term and Transgenerational Effects of Stress Experienced during Different Life Phases in Chickens (*Gallus gallus*). *PLoS One* **2016**, *11*, e0153879, doi:10.1371/journal.pone.0153879.
83. McCormick, G.L.; Robbins, T.R.; Cavigelli, S.A.; Langkilde, T. Ancestry trumps experience: Transgenerational but not early life stress affects the adult physiological stress response. *Horm. Behav.* **2017**, *87*, 115–121, doi:10.1016/j.yhbeh.2016.11.010.
84. Infurna, M.R.; Fuchs, A.; Fischer-Waldschmidt, G.; Reichl, C.; Holz, B.; Resch, F.; Brunner, R.; Kaess, M. Parents' childhood experiences of bonding and parental psychopathology predict borderline personality disorder during adolescence in offspring. *Psychiatry Res.* **2016**, *246*, 373–378, doi:10.1016/j.psychres.2016.10.013.
85. Vågerö, D.; Rajaleid, K. Does childhood trauma influence offspring's birth characteristics? *Int. J. Epidemiol.* **2017**, *46*, 219–229, doi:10.1093/ije/dyw048.
86. Barocas, Harvey A.; Barocas, C.B. Wounds of the Fathers: The Next Generation of Holocaust Victims. *Int. Rev. Psychoanal.* **1979**, *6*, 331–340.
87. Yehuda, R.; Daskalakis, N.P.; Bierer, L.M.; Bader, H.N.; Klengel, T.; Holsboer, F.; Binder, E.B. Holocaust Exposure Induced Intergenerational Effects on FKBP5 Methylation. *Biol. Psychiatry* **2016**, *80*, 372–380, doi:10.1016/j.biopsych.2015.08.005.
88. Yehuda, R.; Schmeidler, J.; Giller, E.L.; Siever, L.J.; Binder-Brynes, K. Relationship between posttraumatic stress disorder characteristics of holocaust survivors and their adult offspring. *Am. J. Psychiatry* **1998**, *155*, 841–843, doi:10.1176/ajp.155.6.841.
89. Yehuda, R.; Bell, A.; Bierer, L.M.; Schmeidler, J. Maternal, not paternal, PTSD is related to increased risk for PTSD in offspring of Holocaust survivors. *J. Psychiatr. Res.* **2008**, *42*, 1104–1111, doi:10.1016/j.jpsychires.2008.01.002.
90. Yehuda, R.; Bierer, L.M.; Schmeidler, J.; Aferiat, D.H.; Breslau, I.; Dolan, S. Low cortisol and risk for

- PTSD in adult offspring of Holocaust survivors. *Am. J. Psychiatry* **2000**, *157*, 1252–1259, doi:10.1176/appi.ajp.157.8.1252.
91. Field, N.P.; Muong, S.; Sochanvimean, V. Parental Styles in the Intergenerational Transmission of Trauma Stemming From the Khmer Rouge Regime in Cambodia. *Am. J. Orthopsychiatry* **2013**, *83*, 483–494, doi:10.1111/ajop.12057.
92. Rieder, H.; Elbert, T. The relationship between organized violence, family violence and mental health: findings from a community-based survey in Muhanga, Southern Rwanda. *Eur. J. Psychotraumatol.* **2013**, *4*, 21329, doi:10.3402/ejpt.v4i0.21329.
93. Wittekind, C.E.; Jelinek, L.; Kellner, M.; Moritz, S.; Muhtz, C. Intergenerational transmission of biased information processing in posttraumatic stress disorder (PTSD) following displacement after World War II. *J. Anxiety Disord.* **2010**, *24*, 953–957, doi:10.1016/j.janxdis.2010.06.023.
94. Phipps, R.M.; Degges-White, S. A new look at transgenerational trauma transmission: Second-generation latino immigrant youth. *J. Multicult. Couns. Devel.* **2014**, *42*, 174–187, doi:10.1002/j.2161-1912.2014.00053.x.
95. Daud, A.; Skoglund, E.; Rydelius, P.-A. Children in families of torture victims: transgenerational transmission of parents' traumatic experiences to their children. *Int. J. Soc. Welf.* **2005**, *14*, 23–32, doi:10.1111/j.1468-2397.2005.00336.x.
96. Rosenheck, R. Impact of Posttraumatic Stress Disorder of World War II on the Next Generation. *J. Nerv. Ment. Dis.* **1986**, *174*, 319–327.
97. Glenn, D.M.; Beckham, J.C.; Feldman, M.E.; Kirby, A.C.; Hertzberg, M.A.; Moore, S.D. Violence and hostility among families of Vietnam veterans with combat-related posttraumatic stress disorder. *Violence Vict.* **2002**, *17*, 473–489, doi:10.1891/vivi.17.4.473.33685.
98. Klaric, M.; Franciskovic, T.; Klaric, B.; Kvesic, A.; Kastelan, A.; Graovac, M.; Lisica, I.D.; M., K.; T., F.; B., K.; et al. Psychological problems in children of war veterans with posttraumatic stress disorder in Bosnia and Herzegovina: Cross-sectional study. *Croat. Med. J.* **2008**, *49*, 491–498, doi:10.3325/cmj.2008.4.491.
99. Grizelj, R.; Bojanić, K.; Vuković, J.; Novak, M.; Rodin, U.; Čorić, T.; Stanojević, M.; Schroeder, D.R.; Weingarten, T.N.; Sprung, J.; et al. Epidemiology and Outcomes of Congenital Diaphragmatic Hernia in Croatia: A Population-Based Study. *Paediatr. Perinat. Epidemiol.* **2016**, *30*, 336–45, doi:10.1111/ppe.12289.
100. Santavirta, T.; Santavirta, N.; Gilman, S.E. Association of the World War II Finnish Evacuation of Children With Psychiatric Hospitalization in the Next Generation. *JAMA Psychiatry* **2018**, *75*, 21, doi:10.1001/jamapsychiatry.2017.3511.
101. Ciabrelli, F.; Comoglio, F.; Fellous, S.; Bonev, B.; Ninova, M.; Szabo, Q.; Xu?reb, A.; Klopp, C.; Aravin, A.; Paro, R.; et al. Stable Polycomb-dependent transgenerational inheritance of chromatin states in Drosophila. *Nat. Genet.* **2017**, *49*, 876–886, doi:10.1038/ng.3848.
102. Gaydos, L.J.; Wang, W.; Strome, S. H3K27me and PRC2 transmit a memory of repression across generations and during development. *Science (80-.).* **2014**, *345*, 1515–1518, doi:10.1126/science.1255023.
103. Rodgers, A.B.; Morgan, C.P.; Leu, N.A.; Bale, T.L. Transgenerational epigenetic programming via sperm

- microRNA recapitulates effects of paternal stress. *Proc. Natl. Acad. Sci.* **2015**, *112*, 13699–13704, doi:10.1073/pnas.1508347112.
104. Short, A.K.; Yeshurun, S.; Powell, R.; Perreau, V.M.; Fox, A.; Kim, J.H.; Pang, T.Y.; Hannan, A.J. Exercise alters mouse sperm small noncoding RNAs and induces a transgenerational modification of male offspring conditioned fear and anxiety. *Transl. Psychiatry* **2017**, *7*, e1114, doi:10.1038/tp.2017.82.
105. Adeoya-Osiguwa, S.A.; Gibbons, R.; Fraser, L.R. Identification of functional alpha2- and beta-adrenergic receptors in mammalian spermatozoa. *Hum. Reprod.* **2006**, *21*, 1555–1563, doi:10.1093/humrep/del016.
106. Fiore, C.; Sticchi, D.; Pellati, D.; Forzan, S.; Bonanni, G.; Bertoldo, A.; Massironi, M.; Calo, L.; Fassina, A.; Rossi, G.P.; et al. Identification of the mineralocorticoid receptor in human spermatozoa. *Int. J. Mol. Med.* **2006**, *18*, 649–652.
107. Naz, R.K. Receptors in Spermatozoa: Are They Real? *J. Androl.* **2006**, *27*, 627–636, doi:10.2164/jandrol.106.000620.
108. Kwon, W.-S.; Park, Y.-J.; Kim, Y.-H.; You, Y.-A.; Kim, I.C.; Pang, M.-G. Vasopressin effectively suppresses male fertility. *PLoS One* **2013**, *8*, e54192, doi:10.1371/journal.pone.0054192.
109. Short, A.K.; Fennell, K.A.; Perreau, V.M.; Fox, A.; O'Bryan, M.K.; Kim, J.H.; Bredy, T.W.; Pang, T.Y.; Hannan, A.J. Elevated paternal glucocorticoid exposure alters the small noncoding RNA profile in sperm and modifies anxiety and depressive phenotypes in the offspring. *Transl. Psychiatry* **2016**, *6*, e837, doi:10.1038/tp.2016.109.
110. Pan, W.; Stone, K.P.; Hsueh, H.; Manda, V.K.; Zhang, Y.; Kastin, A.J. Cytokine signaling modulates blood-brain barrier function. *Curr. Pharm. Des.* **2011**, *17*, 3729–40.
111. Sullivan, R.; Saez, F.; Girouard, J.; Frenette, G. Role of exosomes in sperm maturation during the transit along the male reproductive tract. *Blood Cells, Mol. Dis.* **2005**, *35*, 1–10, doi:10.1016/j.bcmd.2005.03.005.
112. Marré, J.; Traver, E.C.; Jose, A.M. Extracellular RNA is transported from one generation to the next in *Caenorhabditis elegans*. *Proc. Natl. Acad. Sci.* **2016**, *113*, 12496–12501, doi:10.1073/pnas.1608959113.
113. Otero, J.J.; Fu, W.; Kan, L.; Cuadra, A.E.; Kessler, J.A. Beta-catenin signaling is required for neural differentiation of embryonic stem cells. *Development* **2004**, *131*, 3545–3557, doi:10.1242/dev.01218.
114. Denis, H.; Ndlovu, M.N.; Fuks, F. Regulation of mammalian DNA methyltransferases: a route to new mechanisms. *EMBO Rep.* **2011**, *12*, 647–656, doi:10.1038/embor.2011.110.
115. Cheng, T.L.; Wang, Z.; Liao, Q.; Zhu, Y.; Zhou, W.H.; Xu, W.; Qiu, Z. MeCP2 Suppresses Nuclear MicroRNA Processing and Dendritic Growth by Regulating the DGCR8/Drosha Complex. *Dev. Cell* **2014**, *28*, 547–560, doi:10.1016/j.devcel.2014.01.032.
116. Skinner, M.K.; Guerrero-Bosagna, C.; Haque, M.M. Environmentally induced epigenetic transgenerational inheritance of sperm epimutations promote genetic mutations. *Epigenetics* **2015**, *10*, 762–771, doi:10.1080/15592294.2015.1062207.
117. Gapp, K.; Bohacek, J.; Grossmann, J.; Brunner, A.M.; Manuella, F.; Nanni, P.; Mansuy, I.M. Potential of Environmental Enrichment to Prevent Transgenerational Effects of Paternal Trauma. *Neuropsychopharmacology* **2016**, *41*, 2749–2758, doi:10.1038/npp.2016.87.
118. Arai, J.A.; Li, S.; Hartley, D.M.; Feig, L.A. Transgenerational Rescue of a Genetic Defect in Long-Term Potentiation and Memory Formation by Juvenile Enrichment. *J. Neurosci.* **2009**, *29*, 1496–1502,

- doi:10.1523/JNEUROSCI.5057-08.2009.
- 119. Dezsi, G.; Ozturk, E.; Salzberg, M.R.; Morris, M.; O'Brien, T.J.; Jones, N.C. Environmental enrichment imparts disease-modifying and transgenerational effects on genetically-determined epilepsy and anxiety. *Neurobiol. Dis.* **2016**, *93*, 129–136, doi:10.1016/j.nbd.2016.05.005.
 - 120. Murgatroyd, C.A.; Hicks-Nelson, A.; Fink, A.; Beamer, G.; Gurel, K.; Elnady, F.; Pittet, F.; Nephew, B.C. Effects of Chronic Social Stress and Maternal Intranasal Oxytocin and Vasopressin on Offspring Interferon- γ and Behavior. *Front. Endocrinol. (Lausanne)*. **2016**, *7*, 155, doi:10.3389/fendo.2016.00155.
 - 121. Sharma, A. Transgenerational epigenetic inheritance: Resolving uncertainty and evolving biology. *Biomol. Concepts* **2015**, *6*, 87–103.
 - 122. Kun, Á.; Szilágyi, A.; Könnyu, B.; Boza, G.; Zachar, I.; Szathmáry, E. The dynamics of the RNA world: Insights and challenges. *Ann. N. Y. Acad. Sci.* **2015**, *1341*, 75–95, doi:10.1111/nyas.12700.
 - 123. Horn, S.R.; Charney, D.S.; Feder, A. Understanding resilience: New approaches for preventing and treating PTSD. *Exp. Neurol.* **2016**, *284*, 119–132.
 - 124. Sander, J.D.; Joung, J.K. CRISPR-Cas systems for editing, regulating and targeting genomes. *Nat. Biotechnol.* **2014**, *32*, 347–355, doi:10.1038/nbt.2842.

Brief Communication

2. OmniSperm: Multiomic analyses of sperm and offspring production from a single male

This article is in preparation.

Martin Roszkowski conducted animal experiments, performed molecular analyses, interpreted sequencing data and wrote the article.

2.1. Abstract

Multiomics analyses provide essential information about cells and tissues. Their application to gametes remains however limited. We introduce a strategy called OmniSperm for parallel analyses of epigenome and transcriptome, and offspring generation from sperm of single males. We provide proof-of-principle that sperm signatures and their relation to the direct progeny can be profiled in normal and pathological conditions. This provides a novel tool for studies in reproductive biology and epigenetic inheritance.

2.2. Introduction, results and discussion

Recent research in animal models have shown that features induced by environmental factors or life experiences manifested by an exposed parent can be transmitted to the offspring [1,2]. Evidence has accumulated that such transmission can involve the germline and be associated with changes in the epigenome and transcriptome in germ cells [3,4]. While changes in DNA methylation and RNA level have been reported in sperm of exposed males, a direct link with their effects in the offspring generated from that exact sperm has not been provided yet. Obtaining such link is challenging because it requires to analyse the sperm epigenome and/or transcriptome of an exposed male, and generate an offspring from the same sperm for further analyses [5].

Multiomics methods allow to assess multiple molecular features in a given tissue or cell type. They have been extensively used to simultaneously profile the epigenome and transcriptome of somatic cells but their application to germ cells, in particular sperm, has been limited. This is because DNA and RNA is difficult to extract from sperm due to sperm exceptional lysis resistance, particularly in mouse, but also due to its highly condensed haploid chromatin [6] and its low RNA content [7]. Further, sperm itself is rather scarce in mice and can usually be collected only with low yield. Classical swim-up methods select for highly motile sperm cells which represent only a fraction of total sperm. To date, studies on sperm have therefore focused only on one type of epigenetic factor at a time and used pooled sperm from several animals, preventing any direct correlation with the donor male.

We developed a strategy called OmniSperm that integrates optimized methods for sperm collection, DNA/RNA extraction and multiomic analyses, together with artificial insemination to simultaneously profile the sperm epigenome and transcriptome and produce

an offspring in mice [8]. The first step of the strategy was to optimize sperm yield from individual adult male mice. For this, we used a cell strainer to extract sperm from dissected epididymis and vas deferens (Fig. 1a,b). 30 to 45 million sperm cells per male could be yielded, which is $587 \pm 17\%$ and $173 \pm 18\%$ more than classical simple and repeated swim-up method respectively (Fig. 1c). Sperm purity and integrity were confirmed by imaging flow cytometry (Fig. 1d and Supplementary Figure 1) and scanning electron microscopy (Fig. 1e), which showed few non-gametic cells in the initial filtrate but structurally intact sperm cells.

Extracellular vesicles such as epididymosomes have recently been suggested to be sensitive to environmental exposures and able to pass altered cargo to sperm [9]. We collected epididymosomes from the sperm supernatant by a series of centrifugation and ultracentrifugation steps (Fig. 1a). They were characterized by electron microscopy and showed intact epididymosomes and microvesicles (Fig. 1f). Subsequently, we measured the size and concentration by nanoparticle tracking analysis and observed a majority of epididymosomes in the size range from 100 to 350 nm (Supplementary Fig. 2a). Lastly, we confirmed the presence of the epididymosome surface marker *Cd9* in samples prepared by gradient ultracentrifugation (Supplementary Fig. 2b).

30 million sperm cells were used to prepare DNA and RNA. Sperm was treated with lysis buffer to eliminate somatic cells, then lysed in 200 μ l Buffer RLT+ supplemented with TCEP to achieve full lysis of sperm heads. 50 μ l of lysate was used for DNA extraction with DNeasy purification columns and yielded 5 to 15 μ g of high-quality DNA with DNA integrity values between 7 and 9 (Supplementary Fig. 3a). Bisulfite converted DNA was used for whole genome bisulfite sequencing and the data were used to examine the DNA methylation levels of imprinted genes. Such genes are known to be either fully methylated or unmethylated depending on their parental origin [10]. We observed a clear separation in fully methylated paternal imprinted genes and fully demethylated maternal genes (Fig. 1g). Next, sperm RNA was prepared from 100 μ l of lysate by purification using standard Trizol protocol (Supplementary Fig. 3b). RNA was enriched in fragments longer than 200 nucleotides ($DV_{200} = 50 - 70\%$) and was lacking 18S and 28S ribosomal RNAs (rRNA) (Supplementary Fig. 4a), indicating good RNA integrity and no detectable contamination by somatic cells. In contrast, somatic cell samples have longer and intact RNAs, and rRNA peaks are abundant (Supplementary Fig. 4b). Libraries were prepared with SMARTer stranded RNA-seq kit and total RNA sequenced on Illumina HiSeq4000. Notably, the high RNA yield allowed us to

minimize PCR cycles for libraries preparation resulting in low duplication rates (Supplementary Fig. 5a). Comparative analyses with testis and brain transcriptomic data from adult mouse males confirmed that sperm-specific transcripts such as *Prm1*, *Prm2*, *Slfnl1*, *Gapdhs* and *Oxct2a* were expressed in the samples but no lymphocyte marker like *Cd34*, stem cell marker *Kit* or leukocyte marker *Cd47*. Testicular and epididymal isoforms of sperm adhesion molecule 1 (*Spam1*) could also not be detected indicating the absence of immature spermatids (Fig. 1g and Supplementary Fig. 5b). Ubiquitous genes like *Actb* could also be detected.

Further to DNA/RNA preparation, sperm was also used for artificial insemination (AI) to generate embryos [8]. AI was chosen over in vitro fertilization (IVF) or intracytoplasmic sperm injection (ICSI) because it is less intrusive, does not require hormonal treatment and is easy to establish. 6 million sperm cells were used to inseminate 3 females in parallel. After 48 hours, AI dams were sacrificed and 4- to 8-cell embryos collected from their oviducts. Embryos stages and integrity were assessed by light microscopy and then collected for single cell sequencing in 4 µl of Buffer RLT+. The stage of development of each collected embryo was determined by microscopy, then embryos were freed from attached cells, and transferred in lysis buffer (Supplementary Fig. 6a). DNA and polyA⁺ RNA were first separated by magnetic bead separation, and cDNA prepared according to smart-seq2 for single-embryo sequencing (Supplementary Fig. 6b) [11]. In summary, OmniSperm allows high sperm yield from individual mouse males for parallel DNA and RNA preparation and molecular analyses, and for the generation of offspring.

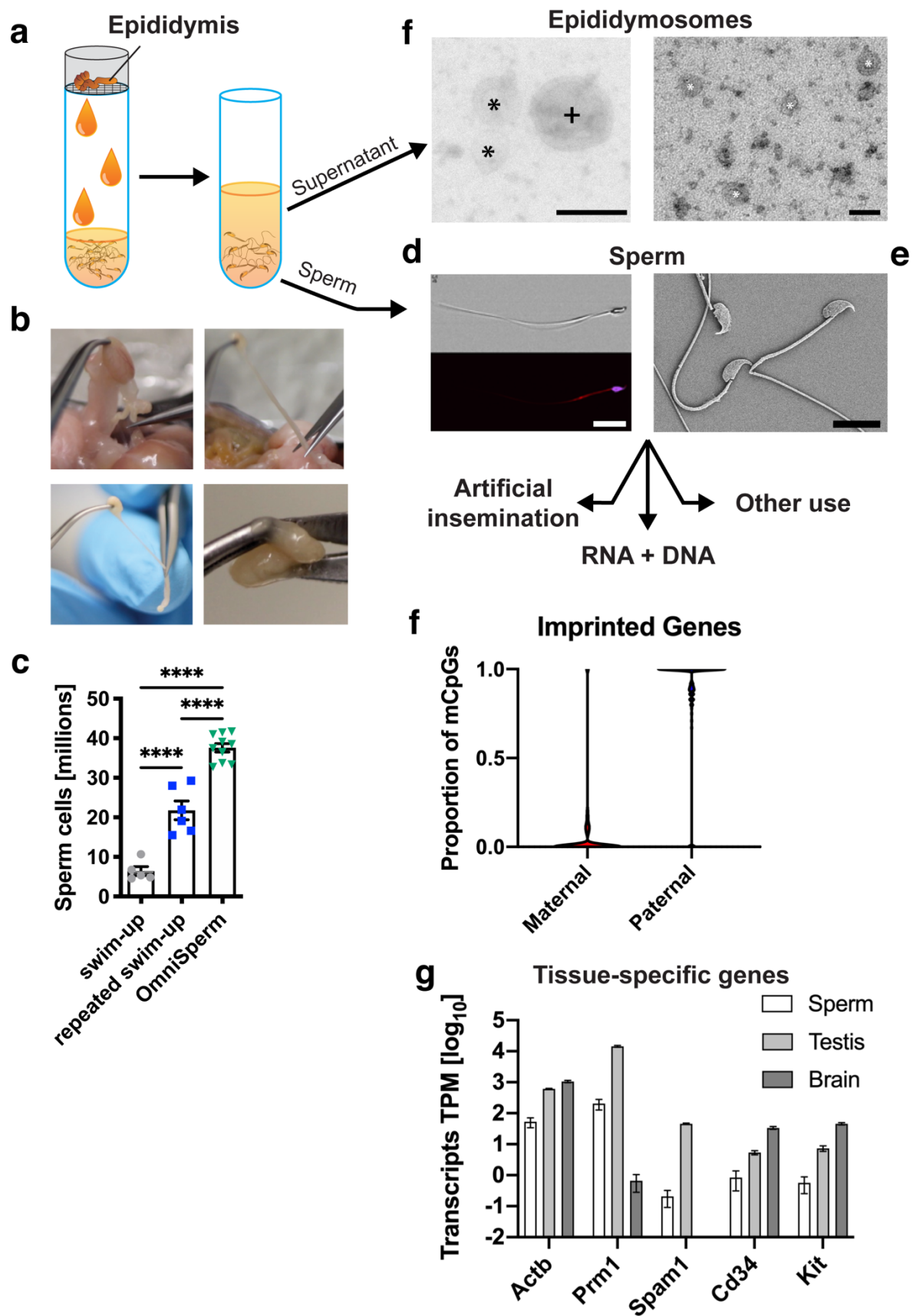


Figure 1: Strategy for RNA and DNA analyses and offspring generation from the sperm of a single male **(a,b)** Cauda epididymis is sliced, placed on a cell strainer and washed with M2

medium to extract sperm, followed by centrifugation for the separation of the sperm pellet from the epididymosome containing supernatant. **(c)** OmniSperm yielded on average 40 million sperm cells from a single mouse, recovering significantly more sperm than by swim-up or repeated swim-up (5 times). **(d)** Crude sperm samples stained for DNA (blue) and mitochondria (red) were analyzed by imaging flow cytometry and quantified by their brightfield and fluorescence properties. Scale bar = 50 μ m. **(e)** Electron micrograph of sperm cells. Scale bar = 20 μ m. **(f)** Transmission electron micrographs of epididymosomes* and microvesicles⁺. Scale bars = 100 nm. **(g,h)** To assess purity, RNA and DNA were extracted from sperm for transcriptome and methylome sequencing. **(f)** Assessment of imprinted genes in sperm ($n = 20$). **(g)** Normalized tissue-specific gene expression in sperm, testis and brain samples in transcripts per million ($n = 5$). Data are represented as mean \pm standard error of mean (SEM). **** adj. p-value < 0.0001.

To demonstrate the potential of OmniSperm, we tested it on a mouse model of postnatal stress (MSUS, Supplementary Fig. 7) known to have altered epigenome and transcriptome, and behavioral and metabolic symptoms transmitted across generations in a sperm-dependent manner [12–14]. We profiled the sperm methylome and transcriptome of exposed males when adult by WGBS and RNA-seq and conducted comparative analyses. We identified differentially methylated loci (DML) near the transcription start site (TSS) of 18 genes with various functions in spermatogenesis (*Syne3*), spermatogonia regulation (*Utf1*), development (*Myom2*), RNA processing (*Rn45s*) and neuronal function (*Spock3*) (Fig. 2b). We also identified multiple dysregulated genes (Fig. 2a and Supplementary Fig. 8). Some genes with high expression had fully methylated TSS (Fig. 2c), consistent with previous observation. Closer examination revealed that genes with fully methylated TSS have an expression profile distinct from preceding spermatogenic stages, suggesting selective retention or expulsion of RNAs from spermatogenic cells during spermatogenesis (Supplementary Fig. 9). We screened for significant DML at TSS of genes with altered gene expression, and identified loci with TF binding sites for known global and germ-line specific regulatory functions such as CREB1, KLF4, CUX1 or EGR1 (Supplementary Fig. 10). Due to chromatin looping, methylation-dependent gene regulatory elements can be distal from the affected gene body. However, we did not identify any statistically significant distal DML that correlated with altered sperm transcripts (Supplementary Fig. 11).

To assess the consequences of an altered sperm methylome and transcriptome in the offspring, we used AI to produce embryos from the same sperm samples used for WGBS and RNA-seq. 4- to 8-cell stage embryos were sequenced by parallel single cell genome and transcriptome sequencing (G&T-seq) revealing sex-specific transcriptomes (Fig. 2d) but also MSUS induced gene expression changes (Fig. 2e). However, we also found differentially expressed genes in sibling embryos, indicating that fathers are a biological source of variance of the embryos' transcriptome (Supplementary Fig. 12). Such inter-sperm differences in the epigenome or possibly the genomic sequence with sperm-specific SNPs or SNVs have previously been observed in human [15,16].

To investigate a potential paternal epigenomic contribution to embryo gene expression, we examined if the observed MSUS embryonic gene expression changes were potentially influenced by methylation dependent changes at genomic locations with known regulatory functions such as binding sites for transcription factors which are crucial for driving gene expression. By estimating TF activity in the sperm methylome and embryo transcriptome, we identified the circadian TF *Clock*, and trans-acting transcription factors (*Sp*) 1, 2 and 3 as potential drivers of embryonic transcription change (Fig. 2f). *Sp1*, *Sp2* and *Sp3* are important mediators of selective gene activation in spermatogenesis [17,18] and were shown to be essential for mouse development [19]. Notably, they have distinct chromatin binding mechanism and are located on different chromosomes, suggesting a coordinated epigenetic regulation between paternal germ-line and developing embryo [19].

In summary, OmniSperm increases the available starting amount of sperm cells, DNAs and RNAs for multiple types of parallel analyses from the same male. Procedures were simplified to be easily implemented without specialized equipment or expertise in reproductive biology. Furthermore, the extended collection of spermatozoa may also improve research in mouse models of impaired sperm motility and morphology. Importantly, OmniSperm reduced non-epigenetic confounders and substantially reduce the number of animals used, and will enable studies of epigenetic inheritance to utilize multiple types of omics. Thus, we expect that widespread application of OmniSperm to future inheritance studies will help elucidate the role of DNA methylation, RNAs and other epigenetic marks without the need to pool multiple sperm samples. The approach is amenable to additional sperm selection or purification steps, and other experimental needs such as sperm cryopreservation and chromatin accessibility techniques.

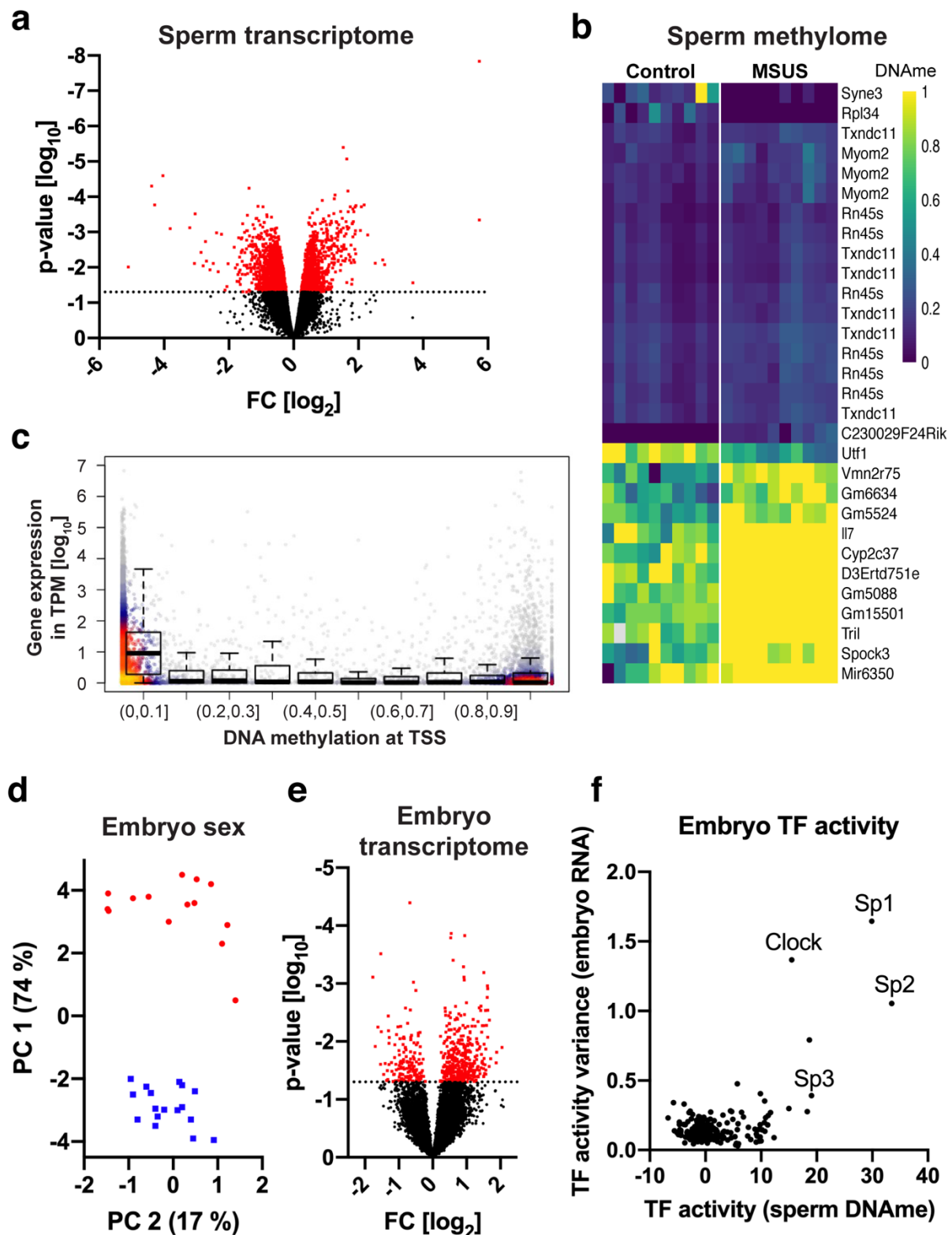


Figure 2: Correlation between epigenetic changes in sperm and consequences for embryo transcriptome. **(a)** Volcano-plot of MSUS-induced transcriptome changes in sperm. ($n = 10$ per group) **(b)** Heatmap of DML in sperm of control and MSUS. Here shown the top 30 altered CpGs at TSS, some genes with multiple CpGs. **(c)** 2D density plot was overlaid with boxplots

of normalized gene expression in sperm compared to the DNA methylation at the corresponding TSS. (n = 20) **(d)** Principle component analysis of embryo gene expression using known sex-linked genes (*Uty*, *Eif2s3y*, *Sry*, *Xist*). 2 distinct clusters emerged indicating an equal distribution of male and female embryos. **(e)** Volcano-plot of MSUS-induced transcriptome changes in embryos. **(f)** TF activity was assessed from TF-binding sites in altered embryo transcriptomes and compared to estimation of corresponding TF activity based on known binding sites in the genome. Negative values indicate a repressed and positive values an increased TF activity because of altered DNA methylation. Dotted lines indicate a p-value of 0.05.

2.3. Materials and Methods

2.3.1. Animals

Animal experiments were conducted in strict adherence to the Swiss Law for Animal Protection and were approved by the cantonal veterinary office in Zürich under license number 57/2015 and 83/2018. C57Bl/6J mice were obtained from Janvier (France) and bred in-house to generate mice for experiments. Mice were housed in groups of 3 to 5 animals in individually ventilated cages. Animals were kept in a temperature- and humidity-controlled facility on a 12h reversed light/dark cycle (light on at 20:00, off at 8:00) with food (M/R Haltung Extrudat, Provimi Kliba SA, Switzerland) and water *ad libitum*. Cages were changed once per week.

2.3.2. Model of postnatal trauma

The unpredictable maternal separation combined with unpredictable maternal stress (MSUS) paradigm was conducted as previously described [12] (Supplementary Fig. 7). In brief, 2-3 month old C57Bl/6J naïve dams were mated with naïve males for 1 week. Mothers were assigned to the control or MSUS group based on the number of male pups born on that day to balance the groups. During MSUS, the pups are separated unpredictably from their mother 3 hours per day from PND1 until PND14 during the active phase. During separation, mothers are subjected to forced swim in cold water (18 °C for 5 min) or restraint in a plastic tube (20 min) at an unpredictable time during the 3h of separation. Control pups were left undisturbed except for weekly cage changes and weight measurements. Pups were weaned at PND21 and assigned to sex and treatment matched cages (4 to 5 mice) between PND22 and PND28 with no co-assignment of siblings to avoid litter effects.

2.3.3. Sperm collection

The intraperitoneal cavity of adult males was cut open with scissors from the sternum to the penis. Cauda epididymis and vas deferens were freed from adipose and connective tissue. The epididymal luminal fluid was extruded from vas deferens with a pair of fine forceps and deposited on cauda epididymis. The empty vas deferens was then cut off and removed. The cauda epididymis was sliced with 20 cuts and placed in 1 ml of M2 medium (Sigma, M7167) in a 2 ml Eppendorf tube and placed at 37 °C for 15 minutes. The tube was gently flicked to detach the tissue from the tube wall and the whole content immediately poured on a 70 µm cell strainer (Falcon, 352350) on top of a 50 ml Falcon tube to allow filtrate collection. The tissue on the nylon mesh was gently rinsed with warm M2 medium using a 1000 µl pipette for a total of 14 ml M2 medium. The filtrate was transferred to a 15 ml conical Falcon tube and the remaining cauda epididymis was snap-frozen for further analysis. The filtrate was centrifuged in a pre-warmed centrifuge at 600 rcf for 5min. The supernatant was transferred to a fresh 15 ml Falcon tube for extracellular vesicles extraction. The sperm pellet was left in 400 µl M2 (a smaller volume can be chosen here to increase sperm concentration) and gently resuspended with a wide-bore pipette tip to minimize shearing and sperm cells damage. An aliquot should be used at this stage to determine sperm concentration and visually confirm that spermatozoa are still motile and not damaged before artificial insemination. The spermatozoa should be kept at 35-37 °C throughout the procedure and processed within one hour for artificial insemination.

2.3.4. Somatic cell lysis treatment and sperm lysis

Sperm were mixed to ensure a homogenous dispersion and 1 ml of cold somatic cell lysis buffer (99 ml MilliQ H₂O, 1 ml of 10 % SDS, 500 µl of Triton X-100) was added. The tube was briefly flicked to mix the solution and incubated at 4 °C for 10 min. Sperm cells were centrifuged at 2'000 rcf for 5 min in 4 °C. The supernatant was discarded and the cell pellet resuspended in 1 ml of 1X PBS pH 7.4 (GIBCO 10010015), centrifuged again then washed a 2 time with PBS. The supernatant was discarded and the sperm pellet snap-frozen for storage at -80 °C.

Sperm was lysed in 200 µl lysis buffer (190 µl Buffer RLT+ (Qiagen, 1053393) and 10 µl 0.5 M TCEP (Sigma, 646547)). The lysate was homogenized for 2 min at 20 Hz using a 0.5 mm stainless steel bead and a TissueLyser II (Qiagen, 85300) then incubated for 5 min at room temperature. Complete lysis of sperm heads was confirmed by microscopy.

2.3.5. DNA extraction

50 µl of sperm lysate was used for DNA extraction with the DNeasy Blood & Tissue Kit (Qiagen, 69506) according to the manufacturer instructions. RNA was separated with an on-column Proteinase K treatment. DNA concentration was determined using a NanoDrop 2000 (Thermofisher). DNA integrity was analysed on a 2200 TapeStation (Agilent) with the Genomic DNA ScreenTape analysis according to manufacturer instructions.

2.3.6. RNA extraction

For 100 µl of sperm lysate were mixed with 1ml Trizol (Life Technologies, 15596026) and RNA prepared according to the standard RNA extraction protocol. All steps were performed at 4 °C. RNA concentration and integrity were analysed on a 2100 Bioanalyzer (Agilent) with a RNA 6000 Pico Kit (Agilent) according to manufacturer instructions. DV₂₀₀ RNA Pico assay was installed on a 2100 Expert Software according to manufacturer instructions for DV₂₀₀ determination for FFPE RNA samples.

2.3.7. Whole genome bisulfite sequencing

Libraries for whole genome bisulfite sequencing were prepared using 100 ng genomic DNA using Ovation UltraLow Methyl-seq DR Multiplex System (NuGen) according to manufacturer recommendation. In brief, DNA was fragmented into 200bp fragments by ultrasonication, followed by purification with Agencourt beads into 14 µl nuclease-free water. End-repair reaction was performed in a preheated thermal cycler by incubating the fragmented DNA at 25 °C for 30 min followed by 10 min at 70 °C. Methylated adaptors were ligated by incubating in a preheated thermal cycler at 25 °C for 30 min followed by 10 min at 70 °C. Post-ligation purification was performed using the Agencourt beads as previously, then samples were eluted in 16 µl of nuclease-free water. Another repair reaction was conducted for 10 min at 60 °C then DNA was subjected to bisulfite conversion by..... Following purification of bisulfite-converted DNA, the optimal number of PCR amplification cycles was determined with a qPCR assay. Linear Rn versus cycle number was plotted and the cycle number corresponding to 1/2 of the maximum fluorescent intensity was calculated and used for PCR amplification. Libraries were purified using the Agencourt RNA Clean XP beads and eluted in 20 µl nuclease-free water. Libraries quality and quantity were assessed using the Bioanalyzer 2100 (Agilent Technologies) on DNA 1000 Chips. Profiles typically displayed a peak around

300 bp, corresponding to 150-200 bp inserts. Paired-end sequencing was performed on an Illumina HiSeq 2500. Reads were trimmed with TrimGalore (-q 30, -l 30) and mapped with Bismark using Bowtie2 to the mm10 reference genome. CpG methylation was assessed using bismark_methylation_extractor and used for further analysis with custom scripts and R packages.

2.3.8. Sperm RNA sequencing

Total RNA libraries were generated starting from 1 ng of DNase treated (AM1906, Invitrogen) sperm RNA using SMARTer Stranded Total RNA-seq Kit v2 – Pico Input Mammalian (Takara Bio) according to manufacturer instructions. In brief, RNA was fragmented in first strand buffer at 94 °C for 90 s. After addition of template switching oligo and reverse transcriptase, samples were incubated at 42 °C for 90 min. Unique Dual Illumina Indexes were added in 5 PCR cycles. Libraries were purified with AMPure XP beads (Beckman Coulter) and rRNAs depleted with ZapR v2 at 37 °C for 60 min. Final libraries were PCR amplified in 12 cycles and purified with AMPure beads. Libraries were quantified with Qubit dsDNA HS kit and profiles assessed using Agilent High Sensitivity DNA Kit. Sequencing was performed on an Illumina HiSeq 4000. Reads were trimmed with TrimGalore (-q 30, -l 30) and quantified using Salmon (--seqBias, --posBias, --gcBias, --dumpEq, --numBootstraps 30). Differential gene expression was assessed using the R-packages edgeR, Limma/voom. Duplicates were marked with Picard Tools and analyzed by dupRadar.

2.3.9. Embryo RNA sequencing

Embryo RNA-seq libraries were generated using G&T-Seq and smart-seq2 protocols [11,20]. In brief, individual embryos were lysed in Buffer RLT+ and gDNA separated from polyA-RNA using magnetic beads (Invitrogen) labeled with dT30VN (MicroSynth). After washing, cDNA was reverse transcribed by Superscript II (Life Technologies) and template switching oligo (IDT) at 42 °C for 90 min and 10 cycles (50 °C for 2min, 42 °C for 2min). cDNA was PCR amplified (20 cycles) using KAPA HiFi HS (Roche) and purified using Ampure XP beads. cDNA library profiles were assessed using Agilent High Sensitivity DNA Kit. Sequencing was performed on the Illumina HiSeq 4000. Reads were trimmed with TrimGalore (-q 30, -l 30) and quantified using Salmon (--seqBias, --posBias, --gcBias, --dumpEq, --numBootstraps 30). Differential gene expression was assessed using the R-

packages edgeR, Limma/voom and dream. TF activity was assessed using the R-packages SETools, viper and TFBSTools.

2.3.10. Epididymosome collection and characterization

To remove cellular debris, the supernatant from sperm collection was subjected to a series of centrifugations of 2'000 rcf for 10 min and 10'000 rcf for 30 min. Supernatants were ultracentrifuged at 120'000 rcf at 4 °C for 2 h (TH 64.1 rotor, Thermo Fisher Scientific). The pellets were washed in PBS at 4 °C and again ultracentrifuged. The pellets were resuspended in 60 µl of PBS. For particle quantification, 10 µl was diluted to a 1:1000 concentration in filtered (0.22 µm) PBS. The number and size distribution of epididymosomes was measured on Nanosight NS300 (Malvern, UK) at 20 °C.

For immunoblot analysis, fractions were prepared. Iodoxanol (OptiPrep) density media (Sigma-Aldrich, St Louis, MO, USA) was used to prepare an OptiPrep gradient (40 %, 20 %, 10 %, 5 %) by diluting OptiPrep with 0.25 M sucrose, 10 mM Tris. The UC pellets resuspended in PBS were layered onto the OptiPrep gradient and ultracentrifuged at 100'000 rcf at 4 °C for 18 h. 12 fractions were collected from top to bottom, and each fraction was diluted with filtered cold PBS and subjected to 120'000 rcf ultracentrifugation for 2 h at 4 °C. The PBS-resuspended pellet was mixed with 10x RIPA (Cell Signaling Technology) and incubated for 5 min at 4 °C. Equal amount of protein was mixed with 4x Laemmli Sample Buffer (Bio-Rad Laboratories, USA) and samples were loaded on 4-20 % Tris-glycine polyacrylamide gels (Bio-Rad, CA, USA). Membranes were blocked in 5 % SureBlock (LubioScience GmbH, Zürich, Switzerland) in Tris-buffered saline with 0.05 % Tween-20 (Sigma-Aldrich, St Louis, MO, USA) for 2 h at room temperature and incubated with primary-antibodies overnight at 4 °C (anti-CD9 [1:3000; System Biosciences, Palo Alto, CA, USA], anti-GAPDH [1:5000; Cell Signaling, Davers, MA, USA; 14C10]). Next, membranes were washed 3 times in TBS-T, and incubated with a corresponding HRP-conjugated secondary antibody (anti-rabbit [1:10000; Santa-Cruz Biotechnology, cs2357], anti-mouse [1:10000; Upstate Biotechnology, 12-349]) for 2 h. WesternBright Sirius western blot detection kit (Advansta, Menlo Park, CA, USA) was used to visualize the signals, following analysis on ImageLab software (Bio-Rad, Hercules, CA, USA).

2.3.11. Artificial insemination

Artificial insemination was performed as previously[8] with slight modifications. To ensure that females ovulate, vaginal smears from acyclic virgin females were collected and oestrus stage assessed shortly before insemination. A 100 µl pipette was used to gently flush the opening of the vaginal canal with sterile PBS and collect the liquid on a glass slide. Only females with vaginal cytology characterized by cornified epithelial cells typical of oestrus were used for insemination. 30 µl of the sperm suspension was loaded into a 200 µl pipette tip (Biorad, 223-9915). Two in-house manufactured Teflon tubes of different size (small speculum: 13 mm; large speculum: 10 mm) were used as speculums to guide the pipette tip through the vagina and localize the cervix. Each female mouse was placed on an angled wire cage top and gently pulled up by the tail to expose the vaginal opening. The smaller speculum (inner diameter, 3.28–3.58 mm, wall 0.38 mm) was first inserted into the vagina until the cervix was reached (slight resistance is felt). The small speculum was then removed and the large speculum (inner diameter, 2.06–2.31 mm, wall 0.38 mm) inserted. The cervical opening was localized by gentle probing with the tip of the pipette, and once in place, the tip was inserted into the cervix for a total of 2 cm and the sperm suspension slowly injected. After removing the large speculum, a small cotton tampon moistened in 0.9 % saline solution was inserted into the vaginal opening to mimic the mating plug and replace the need of mating to a vasectomized male. All inseminations were performed under red light during the active phase of the mice. Between 3 and 5 female mice were inseminated with the sperm of one male.

2.3.12. Embryo collection

Four to eight-cell embryos were collected from the oviducts of inseminated females, 42 hours following mating. In brief, female mice were euthanized with 5 % isoflurane and the oviducts were dissected out and placed in 24-well plates in M2 media at 37 °C. The oviducts were flushed with M2 media by inserting a slightly bent hypodermic 30 G needle through the infundibulum. The procedures were carried out using a stereomicroscope equipped with reflected white light for better visualization of the infundibulum opening. Individual embryos were assessed by light microscopy for cell stage and morphological integrity. Intact 4- to 8-cell embryos were freed from any attached cells, transferred in 4 µl of Buffer RLT+ and frozen.

2.3.13. Data, statistics and visualization

Data are represented as mean \pm standard error of mean (SEM). Graphs were prepared using the software GraphPad Prism 9 and R.

2.4. Conflict of Interest

The authors declare that the research was conducted in the absence of any commercial or financial relationships that could be construed as a potential conflict of interest. Funders had no role in the design of the study; in the collection, analyses, or interpretation of data; in the writing of the manuscript, or in the decision to publish the results.

2.5. Authors and Contributions

Martin Roszkowski, Irina Lazar-Contes, Pierre-Luc Germain, Deepak Tanwar, Anara Alshanbayeva, Niharika Obrist, Ali Jawaid, Gretchen van Steenwyk, Eloïse Kremer, Dalila Korkmaz, Mark Ormiston, Francesca Manuella, Johannes vom Berg, Jörg Tost, Johannes Bohacek, Isabelle M Mansuy

MR, JB and IMM designed experiments. MR established sperm collection and characterization. MR, IL, GvS and FM performed animal experiments. MR, IL, AJ and EK collected sperm. MR, IL and JB performed AI. MR, IL, DK and MO collected embryos. MR and NO processed samples and library preparation. MR and AA collected and characterized epididymosomes. PG and DT performed bioinformatic analyses. MR, JB and PL interpreted experimental results. IMM, JB, JT and JvB acquired funding for the study. MR, JB, IL and IMM wrote the manuscript.

2.6. Funding

This work was supported by University of Zurich, ETH Zurich, Swiss National Science Foundation (31003A_135715), Novartis Foundation (16B097), Roche Postdoctoral Fellowship Program (ID233), the NCCR RNA and Disease, EU project EarlyCause 848158 and the Slack-Gyr foundation. MR was funded by the ETH Zurich Fellowship (ETH-10 15-2).

2.7. Acknowledgments

The authors thank Dr. Silvia Schelbert for administrative support, Dr. Claudia Dumrese from the UZH Cytometry Facility for help with imaging flow cytometry, Dr. Catharina Aquino and Dr. Emilio Yánguez from the Functional Genomics Center Zurich for sequencing services, Dr. Andres Käch and Teresa Colangelo from the UZH Center for Microscopy and Image Analysis for electron microscopy services, and the animal care takers of the Laboratory Animal Services Center.

2.8. Data Availability Statement

The original contributions presented in the study are included in the article, further inquiries can be directed to the corresponding author. Custom scripts are available upon request

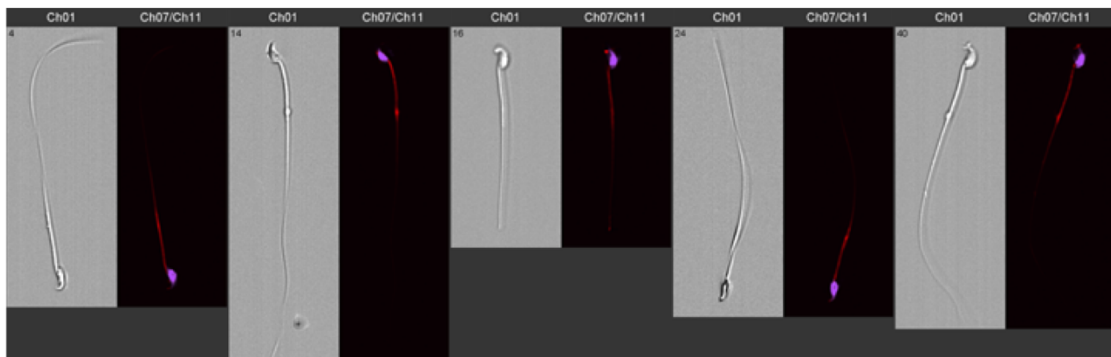
2.9. References

1. Jawaid, A.; Jehle, K.-L.; Mansuy, I.M. Impact of Parental Exposure on Offspring Health in Humans. *Trends Genet.* **2020**, *1*–16, doi:10.1016/j.tig.2020.10.006.
2. Lempradl, A. Germ cell-mediated mechanisms of epigenetic inheritance. *Semin. Cell Dev. Biol.* **2020**, *97*, 116–122, doi:10.1016/j.semcd.2019.07.012.
3. Bohacek, J.; Mansuy, I.M. Molecular insights into transgenerational non-genetic inheritance of acquired behaviours. *Nat. Rev. Genet.* **2015**, *16*, 641–652, doi:10.1038/nrg3964.
4. Chen, Q.; Yan, W.; Duan, E. Epigenetic inheritance of acquired traits through sperm RNAs and sperm RNA modifications. *Nat. Rev. Genet.* **2016**, *17*, 733–743, doi:10.1038/nrg.2016.106.
5. Bohacek, J.; Mansuy, I.M. A guide to designing germline-dependent epigenetic inheritance experiments in mammals. *Nat. Methods* **2017**, *14*, 243–249, doi:10.1038/nmeth.4181.
6. Jung, Y.H.; Sauria, M.E.G.; Lyu, X.; Cheema, M.S.; Ausio, J.; Taylor, J.; Corces, V.G. Chromatin States in Mouse Sperm Correlate with Embryonic and Adult Regulatory Landscapes. *Cell Rep.* **2017**, *18*, 1366–1382, doi:10.1016/j.celrep.2017.01.034.
7. Krawetz, S.A. Paternal contribution: New insights and future challenges. *Nat. Rev. Genet.* **2005**, *6*, 633–642, doi:10.1038/nrg1654.
8. Bohacek, J.; von Werdt, S.; Mansuy, I.M. Probing the germline-dependence of epigenetic inheritance using artificial insemination in mice. *Environ. Epigenetics* **2016**, *2*, 1–10, doi:10.1093/EEP/DVv015.
9. Trigg, N.A.; Eamens, A.L.; Nixon, B. The contribution of epididymosomes to the sperm small RNA profile. *Reproduction* **2019**, *157*, R209–R223, doi:10.1530/REP-18-0480.
10. Xie, W.; Barr, C.L.; Kim, A.; Yue, F.; Lee, A.Y.; Eubanks, J.; Dempster, E.L.; Ren, B. Base-resolution analyses of sequence and parent-of-origin dependent DNA methylation in the mouse genome. *Cell* **2012**, *148*, 816–831, doi:10.1016/j.cell.2011.12.035.
11. Macaulay, I.C.; Teng, M.J.; Haerty, W.; Kumar, P.; Ponting, C.P.; Voet, T. Separation and parallel sequencing of the genomes and transcriptomes of single cells using G&T-seq. *Nat. Protoc.* **2016**, *11*,

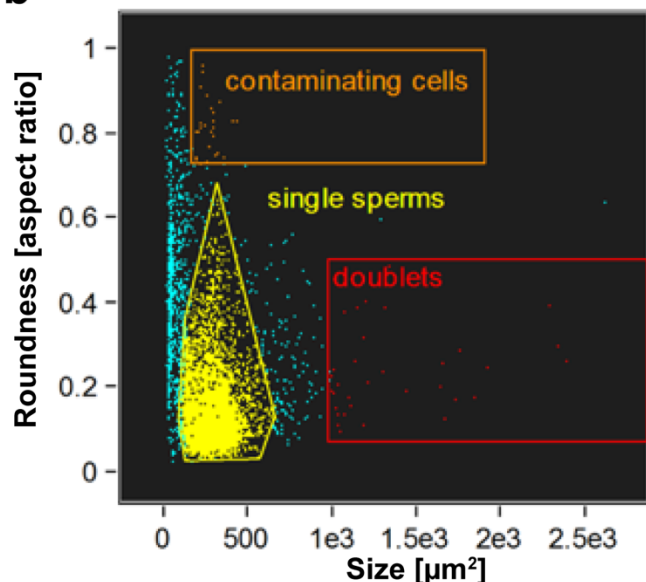
- 2081–2103, doi:10.1038/nprot.2016.138.
- 12. Franklin, T.B.; Russig, H.; Weiss, I.C.; Gräff, J.; Linder, N.; Michalon, A.; Vizi, S.; Mansuy, I.M. Epigenetic transmission of the impact of early stress across generations. *Biol. Psychiatry* **2010**, *68*, 408–15, doi:10.1016/j.biopsych.2010.05.036.
 - 13. Gapp, K.; Jawaid, A.; Sarkies, P.; Bohacek, J.; Pelczar, P.; Prados, J.; Farinelli, L.; Miska, E.; Mansuy, I.M. Implication of sperm RNAs in transgenerational inheritance of the effects of early trauma in mice. *Nat. Neurosci.* **2014**, *17*, 667–669, doi:10.1038/nn.3695.
 - 14. Bohacek, J.; Farinelli, M.; Mirante, O.; Steiner, G.; Gapp, K.; Coiret, G.; Ebeling, M.; Durán-Pacheco, G.; Iniguez, a L.; Manuella, F.; et al. Pathological brain plasticity and cognition in the offspring of males subjected to postnatal traumatic stress. *Mol. Psychiatry* **2015**, *20*, 621–631, doi:10.1038/mp.2014.80.
 - 15. Chen, Y.; Zheng, Y.; Gao, Y.; Lin, Z.; Yang, S.; Wang, T.; Wang, Q.; Xie, N.; Hua, R.; Liu, M.; et al. Single-cell RNA-seq uncovers dynamic processes and critical regulators in mouse spermatogenesis. *Cell Res.* **2018**, *28*, 879–896, doi:10.1038/s41422-018-0074-y.
 - 16. Kirkness, E.F.; Grindberg, R. V.; Yee-Greenbaum, J.; Marshall, C.R.; Scherer, S.W.; Lasken, R.S.; Venter, J.C. Sequencing of isolated sperm cells for direct haplotyping of a human genome. *Genome Res.* **2013**, *23*, 826–832, doi:10.1101/gr.144600.112.
 - 17. Ma, W.; Horvath, G.C.; Kistler, M.K.; Kistler, W.S. Expression Patterns of SP1 and SP3 During Mouse Spermatogenesis: SP1 Down-Regulation Correlates with Two Successive Promoter Changes and Translationally Compromised Transcripts1. *Biol. Reprod.* **2008**, *79*, 289–300, doi:10.1095/biolreprod.107.067082.
 - 18. Thomas, K.; Sung, D.-Y.; Yang, J.; Johnson, K.; Thompson, W.; Millette, C.; McCarrey, J.; Breitberg, A.; Gibbs, R.; Walker, W. Identification, Characterization, and Functional Analysis of Sp1 Transcript Variants Expressed in Germ Cells During Mouse Spermatogenesis1. *Biol. Reprod.* **2005**, *72*, 898–907, doi:10.1095/biolreprod.104.030528.
 - 19. Völkel, S.; Stielow, B.; Finkernagel, F.; Stiewe, T.; Nist, A.; Suske, G. Zinc Finger Independent Genome-Wide Binding of Sp2 Potentiates Recruitment of Histone-Fold Protein Nf-y Distinguishing It from Sp1 and Sp3. *PLOS Genet.* **2015**, *11*, e1005102, doi:10.1371/journal.pgen.1005102.
 - 20. Picelli, S.; Faridani, O.R.; Björklund, Å.K.; Winberg, G.; Sagasser, S.; Sandberg, R. Full-length RNA-seq from single cells using Smart-seq2. *Nat. Protoc.* **2014**, *9*, 171–181, doi:10.1038/nprot.2014.006.
 - 21. Wuertz-Kozak, K.; Roszkowski, M.; Cambria, E.; Block, A.; Kuhn, G.A.; Abele, T.; Hitzl, W.; Drießlein, D.; Müller, R.; Rapp, M.A.; et al. Effects of Early Life Stress on Bone Homeostasis in Mice and Humans. *Int. J. Mol. Sci.* **2020**, *21*, 6634, doi:10.3390/ijms21186634.

2.10. Supplementary Figures

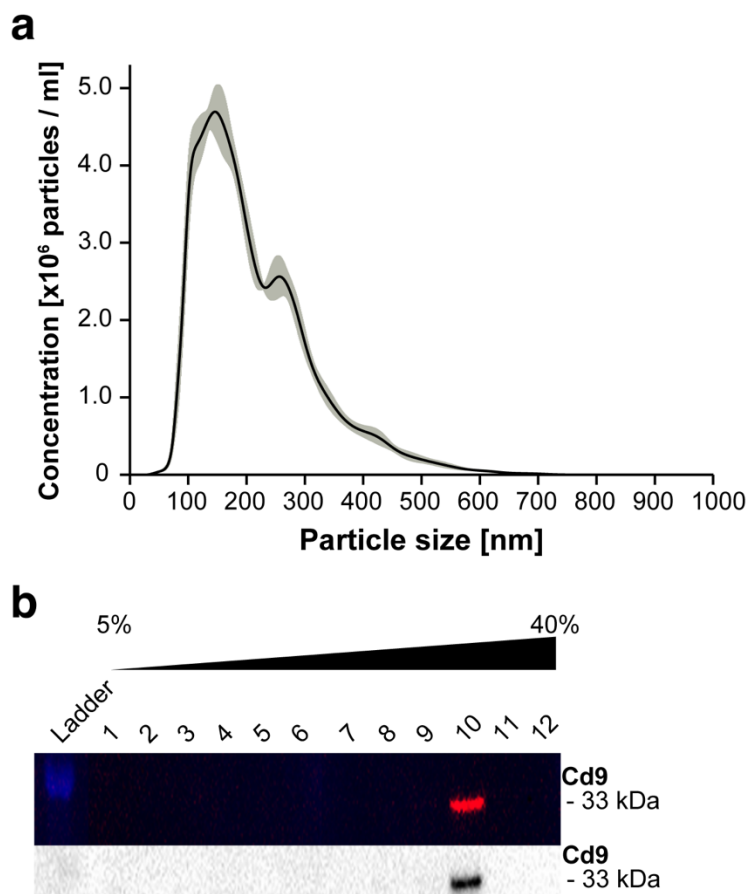
a



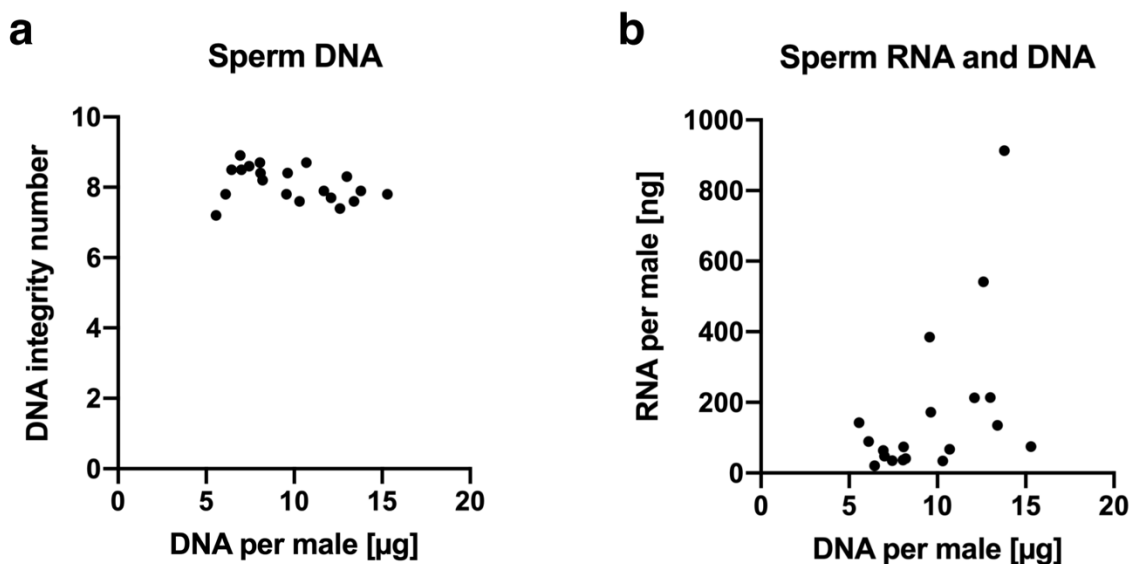
b



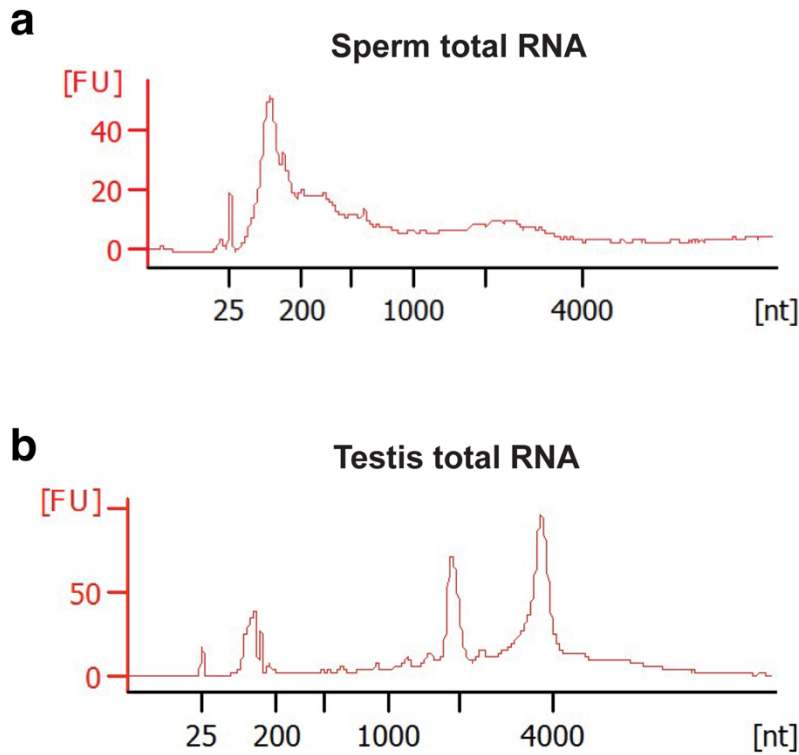
Supplementary Figure 1 – Imaging Flow Cytometry of OmniSperm. **(a)** Brightfield (Channel 1) and overlaid fluorescence images (Channel 7 and 11) of sperm stained with Hoechst 33342 (blue) and MitoTracker Deep Red (red) acquired by imaging flow cytometry. **(b)** Imaging events were quantified based on the detected aspect ratio (with the value 1 equaling a completely round object) and their size in μm^2 . The majority of observed events were sperm cells, indicating few contaminating cells in the crude sperm sample before treatment with somatic cell lysis buffer.



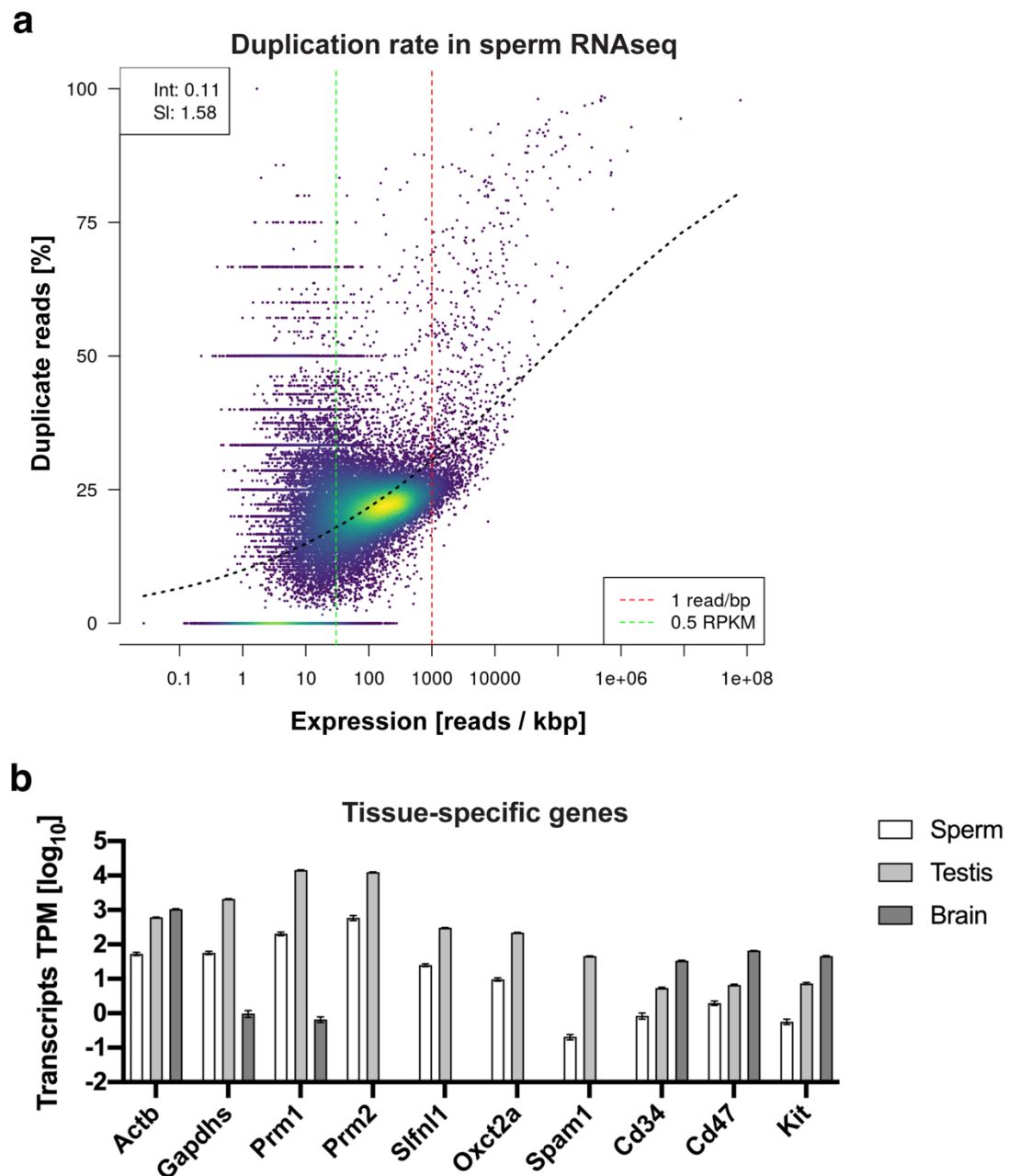
Supplementary Figure 2 – Extracellular vesicles collected by OmniSperm **(a)** Nanoparticle tracking results shown as concentration of detected particles according to their size in nm. The size of isolated extracellular vesicles ranged from 50 nm to 600 nm, with a majority of particles having a size of 147 nm ($n = 5$). Gray area indicates ± 1 SEM. **(b)** Western blot of enriched epididymosomes after gradient ultracentrifugation (5 – 40 % OptiPrep gradient) showed the extracellular vesicle marker Cd9 in the expected fraction.



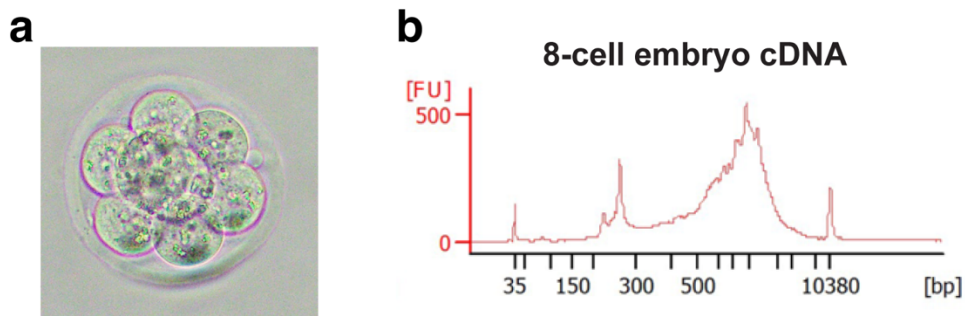
Supplementary Figure 3 – DNA quality and RNA quantity in OmniSperm. (a) Sperm DNA integrity was assessed by gel electrophoresis and plotted against DNA amount collected per mouse. 50 μ l of sperm lysate yielded between 5 and 15 μ g DNA per male with an average DNA integrity number (DIN) of 8. DIN 10 signifies the highest possible DNA integrity. (b) Total amount of untreated sperm RNA collected from a single male plotted against sperm DNA amount. On average, 170 ng of RNA were collected per male.



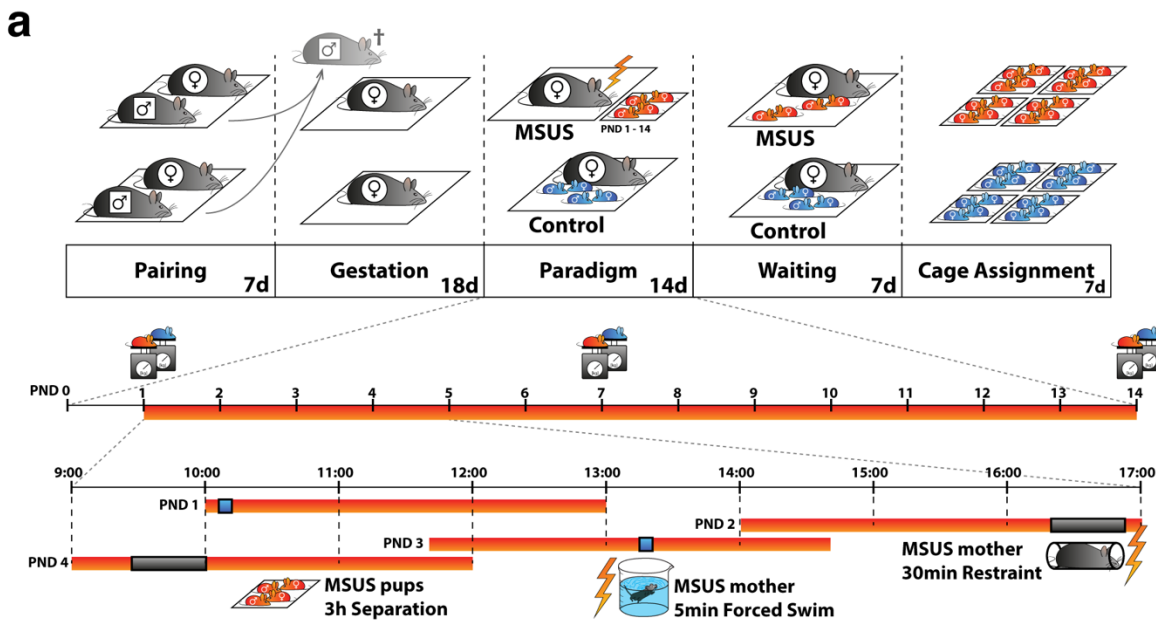
Supplementary Figure 4 – RNA profile of sperm and somatic tissue. **(a,b)** Electropherograms of RNA concentration in fluorescence units (FU) for a given nucleotide length (nt). **(a)** Sperm RNA has mostly short RNAs and no distinct rRNAs. **(b)** Testis RNA has distinct 18S rRNA peak at 1900 nt and 28S rRNA peak at 4700 nt.



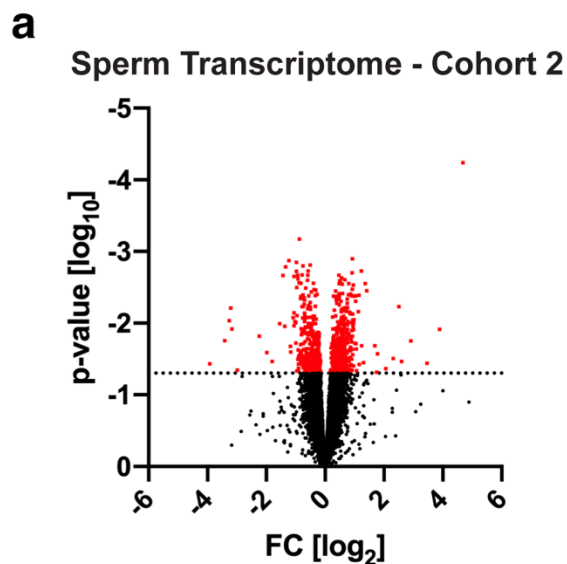
Supplementary Figure 5 – Purity of sperm and quality of RNAseq. **(a)** 2D density plot of quantified read duplication rate in % according to the corresponding transcripts expression level in sperm RNAseq using dupRadar. A high duplication rate of reads belonging to lowly expressed genes could indicate technical PCR artefacts resulting from over-amplified libraries due to insufficient cDNA starting amounts. The logistic regression (dotted black line) indicates a low duplication for low read count transcripts. **(b)** Extended assessment of normalized tissue-specific gene expression in sperm, testis and brain samples in transcripts per million ($n = 5$). Somatic cell markers *Spam1*, *Cd34*, *Cd47* and *Kit* were absent in sperm when compared to germ-line transcripts such as *Actb*, *Gapdhs*, *Prm1*, *Prm2*, *Slfnl1* and *Oxct2a*. Data are represented as mean \pm standard error of mean (SEM).



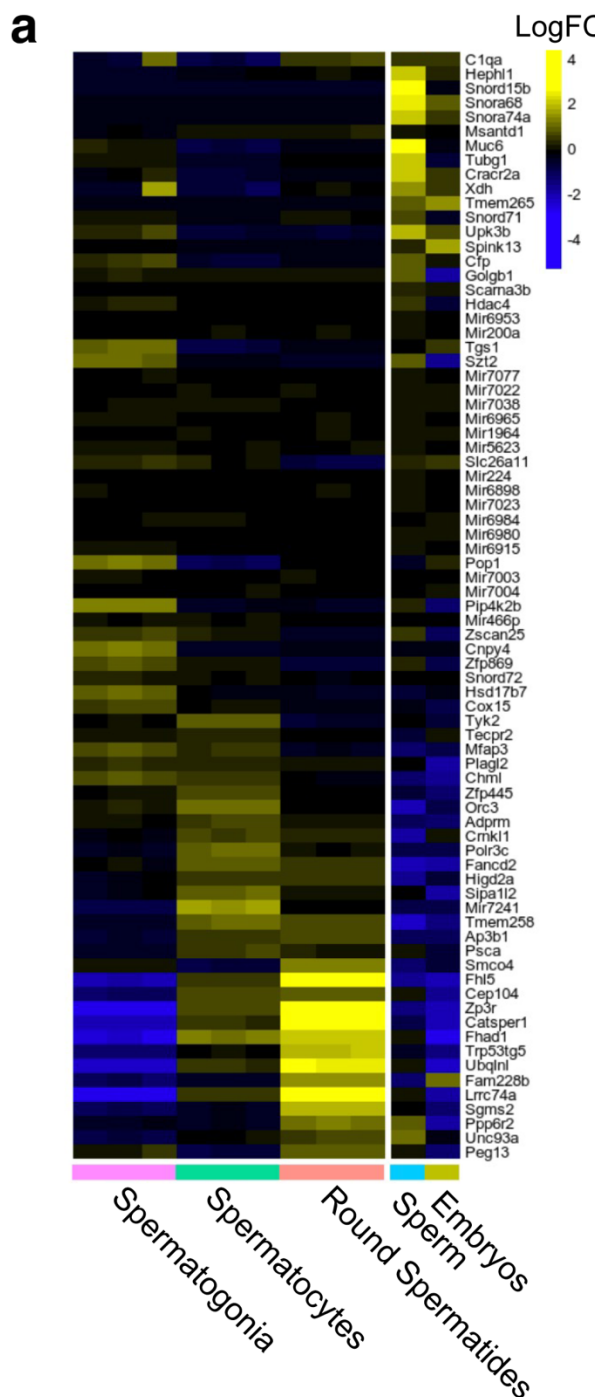
Supplementary Figure 6 – Embryo collection for single cell sequencing. **(a)** Light microscopy picture of 8-cell mouse embryo. **(b)** Electropherograms of DNA concentration in fluorescence units (FU) for a given base pair length (bp). cDNA from 8-cell embryo was prepared by G&T-Seq. The distinct peak between 500 and 8000 bp indicates high-quality cDNA.



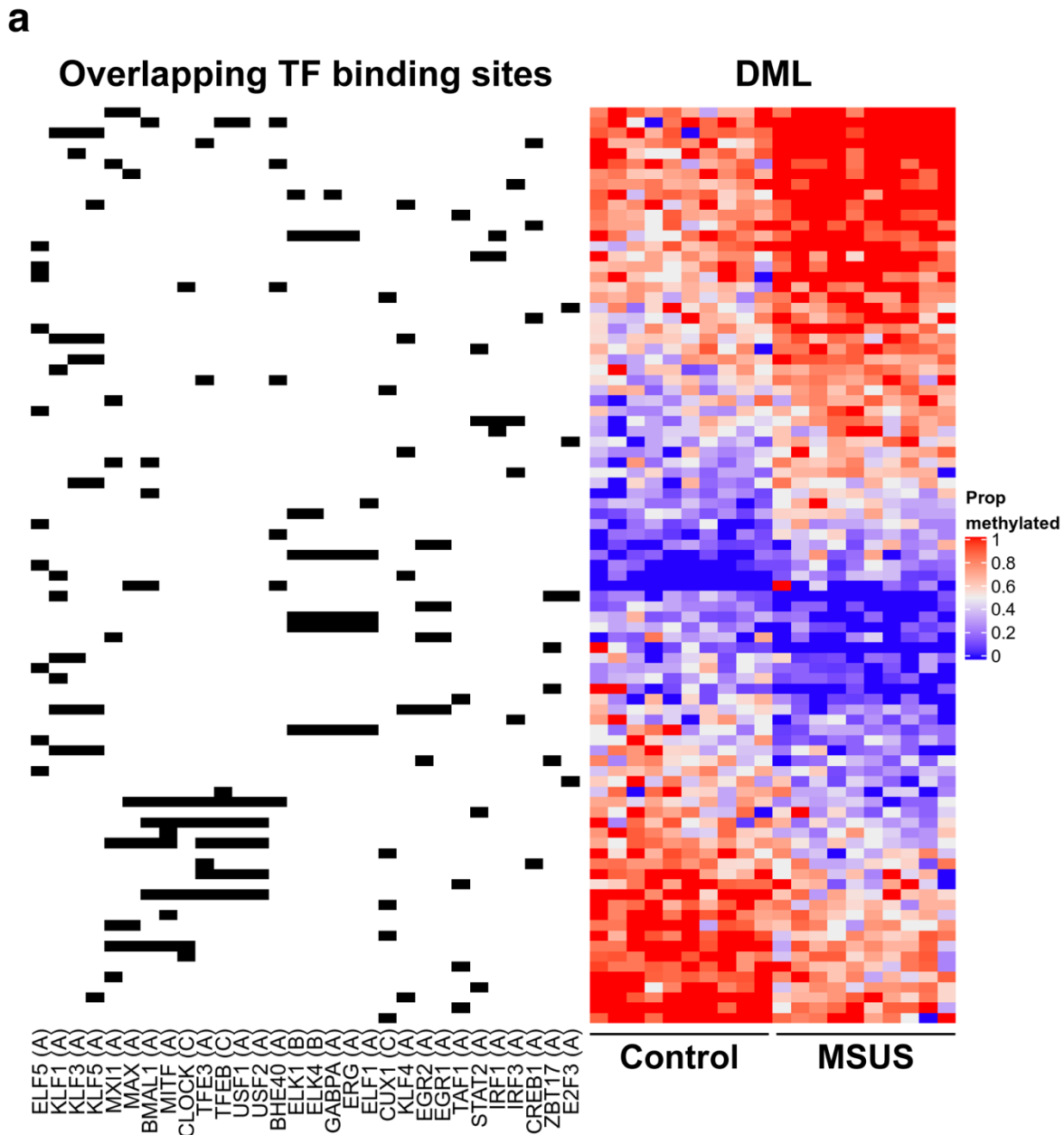
Supplementary Figure 7 – Unpredictable maternal separation and unpredictable maternal stress (MSUS) is an animal model for early life stress. Naïve males are mated with naïve females for 1–7 days. Dams gestate for about 21 days in normal conditions until delivery. The MSUS paradigm (red bar in the timeline) starts at postnatal day 1 (PND1) and lasts until PND14. During MSUS, pups are unpredictably separated from their mothers for 3 h each day at different times of the dark cycle (lights off from 8 am to 8 pm). During separation, the mother is stressed unpredictably by forced swim or restraint as shown in the timeline at the bottom. Pups and dam are left undisturbed from PND15 until weaning at PND21. Gray mice are naïve without any previous stress exposure. Blue pups are controls without any stress exposure. Red pups are exposed to MSUS. (Figure ref. [21])



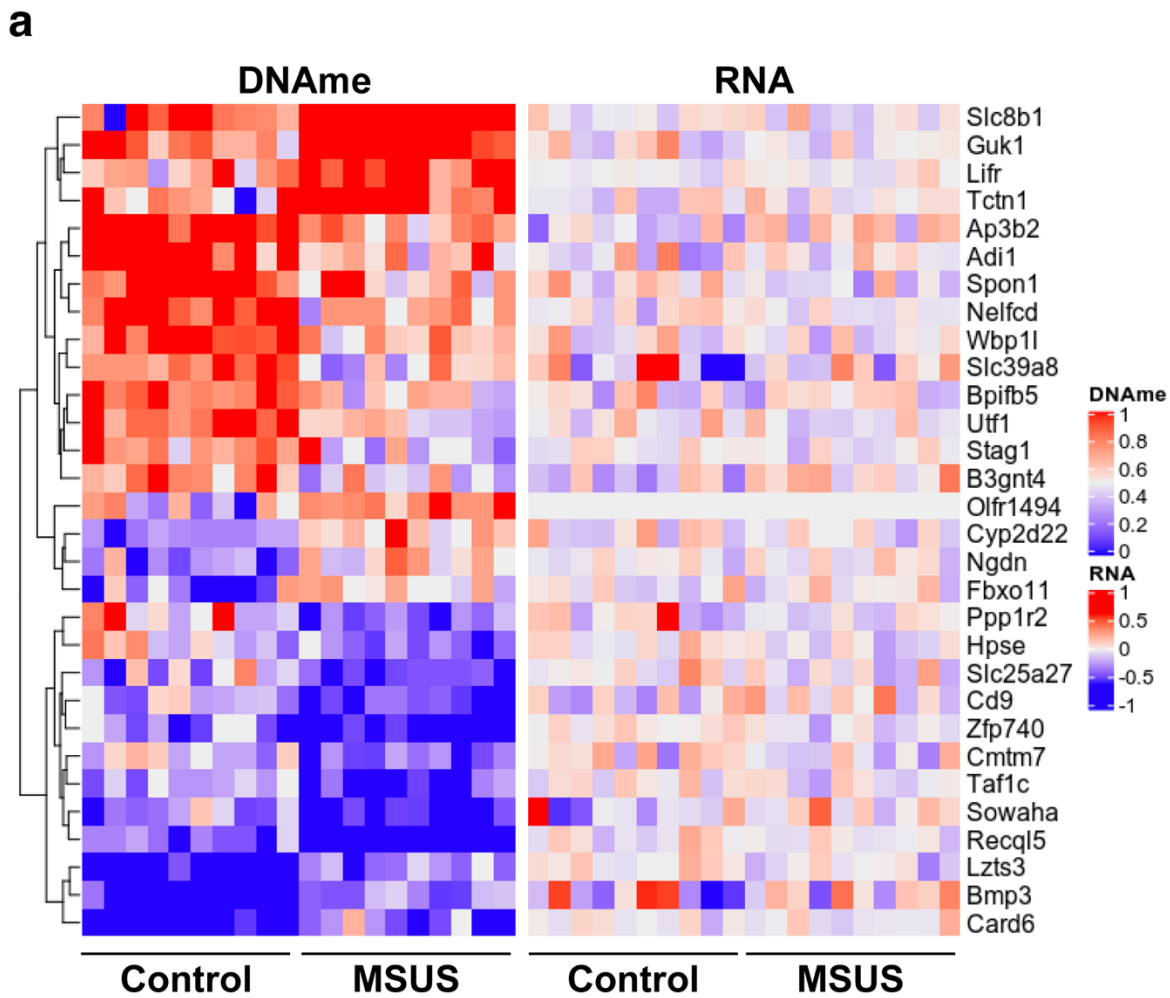
Supplementary Figure 8 – Sperm transcriptome changes after MSUS. **(a)** Volcano-plot of MSUS-induced transcriptome changes in sperm of the second mouse cohort ($n = 5$ per group). Dotted line indicates a p-value of 0.05.



Supplementary Figure 9 – Heatmap of expressed genes at methylated TSS. Sperm transcripts that were expressed despite highly methylated TSS were compared to published datasets of earlier spermatogenesis stages such as spermatogonia, spermatocytes and round spermatides. Divergent expression patterns are present in sperm and embryos when compared to the last spermatogenic stage, including genes involved in spermatogenesis and sperm function such as *Zpr3*, *Catsper1*, *Fhl5*, *miR224*, *Hdac4*, *Upk3b*, *Cracr2a*, and embryo development such as *Peg13*, *Fancd2*, *Zfp445*, *Plagl2*, *Mfap3*, *Hsd17b7*, *Cnpy4*, *Pip4k2b*, *Pop1*, *Tgs1*, *miR200a*, *Golgb1*, *Tubg1*, *Spinck13*.

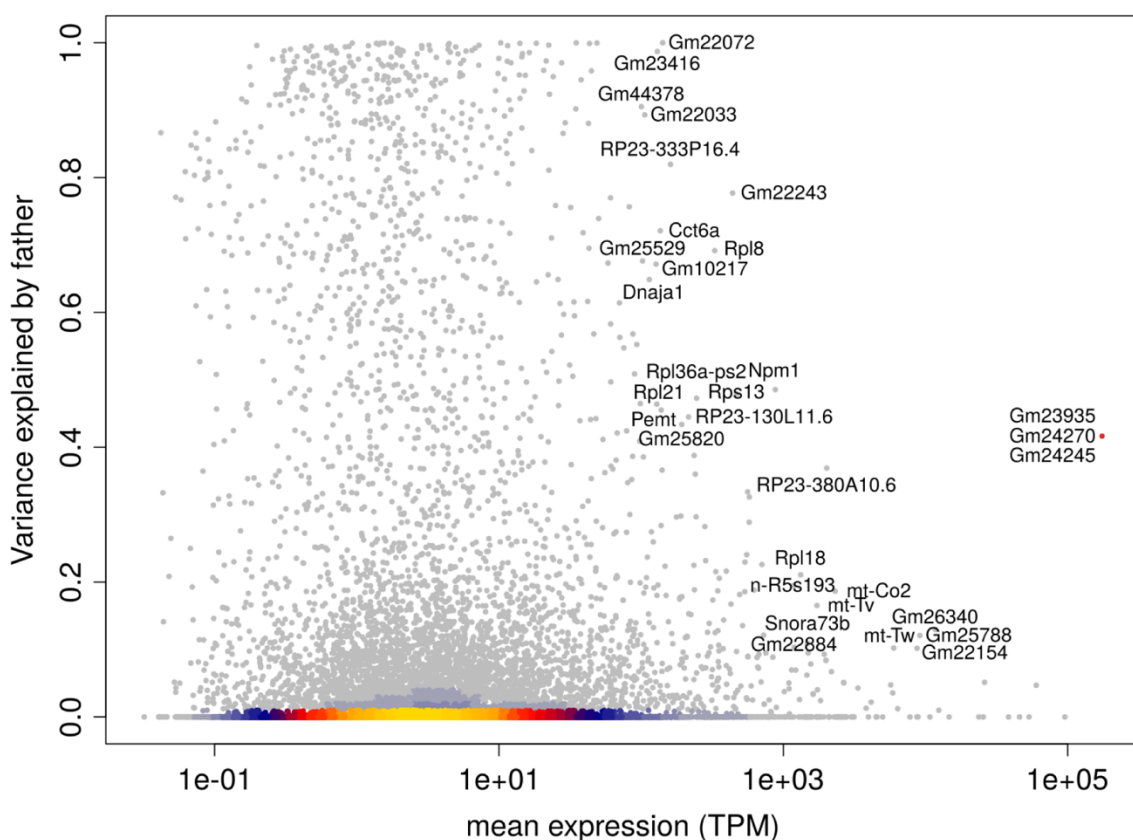


Supplementary Figure 10 – Identification of TFs with binding sites in sperm DML. MSUS-induced DML (rows) in sperm were screened for predicted TF binding sites (columns in black and white). Letters A to C indicate level of evidence for TF binding. Cells filled in black correspond to overlapping TF binding sites at DML.



Supplementary Figure 11 – Distal DML and corresponding gene expression in sperm.
Differential methylated CpGs within 2kb of TSS were screened for corresponding gene expression changes and the strongest correlations plotted. However, we did not observe any statistically significant correlations.

a



Supplementary Figure 12 – Analysis of variance in embryo gene expression. 2D density plot of gene expression from pooled embryos that were generated by the same sperm. Therefore, embryo transcriptome alterations were independent from the mother's uterine environment. This analysis indicated a substantial contribution of the father's sperm to the gene expression of embryos.

Article

3. High efficiency RNA extraction from sperm cells using guanidinium thiocyanate supplemented with tris(2-carboxyethyl)phosphine

Martin Roszkowski¹, Isabelle M. Mansuy¹

¹ Laboratory of Neuroepigenetics, Brain Research Institute of the University of Zurich and Institute for Neuroscience of the ETH Zurich, Zurich, Switzerland

This article has been submitted to *Frontiers in Cell and Developmental Biology* and is in revision.

Martin Roszkowski conducted and analyzed all experiments and wrote the article.

3.1. Abstract

The extraction of high-quality ribonucleic acid (RNA) from tissues and cells is a key step in many biological assays. Guanidinium thiocyanate-phenol-chloroform (AGPC) is a widely used and efficient method to obtain pure RNA from most tissues and cells. However, it is not efficient with some cells like sperm cells because they are resistant to chaotropic lysis solutions containing guanidinium thiocyanate such as Buffer RLT+ and Trizol. Here, we show that disulfide bonds are responsible for the chemical resistance of sperm cells to RNA extraction reagents. We show that while β -mercaptoethanol (β ME) can increase sperm lysis in Buffer RLT+, it has no effect in Trizol and leaves sperm cells intact. We measured the reduction of disulfide bonds in 2,2'-dithiodipyridine (DTDP) and observed that β ME has a pH-dependent activity in chaotropic solutions, suggesting that pH is a limiting factor. We identified tris(2-carboxyethyl)phosphine (TCEP) as an efficient lysis enhancer of AGPC solutions that can retain reducing activity even at acidic pH. Trizol supplemented with TCEP allows the complete and rapid lysis of sperm cells, increasing RNA yield by 100-fold and resulting in RNA with optimal quality for reverse transcription and polymerase chain reaction. Our findings highlight the importance of efficient cell lysis and extraction of various macromolecules for bulk and single-cell assays, and can be applied to other lysis-resistant cells and vesicles, thereby optimizing the amount of required starting material and animals.

3.2. Introduction

Ribonucleic acid (RNA) is a macromolecule essential for many biological processes across all known species. It exists in different forms and length, and has numerous functions. In eukaryotes, messenger RNA (mRNA) is a form of coding RNA that is transcribed from genes and serves as template for translation into proteins [1]. Non-coding RNA is transcribed from intergenic regions, and is not translated into proteins but has various regulatory functions. MicroRNAs and long non-coding RNA are involved in the silencing/degradation of mRNA and in genome regulation, while ribosomal and transfer RNA participate to ribosomal constitution and functions respectively [2,3], and small interfering RNA and Piwi-interacting RNA in genome defence [4,5]. RNA is present in cells and in extracellular vesicles which mediate signalling in-between cells and across tissues [6,7]. It has also been causally involved in the transmission of phenotypes from parent to offspring in vertebrates and invertebrates [8–10].

Purification of high-quality RNA is an important step to investigate biological processes, cellular functions and phenotypes in molecular assays. The successful extraction of short and long RNA relies on the separation from DNA, proteins and cellular debris contained in cell lysate. Reverse transcription of purified RNA results in cDNA that can be amplified by polymerase chain reaction (PCR) for quantification of gene and transcript expression for classical qPCR or digital droplet PCR. Next generation sequencing is another method to quantify RNA, now commonly used to identify molecular signatures of tissues or individual cells and assess differential expression [11].

RNA is purified from lysed cells by mainly two methods: acid guanidinium thiocyanate-phenol-chloroform (AGPC) and silica-based extraction columns [12,13]. AGPC extraction yields RNA of all lengths and is therefore the preferred method to obtain total RNA from cells and tissues [14]. However, RNA purity and quality largely depends on the expertise of the experimenter and on sample handling. Its low cost, simplicity and adaptability to various biological material make it the most popular method in basic research. Silica-based columns allow nucleic acids extraction by binding to silica in the presence of chaotropic salts. It is commonly used in commercially available RNA extraction kits such as Qiagen RNAeasy and is amenable to automation for high throughput. Silica-based columns preferentially capture nucleic acids longer than 200 nucleotides but provide poor recovery of short RNA because they

tightly bind with silica and are less likely to elute [15]. The recovered RNA is highly pure but the yield is usually lower when compared to AGPC.

In this study, we report that some cells, particularly mouse sperm cells are resistant to commercially available AGPC and lysis solutions used for silica-based columns and cannot be properly lysed, resulting in poor RNA yield and significant sample loss. Sperm lysis in AGPC is not improved by the addition of the reducing agent β -mercaptoethanol (β ME) or dithiothreitol (DTT), while it is achieved in silica-based column protocols by β ME in the lysis solution. We observed that the reduction of protein disulfide bonds is necessary for the lysis of sperm heads, and that reduction efficiency is pH-dependent, potentially explaining the difference in sperm lysis efficiency of various solutions. Lastly, we identify tris(2-carboxyethyl)phosphine (TCEP) as a potent enhancer of AGPC RNA extraction and show that it leads to complete lysis of mouse sperm cells.

3.3. Results

3.3.1. Mouse sperm cells are resistant to AGPC RNA extraction

A sperm cell is composed of a head containing a nucleus that carries the paternal genome and RNA, and a flagellum prolonging the head through a mitochondria-rich midpiece, that provides motility (Figure 1A). We incubated mouse sperm cells at room temperature in Trizol, a commercially available AGPC RNA extraction reagent containing guanidinium thiocyanate as chaotropic agent. To separate sperm heads from the midpiece and flagellum, and dissociate cell clumps, we passed the sperm samples 10 times through a 30 G needle at the beginning of Trizol incubation. Despite this treatment, sperm heads remained intact after 5 minutes of incubation, indicating inefficient lysis (Figure 1A). We repeated the procedure and made it more stringent by using longer incubation (30 min) in Trizol and strong homogenization with small steel beads at 20 Hz for 10 minutes. However, intact sperm heads still remained visible (Figure 1A). These results confirm previous observations that 2 M guanidinium does not lyse sperm heads [16].

We examined if other commercially available RNA extraction solutions are more efficient. Buffer RLT+ is a proprietary lysis solution of the Qiagen RNAeasy Mini kit, whose composition is unknown. However, the material safety data sheet suggests that it contains up to 50 % guanidinium thiocyanate, thus resembles chaotropic properties of Trizol. Buffer RLT+

did not allow sperm lysis either (Figure 1A) even with a prolonged incubation of 18 hours at room temperature. However, complete lysis of sperm heads was achieved within 2 minutes when 100 mM β -mercaptoethanol (β ME) was added to Buffer RLT+ at room temperature (Figure 1B). β ME is a commonly used reducing agent that breaks inter- and intradisulfide bonds formed between cysteine residues in proteins. The addition of β ME is recommended by the manufacturer of the RNAeasy Mini kit to inhibit RNase, especially when extracting RNA from pancreas and spleen, tissues rich in RNase.

We extracted RNA from Trizol and Buffer RLT+/ β ME sperm lysates using a standard phenol-chloroform protocol. To exclude contamination by testicular somatic cells, we prepared sperm samples using a swim-up method followed by treatment with a somatic cell lysis buffer. This approach has previously been shown to yield sperm samples free of somatic cells [17,18]. We observed cell debris but no discernible somatic cells in the samples before RNA extraction. We assessed the quality of the extracted RNA by gel electrophoresis. Sperm samples were free of distinct 18S/28S rRNA peaks and had the expected RNA profile (Figure 1C,D), whereas RNA from testes had two characteristic peaks at 1800 and 3800 nt for 18S and 28S ribosomal RNA respectively, and are apparent that indicate high-quality RNA (Figure 1E), suggesting no contamination by somatic cells.

These results indicate that the standard protocol for AGPC RNA extraction is inappropriate to completely lyse mouse sperm cells and is the main reason for poor RNA yield from these cells, and that using Buffer RLT+/ β ME instead of AGPC solutions circumvents this issue.

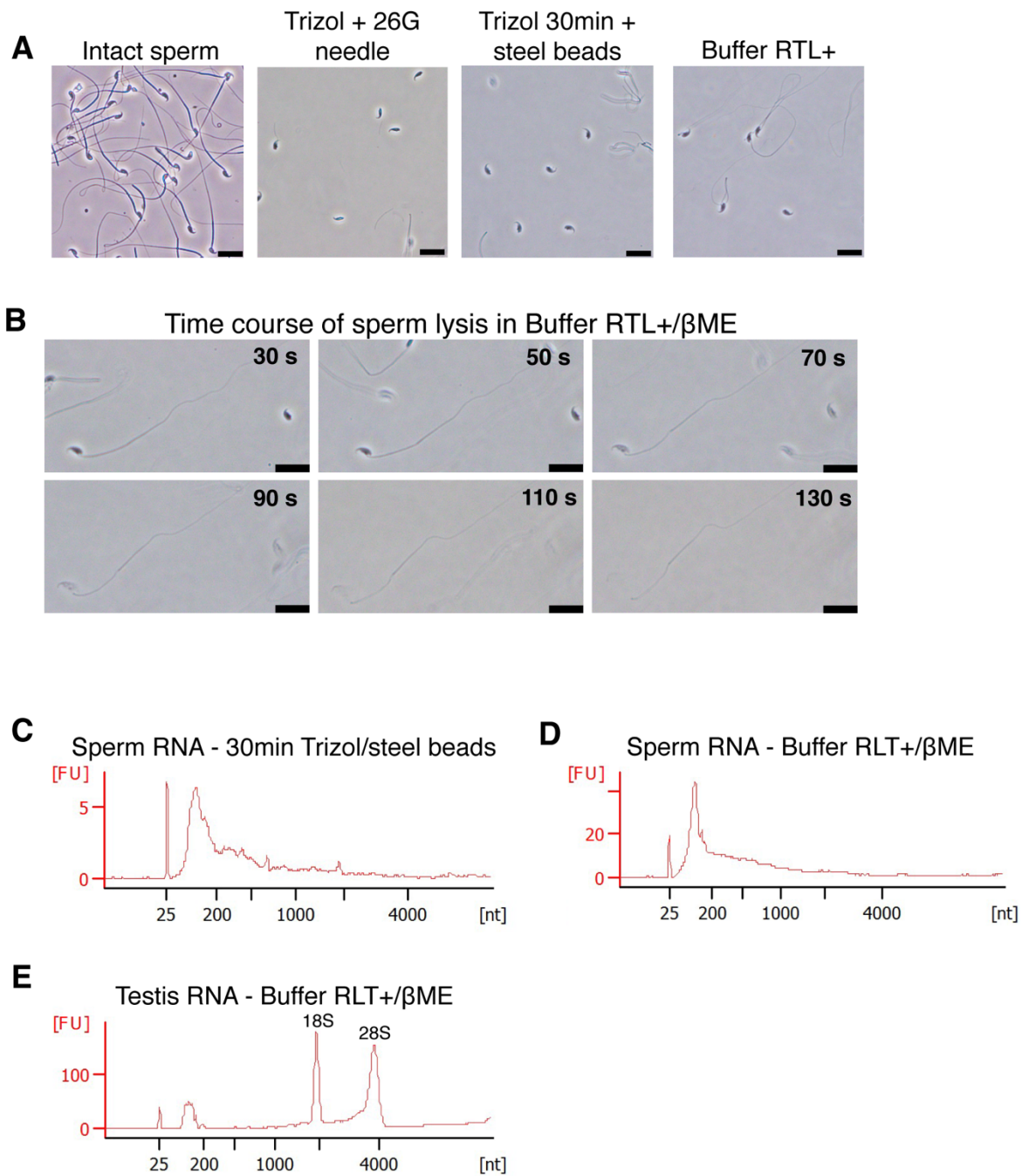


Figure 1: Mouse sperm cells require reducing agents for lysis in chaotropic solutions. **(A)** Mouse sperm was not lysed in Trizol nor Buffer RLT+. Lysis was not improved by mechanical shearing. Scale bars = 20 μ m. **(B)** Mouse sperm is rapidly lysed by Buffer RLT+ supplemented with 50 mM β ME. Scale bars = 20 μ m. **(C-E)** Bioanalyzer electropherograms of RNA concentration in fluorescence units (FU) for a given nucleotide length (nt). Sperm RNA prepared with **(C)** Trizol and homogenized by steel beads, or **(D)** Buffer RLT+ and β ME, and **(E)** testes RNA prepared with Buffer RLT+ and β ME.

3.3.2. Examining sperm lysis properties and reduction of disulfide bonds

We next examined the reason for the lysis-resistance of sperm outer membrane. Sperm cells are only lysed by Buffer RLT+ when supplemented with βME despite the presence of guanidinium thiocyanate as main chaotropic agent. βME is a widely used reducing agent that disrupts disulfide bonds between thiol groups such as cysteine residues, within and between proteins (Figure 2A). During RNA extraction, it inhibits ribonuclease activity, preventing the degradation of RNA released in solution. We tested if adding a reducing agent to AGPC solution results in the successful lysis of sperm cells. Trizol with 100 mM βME however did not result in the lysis of sperm heads, which remained intact (Figure 2C). Similarly, Trizol supplemented with dithiothreitol (DTT, Figure 2B) did not induce lysis (Figure 2C) even if DTT has been shown to decondense sperm heads by reducing disulfide bonds in protamines [16,19].

We then examined if the pH of the lysis solution influences the efficiency of sperm lysis. The pH primarily affects the reactivity of reducing agents and an alkaline pH is necessary for efficient reduction of disulfide bonds by βME and DTT [20]. In contrast, an acidic pH is preferred for protein disulfide bond mapping by mass spectrometry because it preserves disulfide bonds [21]. We measured the pH of several commercially available RNA extraction solutions and observed that Trizol and other AGPC lysis buffers have a pH of 3 while guanidinium thiocyanate in water has a pH of 5 and Buffer RLT+ and lysis buffer from mirVana RNA extraction kit using silica-columns have a pH of 6 (Table 1). The low pH may explain why βME did not improve lysis by Trizol.

Table 1: pH of commercially available lysis solutions for RNA extraction

Commercial Name	RNA Extraction Method	pH
TRIzol reagent	AGPC	3
QIAzol	AGPC	3
Tri Reagent	AGPC	3
TRIsure	AGPC	3
Guanidinium Thiocyanate 1 M	AGPC	5
Buffer RTL+	Silica Columns	6
mirVana Lysis/Binding Buffer	Silica Columns and AGPC	6

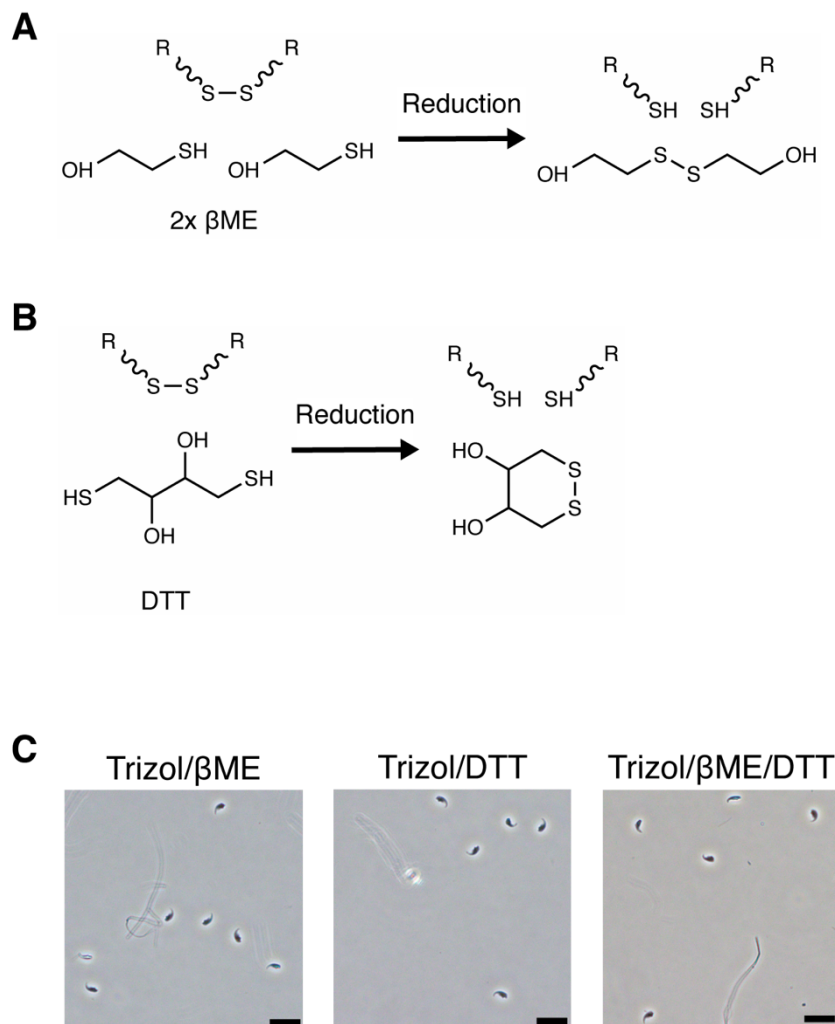
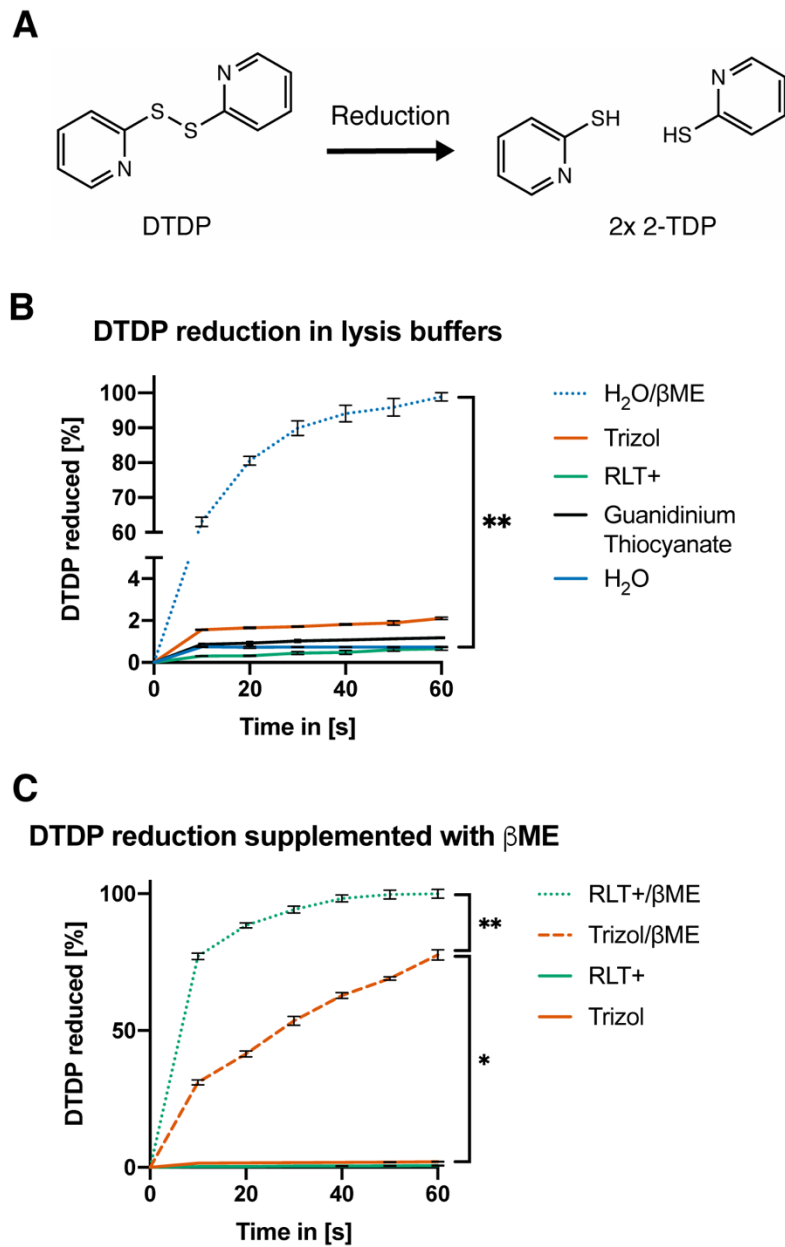


Figure 2. Sperm is not lysed in Trizol supplemented with β ME or DTT. **(A,B)** Chemical reduction of a protein disulfide bond by (A) β ME or (B) DTT. **(C)** Mouse sperm is not lysed in Trizol supplemented with 100 mM β ME, 100 mM DTT or a combination of both. Scale bars = 20 μ m.

Finally, we confirmed the pH-dependent activity of reducing agents by measuring the amount of 2-thiopyridone (2-TPD) formed after reduction of 2,2'-dithiodipyridine (DTDP) in lysis solutions. DTDP mimics protein disulfide bonds between cysteines and absorbance at 343 nm of 2-TPD in solution indicates the amount of disrupted bonds (Figure 3A). Trizol, Buffer RLT+ or 1 M guanidinium thiocyanate did not reduce DTDP. However, Buffer RLT+ supplemented with 50 mM β ME led to rapid (within 40 s) and complete reduction of DTDP in water (Figure 3B, ANOVA, $F(1.000, 6.000) = 31.6$, $p = 0.0014$). When added to Trizol, 50 mM β ME led to only slow and incomplete reduction of DTDP, with 25 % remaining after 60s (Figure 3C, ANOVA, $F(1.171, 7.026) = 29.94$, $p = 0.0007$).

In summary, the supplementation of acidic AGPC solutions with β ME or DTT is not sufficient to lyse mouse sperm, likely because guanidinium thiocyanate cannot reduce disulfide bonds present in the sperm head membrane, and the reactivity of β ME is pH dependent.

Figure 3. DTDP assay reveals pH-dependent activity of reducing agents. **(A)** Reduction of 2,2'-Dithiodipyridine (DTDP) produces 2-thiopyridone (2-TDP). **(B,C)** Measurement of DTDP reduction in % during 60s. **(B)** DTDP was not reduced by Trizol, Buffer RLT+, 1 M guanidinium thiocyanate or water. Water supplemented with 50 mM β ME reduced DTDP within 60 s. **(C)** Buffer RLT+ supplemented with β ME completely reduced DTDP. Trizol supplemented with β ME reduced 75 % of DTDP in the same time. Each condition and timepoint was measured 3 times ($n = 3$). Data are represented as mean \pm standard error of mean (SEM). Significant ANOVAs were followed up with Tukey's post-hoc test, * $p < 0.05$, ** $p < 0.01$.



3.3.3. TCEP enhances AGPC lysis

Tris(2-carboxyethyl)phosphine (TCEP) was previously shown to effectively reduce disulfide bonds across a wide pH range from 1.5 to 8.5 (Figure 4A) [20]. Therefore, we first assessed if TCEP could be an effective reducing agent for acidic lysis solutions. In contrast to β ME, Trizol supplement with 50 mM TCEP rapidly reduced all DTDP within 10 seconds (Figure 4B, ANOVA, $F(1.458, 8.747) = 28.96, p = 0.0002$).

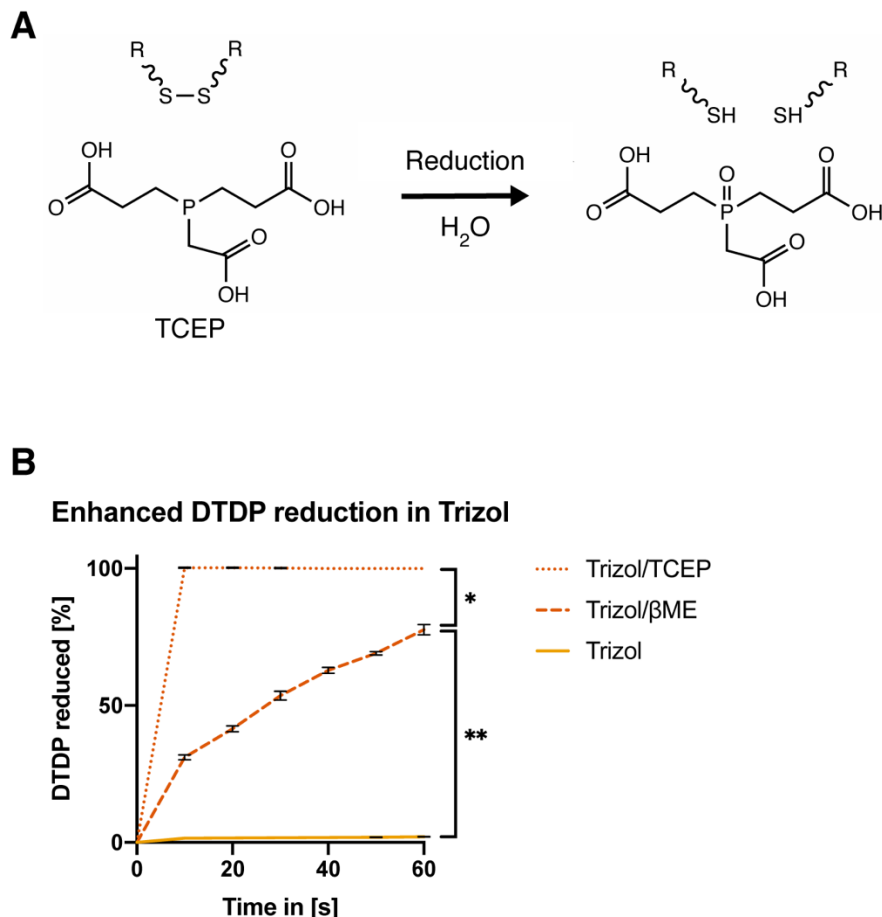
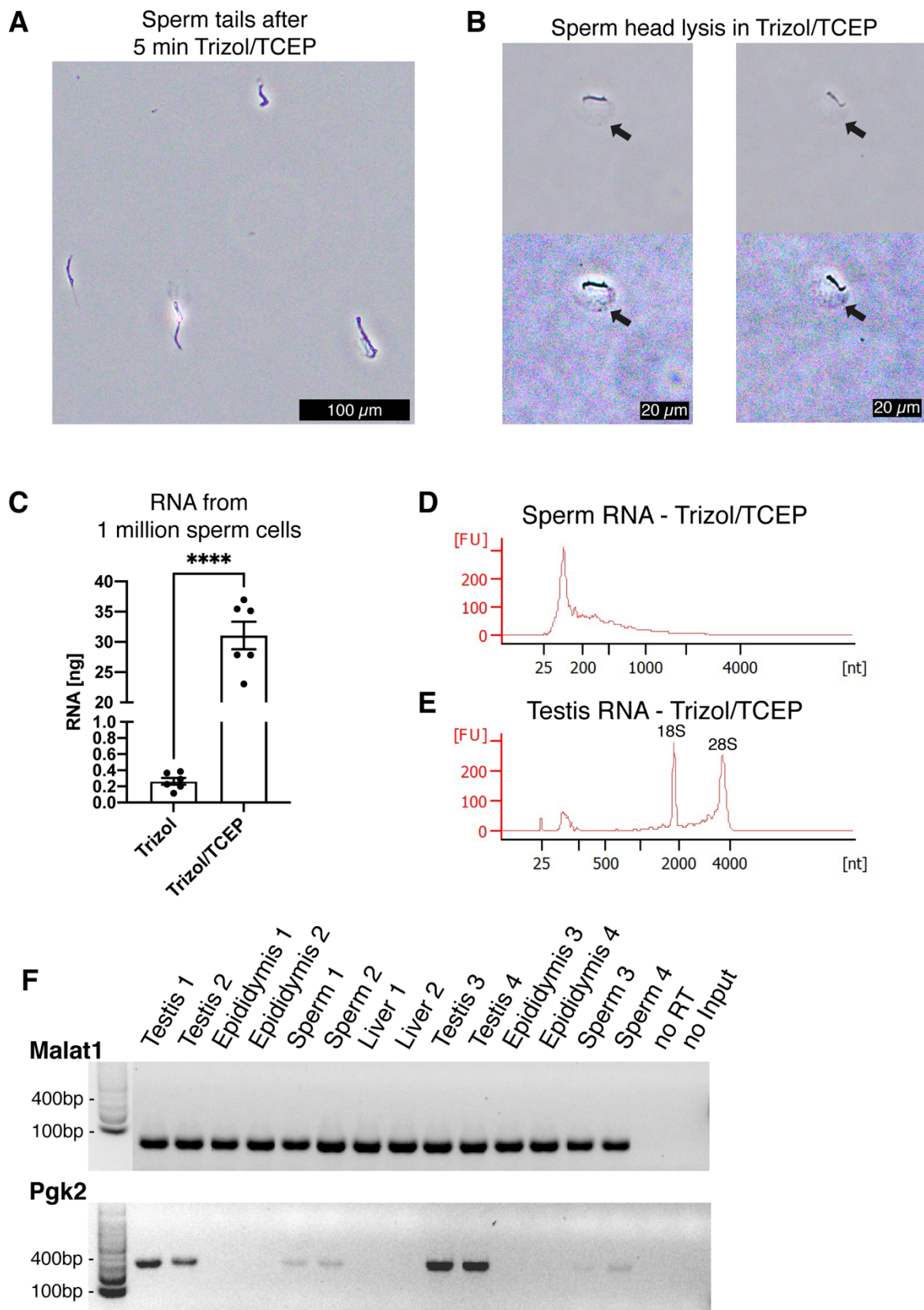


Figure 4. TCEP is a potent reducing agent in AGPC lysis solution. **(A)** Chemical reduction of a protein disulfide bond by TCEP. **(B)** Measurement of DTDP reduction in % during 60 s. DTDP was rapidly reduced in Trizol supplemented with 50 mM TCEP within 10 s. Each condition was measured 3 times ($n = 3$). Data are represented as mean \pm standard error of mean (SEM). Significant ANOVAs were followed up with Tukey's post-hoc test, * $p < 0.05$, ** $p < 0.01$.

Next, we examined if lysis of sperm cells was improved by supplementing AGPC lysis solutions with TCEP. We observed complete lysis of all sperm heads in Trizol with 50 mM TCEP at room temperature within 5 minutes (Figure 5A,B). As expected, complete sperm lysis improved the efficiency of RNA extraction without requiring any adjustment or additional recovery step of the standard AGPC protocol. 1 million sperm cells yielded 30 ng RNA when lysed by Trizol/TCEP, thereby considerably improving RNA yield (Figure 5C). The sperm RNA profile had no distinct 18S/28S ribosomal peaks indicating that the source of increased RNA was from sperm cells rather than contamination by somatic cells (Figure 5D). Similarly to Buffer RTL+/βME, extraction by Trizol/TCEP from testis tissue yielded high-quality RNA (Figure 5E).

Finally, we confirmed that the RNA extracted by Trizol and TCEP was suitable for down-stream applications such as reverse transcription polymerase chain reaction (RT-PCR). We conducted RT-PCR on metastasis associated lung adenocarcinoma transcript 1 (Malat1), an abundant long non-coding RNA (lncRNA) expressed in many mouse tissues [22]. Malat1 amplified in sperm, testis, epididymis and liver RNA samples extracted by Trizol/TCEP (Figure 5F). In contrast, the less abundant germ-cell specific phosphoglycerate kinase 2 (Pgk2) only amplified in sperm and testis samples (Figure 5F).

In conclusion, the supplementation of AGPC with TCEP enhanced lysis and increased the RNA yield from lysis-resistant sperm samples.



(Figure legend on next page)

Figure 5. TCEP enhances AGPC lysis and increases sperm RNA yield. **(A)** Mouse sperm cells are rapidly lysed in Trizol supplemented with 50 mM TCEP. Only clumped sperm tails remain visible indicating complete lysis of sperm heads. Scale bar = 100 μ m. **(B)** Details of mouse sperm lysis in Trizol/TCEP. In comparison to lysis of mouse sperm in Buffer RLT+/ β ME, the acrosome remains visible for longer and a distinct swelling of the nucleus containing sperm head is observed (black arrows). In the second row, color contrast of microscopy pictures was increased to highlight the swelling. Scale bars = 20 μ m. **(C)** Comparison between RNA yield in ng from 1 millions sperm cells when extracted with only Trizol or Trizol supplemented with TCEP. Trizol/TCEP extraction increased the RNA yield to an average of 30 ng. ($n = 6$). **(D,E)** Bioanalyzer electropherograms of RNA concentration in fluorescence units (FU) for a given nucleotide length (nt). **(D)** Sperm RNAs extracted from Trizol/TCEP were comprised mostly of RNAs shorter than 200 nt. **(E)** Testis RNA extracted from Trizol/TCEP was comprised of longer RNAs with distinct peaks at 1800 nt and 3800 nt. **(F)** lncRNA Malat1 was detected by RT-PCR in Trizol/TCEP samples from sperm ($n = 4$), testis ($n = 4$), epididymis ($n = 4$) and liver ($n = 2$). The germ-line specific transcript Pgk2 was only present in sperm and testis. noRT = RNA not reverse transcribed. NoInput = Sample without RNA. Data are represented as mean \pm standard error of mean (SEM). ***p < 0.0001.

3.4. Discussion

This study shows that mouse sperm cells are resistant to RNA extraction by AGPC and that supplementation with TCEP solves this issue by allowing complete lysis and thereby high RNA yield. The results indicate that a disulfide reducing agent is necessary to lyse sperm cells suggesting a critical role for disulfide bonds in conferring chemical resistance of sperm cells in mouse and potentially other species.

The effectiveness of AGPC extraction methods depends on the complete lysis of cells in the presence of chaotropic guanidinium (Gdm^+) and thiocyanate (SCN^-) ions and additional factors such as mechanical shearing, degrading conditions and osmotic pressure. Gdm^+ and SCN^- ions are strong protein denaturants that partially disrupt accessible hydrophilic bonds, and are commonly used in studies of protein stability and folding [23,24]. They also strongly inhibit the enzymatic activity of ribonucleases released during cell lysis, thus prevent the degradation of RNA in solution and contribute to the acidification of the lysate [25]. An acidic

pH is necessary during phenol-chloroform separation where DNA and proteins move to the organic phase while RNA remains in the aqueous phase [12,26].

Despite the general applicability and potency of AGPC lysis solutions, we observed that mouse sperm cells are not effectively lysed and require the presence of pH-compatible denaturing agents. Specifically, we show that TCEP improves lysis at acidic pH. TCEP is also used to stabilize extracted RNA, for the reduction of proteomic samples and the preparation of protein:RNA crystallization samples [27–29].

Sperm cells are specialized cells whose functions are to maintain the paternal genome and transfer it to an oocyte to generate offspring. During spermatogenesis, most histones are replaced by protamines with the exception of about 1 % of retained histones in mouse and 15 % in human at specific genomic regions such as transcription start sites, promoters and enhancers [30,31]. In contrast to histones, protamines are highly enriched in disulfide bonds forming intra- and interprotamine bonds that mediate and stabilize the crystalline-like toroid DNA packaging, requiring detergents for decondensation [32]. The highly condensed sperm nucleus is surrounded by the acrosome which in mice, has a distinct hook-like shape for cooperative cell motility, and carries enzymes necessary for successful sperm-oocyte fusion [33]. The acrosome protects the sperm nucleus from the environment of the vagina and uterus during transit to the oviduct. It is primarily composed of proteins, ceramides and sphingomyelins with very long chain (carbon length 24 to 34) polyunsaturated fatty acids (PUFA) [34]. The acrosome composition varies between mouse, rat and human with predominantly very long chain PUFA (C30) in mouse, (C28) in rat and (C16) in human [35,36]. Molecular dynamics simulations have shown that the composition regulates the stability and mechanical rigidity of bilayer membranes and changes in very long chain PUFA composition have been implicated in reduced sperm quality [36,37]. Our findings suggest a critical role for disulfide bonds in conveying chemical resistance of sperm cells, which has not been described previously.

The resistance of mouse sperm cells to an acidic pH may be a cellular adaptation to protect sperm cells during transit in the vagina and uterus. While the testicular environment and epididymis are chemically stable in male mice, the uterus and vaginal milieu in females undergo substantial changes during the estrous cycle. The mouse vagina has typically a slightly acidic pH to suppress the growth of undesired bacteria and fungi. Importantly, the acidic

environment together with other secreted enzymes contributes to the capacitation of sperm cells. The vaginal pH fluctuates with the estrous cycle and is particularly acidic (pH 4.5) during the estrous phase [38]. This is a time when females are the most receptive for copulation [39], thus the sperm is naturally exposed to an acidic environment. Its ability to resist such environment therefore allows it to regulate intracellular pH and maintain physiologically relevant functions [40].

A low RNA yield is expected from sperm samples, because these cells are transcriptionally silent. In sperm cells, protein synthesis is suppressed by cleavage of ribosomal RNA and most of the RNA contained in the cytoplasm is expulsed during spermatogenesis. A single sperm cell is presumed to contain only 10 to 100 fg RNA [41]. Thus, an efficient method for RNA extraction is essential to recover sufficient RNA for RT-PCR and sequencing to avoid pooling several sperm samples. Furthermore, low RNA yield can also confound downstream analyses because some RNA species such as specific miRNAs can be selectively lost during AGPC RNA extraction from a small number of cells [42]. With the improved lysis of sperm heads, we obtained on average 30 fg RNA per sperm cell, consistent with previous studies [8].

While we focused on the lysis of mouse sperm cells, similar issues and resistance to AGPC or other chaotropic solutions have been reported for extracellular vesicles [43], non-enveloped viruses [44] and sperm from other species such as human [17], bovine [45] and chicken [46]. Further to RNA, other macromolecules such as DNA, proteins or metabolites will also benefit from the improved lysis method. Further, with the availability of single cell sequencing, the reliable lysis and characterization of each cell becomes even more important. For example, easy to implement protocols such as genome and transcriptome sequencing (G&T-seq) allow parallel sequencing of genomic DNA and RNA from single cells [47]. However, G&T-seq uses Buffer RLT+ without any reducing agent to lyse cells. Supplementing Buffer RLT+ with TCEP may lead to faster and more robust cell lysis. Therefore, our findings can benefit other model organisms and single-cell applications requiring efficient cell lysis.

3.5. Materials and Methods

3.5.1. Animals

Animal experiments were conducted in strict adherence to the Swiss Law for Animal Protection and were approved by the cantonal veterinary office in Zürich under license number 57/2015 and 83/2018. C57Bl/6J mice were obtained from Janvier (France) and bred in-house to generate male mice ($n = 16$, 5 months old) for experiments. Mice were housed in groups of 3 to 5 animals in individually ventilated cages. Animals were kept in a temperature- and humidity-controlled facility on a 12h reversed light/dark cycle (light on at 20:00, off at 8:00) with food (M/R Haltung Extrudat, Provimi Kliba SA, Switzerland) and water *ad libitum*. Cages were changed weekly.

3.5.2. Mouse sperm collection

Epididymidis from both sides was incised by several cuts with a fine scissor and placed in 2 ml M2 medium (M7167-100ml, Sigma-Aldrich). Sperm cells were incubated at 37 °C for 30 min. 1 ml of supernatant containing motile sperm was collected and centrifuged at 2'000 rcf for 5 min. The supernatant was again collected, mixed with 1 ml of somatic cell lysis buffer (0.1 % sodium dodecyl sulfate and 0.05 % Triton X-100 in MilliQ water) and incubated at 4 °C for 10 min. Sperm samples were centrifuged at 2'000 rcf for 5 min, sperm pellets were washed twice in phosphate buffer saline (10010-015, Gibco) then snap-frozen and stored at -80 °C until further processing. For lysis experiments, sperm samples were immediately resuspended in 250 µl water, lysis solutions were added and sperm observed under a light microscope.

3.5.3. Cell lysis

Sperm pellets and small pieces of testis, liver or epididymis were lysed in 1 ml of Trizol (15596026, Life Technologies) or 1 ml of Buffer RLT+ (1053393, Qiagen) depending on the experiments. Lysis buffer was supplemented with 100 mM β-mercaptoethanol (M3148, Sigma-Aldrich), 100 mM dithiothreitol (646563-10X.5ml, Sigma-Aldrich) or 100 mM tris(2-carboxyethyl)phosphine (646547-10X1ml, Sigma-Aldrich). Sperm samples were either resuspended in lysis buffer by passage through a 30 G syringe or in the presence of 0.2 mm steel beads (SSB02-RNA, NextAdvance) at 20 Hz for up to 10 min in a TissueLyser II (85300, Qiagen). Since the lysis of sperm cells depends primarily on chemical lysis, we recommend future users a simple homogenization to sufficiently break up the cell pellet to obtain a single-

cell suspension using 5 mm steel beads for 2 min (69989, Qiagen). We did not observe any differences between sperm lysis using small or large steel beads. Tissue samples were homogenized in a TissueLyser II using 5 mm steel beads at 20 Hz for 2 min.

3.5.4. RNA extraction

For RNA extraction by phenol chloroform phase separation, 100 µl of sample lysed in Buffer RLT+ were added to 900 µl Trizol and extracted using the standard Trizol protocol. All centrifugation steps were at 4 °C and samples kept on ice unless noted otherwise. In brief, 200 µl chloroform was added to 1 ml lysate, shaken for 15 s and then incubated at room temperature for 3 min. Samples were centrifuged at 12'000 rcf for 15 min. The aqueous phase was transferred to a fresh tube, 10 µl glycogen was added and the tube inverted 4 times for mixing. 500 µl isopropanol was then added and the tube inverted again 4 times. After an incubation at room temperature for 10 min, samples were centrifuged at 12'000 rcf for 10 min. The supernatant was removed and the pellet washed twice in 75 % ethanol. After a final centrifugation at 7'500 rcf for 5 min, the supernatant was carefully removed. The pellet was dried in a concentrator (Speed-vac, Eppendorf) at 45 °C for 4 to 6 min. Sperm RNA was resuspended in 20 µl nuclease-free water and tissue RNA in 100 µl nuclease-free water (A7398,500, ITW Reagents). Finally, the solution was incubated at 55 °C for 15 min. RNA was stored at -80 °C.

3.5.5. RNA quantification and characterization

RNA concentration and integrity were analysed on the 2100 Bioanalyzer (G2939BA, Agilent) with the RNA 6000 Pico Kit (5067-1513, Agilent) according to manufacturer instructions. RNA was DNase treated with the DNA-free Kit (AM1906, Invitrogen) and reverse-transcribed with the GoScript Reverse Transcription System (A5000, Promega) using random hexamers according to manufacturer instructions. A testis sample without GoScript reverse transcriptase (noRT) and a sample without RNA (no Input) was processed in parallel and served as negative controls. 5 ng of cDNA was amplified by GoTaq G2 HS Polymerase (M7405, Promega) for 30 cycles using specific primers for Malat1 (Forward (5'-3'): ATCGATTAAAGTAAATGGGCTA, reverse (5'-3'): TTACATGCAGGAACATTGACA) and Pgk2 (Forward (5'-3'): AAGTTTGATGAGAACATGCTAAAGT, reverse (5'-3'): CCTCCTCCTATAATGGTGACA). PCR products size was assessed by agarose gel electrophoresis. In Figure 5F, a part of the gel between the DNA ladder and Malat1 PCR

products was cut out because it contained an RT-PCR with a different primer set. For sperm, RNA concentration was assessed from 6 males per extraction method.

3.5.6. Quantification of disulfide bond reduction

The reduction of disulfide bonds was performed as described previously [20]. 1 mM 2,2'-dithiodipyridine (43791-1G, Sigma-Aldrich) was prepared in nuclease-free water and stored at 4 °C. Lysis buffers were prepared as follows and used for absorption reference measurement: Trizol, Buffer RLT+, 1 M guanidinium thiocyanate (G9277-100g, Sigma-Aldrich) in nuclease-free water, 50 mM β-mercaptoethanol (βME) in nuclease-free water, Trizol supplemented with 50 mM βME (Trizol/βME), Buffer RLT+ supplemented with 50 mM βME (RLT+/βME) and Trizol supplemented with 50 mM TCEP (Trizol/TCEP). The reduction of DTDP was quantified by measuring the absorption of 2-thiopyridone (2-TPD) at 343 nm using an Ultrospec 2000 (80-2106-00, Pharmacia Biotech). 980 µl of lysis solution was prepared in UV-cuvettes and 20 µl of 1 mM DTDP solution added. The solution was briefly mixed by pipetting and absorption measurements started 10 s after DTDP addition. All measurements for each solution were conducted in triplicates ($n = 3$).

3.5.7. Data, statistics and visualization

Data are represented as mean ± standard error of mean (SEM). Two groups were compared by unpaired t-test ($p < 0.05$). For comparisons in the DTDP assay, groups were analyzed by repeated measures one-way analysis of variance (ANOVA, $p < 0.05$) and significant effects were further analyzed by multiple comparison with Tukey's post-hoc test (adjusted p-value < 0.05). Graphs and statistics were prepared using the software GraphPad Prism 9. Contrast in microscopy pictures of Figure 5B was enhanced in Adobe PhotoShop 2021. Chemical reactions were drawn in ChemDraw19.

3.6. Conflict of Interest

The authors declare that the research was conducted in the absence of any commercial or financial relationships that could be construed as a potential conflict of interest. Funders had no role in the design of the study; in the collection, analyses, or interpretation of data; in the writing of the manuscript, or in the decision to publish the results.

3.7. Author Contributions

MR designed, performed, analyzed and interpreted all experimental work. IMM supervised and acquired funding for the study. MR and IMM wrote the manuscript. Both authors discussed the results and approved the final version of the manuscript.

3.8. Funding

This work was supported by University of Zurich, ETH Zurich, Swiss National Science Foundation (31003A_175742/1) and Slack-Gyr Foundation. MR was funded by the ETH Zurich Fellowship (ETH-10 15-2). The APC was funded by ETH Zurich.

3.9. Acknowledgments

The authors thank Dr. Irina-Elena Lazar-Contes and Maria-Andreea Dimitriu for discussions and critical comments on the original draft, Dr. Florentine Veenstra for advice on the DTDP assay, Prof. Johannes Bohacek for conceptual discussions, Dr. Silvia Schelbert for administrative support, and the animal care takers of the Laboratory Animal Services Center.

3.10. Data Availability Statement

The original contributions presented in the study are included in the article, further inquiries can be directed to the corresponding author.

3.11. Abbreviations

βME, β-mercaptoethanol; RNA, ribonucleic acid; 2-TDP, 2-thiopyridone; AGPC, Guanidinium thiocyanate-phenol-chloroform; PUFA, polyunsaturated fatty acids; TCEP, Tris(2-carboxyethyl)phosphine; DTDP, 2,2'-dithiodipyridine; RT-PCR, reverse transcription polymerase chain reaction; DTT, dithiothreitol; G&T-seq, genome and transcriptome sequencing; ANOVA, analysis of variance.

3.12. References

1. Buccitelli, C.; Selbach, M. mRNAs, proteins and the emerging principles of gene expression control. *Nat. Rev. Genet.* **2020**, doi:10.1038/s41576-020-0258-4.
2. Holoch, D.; Moazed, D. RNA-mediated epigenetic regulation of gene expression. *Nat. Rev. Genet.* **2015**, *16*, 71–84, doi:10.1038/nrg3863.
3. Quinn, J.J.; Chang, H.Y. Unique features of long non-coding RNA biogenesis and function. *Nat. Rev. Genet.* **2016**, *17*, 47–62, doi:10.1038/nrg.2015.10.
4. Landry, C.D.; Kandel, E.R.; Rajasethupathy, P. New mechanisms in memory storage: piRNAs and epigenetics. *Trends Neurosci.* **2013**, *36*, 535–42, doi:10.1016/j.tins.2013.05.004.
5. Ozata, D.M.; Gainetdinov, I.; Zoch, A.; O’Carroll, D.; Zamore, P.D. PIWI-interacting RNAs: small RNAs with big functions. *Nat. Rev. Genet.* **2019**, *20*, 89–108, doi:10.1038/s41576-018-0073-3.
6. Baldrich, P.; Rutter, B.D.; Karimi, H.Z.; Podicheti, R.; Meyers, B.C.; Innes, R.W. b. Plant extracellular vesicles contain diverse small RNA species and are enriched in 10- to 17-nucleotide “Tiny” RNAs. *Plant Cell* **2019**, *31*, 315–324, doi:10.1105/tpc.18.00872.
7. O’Brien, K.; Breyne, K.; Ughetto, S.; Laurent, L.C.; Breakefield, X.O. RNA delivery by extracellular vesicles in mammalian cells and its applications. *Nat. Rev. Mol. Cell Biol.* **2020**, *21*, 585–606, doi:10.1038/s41580-020-0251-y.
8. Krawetz, S.A. Paternal contribution: New insights and future challenges. *Nat. Rev. Genet.* **2005**, *6*, 633–642, doi:10.1038/nrg1654.
9. Bohacek, J.; Mansuy, I.M. Molecular insights into transgenerational non-genetic inheritance of acquired behaviours. *Nat. Rev. Genet.* **2015**, *16*, 641–652, doi:10.1038/nrg3964.
10. Rechavi, O.; Lev, I. Principles of Transgenerational Small RNA Inheritance in *Caenorhabditis elegans*. *Curr. Biol.* **2017**, *27*, R720–R730, doi:10.1016/j.cub.2017.05.043.
11. Stark, R.; Grzelak, M.; Hadfield, J. RNA sequencing: the teenage years. *Nat. Rev. Genet.* **2019**, *20*, 631–656, doi:10.1038/s41576-019-0150-2.
12. Chomczynski, P.; Sacchi, N. Single-step method of RNA isolation by acid guanidinium thiocyanate-phenol-chloroform extraction. *Anal. Biochem.* **1987**, *162*, 156–159, doi:10.1016/0003-2697(87)90021-2.
13. Boom, R.; Sol, C.J.A.; Salimans, M.M.M.; Jansen, C.L.; Wertheim-van Dillen, P.M.; van der Noordaa, J. Rapid and simple method for purification of nucleic acids. *J. Clin. Microbiol.* **1990**, *28*, 495–503, doi:10.1128/JCM.28.3.495-503.1990.
14. Toni, L.S.; Garcia, A.M.; Jeffrey, D.A.; Jiang, X.; Stauffer, B.L.; Miyamoto, S.D.; Sucharov, C.C. Optimization of phenol-chloroform RNA extraction. *MethodsX* **2018**, *5*, 599–608, doi:10.1016/j.mex.2018.05.011.
15. Ali, N.; Rampazzo, R.D.C.P.; Costa, A.Di.T.; Krieger, M.A. Current Nucleic Acid Extraction Methods and Their Implications to Point-of-Care Diagnostics. *Biomed. Res. Int.* **2017**, *2017*, 1–13, doi:10.1155/2017/9306564.
16. Flaherty, S.P.; Breed, W.G. The sperm head of the plains mouse, *Pseudomys australis*: Ultrastructure and effects of chemical treatments. *Gamete Res.* **1983**, *8*, 231–244, doi:10.1002/mrd.1120080304.
17. Bianchi, E.; Stermer, A.; Boekelheide, K.; Sigman, M.; Hall, S.J.; Reyes, G.; Dere, E.; Hwang, K. High-quality human and rat spermatozoal RNA isolation for functional genomic studies. *Andrology* **2018**, *6*,

- 374–383, doi:10.1111/andr.12471.
18. Peng, H.; Shi, J.; Zhang, Y.; Zhang, H.; Liao, S.; Li, W.; Lei, L.; Han, C.; Ning, L.; Cao, Y.; et al. A novel class of tRNA-derived small RNAs extremely enriched in mature mouse sperm. *Cell Res.* **2012**, *22*, 1609–1612, doi:10.1038/cr.2012.141.
19. Zirkin, B.R.; Naish, S.J.; Perreault, S.D. Formation and Function of the Male Pronucleus during Mammalian Fertilization. In *The Molecular Biology of Fertilization*; Elsevier, 1989; pp. 91–114.
20. Han, J.C.; Han, G.Y. A Procedure for Quantitative Determination of Tris(2-Carboxyethyl)phosphine, an Odorless Reducing Agent More Stable and Effective Than Dithiothreitol. *Anal. Biochem.* **1994**, *220*, 5–10, doi:10.1006/abio.1994.1290.
21. Lakbub, J.C.; Shipman, J.T.; Desaire, H. Recent mass spectrometry-based techniques and considerations for disulfide bond characterization in proteins. *Anal. Bioanal. Chem.* **2018**, *410*, 2467–2484, doi:10.1007/s00216-017-0772-1.
22. Hutchinson, J.N.; Ensminger, A.W.; Clemson, C.M.; Lynch, C.R.; Lawrence, J.B.; Chess, A. A screen for nuclear transcripts identifies two linked noncoding RNAs associated with SC35 splicing domains. *BMC Genomics* **2007**, *8*, 39, doi:10.1186/1471-2164-8-39.
23. Mason, P.E.; Neilson, G.W.; Dempsey, C.E.; Barnes, A.C.; Cruickshank, J.M. The hydration structure of guanidinium and thiocyanate ions: Implications for protein stability in aqueous solution. *Proc. Natl. Acad. Sci.* **2003**, *100*, 4557–4561, doi:10.1073/pnas.0735920100.
24. Baldwin, R.L. How Hofmeister ion interactions affect protein stability. *Biophys. J.* **1996**, *71*, 2056–2063, doi:10.1016/S0006-3495(96)79404-3.
25. Chang, J.Y.; Li, L. The unfolding mechanism and the disulfide structures of denatured lysozyme. *FEBS Lett.* **2002**, *511*, 73–78, doi:10.1016/S0014-5793(01)03284-7.
26. Chomczynski, P.; Sacchi, N. The single-step method of RNA isolation by acid guanidinium thiocyanate–phenol–chloroform extraction: twenty-something years on. *Nat. Protoc.* **2006**, *1*, 581–585, doi:10.1038/nprot.2006.83.
27. Thomas, S.N.; Friedrich, B.; Schnaubelt, M.; Chan, D.W.; Zhang, H.; Aebersold, R. Orthogonal Proteomic Platforms and Their Implications for the Stable Classification of High-Grade Serous Ovarian Cancer Subtypes. *iScience* **2020**, *23*, 101079, doi:10.1016/j.isci.2020.101079.
28. Ripin, N.; Boudet, J.; Duszczak, M.M.; Hinniger, A.; Faller, M.; Krepl, M.; Gadi, A.; Schneider, R.J.; Šponer, J.; Meisner-Kober, N.C.; et al. Molecular basis for AU-rich element recognition and dimerization by the HuR C-terminal RRM. *Proc. Natl. Acad. Sci.* **2019**, *116*, 2935–2944, doi:10.1073/pnas.1808696116.
29. Rhee, S.S.; Burke, D.H. Tris(2-carboxyethyl)phosphine stabilization of RNA: Comparison with dithiothreitol for use with nucleic acid and thiophosphoryl chemistry. *Anal. Biochem.* **2004**, *325*, 137–143, doi:10.1016/j.ab.2003.10.019.
30. Lismer, A.; Siklenka, K.; Lafleur, C.; Dumeaux, V.; Kimmins, S. Sperm histone H3 lysine 4 trimethylation is altered in a genetic mouse model of transgenerational epigenetic inheritance. *Nucleic Acids Res.* **2020**, *48*, 11380–11393, doi:10.1093/nar/gkaa712.
31. Jung, Y.H.; Sauria, M.E.G.; Lyu, X.; Cheema, M.S.; Ausio, J.; Taylor, J.; Corces, V.G. Chromatin States in Mouse Sperm Correlate with Embryonic and Adult Regulatory Landscapes. *Cell Rep.* **2017**, *18*, 1366–

- 1382, doi:10.1016/j.celrep.2017.01.034.
32. Hutchison, J.M.; Rau, D.C.; DeRouchey, J.E. Role of Disulfide Bonds on DNA Packaging Forces in Bull Sperm Chromatin. *Biophys. J.* **2017**, *113*, 1925–1933, doi:10.1016/j.bpj.2017.08.050.
33. Moore, H.; Dvoráková, K.; Jenkins, N.; Breed, W. Exceptional sperm cooperation in the wood mouse. *Nature* **2002**, *418*, 174–177, doi:10.1038/nature00832.
34. Robinson, B.S.; Johnson, D.W.; Poulos, A. Novel molecular species of sphingomyelin containing 2-hydroxylated polyenoic very-long-chain fatty acids in mammalian testes and spermatozoa. *J. Biol. Chem.* **1992**, *267*, 1746–51.
35. Zanetti, S.R.; de los Ángeles Monclús, M.; Rensetti, D.E.; Fornés, M.W.; Aveldaño, M.I. Ceramides with 2-hydroxylated, very long-chain polyenoic fatty acids in rodents: From testis to fertilization-competent spermatozoa. *Biochimie* **2010**, *92*, 1778–1786, doi:10.1016/j.biochi.2010.08.012.
36. Craig, L.B.; Brush, R.S.; Sullivan, M.T.; Zavy, M.T.; Agbaga, M.-P.; Anderson, R.E. Decreased very long chain polyunsaturated fatty acids in sperm correlates with sperm quantity and quality. *J. Assist. Reprod. Genet.* **2019**, *36*, 1379–1385, doi:10.1007/s10815-019-01464-3.
37. Ahumada-Gutierrez, H.; Peñalva, D.A.; Enriz, R.D.; Antollini, S.S.; Cascales, J.J.L. Mechanical properties of bilayers containing sperm sphingomyelins and ceramides with very long-chain polyunsaturated fatty acids. *Chem. Phys. Lipids* **2019**, *218*, 178–186, doi:10.1016/j.chemphyslip.2018.12.008.
38. Ganesan, M.; Kadalmali, B. Phase dependent discrepancy in murine vaginal micro-environment: A correlative analysis of PH, glycogen and Serum Estrogen upon exposure to Lapatinib Ditosylate. *Int. J. Pharm. Pharm. Sci.* **2016**, *8*, 404–407.
39. Byers, S.L.; Wiles, M. V.; Dunn, S.L.; Taft, R.A. Mouse estrous cycle identification tool and images. *PLoS One* **2012**, *7*, 2–6, doi:10.1371/journal.pone.0035538.
40. Nishigaki, T.; José, O.; González-Cota, A.L.; Romero, F.; Treviño, C.L.; Darszon, A. Intracellular pH in sperm physiology. *Biochem. Biophys. Res. Commun.* **2014**, *450*, 1149–1158, doi:10.1016/j.bbrc.2014.05.100.
41. Pessot, C.A.; Brito, M.; Figueroa, J.; Concha, I.I.; Yañez, A.; Burzio, L.O. Presence of RNA in the sperm nucleus. *Biochem. Biophys. Res. Commun.* **1989**, *158*, 272–278, doi:10.1016/S0006-291X(89)80208-6.
42. Kim, Y.-K.; Yeo, J.; Kim, B.; Ha, M.; Kim, V.N. Short Structured RNAs with Low GC Content Are Selectively Lost during Extraction from a Small Number of Cells. *Mol. Cell* **2012**, *46*, 893–895, doi:10.1016/j.molcel.2012.05.036.
43. Tang, Y.T.; Huang, Y.Y.; Zheng, L.; Qin, S.H.; Xu, X.P.; An, T.X.; Xu, Y.; Wu, Y.S.; Hu, X.M.; Ping, B.H.; et al. Comparison of isolation methods of exosomes and exosomal RNA from cell culture medium and serum. *Int. J. Mol. Med.* **2017**, *40*, 834–844, doi:10.3892/ijmm.2017.3080.
44. Schlegel, A.; Immelmann, A.; Kempf, C. Virus inactivation of plasma-derived proteins by pasteurization in the presence of guanidine hydrochloride. *Transfusion* **2001**, *41*, 382–389, doi:10.1046/j.1537-2995.2001.41030382.x.
45. Gilbert, I.; Bissonnette, N.; Boissonneault, G.; Vallée, M.; Robert, C. A molecular analysis of the population of mRNA in bovine spermatozoa. *Reproduction* **2007**, *133*, 1073–1086, doi:10.1530/REP-06-0292.

High efficiency RNA extraction from sperm cells using guanidinium thiocyanate supplemented with tris(2-carboxyethyl)phosphine

46. Shafeequ, C.M.; Singh, R.P.; Sharma, S.K.; Mohan, J.; Sastry, K.V.H.; Kolluri, G.; Saxena, V.K.; Tyagi, J.S.; Kataria, J.M.; Azeez, P.A. Development of a new method for sperm RNA purification in the chicken. *Anim. Reprod. Sci.* **2014**, *149*, 259–265, doi:10.1016/j.anireprosci.2014.06.032.
47. Macaulay, I.C.; Haerty, W.; Kumar, P.; Li, Y.I.; Hu, T.X.; Teng, M.J.; Goolam, M.; Saurat, N.; Coupland, P.; Shirley, L.M.; et al. G&T-seq: parallel sequencing of single-cell genomes and transcriptomes. *Nat. Methods* **2015**, *12*, 519–522, doi:10.1038/nmeth.3370.

Article

4. Chronic postnatal stress dysregulates maternal milk composition and alters offspring's early life physiology

This article is in preparation.

Martin Roszkowski conducted animal experiments, established and performed milk collection, analyzed and interpreted milk data, and wrote the article.

4.1. Abstract

Mothers milk is the main source of nutrients for infants and has been shown to modulate offspring's development, physiology and behaviour. However, the molecular mechanisms underlying this modulation and the effects of adverse conditions and mental states of the mother such as malnutrition, stress and depression on milk have yet to be clarified. This study examined the impact of chronic postnatal stress (CPS) on the mother's milk and the offspring's physiology using an established mouse model of early life trauma. At the end of the paradigm, dams' milk was collected by a newly established method, wherein mammary glands were excised and the milk retrieved through centrifugation. miRNAs were quantified in mammary gland milk and partially digested milk collected from pups' stomachs. Dams milk was analyzed by milk composition analysis and metabolomics. To investigate the potential effects in the offspring, pups' serum and plasma were analyzed by metabolomics and targeted amino acids analyses. Chronic postnatal stress stunted body weight development in dams and pups, and led to widespread dysregulation of milk macronutrients and metabolites. miR-16 and miR-375 were increased in CPS milk from mammary glands and partially mimicked in the milk retrieved from pups' stomachs. Individual metabolites were dysregulated in both dams' milk and pup serum. Network-based enrichment analysis of metabolites revealed dysregulated metabolite networks and amino acid imbalances in dams' milk and pups' blood, such as AGE-RAGE signaling or protein digestion and absorption. These changes were validated by targeted amino acid analysis. In the current study we bring evidence for CPS-induced metabolome and miRNA expression changes in the dams and their offspring, with potential metabolic and immunological consequences for the developing pups. Furthermore, our new milk collection method enables the parallel analysis of multiple biologically active compounds. Although our study could not provide causal evidence for the parent-offspring transmission of such compounds, our findings warrant further investigation on the effects of postnatal stress on lactation, consequences for the developing offspring, mechanisms of transmission and mitigation strategies.

4.2. Introduction

The postnatal period is a challenging and stressful time for mothers. Multiple factors such as sleep deprivation, hormonal changes, and demands of caring for the infant can contribute to postnatal stress, which can manifest as the relatively mild baby blues to a more severe postnatal stress syndrome. Any form of postnatal stress can serve as a precursor to the more serious postnatal depression, which has a reported incidence of 10 % to 20 % of all pregnancies [1]. These conditions are often accompanied by maternal separation anxiety, whereby the mothers feel extremely anxious when separated from their infant, even for short durations [2]. Critically, several epidemiological studies indicate an increased risk of psychological and physiological perturbations in offspring of mothers experiencing postnatal stress and depression [3–5].

However, the mediators of these effects to the offspring remain unclear. While impairment of maternal care [6] and energy provided through the milk [7] are likely contributors, it is plausible that stressed mothers actively transmit additional biological mediators to alter the offspring's physiology, behaviour and immune response. Lactation is a critical form of communication through which such biologically active compounds are transmitted from the mother to the offspring [8]. For example, infant behaviour was shown to be modulated by stress hormones such as cortisol [9] or endogenous opiates in the maternal milk [10].

These biological mediators can be influenced by the mothers physical and mental state and previous research in human and mouse indicates that maternal milk can alter the offspring's early development. Notably, stressed mothers transmit through milk to their offspring the stress hormone cortisol and the cytokine TNF- α , which have functional consequences for development [9,11]. On the contrary, positive environmental exposures, such as exercise, were shown to alter the oligosaccharide content of milk which improved the offspring's cardiac and metabolic health [12]. Similarly, protein-bound and free amino acids are on one hand important sources of nitrogenous components but have also been associated with weight gain and immune functions [13–15].

Furthermore, the mother's milk also contains nucleic acids in the form of RNAs and free monomeric nucleotides that may have a critical role in early development of the offspring [16]. Non-coding RNAs in milk, such as, microRNAs (miRNAs) can also serve as vectors of molecular communication between the mothers and offspring. miRNAs are packaged by extracellular vesicles or lipoproteins in the milk, which allow their preservation and may also help in their absorption. However, whether miRNAs are absorbed by the gut and competent to regulate gene expression in the intestinal epithelial cells and/or distal tissue is controversial. A study on mice with knock-out of miR-375 and miR-200c fed on milk from foster mothers that contained miR-375 and miR-200c did not reveal an uptake of these miRNAs in the majority of the pups' tissue. When the miRNAs were detected in the tissues, their copy numbers were too low for post-transcriptional regulation of their targets. Instead, it has been proposed that miRNAs in milk have a nutritional value [17,18]. On the contrary, other studies indicate the milk RNAs can be efficiently absorbed and delivered to tissues, such as spleen and liver [19].

Although human breast milk is readily collectible from breastfeeding mothers, investigating the effects of severe postnatal stress poses experimental and ethical challenges. Several rodent models were shown to induce behavioral and metabolic changes, particularly pre- and postnatal chronic stress. However, in contrast to humans, the collection of milk from mouse is challenging. Existing methods of milk collection in mice yield only limited amounts, thus precluding parallel characterization of milk composition, RNAs, and metabolites. Additionally, these methods typically involve prior stimulation with oxytocin that may impact the molecular composition of milk [11,12].

In this study, we established a novel milk collection method, which substantially increased the amount of milk retrieved from a single mouse, without the use of any potentially confounding agents. Using this method, we show that chronic postnatal stress affects lactating dams and induces substantial alterations in milk composition, and causes persistent miRNAs changes. By comparing the maternal milk metabolome with previously published pup serum metabolome changes using the same postnatal stress paradigm, we were able to identify commonly dysregulated metabolites with important functions for thermoregulation, energy metabolism, immune functions and organ development.

4.3. Results

4.3.1. Chronic postnatal stress dysregulates early life development and maternal milk macronutrients

Using an established mouse model of unpredictable maternal separation combined with unpredictable maternal stress [20], we assessed the maternal milk and offspring's physiology for the effects of chronic postnatal stress (CPS). The CPS paradigm consisted of unpredictable separation of the dams from their pups for three hours daily during postnatal day (PND) 1 to 14. During the separation, the dams were subjected to acute stress through forced swim and chronic restraint, and pups were placed outside the dams cage without nesting material [20]. Compared to control dams, CPS stunted the postnatal body weight development of dams (Figure 1A). Similarly, body weight of male and female pups from CPS mothers were decreased during development (Figure 1B,C). In addition to the stress of separation and disrupted feeding schedule, we observed that the pups nest temperature dropped significantly during the 3 hours of separation (Figure 1D). The stunted body weight development, particularly in pups, raised the question whether maternal milk composition was altered as a consequence of the unpredictable stress in dams and pups.

To obtain sufficient starting material for parallel analyses of maternal milk composition, metabolites and RNAs, we established a new method of milk collection without the need for hormonal stimulation and sedation for manual milk pumping. In brief, dams were euthanized and the abdominal skin was carefully separated from the abdominal wall muscles (Figure 2A). The clearly visible mammary glands were then carefully separated from surrounding tissues and stored on ice (Figure 2B,C, Supplementary Figure 1). The cut mammary gland tissues were then placed on 70 µm cell strainers and centrifuged at 2'000 rcf (Figure 2D). As a result, the milk was forced out of the cut mammary glands through centrifugal force and pooled in the collection tube. Our method of milk collection consistently yields 400 to 500 µl of milk per dam when performed at PND 14 (Figure 2E). The collected milk was then stored at -80 °C and used for differential analyses between the stressed and control dams.

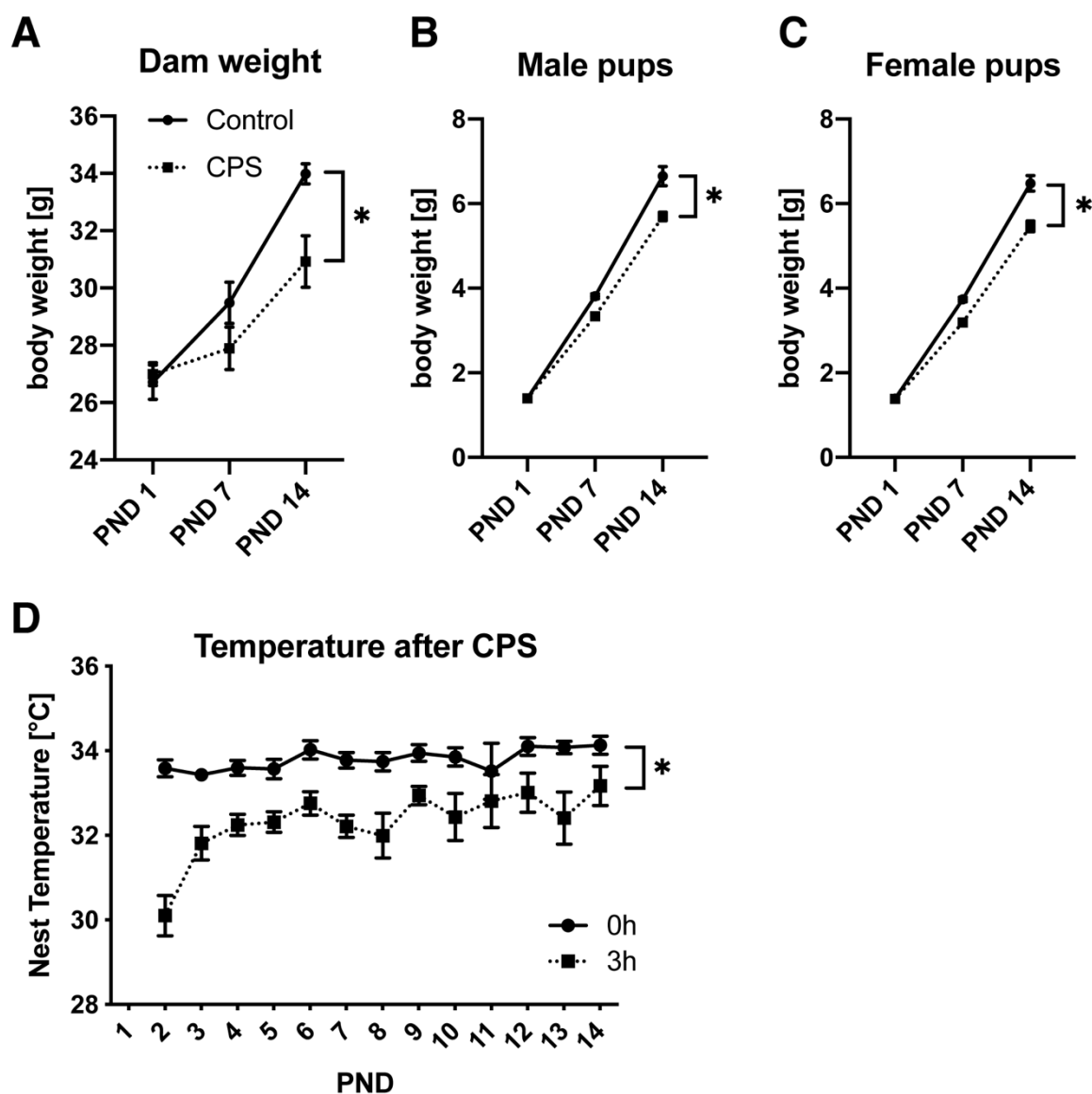


Figure 1: Chronic postnatal stress impaired weight development and decreased nest temperature. **(A)** Dam weight is decreased by CPS. **(B,C)** Weight of female and male pups is decreased by CPS. **(D)** Nest temperature in °C at the beginning (0h, black) and end (3h, blue) of the CPS paradigm from PND 2 until PND 14. Temperature of CPS nests was decreased at the end of the separation. *p-value < 0.05.

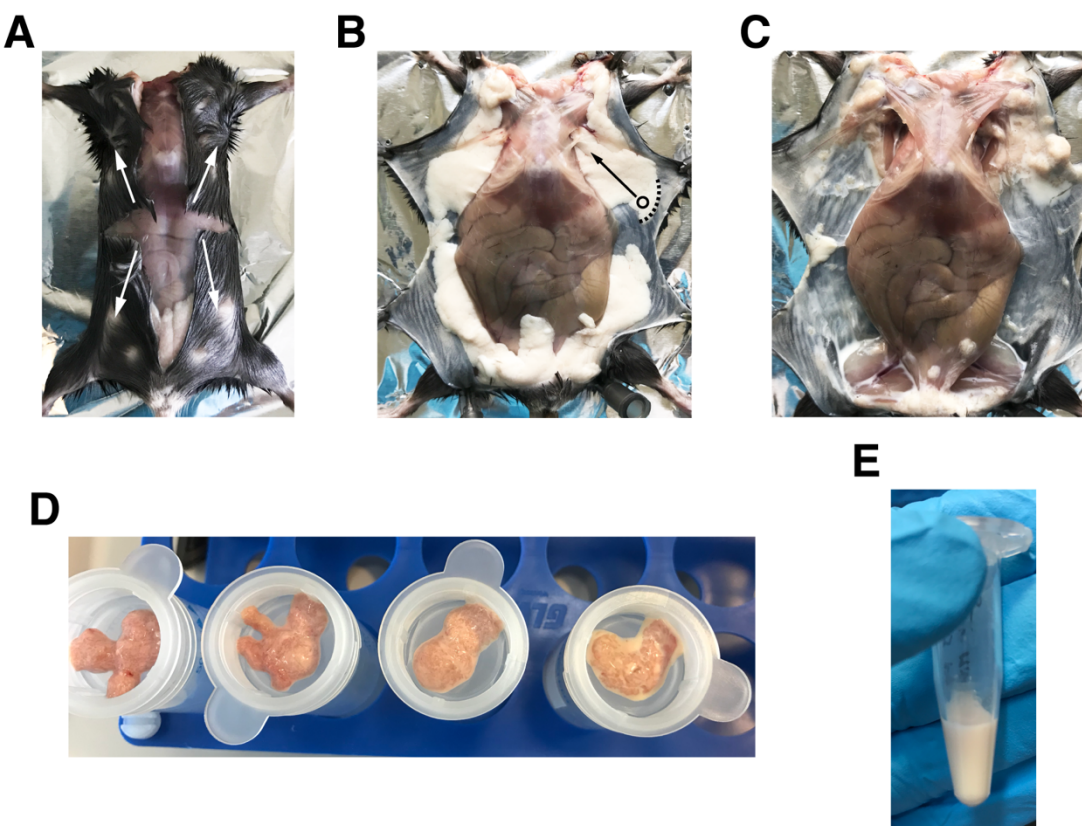


Figure 2: Collection of milk from mammary glands. **(A)** Separation of skin flaps from the abdominal muscle wall. **(B)** Visible mammary glands. Circle indicated holding point for forceps, dotted line indicates the site for initiating the separation of mammary glands from the skin and the arrow indicates the direction of separation. **(C)** Example of dam with excised mammary glands. **(D)** Mammary glands on cell strainers before centrifugation. **(E)** Example of approximately 500 μ l mouse milk collected from a single lactating dam.

4.3.2. Chronic postnatal stress increased miRNAs in maternal milk and digested milk from pups

Previously, we reported that CPS altered miRNAs such as miR-375 in the germ-line and serum [21] and lead to life-long and heritable dysregulation of glucose metabolism and insulin response [22,23]. A critical role in metabolic functions was previously shown for let-7-a, miR-16, miR-29a, and miR-375. Particularly miR-375 has been shown to be highly abundant in murine milk and was originally described as an important regulator of glucose metabolism and insulin secretion from pancreas [17,24,25]. Therefore, we first assessed whether CPS altered the milk miRNA signature.

Quantitative PCR-based quantification of miRNAs using *C.elegans* miR-39 as a spike-in control revealed a significant increase in miR-16 and miR-375 in the milk collected from CPS mothers (Figure 3A). We then investigated if these miRNAs were similarly altered in the partially digested milk clot extracted from the pups' stomach. However, changes in miRNA levels in partially digested milk were less pronounced with a trend towards increased miR-16 and significant increase in miR-29a (Figure 3B). Although miR-375 showed a similar increase as in the maternal milk, it was statistically not significant. As the milk in the pups' stomachs is present prior to the sacrifice of their mothers, this also indicates that the miRNA changes in the maternal milk are related to chronic postnatal stress and not acutely induced at the time of the sacrifice. To exclude a potential false miRNA signal by contaminating cells from the mammary gland tissue, we quantified the miRNAs in the mammary gland tissue of the dams and did not detect similar miRNA changes (Supplementary Figure 2).

In summary, we found that CPS increased miRNAs in the maternal milk which was recapitulated in the partially digested milk retrieved from the pups' stomachs.

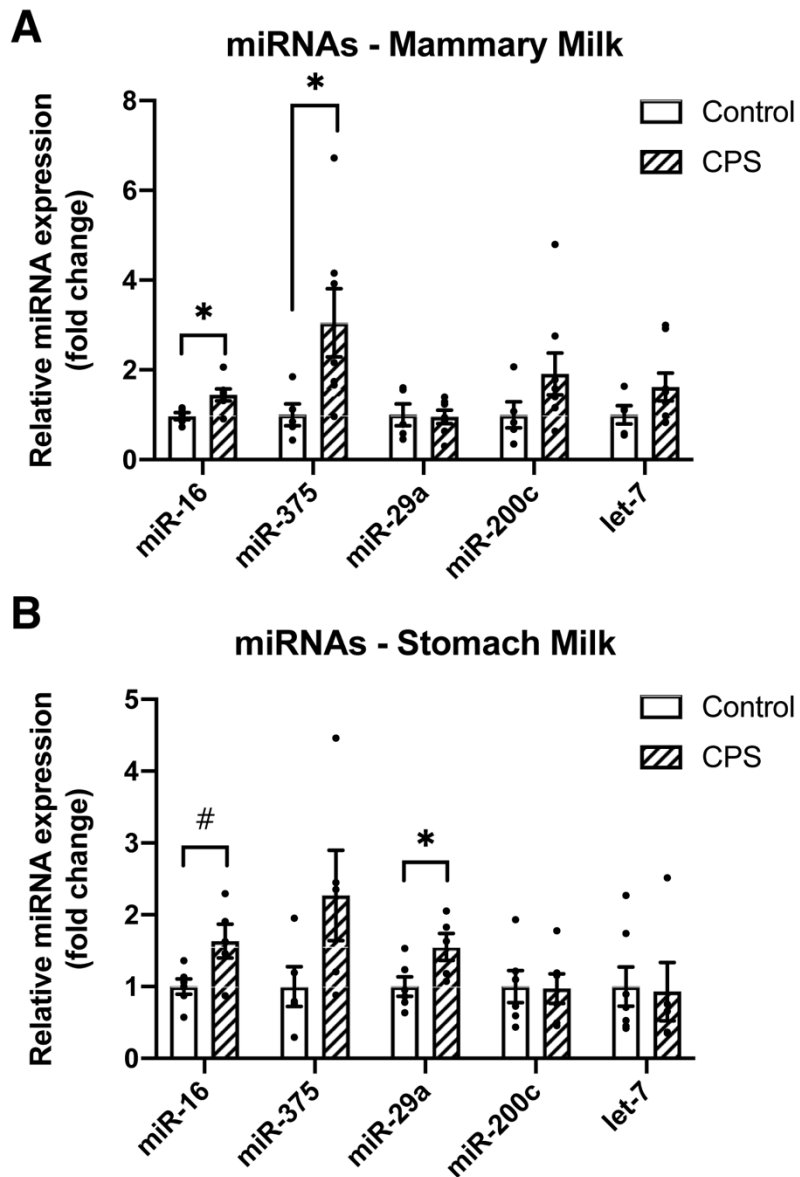


Figure 3: miRNAs quantified in milk from mammary glands and pup stomachs. **(A)** miR-16 and miR-375 was increased in CPS dams. **(B)** miR-29a was increased in CPS milk retrieved from pup stomachs. miR-16 and miR-375 were only marginally increased. n = 6 per group. #p-value < 0.06, *p-value < 0.05.

4.3.3. Maternal milk macronutrients and metabolites are dysregulated by chronic postnatal stress

A decreased miR-375 expression was previously shown to increase insulin secretion and glucose levels [25]. To assess a potential impact on maternal milk composition, we quantified the main macronutrients by targeted chemistry composition analysis. In CPS maternal milk, glucose was significantly decreased (Figure 4A) and albumin marginally increased (Figure 4B). There were no significant differences in triglycerides (Figure 4C) and cholesterol was below the detection range of the analyzer (data not shown). However, these macronutrients are composed of many individual metabolites which were not distinguishable by the chemistry analysis.

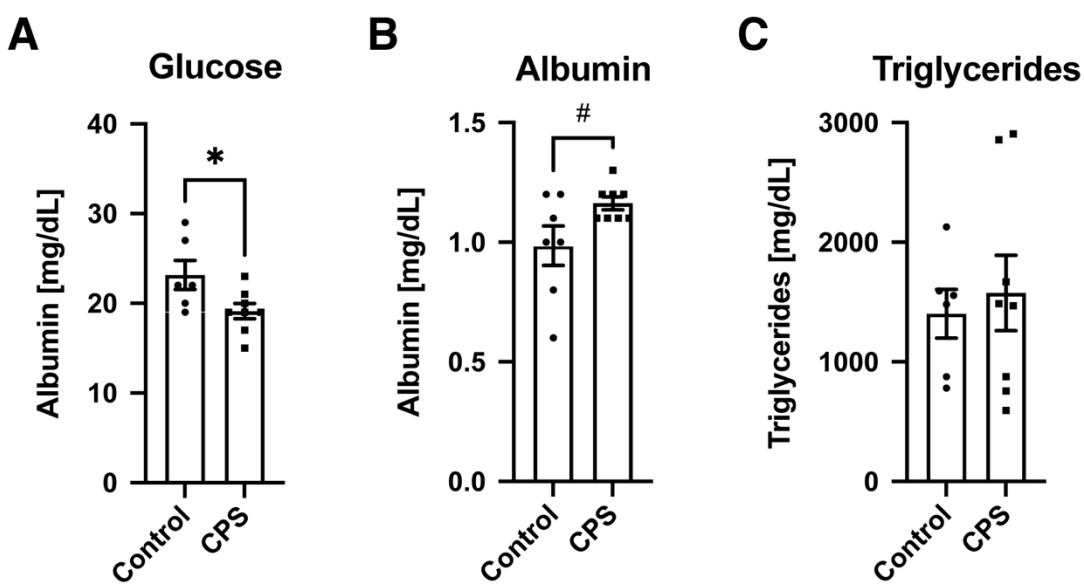
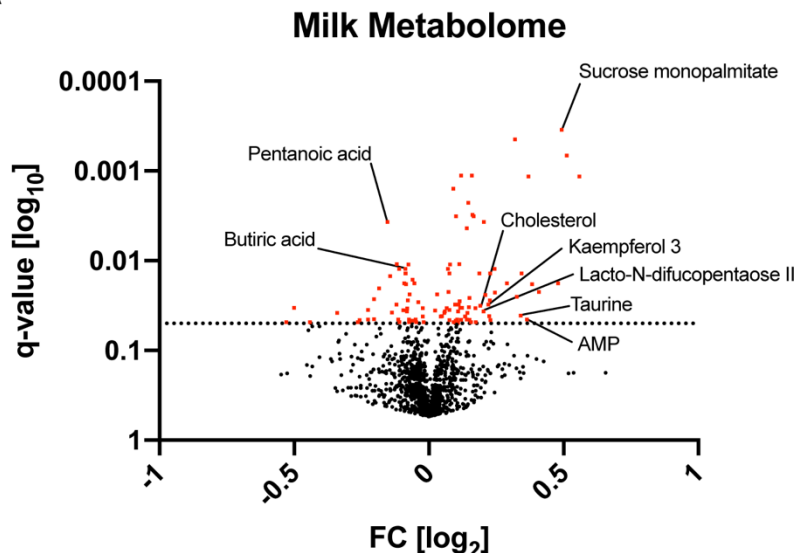


Figure 4: Quantification of mammary milk macronutrients. (A-C) Measurement of glucose, albumin and triglycerides in milk from mammary glands by chemistry analysis. ($n = 6$) (A) Glucose was significantly decreased and (B) albumin marginally increased in CPS milk. (C) Triglycerides were not changed by CPS. # p -value < 0.6, * p -value < 0.05.

To address these limitations, we investigated the maternal milk metabolome by mass spectrometry and annotated the 1425 detected metabolites using the human metabolome database (HMDB) and the Kyoto Encyclopedia of Genes and Genomes (KEGG). In CPS maternal milk, 45 metabolites were significantly decreased and 69 increased (Figure 5A, Supplementary Table 1, q -value < 0.05). The increased sensitivity of the mass spectrometry found that cholesterol, an essential lipid component for membranes and precursor for steroid hormones [26], was increased in CPS milk. Similarly, we found butyric and pentanoic acid,

both short-chain fatty acids making up triglycerides, to be decreased in CPS milk. In conclusion we found that macronutrients in maternal milk were affected by CPS and further metabolome analysis revealed over 100 hundred affected metabolites.

A



B

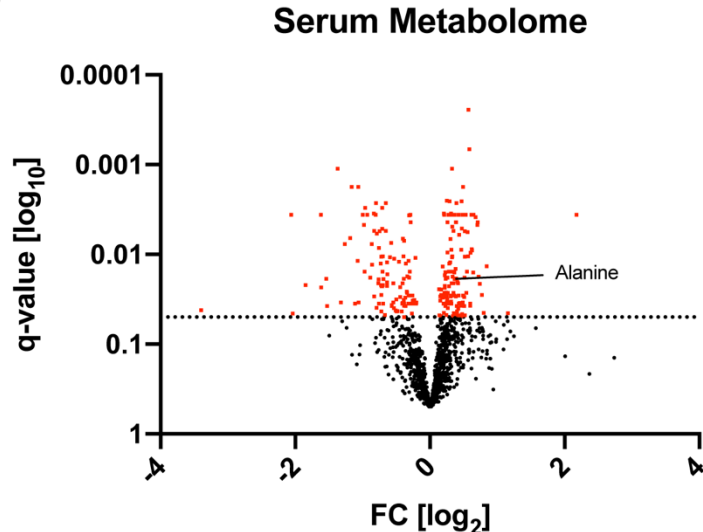


Figure 5: Metabolomics of maternal milk and PND14 serum after CPS. **(A,B)** Volcano plot of altered metabolites. Altered metabolites with $q\text{-value} < 0.05$ are highlighted as red squares and were plotted against their log-fold change. **(A)** CPS altered the maternal milk metabolome ($n = 12$ per group) and **(B)** previously published serum metabolome of offspring ($n = 5$ per group, see Ref. [23]). Dotted line indicates $q\text{-values} < 0.05$.

4.3.4. Chronic postnatal stress dysregulates physiologically important metabolites and networks in maternal milk and offspring blood

To assess the potential consequences of altered maternal milk metabolites and miRNAs for pups, we included previously published serum metabolome changes of PND14 pups subjected to CPS in our subsequent analyses (Figure 5B, Supplementary Table 2, see Ref. [23]). First, we compared metabolites that were significantly altered by CPS in both maternal milk and pup serum (Figure 6A, Supplementary Table 3, p-value < 0.05). For further analysis of the 23 dysregulated metabolites, we grouped them into three classes using the chemical classification by ClassyFire and literature search (Supplementary Table 3) [27]. This revealed that the majority of concomitantly altered metabolites belonged to the two sub-classes “lipid metabolism” (Figure 6A, blue triangles) and “amino acids, peptides, and analogues” (Figure 6A, red squares) which are important for the developing mouse metabolism. Furthermore, 4 metabolites from various classes with previously known functions in mouse physiology were also observed in both maternal milk and pup serum (Figure 6A, black dots).

In summary, we observed that CPS altered metabolites in maternal milk and the offsprings' serum. The classification of altered metabolites revealed that they primarily belonged to the classes of lipids and amino acids indicating a dysregulation with potential consequences for the pups physiological response to environmental challenges and stress.

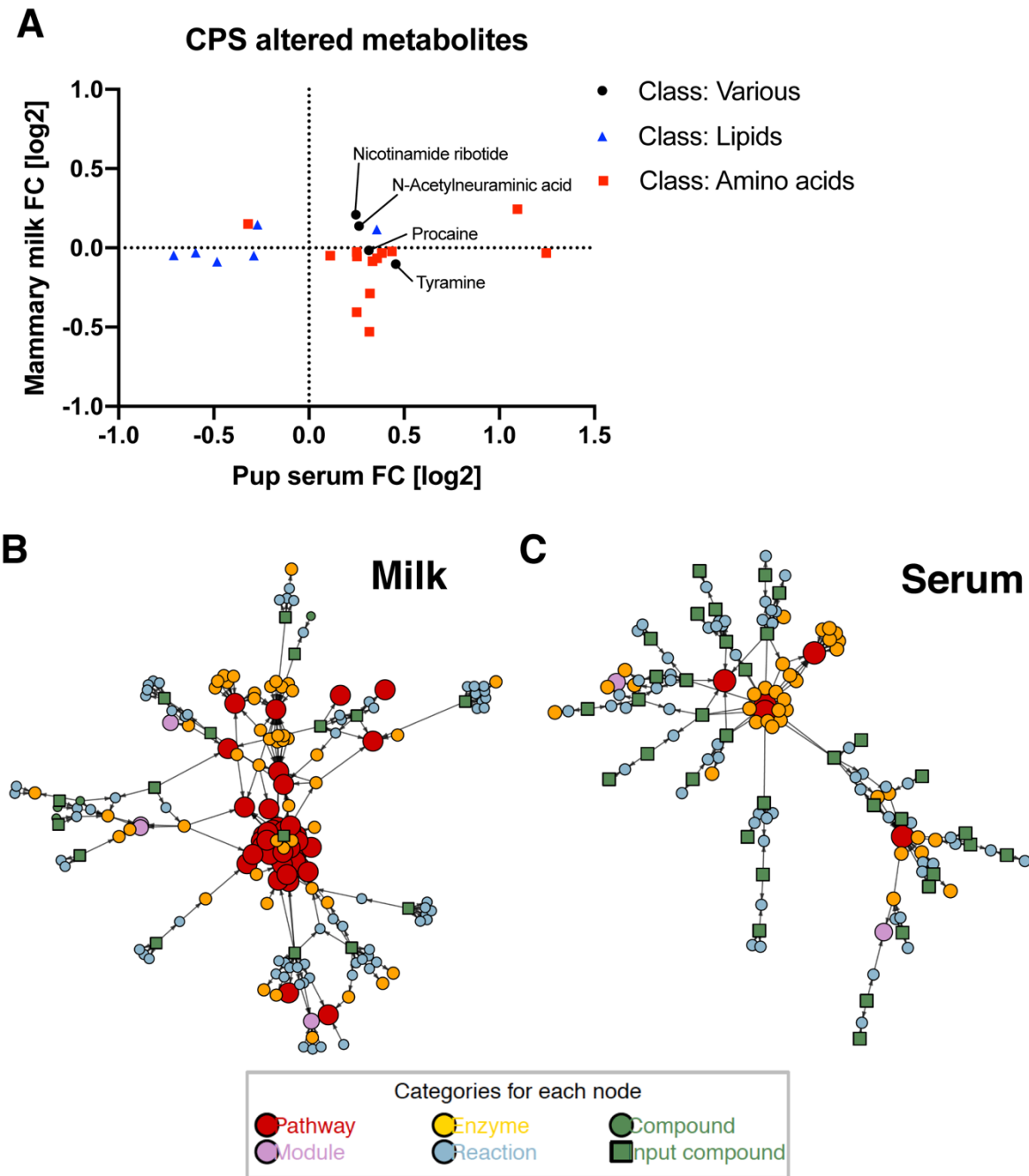


Figure 6: Comparison and network-enrichment of altered maternal milk and pup serum metabolites. **(A)** Metabolites that were significantly altered by CPS in maternal milk and pup serum were plotted according to their fold change. Based on their chemical properties, they were grouped in the classes lipids, amino acids and various. **(B)** Network-enrichment analysis of significantly altered metabolites in mammary gland milk and **(C)** pup serum. Nodes represent enriched KEGG pathways (red), modules (violet), enzymes (yellow), reactions (blue) and compounds (green circles). The significantly altered metabolites used as input are highlighted as green squares.

4.3.5. Dysregulated metabolite networks and amino acid imbalances in maternal milk and pup serum

To further elucidate the potential impact of the CPS altered metabolites on the offspring's development, we performed a network-based enrichment analysis on the significantly altered maternal milk and pup serum metabolites [28]. In maternal milk, 36 KEGG pathways were enriched after CPS (Figure 6B, Supplementary Table 4), notably the pathways for AGE-RAGE signaling, pancreatic secretion, protein digestion and absorption, and cholesterol metabolism. Network-based analysis of the offspring serum metabolome identified enriched KEGG pathways for glycine, serine and threonine metabolism, renin-angiotensin system, mineral absorption, central carbon metabolism and protein digestion and absorption (Figure 6C, Supplementary Table 5).

Comparing the enriched networks, we found that the pathway for protein digestion and absorption was enriched in CPS maternal milk (Supplementary Figure 3) and offspring serum (Supplementary Figure 4). The network-based enrichment in offspring serum also revealed several intermediate amino acids in this pathway (Supplementary Figure 4, blue dots) and metabolites that were shared with the pancreatic secretion pathway (Supplementary Figure 5). These findings complemented our initial observation that amino acids were dysregulated by CPS in maternal milk and pup serum (Figure 6A).

However, our initial metabolomics screen was unable to resolve certain amino acids in sufficient resolution and they were collapsed into groups, such as alanine, β -alanine and sarcosine which have a very similar chemical composition and mass. Despite their similarities, the blood concentration and physiological importance of such amino acids is vastly different. To further investigate a potential amino acid dysregulation, we performed targeted amino acid analysis in pup serum from a different CPS cohort (Supplementary Table 6). This targeted analysis revealed that alanine was not altered in CPS serum of the second cohort (Figure 7A), unlike the initial analysis where alanine-like metabolites were significantly increased in the serum metabolomics analysis (Figure 5B). The targeted analysis revealed that β -alanine was significantly decreased and sarcosine increased in CPS serum of the second cohort (Figure 7B,C). β -alanine is a non-proteinogenic amino acid and primarily metabolized to form carnosine in brain and muscles, a dipeptide of particular importance for improved skeletal muscle performance. Sarcosine is a byproduct of glycine synthesis and is increased by dietary

restriction [29]. Furthermore, the semi-essential amino acids arginine and cysteine were increased in PND14 serum (Figure 7D,E).

Our targeted amino acid analysis using pups from a different cohort substantiated the initial metabolome screen and network-based enrichment analysis that alanine-like metabolites (alanine, β -alanine and sarcosine) and other amino acid pathways were dysregulated by CPS in maternal milk and pup serum.

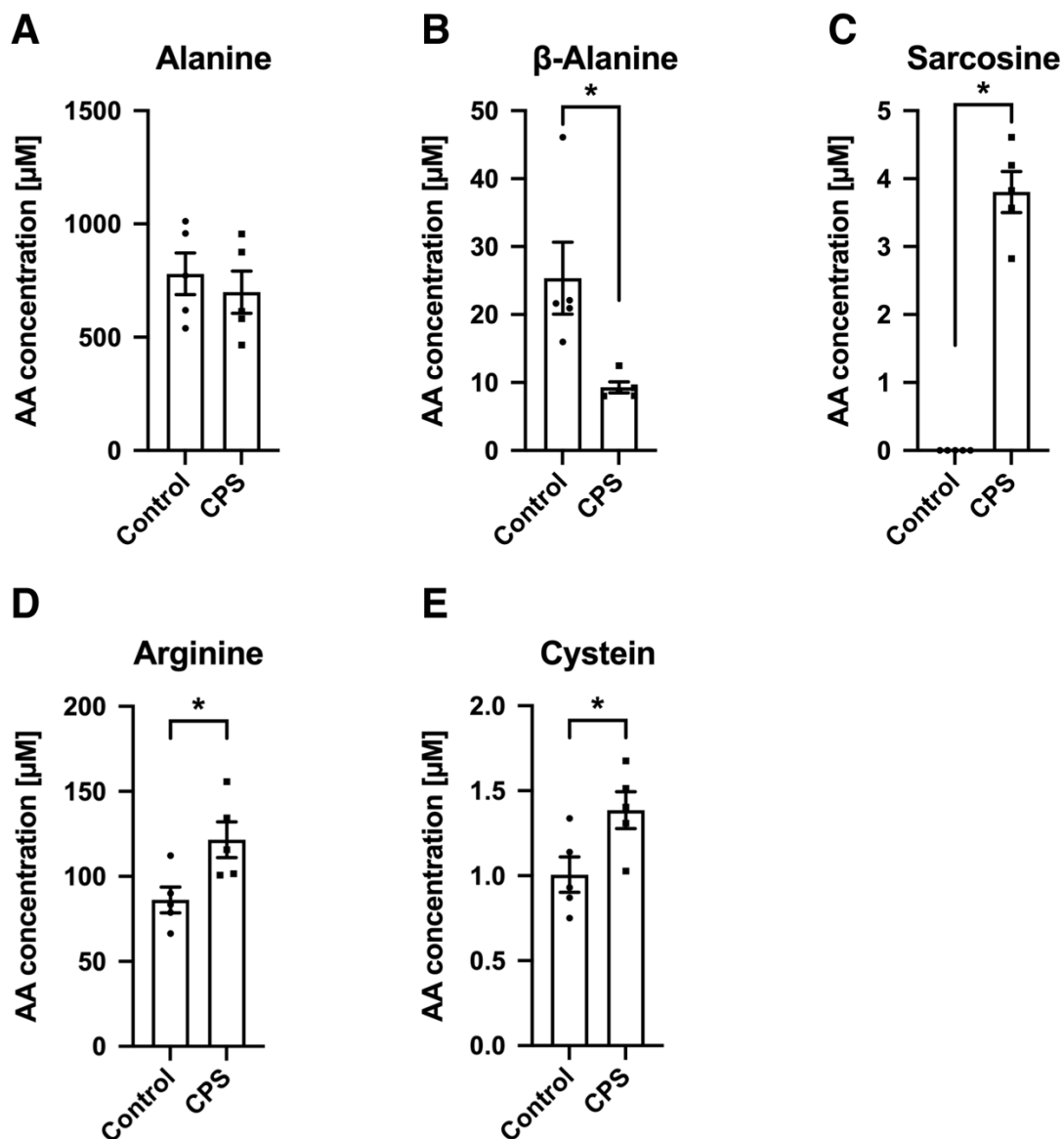


Figure 7: Comparison Targeted amino acid analysis of pup serum. (A-E) Amino acid concentration in μM from serum of control and CPS pups. ($n = 5$ per group) (A) Alanine was not changed by CPS. (B) β -alanine was significantly decreased after CPS. (C) Sarcosine was absent in serum from control pups and increased after CPS. (D) Arginine and (E) cysteine were increased in CPS serum. * p -value < 0.05.

4.4. Discussion

Milk is a direct form of communication between the mother and the pups during early life. Understanding if biologically active components of the milk were altered by CPS and whether they could act upon the developing offspring with potentially life-long consequences was important for understanding long-term effects. Previously, we've shown that CPS also affects offspring's behavior, metabolism, bones and the germline, which also affect subsequent generations [21–23,30–37]. This study showed that CPS can alter the composition of milk. The observed changes were associated with stunted weight development in CPS pups that mirrors the stunted weight of the CPS dams during the same time period, suggesting a dysregulation in early life metabolism of these pups.

Our analyses revealed that the miRNA signature was altered in maternal milk as well as the ingested milk in pups' stomachs. We could not conclusively show a direct modulatory role of the upregulated miR-375, miR16 and miR-29a on the early life development and metabolic regulation in pups. However, our comparisons between maternal milk and pup serum metabolomes revealed numerous changes which in parts also overlapped between the two. The altered metabolites have functional properties for milk, nutrition and digestion, such as sucrose monopalmitate, an important fatty acid for milk emulsion [38]; kaempferol 3, a common flavonoid in human breast milk [39]; lacto-N-difucopentasoe II, an oligosaccharide and substrate for bacterial metabolism in intestine [40] and adenosine monophosphate, a nucleotide which contributes to energy and RNA metabolism [41]. We also observed taurine to be increased after CPS in maternal milk. Taurine is highly abundant in milk [42,43] and a previous study in mice showed that chronic restrain stress in lactating dams increased the level of amino acids taurine and cystathionine in milk that, in case of taurine, also correlated with the level of corticosterone in the dams' blood [44].

The decreased nest temperature after the separation from the dams, the stunted pup weight development and changes in maternal milk glucose raised the question whether thermogenesis and regulation were affected by CPS. Considering that pups lack developed brown adipose tissue, which is usually the main source of thermogenesis in adult mice, they rely primarily on passive body heat provided by the mother and thermal insulation in their nest. Muscle shivering thermogenesis is a known alternative to generate body heat [45] and more milk albumin may contribute to the buildup of muscle mass in pups to facilitate such a switch.

Furthermore, we found 4 metabolites that were dysregulated in maternal milk and offsprings' serum with potential thermoregulatory functions. Procaine is a known vasoconstrictor and was previously shown to increase body temperature in rats [46]. Tyramine is derived from the amino acid tyrosine and serves as a substrate for adrenergic uptake systems and monoamine oxidase, thereby prolonging the actions of adrenergic transmitters. Tyramine increase was previously reported to be a nutritional stress response [47] and to amplify thermoregulation [48]. Nicotinamide ribotide is a potent NAD⁺ precursors which has previously been shown to improve mitochondrial capacity and biogenesis in skeletal muscles of rodents, and reduce circulating inflammatory cytokines in human [49,50]. N-Acetylneurameric acid is the most abundant sialic acid and implicated in brain development and immunity [51].

Previous work from our lab has shown that fatty acid metabolism and arachidonic acid precursors are altered in the blood of male mice exposed to early-life traumatic stress [23]. Therefore, our initial interpretation of the altered metabolites focused primarily on pathways important for the energy metabolism of developing pups. However, our analyses of miRNAs, metabolites and amino acids also suggested an impact of CPS on the developing immune system. For example, miR-16 has anti-inflammatory functions and was increased in CPS milk [52]. miR-16 is a constitutive modulator of immune response and known regulator of TNF- α . Similarly, we saw an increase in circulating amino acids such as arginine and cysteine. Arginine is primarily known as a precursor in protein biosynthesis. However, arginine metabolism has also been extensively studied in its regulatory function of the immune response [53]. More broadly, our metabolite network analysis flagged the AGE-RAGE signaling pathway to be enriched in maternal milk and pup serum, and warrants further investigation on the potential impact of CPS on the developing immune system.

Despite our advancements in milk collection and analysis, further challenges remain in establishing causality between changes in the composition, miRNA or metabolite content of mother's milk and the complex physiological changes in pups. The weight loss in the pups could be influenced by impairment of maternal care due to postnatal stress or due to maternal separation during the time the mother is exposed to stress. In follow-up investigations, it will be important to control for these confounding factors by adopting cross-fostering or cross-lactation strategies, in which pups born to non-stressed mothers are fostered by dams exposed to postnatal stress and vice-versa. Subsequently, it will be of interest to investigate whether pups can signal their changed nutritional demand to their mothers through biological mediators

or other currently unknown behavioural or acoustic cues. Finally, it is vital to identify if dietary supplementation and/or environmental enrichment could mitigate the effects of maternal postnatal stress on milk composition, metabolites, and miRNAs. Ongoing work to prove a causal link between postnatal stress and these changes, as well as, between these changes and offspring development could have important implications for breastfeeding, the composition of milk formulas and wellbeing of infants.

4.5. Materials and Methods

4.5.1. Animals

Animal experiments were conducted in strict adherence to the Swiss Law for Animal Protection and were approved by the cantonal veterinary office in Zürich under license number 57/2015 and 83/2018. C57Bl/6J mice were obtained from Janvier (France) and bred in-house to generate mice for experiments. Mice were housed in groups of 3 to 5 animals in individually ventilated cages. Animals were kept in a temperature- and humidity-controlled facility on a 12h reversed light/dark cycle (light on at 20:00, off at 8:00) with food (M/R Haltung Extrudat, Provimi Kliba SA, Switzerland) and water *ad libitum*. Cages were changed weekly.

4.5.2. Chronic postnatal stress, body weight and temperature measurements

3-month old C57Bl/6J primiparous females were paired with age-matched males for one week. Following birth of pups, dams were randomly assigned to chronic postnatal stress (CPS) or control groups. Assignment was done in a way to balance litter size and number of animals across groups. Dams assigned to CPS group were separated from their pups for 3 hours per day unpredictably from postnatal day (PND) 1 to 14 as described previously [20]. Separation onset was at an unpredictable time within the 3 hours, and during separation, each mother was exposed to an acute swim in cold water (18 °C for 5 min) or restraint for 30 min. Control animals were undisturbed apart from cage changes once per week. Weight of mothers and pups was measured during weekly cage changes. Nest temperature was measured with an electronic thermometer at the beginning and end of the CPS paradigm.

4.5.3. Milk collection

After decapitation, place the mouse on its back on a 20 cm x 20 cm styrofoam pad wrapped in aluminium foil. We recommend the decapitation of mice and blood drainage to reduce the potential of blood spilling onto mammary tissue during the dissection procedure.

Stretch the limbs perpendicularly to the body axis and fix each paw with a pin needle to the pad. After dousing the fur with 70 % ethanol, perform an anterior to posterior incision with a pair of scissors along the ventral mid-line starting from the decapitated neck down to the urethral orifice. Next, cut the skin laterally along the thorax-abdomen division (Figure 2A). Pay attention to only cut the ventral skin but not the abdominal wall muscles. As indicated by the arrows in (Figure 2A), pull the skin at the incised corners with forceps and carefully separate with a new No. 10 scalpel the skin from the abdominal wall. Pull the skin perpendicular to the body axis and fix it with pin needles to the pad. In our experience, unwanted damage to the mammary glands can be avoided by applying sufficient tension between the skin and abdominal wall (by pulling the skin and if necessary, stretching the limbs more) and running the scalpel along the connective tissue without applying any pressure to the blade. The mammary glands are located between the skin and abdominal wall and remain attached to the skin (Figure 2B). Typically, a lactating mouse will have pronounced mammary glands that are visibly white and swollen by the milk (Supplementary Figure 1A,B, right). In contrast, empty mammary glands have a yellow to orange colour (Supplementary Figure 1A,B, left).

To collect the mammary glands, hold the lateral corner of the gland with serrated forceps (Figure 2B, circle) and cut the connecting tissue between the skin and mammary gland with the scalpel (Figure 2B, dashed line). Similar to the separation of skin from the abdominal muscles, not a lot of pressure is required on the blade and instead the tension between glands and skin should be kept high. The skin can be stretched with additional pin needles to facilitate this step. The mammary glands are more strongly connected to the skin at the nipples and may require multiple cuts for separation. Proceed with the separation from the skin towards the armpits of the mouse (Figure 2B, arrow direction). Lift the mammary gland for the final separation from the skin and muscle wall as we noticed that a major blood vessel in the armpit and hip of the mouse is typically nicked during the last cuts (Supplementary Figure 1C, dashed circles). By lifting the mammary gland, unwanted contact with blood can be reduced. Alternatively, the blood vessel can be cut beforehand and the escaping blood soaked up with pieces of tissue. Finally, place the collected mammary gland in a plastic petri dish on ice until further processing. We recommend to first collect the cervical and thoracic mammary glands before proceeding to the abdominal and inguinal mammary glands. The pad with the mouse can be turned between the collection of the right and left mammary glands so that the

experimenter can comfortably and steadily perform the cuts. Instead of cutting, the surgical blade can be also used to gently scrap the skin while pulling the mammary gland tissue.

After the dissection of all mammary glands (Figure 2C) the mammary glands are perforated with the surgical blade. Hold the mammary glands with the forceps and make deep cuts with the scalpel. We recommend performing 20 cuts and then turn the mammary gland to cut the other side also 20 times. Place the perforated mammary glands in a 70 µm cell strained. We recommend using 4 cell strainers per mouse to avoid a clogging of the mesh by excess tissue (Figure 2D). Milk may already escape the mammary glands during the dissection or the perforation steps. To maximize the recovery, we suggest collecting such milk with a pipette and transfer it either directly to the collection tube or add it to the mammary glands in the cell strainer. Avoid the collection of milk that came in contact with escaped blood.

Finally, centrifuge the mammary glands at 2'000 rcf in a swinging bucket rotor for 5 min. This step forces the milk out of the mammary glands into the collection tube. After centrifugation, first remove the small blood pellet at the bottom of the tube with a 20 µl pipette. We suggest to first perfuse the mice with PBS if any contact between milk and blood has to be excluded for experimental reason. Next, transfer and pool the milk from all 4 tubes for final storage or further processing (Figure 2E). Note, that during the centrifugation the fatty milk components can separate from the aqueous milk components. To collect all milk, use a wide-bore pipette (e.g. 1000 µl pipette) to resuspend the fatty milk components found at the bottom and the walls of the tube using the aqueous milk. Alternatively, any fatty milk remaining in the tube can be resuspended with 100 µl PBS.

4.5.4. Metabolite quantification and enrichment analysis

Metabolites were extracted from 10 µl milk 3 times with 70 % ethanol at 75 °C. Extracts were analysed using flow injection – time of flight mass spectrometry (Agilent 6550 QTOF) operated in negative mode, as described previously [23]. Distinct mass-to-charge (m/z) ratio could be identified in each batch of samples (typically with 5,000-12,000 ions). Ions were annotated by aligning their measured mass to compounds defined by the HMDB and KEGG database, allowing a tolerance of 0.001 Da. Only deprotonated ions (without adducts) were considered in the analysis. When multiple matches were identified, such as in the case of structural isomers, all candidates were retained.

Altered milk or serum metabolites (q -value < 0.05) were used for network-enrichment of mouse KEGG components such as pathways, reactions and enzymes by FELLA R package [28]. In brief, metabolites with a KEGG identifier were enriched using the heat diffusion method, followed by statistical normalization using parametric z-scores. Enriched components (p -value < 0.05) are listed in Supplementary Tables 4 and 5. Enriched networks were visualized using the FELLA plot function with the function “diffusion” and a node limit of 250.

4.5.5. Targeted amino acid analysis

Samples were centrifuged at 1300 rpm for 5 min. 20 μ l of the supernatant were precipitated with 10 % SSA/250 μ M Norvaline. The solution was centrifuged again at 13000 rpm for 5 min. 20 μ l of supernatant was mixed with 60 μ l 0.5 M borate buffer (pH 9) and 20 μ l 2AMassTrak were derivatized for 10 min at 50 °C. 1/100 μ l of sample were injected and run on MassTrak. Data were acquired for 45 min.

4.5.6. miRNA expression analysis

For miRNA expression assays, RNA was extracted using a phenol/chloroform extraction method (Trizol; Thermo Fischer Scientific). Reverse transcription was performed on purified RNA samples with miScript II RT reagents (Qiagen) using HiFlex buffer. RT-qPCR was performed with QuantiTect SYBR (Qiagen) on a Light Cycler II 480 (Roche) using miScript Primers Assays (Qiagen) for miR-16, miR-375, miR-29a, miR-200c, let-7-a and the *C. elegans* spike-in control miR-39. All samples were run in triplicate under the following cycling conditions: 95° C for 15 min, 45 cycles of 15 sec at 94° C, 30 sec at 55° C, 30 sec at 70° C, followed by melt curve with gradual temperature increase until temperature reached 95° C. Melt curve analysis confirmed amplification of single products for each primer. Primer sequences are proprietary (Qiagen).

4.5.7. Data, statistics and visualization

Data are represented as mean \pm standard error of mean (SEM). Statistical outliers were identified by the ROUT method ($Q = 0.5\%$) and removed for further analysis. Dam and pup body weight development was analyzed using a mixed-effects model using maximum likelihood method ($p < 0.05$). Two groups were compared using unpaired t-test ($p < 0.05$). Graphs were prepared using the software GraphPad Prism 9 and R.

4.6. Conflict of Interest

The authors declare that the research was conducted in the absence of any commercial or financial relationships that could be construed as a potential conflict of interest. Funders had no role in the design of the study; in the collection, analyses, or interpretation of data; in the writing of the manuscript, or in the decision to publish the results.

4.7. Authors and Contributions

Martin Roszkowski, Ali Jawaid, Irina Lazar-Contes, Gretchen van Steenwyk, Marina Kunzi, Francesca Manuella, Nicola Zamboni, Isabelle Mansuy

MR, AJ and IMM designed experiments. MR, IL, GvS and FM performed animal experiments. MR and AJ established milk collection method. MR, AJ and MK performed and analyzed all milk related experiments. GvS performed targeted amino acid analysis. NZ performed and analyzed metabolomics. MR performed bioinformatics analyses. MR and AJ interpreted experimental results. IMM and AJ acquired funding for the study. MR, AJ, IL and IMM wrote the manuscript.

4.8. Funding

This work was supported by University of Zurich, ETH Zurich, Swiss National Science Foundation (31003A_175742/1) and Slack-Gyr Foundation. MR was funded by the ETH Zurich Fellowship (ETH-10 15-2).

4.9. Acknowledgments

The authors thank Maria-Andreea Dimitriu for discussions and critical comments on the original draft, Dr. Eloïse Kremer for conceptual discussions, Niharika Obrist for experimental support, Deepak K. Tanwar for bioinformatics support, Dr. Silvia Schelbert for administrative support, the Functional Genomics Center for proteomics and targeted amino acid analysis, and the animal care takers of the Laboratory Animal Services Center.

4.10. Data Availability Statement

The original contributions presented in the study are included in the article, further inquiries can be directed to the corresponding author.

4.11. References

1. Norhayati, M.N.; Nik Hazlina, N.H.; Asrennee, A.R.; Wan Emilin, W.M.A. Magnitude and risk factors for postpartum symptoms: A literature review. *J. Affect. Disord.* **2015**, *175*, 34–52, doi:10.1016/j.jad.2014.12.041.
2. Scher, A.; Hershkovitz, R.; Harel, J. Maternal separation anxiety in infancy: Precursors and outcomes. *Child Psychiatry Hum. Dev.* **1998**, *29*, 103–111, doi:10.1023/A:1025031931770.
3. Oyetunji, A.; Chandra, P. Postpartum stress and infant outcome: A review of current literature. *Psychiatry Res.* **2020**, *284*, 112769, doi:10.1016/j.psychres.2020.112769.
4. Verbeek, T.; Bockting, C.L.H.; van Pampus, M.G.; Ormel, J.; Meijer, J.L.; Hartman, C.A.; Burger, H. Postpartum depression predicts offspring mental health problems in adolescence independently of parental lifetime psychopathology. *J. Affect. Disord.* **2012**, *136*, 948–954, doi:10.1016/j.jad.2011.08.035.
5. Farias-Antúnez, S.; Xavier, M.O.; Santos, I.S. Effect of maternal postpartum depression on offspring's growth. *J. Affect. Disord.* **2018**, *228*, 143–152, doi:10.1016/j.jad.2017.12.013.
6. Weaver, I.C.G.; Meaney, M.J.; Szyf, M. Maternal care effects on the hippocampal transcriptome and anxiety-mediated behaviors in the offspring that are reversible in adulthood. *Proc. Natl. Acad. Sci. U. S. A.* **2006**, *103*, 3480–3485, doi:10.1073/pnas.0507526103.
7. Hinde, K.; Capitanio, J.P. Lactational programming? Mother's milk energy predicts infant behavior and temperament in rhesus macaques (*Macaca mulatta*). *Am. J. Primatol.* **2010**, *72*, 522–529, doi:10.1002/ajp.20806.
8. Shukri, N.H.M.; Wells, J.; Mukhtar, F.; Lee, M.H.S.; Fewtrell, M. Study protocol: An investigation of mother-infant signalling during breastfeeding using a randomised trial to test the effectiveness of breastfeeding relaxation therapy on maternal psychological state, breast milk production and infant behaviour and growth. *Int. Breastfeed. J.* **2017**, *12*, 1–14, doi:10.1186/s13006-017-0124-y.
9. Grey, K.R.; Davis, E.P.; Sandman, C.A.; Glynn, L.M. Human milk cortisol is associated with infant temperament. *Psychoneuroendocrinology* **2013**, *38*, 1178–1185, doi:10.1016/j.psyneuen.2012.11.002.
10. Zanardo, V.; Nicolussi, S.; Carlo, G.; Marzari, F.; Faggian, D.; Favaro, F.; Plebani, M. Beta endorphin concentrations in human milk. *J. Pediatr. Gastroenterol. Nutr.* **2001**, *33*, 160–164, doi:10.1097/00005176-200108000-00012.
11. Liu, B.; Zupan, B.; Laird, E.; Klein, S.; Gleason, G.; Bozinowski, M.; Gal Toth, J.; Toth, M. Maternal hematopoietic TNF, via milk chemokines, programs hippocampal development and memory. *Nat. Neurosci.* **2014**, *17*, 97–105, doi:10.1038/nn.3596.
12. Harris, J.E.; Pinckard, K.M.; Wright, K.R.; Baer, L.A.; Arts, P.J.; Abay, E.; Shettigar, V.K.; Lehnig, A.C.; Robertson, B.; Madaris, K.; et al. Exercise-induced 3'-sialyllactose in breast milk is a critical mediator to improve metabolic health and cardiac function in mouse offspring. *Nat. Metab.* **2020**, *2*, 678–687, doi:10.1038/s42255-020-0223-8.
13. Baldeón, M.E.; Zertuche, F.; Flores, N.; Fornasini, M. Free amino acid content in human milk is associated with infant gender and weight gain during the first four months of lactation. *Nutrients* **2019**, *11*, doi:10.3390/nu11092239.
14. van Sadelhoff, J.H.J.; Wiertsema, S.P.; Garssen, J.; Hogenkamp, A. Free Amino Acids in Human Milk:

- A Potential Role for Glutamine and Glutamate in the Protection Against Neonatal Allergies and Infections. *Front. Immunol.* **2020**, *11*, 1–14, doi:10.3389/fimmu.2020.01007.
15. Coleman, D.N.; Lopreiato, V.; Alharthi, A.; Loor, J.J. Amino acids and the regulation of oxidative stress and immune function in dairy cattle. *J. Anim. Sci.* **2020**, *98*, S175–S193, doi:10.1093/jas/skaa138.
16. Zamanillo, R.; Sánchez, J.; Serra, F.; Palou, A. Breast milk supply of microrna associated with leptin and adiponectin is affected by maternal overweight/obesity and influences infancy bmi. *Nutrients* **2019**, *11*, doi:10.3390/nu11112589.
17. Title, A.C.; Denzler, R.; Stoffel, M. Uptake and Function Studies of Maternal Milk-derived MicroRNAs. *J. Biol. Chem.* **2015**, *290*, 23680–23691, doi:10.1074/jbc.M115.676734.
18. Laubier, J.; Castille, J.; Le Guillou, S.; Le Provost, F. No effect of an elevated miR-30b level in mouse milk on its level in pup tissues. *RNA Biol.* **2015**, *12*, 26–29, doi:10.1080/15476286.2015.1017212.
19. Manca, S.; Upadhyaya, B.; Mutai, E.; Desaulniers, A.T.; Cederberg, R.A.; White, B.R.; Zempleni, J. Milk exosomes are bioavailable and distinct microRNA cargos have unique tissue distribution patterns. *Sci. Rep.* **2018**, *8*, 1–11, doi:10.1038/s41598-018-29780-1.
20. Franklin, T.B.; Russig, H.; Weiss, I.C.; Grff, J.; Linder, N.; Michalon, A.; Vizi, S.; Mansuy, I.M. Epigenetic transmission of the impact of early stress across generations. *Biol. Psychiatry* **2010**, *68*, 408–415, doi:10.1016/j.biopsych.2010.05.036.
21. Gapp, K.; Jawaid, A.; Sarkies, P.; Bohacek, J.; Pelczar, P.; Prados, J.; Farinelli, L.; Miska, E.; Mansuy, I.M. Implication of sperm RNAs in transgenerational inheritance of the effects of early trauma in mice. *Nat. Neurosci.* **2014**, *17*, 667–669, doi:10.1038/nn.3695.
22. van Steenwyk, G.; Roszkowski, M.; Manuella, F.; Franklin, T.B.; Mansuy, I.M. Transgenerational inheritance of behavioral and metabolic effects of paternal exposure to traumatic stress in early postnatal life: evidence in the 4th generation. *Environ. Epigenetics* **2018**, *4*, 1–8, doi:10.1093/eep/dvy023.
23. Steenwyk, G.; Gapp, K.; Jawaid, A.; Germain, P.; Manuella, F.; Tanwar, D.K.; Zamboni, N.; Gaur, N.; Efimova, A.; Thumfart, K.M.; et al. Involvement of circulating factors in the transmission of paternal experiences through the germline. *EMBO J.* **2020**, *39*, 1–16, doi:10.15252/embj.2020104579.
24. Poy, M.N.; Haussler, J.; Trajkovski, M.; Braun, M.; Collins, S.; Rorsman, P.; Zavolan, M.; Stoffel, M. miR-375 maintains normal pancreatic α - and β -cell mass. *Proc. Natl. Acad. Sci. U. S. A.* **2009**, *106*, 5813–5818, doi:10.1073/pnas.0810550106.
25. Dumortier, O.; Fabris, G.; Pisani, D.F.; Casamento, V.; Gautier, N.; Hinault, C.; Lebrun, P.; Duranton, C.; Tauc, M.; Dalle, S.; et al. microRNA-375 regulates glucose metabolism-related signaling for insulin secretion. *J. Endocrinol.* **2020**, *244*, 189–200, doi:10.1530/JOE-19-0180.
26. Delplanque, B.; Gibson, R.; Koletzko, B.; Lapillonne, A.; Strandvik, B. Lipid Quality in Infant Nutrition: Current Knowledge and Future Opportunities. *J. Pediatr. Gastroenterol. Nutr.* **2015**, *61*, 8–17, doi:10.1097/MPG.0000000000000818.
27. Djoumbou Feunang, Y.; Eisner, R.; Knox, C.; Chepelev, L.; Hastings, J.; Owen, G.; Fahy, E.; Steinbeck, C.; Subramanian, S.; Bolton, E.; et al. ClassyFire: automated chemical classification with a comprehensive, computable taxonomy. *J. Cheminform.* **2016**, *8*, 1–20, doi:10.1186/s13321-016-0174-y.
28. Picart-Armada, S.; Fernández-Albert, F.; Vinaixa, M.; Yanes, O.; Perera-Lluna, A. FELLA: An R package to enrich metabolomics data. *BMC Bioinformatics* **2018**, *19*, 1–9, doi:10.1186/s12859-018-2487-5.

29. Walters, R.O.; Arias, E.; Diaz, A.; Burgos, E.S.; Guan, F.; Tiano, S.; Mao, K.; Green, C.L.; Qiu, Y.; Shah, H.; et al. Sarcosine Is Uniquely Modulated by Aging and Dietary Restriction in Rodents and Humans. *Cell Rep.* **2018**, *25*, 663–676.e6, doi:10.1016/j.celrep.2018.09.065.
30. Wuertz-Kozak, K.; Roszkowski, M.; Cambria, E.; Block, A.; Kuhn, G.A.; Abele, T.; Hitzl, W.; Drießlein, D.; Müller, R.; Rapp, M.A.; et al. Effects of Early Life Stress on Bone Homeostasis in Mice and Humans. *Int. J. Mol. Sci.* **2020**, *21*, 6634, doi:10.3390/ijms21186634.
31. Gapp, K.; Soldado-Magraner, S.; Alvarez-Sánchez, M.; Bohacek, J.; Vernaz, G.; Shu, H.; Franklin, T.B.; Wolfer, D.; Mansuy, I.M. Early life stress in fathers improves behavioural flexibility in their offspring. *Nat. Commun.* **2014**, *5*, 5466, doi:10.1038/ncomms6466.
32. Bohacek, J.; Farinelli, M.; Mirante, O.; Steiner, G.; Gapp, K.; Coiret, G.; Ebeling, M.; Durán-Pacheco, G.; Iniguez, L.; Manuella, F.; et al. Pathological brain plasticity and cognition in the offspring of males subjected to postnatal traumatic stress. *Mol. Psychiatry* **2015**, *20*, 621–631, doi:10.1038/mp.2014.80.
33. Weiss, I.C.; Franklin, T.B.; Vizi, S.; Mansuy, I.M. Inheritable effect of unpredictable maternal separation on behavioral responses in mice. *Front. Behav. Neurosci.* **2011**, *5*, 3, doi:10.3389/fnbeh.2011.00003.
34. Razoux, F.; Russig, H.; Mueggler, T.; Baltes, C.; Dilkaou, K.; Rudin, M.; Mansuy, I.M. Transgenerational disruption of functional 5-HT 1A R-induced connectivity in the adult mouse brain by traumatic stress in early life. *Mol. Psychiatry* **2017**, *22*, 519–526, doi:10.1038/mp.2016.146.
35. Gapp, K.; Bohacek, J.; Grossmann, J.; Brunner, A.M.; Manuella, F.; Nanni, P.; Mansuy, I.M. Potential of Environmental Enrichment to Prevent Transgenerational Effects of Paternal Trauma. *Neuropharmacology* **2016**, *41*, 2749–2758, doi:10.1038/npp.2016.87.
36. Gapp, K.; Corcoba, A.; van Steenwyk, G.; Mansuy, I.M.; Duarte, J.M.N. Brain metabolic alterations in mice subjected to postnatal traumatic stress and in their offspring. *J. Cereb. Blood Flow Metab.* **2017**, *37*, 2423–2432, doi:10.1177/0271678X16667525.
37. Franklin, T.B.; Linder, N.; Russig, H.; Thöny, B.; Mansuy, I.M. Influence of Early Stress on Social Abilities and Serotonergic Functions across Generations in Mice. *PLoS One* **2011**, *6*, e21842, doi:10.1371/journal.pone.0021842.
38. Rao, J.; McClements, D.J. Food-grade microemulsions, nanoemulsions and emulsions: Fabrication from sucrose monopalmitate & lemon oil. *Food Hydrocoll.* **2011**, *25*, 1413–1423, doi:10.1016/j.foodhyd.2011.02.004.
39. Song, B.J.; Jouni, Z.E.; Ferruzzi, M.G. Assessment of phytochemical content in human milk during different stages of lactation. *Nutrition* **2013**, *29*, 195–202, doi:10.1016/j.nut.2012.07.015.
40. Coppa, G. V.; Pierani, P.; Zampini, L.; Bruni, S.; Carloni, I.; Gabrielli, O. Characterization of Oligosaccharides in Milk and Feces of Breast-Fed Infants by High-Performance Anion-Exchange Chromatography. In *Bioactive Components of Human Milk*; Springer: Boston, 2001; pp. 307–314.
41. Italianer, M.F.; Naninck, E.F.G.; Roelants, J.A.; van der Horst, G.T.J.; Reiss, I.K.M.; Goudoever, J.B. van; Joosten, K.F.M.; Chaves, I.; Vermeulen, M.J. Circadian Variation in Human Milk Composition, a Systematic Review. *Nutrients* **2020**, *12*, 2328, doi:10.3390/nu12082328.
42. Zhang, Z.; Adelman, A.S.; Rai, D.; Boettcher, J.; Lonnerdal, B. Amino acid profiles in term and preterm human milk through lactation: A systematic review. *Nutrients* **2013**, *5*, 4800–4821, doi:10.3390/nu5124800.

43. Verner, A.; Craig, S.; McGuire, W. Effect of taurine supplementation on growth and development in preterm or low birth weight infants. *Cochrane Database Syst. Rev.* **2007**, doi:10.1002/14651858.CD006072.pub2.
44. Nishigawa, T.; Nagamachi, S.; Ikeda, H.; Chowdhury, V.S.; Furuse, M. Restraint stress in lactating mice alters the levels of sulfur-containing amino acids in milk. *J. Vet. Med. Sci.* **2018**, *80*, 503–509, doi:10.1292/jvms.17-0661.
45. Lømo, T.; Eken, T.; Bekkestad Rein, E.; Njå, A. Body temperature control in rats by muscle tone during rest or sleep. *Acta Physiol.* **2020**, *228*, 1–26, doi:10.1111/apha.13348.
46. Shibata, M.; Iriki, M.; Arita, J.; Kiyohara, T.; Nakashima, T.; Miyata, S.; Matsukawa, T. Procaine microinjection into the lower midbrain increases brown fat and body temperatures in anesthetized rats. *Brain Res.* **1996**, *716*, 171–179, doi:10.1016/0006-8993(96)00040-6.
47. Bhave, S. V.; Telang, S.D.; Durden, D.A.; Juorio, A. V. Effects of nutritional stress on brain tyramine concentration and dopamine turnover. *Neurochem. Res.* **1988**, *13*, 567–570, doi:10.1007/BF00973299.
48. Wingo, J.E.; Matthew Brothers, R.; Del Coso, J.; Crandall, C.G. Intradermal administration of ATP does not mitigate tyramine-stimulated vasoconstriction in human skin. *Am. J. Physiol. - Regul. Integr. Comp. Physiol.* **2010**, *298*, 1417–1420, doi:10.1152/ajpregu.00846.2009.
49. Elhassan, Y.S.; Kluckova, K.; Fletcher, R.S.; Schmidt, M.S.; Garten, A.; Doig, C.L.; Cartwright, D.M.; Oakey, L.; Burley, C. V.; Jenkinson, N.; et al. Nicotinamide Riboside Augments the Aged Human Skeletal Muscle NAD⁺ Metabolome and Induces Transcriptomic and Anti-inflammatory Signatures. *Cell Rep.* **2019**, *28*, 1717–1728.e6, doi:10.1016/j.celrep.2019.07.043.
50. Crisol, B.M.; Veiga, C.B.; Braga, R.R.; Lenhare, L.; Baptista, I.L.; Gaspar, R.C.; Muñoz, V.R.; Cordeiro, A. V.; da Silva, A.S.R.; Cintra, D.E.; et al. NAD⁺ precursor increases aerobic performance in mice. *Eur. J. Nutr.* **2020**, *59*, 2427–2437, doi:10.1007/s00394-019-02089-z.
51. Oliveros, E.; Vázquez, E.; Barranco, A.; Ramírez, M.; Gruart, A.; Delgado-García, J.M.; Buck, R.; Rueda, R.; Martín, M.J. Sialic acid and sialylated oligosaccharide supplementation during lactation improves learning and memory in rats. *Nutrients* **2018**, *10*, doi:10.3390/nu10101519.
52. Lindsay, M.A. microRNAs and the immune response. *Trends Immunol.* **2008**, *29*, 343–351, doi:10.1016/j.it.2008.04.004.
53. Bronte, V.; Zanovello, P. Regulation of immune responses by L-arginine metabolism. *Nat. Rev. Immunol.* **2005**, *5*, 641–654, doi:10.1038/nri1668.

4.12. Supplementary Figures

A



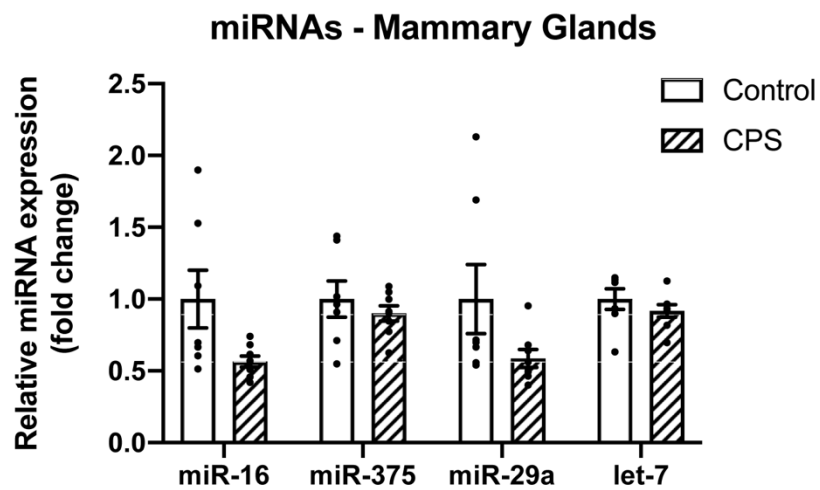
B



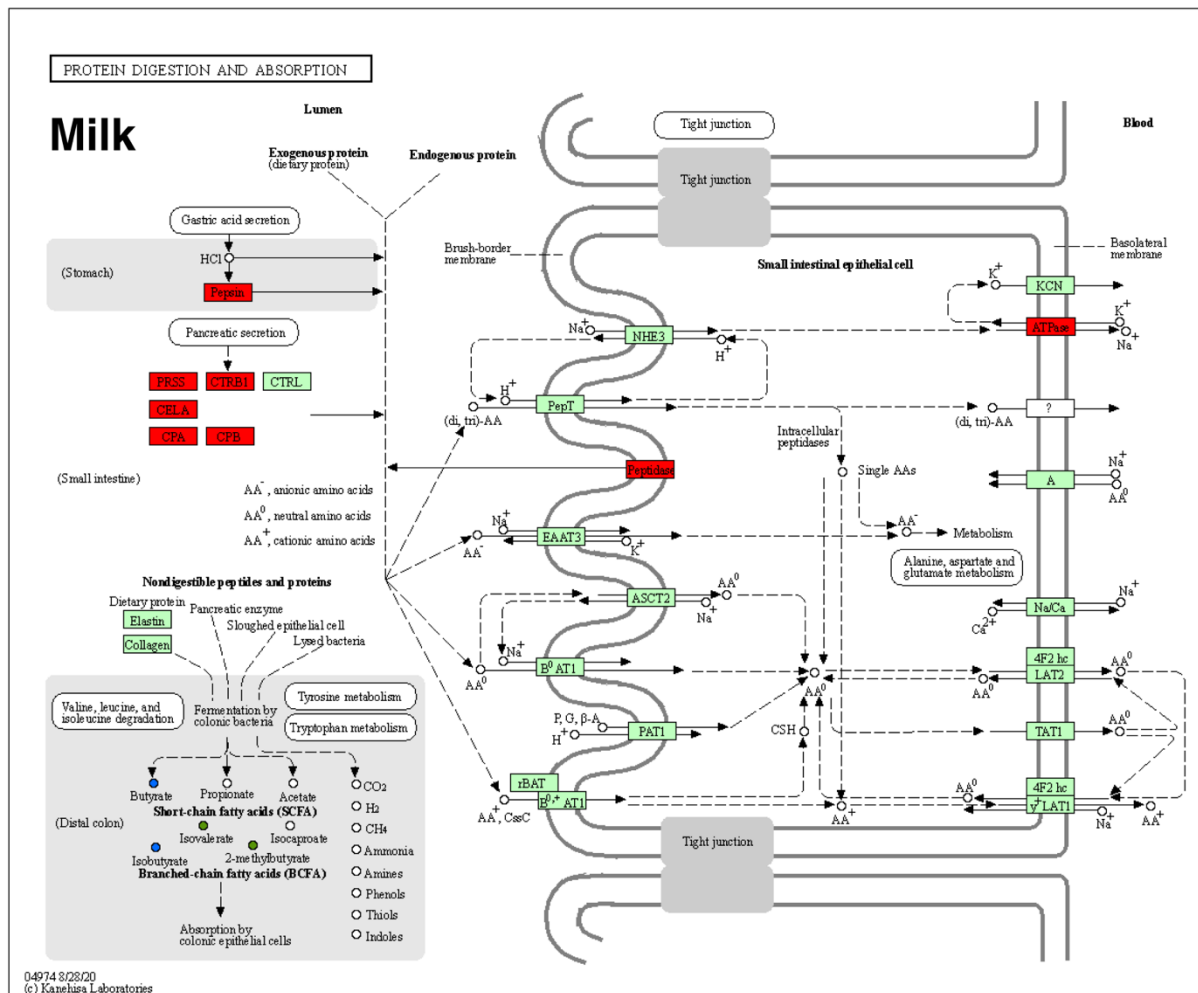
C



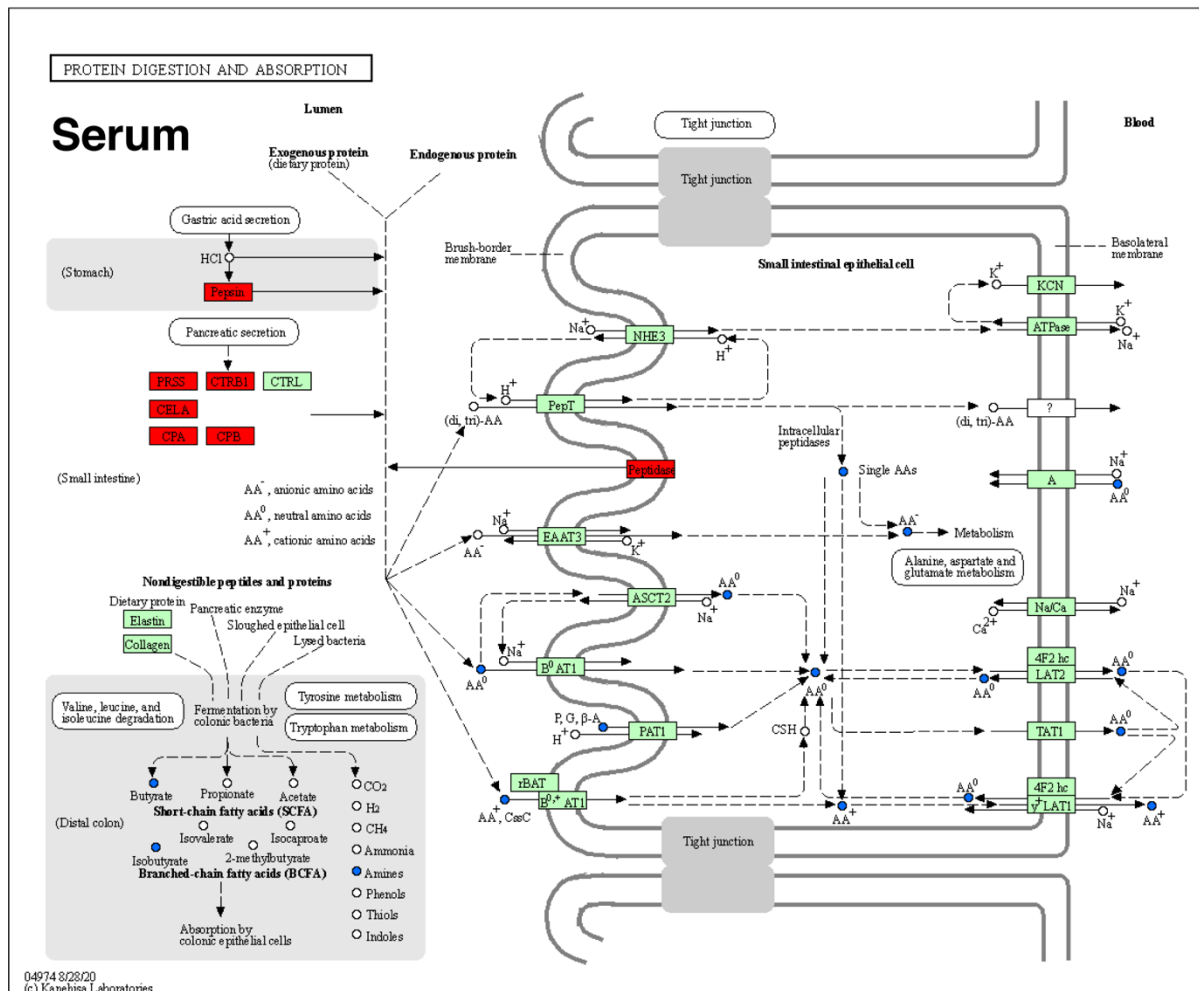
Supplementary Figure 1 – Additional observations for mammary gland collection. **(A,B)** Comparison of mammary glands without visible milk (left) versus mammary glands with milk (right). **(C)** Dashed circles highlight two large blood vessels supplying the mammary glands. Their nicking during mammary gland excision should be avoided.



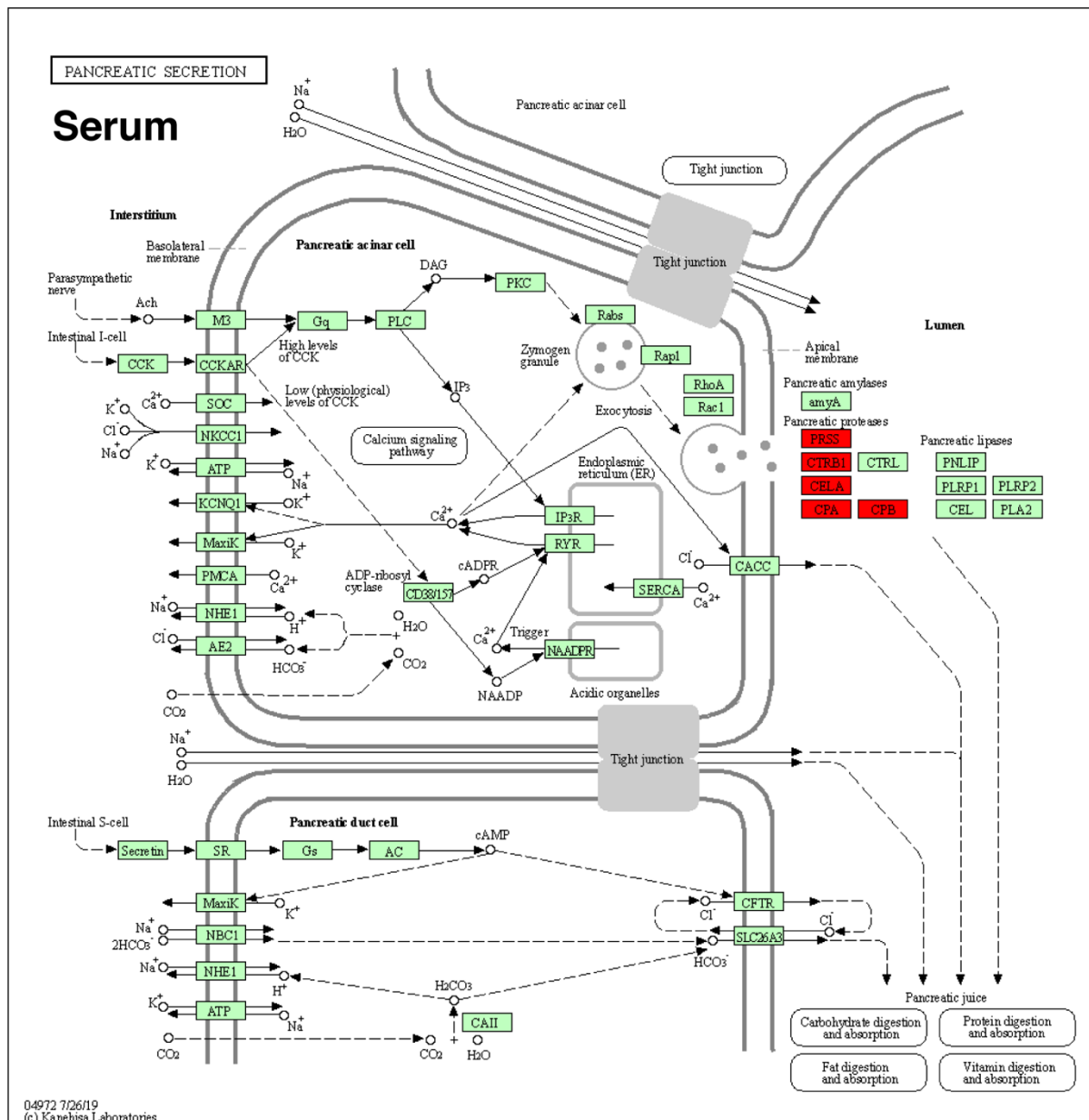
Supplementary Figure 2 - miRNA quantification in mammary gland tissue. In contrast to milk, miR-16 and miR-29a were decreased in CPS mammary glands but the differences were statistically not significant.



Supplementary Figure 3 – KEGG Pathway visualization of enriched “Protein digestion and absorption” KEGG pathway in maternal milk after CPS. Enriched pathway components were highlighted in red (enzymes) and blue (metabolites).



Supplementary Figure 4 – KEGG Pathway visualization of enriched “Protein digestion and absorption” pup serum after CPS. Enriched pathway components were highlighted in red (enzymes) and blue (metabolites).



Supplementary Figure 5 – KEGG Pathway visualization of enriched “Pancreatic secretion” in CPS pup serum after CPS. Enriched pathway components were highlighted in red (enzymes) and blue (metabolites).

4.13. Supplementary Tables

Supplementary Table 1 – Significantly altered compounds in mammary milk.

Compound	FC [\log_2]	q-value (Storey)
Sucrose monopalmitate	0.4931	0.0003
3"-N-Acetyl-4"-O-(9-octadecenoyl)fusarochromanone	0.3195	0.0004
Ponasteroside A	0.5122	0.0007
(3b,6b,8a,12a)-8,12-Epoxy-7(11)-eremophilene-6,8,12-trimethoxy-3-ol	0.1199	0.0011
Madlongiside C	0.1599	0.0011
Benzylpenicilloyl Polylysine	0.3693	0.0012
Licoagrodin	0.5579	0.0012
N-[(4E,8Z)-1,3-dihydroxyoctadeca-4,8-dien-2-yl]hexadecanamide 1-glucoside	0.0906	0.0016
Tejedine	0.1466	0.0023
9-Oxoasimicinone	0.1620	0.0031
simvastatin hydroxy acid	0.1656	0.0032
Varanic acid	0.1003	0.0032
Pentanoic acid	-0.1540	0.0037
Thymol Sulfate	0.2043	0.0037
Mactraxanthin	0.1409	0.0044
Undecanoic acid	-0.1198	0.0109
18alpha-Hydroxyglycyrrhetic acid	0.1126	0.0109
5-Hydroxyindoleacetyl glycine	-0.0756	0.0110
Taurocholic acid	0.0783	0.0110
C4:0 (Butyric acid)	-0.0867	0.0123
5-phosphonoxy-L-lysine	0.2436	0.0123
C16:4	-0.1106	0.0123
LPA(18:2(9Z,12Z)/0:0)	0.0710	0.0123
Tryptamine	-0.0862	0.0139
C13:0	-0.0876	0.0139
Carnosine	0.1868	0.0139
LPA(0:0/18:1(9Z))	0.0756	0.0139
1-Arachidonoylglycerophosphoinositol	0.2270	0.0139
6-{4-[(1E)-3-[(6-{[3,4-dihydroxy-2,5-bis(hydroxymethyl)oxolan-2-yl]oxy}-3,4,5-trihydroxyoxan-2-yl)methoxy]-3-oxoprop-1-en-1-yl]-2-hydroxyphenoxy}-3,4,5-trihydroxyoxane-2-carboxylic acid	0.3433	0.0139
Ethyl isovalerate	-0.1441	0.0149
(10S,11S)-Pterosin C	-0.0606	0.0163
Anisidine	-0.0540	0.0178
10-Undecenyl acetate	-0.0915	0.0178

Continued

Supplementary Table 1 – Significantly altered metabolites in mammary milk. - Continued

Compound	FC [\log_2]	q-value (Storey)
(4-{3,5-dihydroxy-8,8-dimethyl-4-oxo-4H,8H-pyrano[2,3-f]chromen-2-yl}phenyl)oxidanesulfonic acid	0.4791	0.0178
3beta,7alpha-Dihydroxy-5-cholestenoate	0.2889	0.0178
Gemfibrozil	-0.0855	0.0183
CE(16:0)	0.3831	0.0183
cis- and trans-5-Ethyl-4-methyl-2-(2-butyl)-thiazoline	-0.1847	0.0203
Faradiol laurate	0.4088	0.0222
PA(16:0/18:1(11Z))	0.0729	0.0222
PA(16:1(9Z)/15:0)	0.2453	0.0227
DG(8:0/0:0/i-15:0)	0.0306	0.0237
C9:1	-0.0712	0.0238
Nicotinamide ribotide	0.2091	0.0241
Histidinyl-Serine	0.3258	0.0253
5,7-dihydroxy-3-(3-hydroxyphenyl)-4H-chromen-4-one	0.1507	0.0260
Tartaric acid	-0.2043	0.0268
2-Methyl-2-(methyldithio)propanal	-0.2043	0.0268
9-(beta-D-Ribofuranosyl)zeatin	-0.0788	0.0278
PA(15:0/20:5(5Z,8Z,11Z,14Z,17Z))	0.2256	0.0278
PA(15:0/20:0)	0.1144	0.0283
C15:0	-0.0393	0.0289
Hydroxymalonic acid	-0.1205	0.0307
1,3-Dithiane	-0.1205	0.0307
CE(18:2(9Z,12Z))	0.0970	0.0307
PS(14:1(9Z)/18:3(9Z,12Z,15Z))	0.1103	0.0307
Kaempferol 3-(2'''-rhamnosyl-6'''-acetylgalactoside) 7-rhamnoside	0.2205	0.0307
Cholesterol	0.1910	0.0318
Hydratopyrrhocanthinol	0.1481	0.0329
4-Methyl-2-oxopentanoate	-0.5004	0.0334
3"-Azido-3"-deoxy-5"- O-beta-D-glucopyranuronosylthymidine	0.1157	0.0334
Gingerglycolipid C	0.1231	0.0334
cis-4-Hydroxycyclohexylacetic acid	-0.0224	0.0339
Caffeoylcycloartenol	0.1730	0.0339
CE(20:3(8Z,11Z,14Z))	0.0666	0.0339
4-Methoxycinnamic acid	-0.0809	0.0341
DG(16:0/22:5(4Z,7Z,10Z,13Z,16Z)/0:0)	0.0763	0.0353

Continued

Supplementary Table 1 – Significantly altered metabolites in mammary milk. - Continued

Compound	FC [\log_2]	q-value (Storey)
3,4,5-trihydroxy-6-({17-hydroxy-11,18-dimethoxy-13-oxo-6,8,20-trioxapentacyclo[10.8.0.0 ^{2,9} .0 ^{3,7} .0 ^{14,19}]icosanoate-1(12),2(9),4,10,14,16,18-heptaen-15-yl}oxy)oxane-2-carboxylic acid	-0.2257	0.0354
Oleoside 11-methyl ester	-0.0954	0.0357
2-(6-{2,4-dihydroxy-3-[(1E)-3-methylbut-1-en-1-yl]benzoyl}-5-(2,4-dihydroxyphenyl)-3-(hydroxymethyl)cyclohex-2-en-1-yl)benzene-1,3-diol	0.0230	0.0360
Ibuprofen	-0.0819	0.0367
Glutaminyltyrosine	0.0590	0.0368
Trimethobenzamide	0.1088	0.0368
Lacto-N-difucopentaose II	0.2028	0.0368
N-Acetylputrescine	-0.1376	0.0379
[(3-methylbut-2-en-1-yl)oxy]sulfonic acid	-0.3411	0.0381
6-Methylmercaptopurine	-0.3411	0.0381
Sulfolithocholylglycine	0.0568	0.0381
Janthitrem G	0.1425	0.0381
Taurine	0.3409	0.0408
1-(sn-Glycero-3-phospho)-1D-myo-inositol	0.2244	0.0414
Notoginsenoside R1	0.0488	0.0414
Acetylornithine	-0.0227	0.0419
Asparaginyl-Threonine	0.1354	0.0419
(±)-threo-1-(p-Hydroxyphenyl)propylene glycol 4"-glucoside	0.1334	0.0419
Pseudomonine	0.1334	0.0419
Androsterone glucuronide	0.0444	0.0419
Pyridoxal	-0.2034	0.0450
4-(1,1,3,3-Tetramethylbutyl)-phenol	-0.1142	0.0450
C13:2	-0.0491	0.0450
Geranyl acetoacetate	-0.0739	0.0450
2-Dodecylbenzenesulfonic acid	0.1050	0.0450
AMP	0.3639	0.0450
Isocarlinoside	-0.2258	0.0450
PE(14:0/P-16:0)	0.1408	0.0450
(3a,5b,7a)-23-Carboxy-7-hydroxy-24-norcholan-3-yl-β-D-Glucopyranosiduronic acid	0.1195	0.0457
S-(11-hydroxy-9-deoxy-delta12-PGD2)-glutathione	0.1500	0.0457
1,3,11-Tridecatriene-5,7,9-triyne	-0.2572	0.0459
Cloversaponin I	0.2286	0.0459
PE(14:0/P-18:0)	0.0756	0.0459
Acetyl tropine	-0.0603	0.0466

Continued

Supplementary Table 1 – Significantly altered metabolites in mammary milk. - Continued

Compound	FC [\log_2]	q-value (Storey)
3,4-Dihydroxyphenylglycol O-sulfate	-0.0493	0.0466
PS(18:1(11Z)/24:1(15Z))	0.0994	0.0466
Urocanate	-0.0193	0.0482
3-(3-Hydroxyphenyl)propanoic acid	-0.5296	0.0482
4-hydroxy-3-(sulfoxy)benzoic acid	-0.1099	0.0482
6-(2-formyl-3,4,5-trihydroxyphenoxy)-3,4,5-trihydroxyoxane-2-carboxylic acid	-0.0738	0.0482
{4-[(E)-2-{3,5-dihydroxy-4-[3-(propan-2-yl)oxiran-2-yl]phenyl}ethenyl]phenyl}oxidanesulfonic acid	-0.2635	0.0482
Agnuside	0.1741	0.0482
Clomocycline	-0.4417	0.0482
PGP(16:0/16:1(9Z))	0.0921	0.0482
3"-p-Hydroxypaclitaxel	0.1566	0.0482
Tragopogonsaponin M	-0.0467	0.0482
CE(5M5)	0.1078	0.0491

Supplementary Table 3 – Concomitantly altered metabolites in maternal milk and pup serum.

Compound	Milk FC [log ₂]	Milk p- value	Serum FC [log ₂]	Serum p- value
Tragopogonsaponin M	-0.047	0.007	-0.711	0.005
PIP(16:0/20:1(11Z))	-0.032	0.049	-0.595	0.001
C4:0 (Butyric acid)	-0.087	0.000	-0.483	0.015
S-(11-hydroxy-9-deoxy-delta12-PGD2)-glutathione	0.150	0.006	-0.321	0.011
C13:2	-0.049	0.005	-0.290	0.000
4-(Methylnitrosamino)-1-(3-pyridyl)-1-butanol	0.145	0.032	-0.270	0.047
(2R,2"S)-Isobuteine	-0.049	0.031	0.112	0.028
Nicotinamide ribotide	0.209	0.001	0.246	0.007
Arginine	-0.027	0.009	0.251	0.010
Phenylacetaldehyde	-0.406	0.008	0.251	0.000
Valine; Betaine	-0.054	0.027	0.251	0.010
N-Acetylneurameric acid	0.138	0.027	0.263	0.006
Procaine	-0.015	0.015	0.315	0.000
3-(3-Hydroxyphenyl)propanoic acid	-0.530	0.007	0.317	0.010
Acetyl-Leucine	-0.287	0.037	0.320	0.004
Isovalerylglutamic acid	-0.085	0.038	0.335	0.003
Nnal-N-oxide	0.116	0.031	0.356	0.031
Alanyl-Proline	-0.065	0.020	0.357	0.048
Serine	-0.033	0.033	0.383	0.007
Acetyltornithine	-0.023	0.004	0.435	0.021
Tyramine	-0.102	0.041	0.456	0.012
5-phosphonooxy-L-lysine	0.244	0.000	1.096	0.027
Alanyl-Alanine	-0.032	0.032	1.247	0.047

Supplementary Table 4 – Enriched KEGG pathways, modules, enzymes, reactions and metabolites in mammary milk.

KEGG ID	Type	KEGG name	p-value
mmu00563	pathway	Glycosylphosphatidylinositol (GPI)-anchor biosynthesis	1.00E-06
mmu01521	pathway	EGFR tyrosine kinase inhibitor resistance	1.00E-06
mmu04012	pathway	ErbB signaling pathway	1.00E-06
mmu04014	pathway	Ras signaling pathway	1.52E-04
mmu04015	pathway	Rap1 signaling pathway	1.00E-06
mmu04064	pathway	NF-kappa B signaling pathway	1.00E-06
mmu04072	pathway	Phospholipase D signaling pathway	7.57E-05
mmu04136	pathway	Autophagy - other	1.00E-06
mmu04140	pathway	Autophagy - animal	7.08E-04
mmu04650	pathway	Natural killer cell mediated cytotoxicity	1.00E-06
mmu04658	pathway	Th1 and Th2 cell differentiation	1.00E-06
mmu04659	pathway	Th17 cell differentiation	9.74E-05
mmu04660	pathway	T cell receptor signaling pathway	1.00E-06
mmu04662	pathway	B cell receptor signaling pathway	1.00E-06
mmu04666	pathway	Fc gamma R-mediated phagocytosis	1.00E-06
mmu04722	pathway	Neurotrophin signaling pathway	3.68E-06
mmu04723	pathway	Retrograde endocannabinoid signaling	1.36E-04
mmu04724	pathway	Glutamatergic synapse	1.00E-06
mmu04725	pathway	Cholinergic synapse	2.56E-05
mmu04728	pathway	Dopaminergic synapse	6.30E-05
mmu04730	pathway	Long-term depression	1.34E-06
mmu04912	pathway	GnRH signaling pathway	1.00E-06
mmu04913	pathway	Ovarian steroidogenesis	4.47E-06
mmu04915	pathway	Estrogen signaling pathway	4.77E-05
mmu04926	pathway	Relaxin signaling pathway	1.00E-06
mmu04933	pathway	AGE-RAGE signaling pathway in diabetic complications	2.68E-05

Continued

Supplementary Table 4 – Enriched KEGG pathways, modules, enzymes, reactions and metabolites in mammary milk. - Continued

KEGG ID	Type	KEGG name	p-value
mmu04972	pathway	Pancreatic secretion	8.35E-05
mmu04974	pathway	Protein digestion and absorption	1.00E-06
mmu04979	pathway	Cholesterol metabolism	1.00E-06
mmu05163	pathway	Human cytomegalovirus infection	1.11E-03
mmu05167	pathway	Kaposi sarcoma-associated herpesvirus infection	1.00E-06
mmu05170	pathway	Human immunodeficiency virus 1 infection	3.98E-06
mmu05212	pathway	Pancreatic cancer	3.51E-04
mmu05214	pathway	Glioma	1.00E-06
mmu05217	pathway	Basal cell carcinoma	1.00E-06
mmu05235	pathway	PD-L1 expression and PD-1 checkpoint pathway in cancer	1.00E-06
M00045	module	Histidine degradation, histidine => N-formiminoglutamate => glutamate	2.78E-05
M00065	module	GPI-anchor biosynthesis, core oligosaccharide	1.00E-06
M00135	module	GABA biosynthesis, eukaryotes, putrescine => GABA	1.00E-06
1.1.1.2	enzyme	alcohol dehydrogenase (NADP+)	1.00E-06
1.3.1.72	enzyme	Delta24-sterol reductase	4.53E-04
2.1.1.22	enzyme	carnosine N-methyltransferase	1.00E-06
2.1.1.67	enzyme	thiopurine S-methyltransferase	7.77E-04
2.3.1.22	enzyme	2-acylglycerol O-acyltransferase	3.01E-04
2.3.1.26	enzyme	sterol O-acyltransferase	1.00E-06
2.3.1.57	enzyme	diamine N-acetyltransferase	1.00E-06
2.3.1.65	enzyme	bile acid-CoA:amino acid N-acyltransferase	1.00E-06
2.4.1.17	enzyme	glucuronosyltransferase	1.00E-06
2.4.2.12	enzyme	nicotinamide phosphoribosyltransferase	1.00E-06
2.7.1.107	enzyme	diacylglycerol kinase (ATP)	8.04E-06

Continued

Supplementary Table 4 – Enriched KEGG pathways, modules, enzymes, reactions and metabolites in mammary milk. - Continued

KEGG ID	Type	KEGG name	p-value
2.7.1.22	enzyme	ribosylnicotinamide kinase	5.46E-05
2.7.1.81	enzyme	hydroxylysine kinase	1.53E-06
2.7.7.41	enzyme	phosphatidate cytidyltransferase	4.96E-05
2.7.8.29	enzyme	L-serine-phosphatidylethanolamine phosphatidyltransferase	3.48E-04
3.1.1.3	enzyme	triacylglycerol lipase	3.65E-06
3.1.1.34	enzyme	lipoprotein lipase	7.20E-05
3.1.3.81	enzyme	diacylglycerol diphosphate phosphatase	2.51E-05
3.1.4.4	enzyme	phospholipase D	1.00E-06
3.1.4.50	enzyme	glycosylphosphatidylinositol phospholipase D	1.00E-06
3.1.4.54	enzyme	N-acetylphosphatidylethanolamine-hydrolysing phospholipase D	1.36E-04
3.2.1.31	enzyme	beta-glucuronidase	4.24E-04
3.4.11.9	enzyme	Xaa-Pro aminopeptidase	1.00E-06
3.4.13.18	enzyme	cytosol nonspecific dipeptidase	1.00E-06
3.4.13.20	enzyme	beta-Ala-His dipeptidase	9.53E-05
3.4.14.5	enzyme	dipeptidyl-peptidase IV	1.00E-06
3.4.16.2	enzyme	lysosomal Pro-Xaa carboxypeptidase	1.00E-06
3.4.17.1	enzyme	carboxypeptidase A	1.00E-06
3.4.17.15	enzyme	carboxypeptidase A2	1.00E-06
3.4.17.2	enzyme	carboxypeptidase B	1.00E-06
3.4.17.20	enzyme	carboxypeptidase U	1.00E-06
3.4.21.1	enzyme	chymotrypsin	1.00E-06
3.4.21.35	enzyme	tissue kallikrein	2.28E-04
3.4.21.4	enzyme	trypsin	1.00E-06
3.4.21.70	enzyme	pancreatic endopeptidase E	1.00E-06
3.4.21.71	enzyme	pancreatic elastase II	1.00E-06
3.4.23.1	enzyme	pepsin A	1.00E-06

Continued

Supplementary Table 4 – Enriched KEGG pathways, modules, enzymes, reactions and metabolites in mammary milk. - Continued

KEGG ID	Type	KEGG name	p-value
3.4.24.11	enzyme	nephrilysin	1.00E-06
3.4.24.18	enzyme	meprin A	1.00E-06
3.4.24.63	enzyme	meprin B	1.00E-06
3.4.24.80	enzyme	membrane-type matrix metalloproteinase-1	2.22E-05
3.5.1.89	enzyme	N-acetylglucosaminylphosphatidylinositol deacetylase	1.00E-06
4.1.1.105	enzyme	L-tryptophan decarboxylase	1.00E-06
4.1.1.65	enzyme	phosphatidylserine decarboxylase	1.28E-04
4.2.1.49	enzyme	urocanate hydratase	1.00E-06
4.2.3.134	enzyme	5-phosphonoxy-L-lysine phospho-lyase	1.00E-06
4.3.1.3	enzyme	histidine ammonia-lyase	1.00E-06
5.3.3.5	enzyme	cholestenol Delta-isomerase	1.65E-06
6.2.1.2	enzyme	medium-chain acyl-CoA ligase	1.00E-06
6.5.1.6	enzyme	DNA ligase (ATP or NAD+)	1.00E-06
7.2.2.13	enzyme	Na+/K+-exchanging ATPase	1.18E-04
R00103	reaction	NAD+ phosphohydrolase	1.00E-06
R00137	reaction	ATP:nicotinamide-nucleotide adenylyltransferase	1.00E-06
R00173	reaction	pyridoxal-5'-phosphate phosphohydrolase	1.00E-06
R00174	reaction	ATP:pyridoxal 5'-phosphotransferase	1.17E-06
R00669	reaction	N2-Acetyl-L-ornithine amidohydrolase	1.00E-06
R00685	reaction	L-tryptophan decarboxy-lyase	1.00E-06
R01088	reaction	L-leucine:NAD+ oxidoreductase (deaminating)	1.00E-06
R01090	reaction	L-Leucine:2-oxoglutarate aminotransferase	1.00E-06
R01154	reaction	acetyl-CoA:putrescine N-acetyltransferase	1.00E-06
R01156	reaction	N-Acetylputrescine acetylhydrolase	1.00E-06
R01164	reaction	L-histidine:beta-alanine ligase (ADP-forming)	1.00E-06

Continued

Supplementary Table 4 – Enriched KEGG pathways, modules, enzymes, reactions and metabolites in mammary milk. - Continued

KEGG ID	Type	KEGG name	p-value
R01166	reaction	Nalpha-(beta-alanyl)-L-histidine hydrolase	1.00E-06
R01168	reaction	L-histidine ammonia-lyase (urocanate-forming)	1.00E-06
R01176	reaction	Butanoate:CoA ligase (AMP-forming)	1.00E-06
R01179	reaction	butanoyl-CoA:acetate CoA-transferase	1.00E-06
R01270	reaction	Nicotinamide D-ribonucleotide phosphoribohydrolase	1.00E-06
R01271	reaction	nicotinamide-D-ribonucleotide:diphosphate phospho-alpha-D-ribosyltransferase	1.00E-06
R01310	reaction	phosphatidylcholine phosphatidohydrolase	1.00E-06
R01365	reaction	Butanoyl-CoA:acetoacetate CoA-transferase	1.00E-06
R01370	reaction	Phenyllactate:NAD ⁺ oxidoreductase	1.00E-06
R01371	reaction	phenyllactate:NADP ⁺ oxidoreductase	1.00E-06
R01383	reaction	UDPglucuronate beta-D-glucuronosyltransferase (acceptor-unspecific)	1.00E-06
R01461	reaction	Acyl-CoA:cholesterol O-acyltransferase	1.00E-06
R01462	reaction	cholesterol ester acylhydrolase	1.00E-06
R01478	reaction	beta-D-glucuronoside glucuronosohydrolase	1.00E-06
R01562	reaction	adenosine 3'-phosphate phosphohydrolase	1.00E-06
R01682	reaction	3-Sulfo-L-alanine carboxy-lyase (taurine-forming)	2.05E-06
R01684	reaction	taurine:2-oxoglutarate aminotransferase	1.00E-06
R01685	reaction	taurine:ferricytochrome-c oxidoreductase (deaminating)	8.12E-06
R01688	reaction	ATP:butanoate 1-phosphotransferase	4.20E-04
R01708	reaction	Pyridoxine:NADP ⁺ 4-oxidoreductase	2.72E-06
R01710	reaction	Pyridoxamine:oxygen oxidoreductase (deaminating)	2.37E-06

Continued

Supplementary Table 4 – Enriched KEGG pathways, modules, enzymes, reactions and metabolites in mammary milk. - Continued

KEGG ID	Type	KEGG name	p-value
R01711	reaction	pyridoxine:oxygen oxidoreductase (deaminating)	1.75E-06
R01712	reaction	pyridoxamine:pyruvate aminotransferase	1.86E-06
R01713	reaction	Pyridoxamine:oxaloacetate aminotransferase	1.94E-06
R01797	reaction	CDP-diacylglycerol phosphatidylhydrolase	1.00E-06
R01799	reaction	CTP:phosphatidate cytidyltransferase	2.09E-06
R01910	reaction	Primary alcohol:(acceptor) oxidoreductase	1.00E-06
R02051	reaction	phosphatidylethanolamine phosphatidohydrolase	1.00E-06
R02052	reaction	Phosphatidylethanolamine ethanolaminephosphohydrolase	1.00E-06
R02055	reaction	Phosphatidyl-L-serine carboxy-lyase	5.75E-05
R02057	reaction	CDPethanolamine:1,2-diacylglycerol ethanolaminephosphotransferase	6.31E-04
R02144	reaction	S-adenosyl-L-methionine:carnosine N-methyltransferase	1.00E-06
R02173	reaction	Tryptamine:oxygen oxidoreductase(deaminating)	1.00E-06
R02239	reaction	1,2-diacyl-sn-glycerol 3-phosphate phosphohydrolase	1.00E-06
R02240	reaction	ATP:1,2-diacylglycerol 3-phosphotransferase	1.00E-06
R02241	reaction	acyl-CoA:1-acyl-sn-glycerol-3-phosphate 2-O-acyltransferase	1.00E-06
R02252	reaction	phenylpropanoate:NAD ⁺ delta2-oxidoreductase	5.15E-05
R02282	reaction	N2-Acetyl-L-ornithine:L-glutamate N-acetyltransferase	1.00E-06

Continued

Supplementary Table 4 – Enriched KEGG pathways, modules, enzymes, reactions and metabolites in mammary milk. - Continued

KEGG ID	Type	KEGG name	p-value
R02283	reaction	N2-Acetyl-L-ornithine:2-oxoglutarate aminotransferase	1.00E-06
R02322	reaction	nicotinamide-D-ribonucleotide amidohydrolase	1.00E-06
R02323	reaction	nicotinamide ribonucleotide phosphohydrolase	9.37E-06
R02324	reaction	ATP:N-ribosylnicotinamide 5'-phosphotransferase	9.10E-06
R02478	reaction	UDPglucuronate beta-D-glucuronosyltransferase (acceptor-unspecific)	1.00E-06
R02692	reaction	1,2-Diacyl-sn-glycerol:sterol O-acyltransferase	1.00E-06
R02797	reaction	Taurocholate amidohydrolase	1.00E-06
R02914	reaction	4,5-Dihydro-4-oxo-5-imidazolepropanoate hydro-lyase	1.00E-06
R03353	reaction	5alpha-Cholest-7-en-3beta-ol delta7-delta8-isomerase	1.00E-06
R03369	reaction	3-(2-hydroxyphenyl)propanoate,NADH2:oxygen oxireductase(3-hydroxylating)	1.00E-06
R03378	reaction	GTP:5-hydroxy-L-lysine O-phosphotransferase	1.23E-06
R03401	reaction	8-[(1R,2R)-3-oxo-2-{(Z)-pent-2-enyl}cyclopentyl]octanoate-NADP+ 4-oxidoreductase	1.00E-06
R03537	reaction	2',3'-Cyclic AMP 3'-nucleotidohydrolase	1.00E-06
R03709	reaction	3-(2-Hydroxyphenyl)propanoate:NAD+ oxidoreductase	1.00E-06

Continued

Supplementary Table 4 – Enriched KEGG pathways, modules, enzymes, reactions and metabolites in mammary milk. - Continued

KEGG ID	Type	KEGG name	p-value
R03720	reaction	Choloyl-CoA:glycine N-choloyltransferase	1.00E-06
R04025	reaction	N-Acetylputrescine:oxygen oxidoreductase(deaminating) (flavin-containing)	1.00E-06
R04352	reaction	UDPglucuronate beta-D-glucuronosyltransferase (acceptor-unspecific)	1.00E-06
R04413	reaction	Acyl-CoA:1-alkenylglycerophosphoethanolamine O-acyltransferase	1.00E-06
R04888	reaction	3-Methoxy-4-hydroxyphenylacetaldehyde:NAD+ oxidoreductase	1.00E-06
R04889	reaction	3-Methoxy-4-hydroxyphenylacetaldehyde:NADP+ oxidoreductase	1.00E-06
R04890	reaction	3-Methoxytyramine:oxygen oxidoreductase (deaminating) (copper-containing)	1.00E-06
R04899	reaction	3-(2-Hydroxyphenyl)propanoate <=> Phenylpropanoate	1.00E-06
R04903	reaction	5-Hydroxyindoleacetaldehyde:NAD+ oxidoreductase	3.24E-05
R04904	reaction	5-hydroxyindoleacetaldehyde:oxygen oxidoreductase	1.98E-05
R04906	reaction	5-Hydroxyindoleacetate <=> 5-Hydroxyindoleacetylglycine	1.00E-06
R05084	reaction	isopyridoxal:NAD+ oxidoreductase (5-pyridolactone-forming)	1.00E-06
R05099	reaction	6-oxohexanoate:NADP+ oxidoreductase	1.00E-06

Continued

Supplementary Table 4 – Enriched KEGG pathways, modules, enzymes, reactions and metabolites in mammary milk. - Continued

KEGG ID	Type	KEGG name	p-value
R05364	reaction	2-Hydroxy-6-oxo-7-methylocta-2,4-dienoate acylhydrolase	1.00E-06
R05507	reaction	6-Aminohexanoate + 2-Oxoglutarate aminotransferase	1.00E-06
R05652	reaction	taurine:pyruvate aminotransferase	1.00E-06
R05839	reaction	pyridoxamine:2-oxoglutarate aminotransferase	2.19E-05
R05919	reaction	Dolichyl phosphate D-mannose + G00145 => Dolichyl phosphate + G00146	1.00E-06
R05922	reaction	Dolichyl phosphate D-mannose + G00148 => Dolichyl phosphate + G00149	1.00E-06
R05924	reaction	Phosphatidylethanolamine + G00141 => 1,2-Diacyl-sn-glycerol + G00151	1.00E-06
R06623	reaction	glycoprotein-phosphatidylinositol phosphatidohydrolase	1.00E-06
R06780	reaction	Phenylpropanoate => 3-(3-Hydroxyphenyl)propanoic acid	1.00E-06
R06786	reaction	3-(3-hydroxyphenyl)propanoate,NADH:oxygen oxidoreductase (2-hydroxylating)	1.00E-06
R07016	reaction	1,2-Dihydronaphthalene-1,2-diol, NADPH:oxygen oxidoreductase (RH-hydroxylating or -epoxidizing)	1.00E-06
R07129	reaction	Dolichyl phosphate D-mannose + G00149 => Dolichyl phosphate + G00140	1.00E-06
R07245	reaction	carbamoyl-phosphate:N2-acetyl-L-ornithine carbamoyltransferase	6.47E-06
R07376	reaction	L-1-phosphatidylethanolamine:L-serine phosphatidyltransferase	1.34E-04

Continued

Supplementary Table 4 – Enriched KEGG pathways, modules, enzymes, reactions and metabolites in mammary milk. - Continued

KEGG ID	Type	KEGG name	p-value
R07379	reaction	plasmenylethanolamine 2-acylhydrolase	1.00E-06
R07381	reaction	Plasmenylethanolamine ethanolamine phosphohydrolase	5.19E-06
R07384	reaction	O-1-Alk-1-enyl-2-acyl-sn-glycero-3-phosphoethanolamine + CMP <=> 1-Alkenyl-2-acylglycerol + CDP-ethanolamine	8.10E-05
R07385	reaction	O-1-Alk-1-enyl-2-acyl-sn-glycero-3-phosphoethanolamine + H2O <=> 2-Acyl-1-(1-alkenyl)-sn-glycero-3-phosphate + Ethanolamine	2.04E-05
R07386	reaction	O-1-Alk-1-enyl-2-acyl-sn-glycero-3-phosphoethanolamine + Choline <=> Plasmethylcholine + Ethanolamine	5.14E-06
R07498	reaction	Zymosterol + NADPH + H+ <=> 5alpha-Cholest-8-en-3beta-ol + NADP+	1.00E-06
R07887	reaction	ATP + 8-[(1R,2R)-3-Oxo-2-{(Z)-pent-2-enyl}cyclopentyl]octanoate + CoA <=> AMP + Diphosphate + OPC8-CoA	1.00E-06
R08107	reaction	Phosphatidylethanolamine + G00149 <=> 1,2-Diacyl-sn-glycerol + G13044	1.00E-06
R08236	reaction	S-adenosyl-L-methionine:6-mercaptopurin S-methyltransferase	1.00E-06
R08238	reaction	6-methylthiopurine 5'-monophosphate ribonucleotide:diphosphate phospho-D-ribosyltransferase	1.00E-06

Continued

Supplementary Table 4 – Enriched KEGG pathways, modules, enzymes, reactions and metabolites in mammary milk. - Continued

KEGG ID	Type	KEGG name	p-value
R08325	reaction	Valproic acid + NADPH + H+ + Oxygen => 4-Hydroxyvalproic acid + NADP+ + H2O	1.13E-05
R08327	reaction	Valproic acid + NADPH + H+ + Oxygen => 3- Hydroxyvalproic acid + NADP+ + H2O	1.00E-06
R08330	reaction	4-Hydroxyvalproic acid => 2-n-Propyl-4-oxopentanoic acid	1.00E-06
R08333	reaction	2-n-Propyl-4-oxopentanoic acid => 2-Propylsuccinic acid	1.00E-06
R08335	reaction	3-Hydroxyvalproic acid => 3-Oxovalproic acid	1.00E-06
R08338	reaction	2-n-Propyl-2-pentenoic acid => 3-Hydroxyvalproic acid	1.51E-05
R08566	reaction	4-methyl-2-oxopentanoate:ferredoxin oxidoreductase (decarboxylating; CoA-3-methylbutanoylating)	3.31E-04
R08615	reaction	UDP-glucuronate glucuronohydrolase	1.27E-04
R08727	reaction	3beta-hydroxy-5-cholestenoate,NADPH:oxygen oxidoreductase (7alpha-hydroxylating)	1.00E-06
R08728	reaction	3beta,7alpha-dihydroxy-5-cholestenoate:NAD+ 3-oxidoreductase	1.00E-06
R09944	reaction	CTP:1,2-diacyl-sn-glycerol 3-phosphotransferase	1.00E-06
R10052	reaction	(2R,3S)-3-isopropylmalate:NAD+ oxidoreductase	1.29E-04

Continued

Supplementary Table 4 – Enriched KEGG pathways, modules, enzymes, reactions and metabolites in mammary milk. - Continued

KEGG ID	Type	KEGG name	p-value
R10270	reaction	(5R)-5-phosphoxy-L-lysine phosphate-lyase (deaminating; (S)-2-amino-6-oxohexanoate-forming)	1.00E-06
R10330	reaction	dihydrourocanate:acceptor oxidoreductase	9.18E-05
R12265	reaction	isopyridoxal:NAD ⁺ oxidoreductase (5-pyridoxate-forming)	1.00E-06
R12350	reaction	G00146 + Dolichyl phosphate D-mannose <=> G13128 + Dolichyl phosphate	1.00E-06
R12351	reaction	G13128 + Phosphatidylethanolamine <=> G00148 + 1,2-Diacyl-sn-glycerol	1.00E-06
C00165	compound	Diacylglycerol	1.00E-06
C00167	compound	UDP-glucuronate	1.05E-04
C00187	compound	Cholesterol	1.00E-06
C00233	compound	4-Methyl-2-oxopentanoate	1.00E-06
C00245	compound	Taurine	1.00E-06
C00246	compound	Butanoic acid	1.00E-06
C00250	compound	Pyridoxal	1.00E-06
C00350	compound	Phosphatidylethanolamine	1.00E-06
C00386	compound	Carnosine	1.00E-06
C00398	compound	Tryptamine	1.00E-06
C00416	compound	Phosphatidate	1.00E-06
C00437	compound	N-Acetylornithine	1.00E-06
C00455	compound	Nicotinamide D-ribonucleotide	1.00E-06
C00785	compound	Urocanate	1.00E-06
C01198	compound	3-(2-Hydroxyphenyl)propanoate	1.00E-06
C01367	compound	3'-AMP	1.00E-06
C02530	compound	Cholesterol ester	1.00E-06
C02632	compound	2-Methylpropanoate	1.00E-06
C02714	compound	N-Acetylputrescine	1.00E-06

Continued

Supplementary Table 4 – Enriched KEGG pathways, modules, enzymes, reactions and metabolites in mammary milk. - Continued

KEGG ID	Type	KEGG name	p-value
C03033	compound	beta-D-Glucuronoside	1.00E-06
C03366	compound	5-Phosphoxy-L-lysine	1.00E-06
C03845	compound	5alpha-Cholest-8-en-3beta-ol	1.00E-06
C04756	compound	O-1-Alk-1-enyl-2-acyl-sn-glycero-3-phosphoethanolamine	1.00E-06
C04780	compound	8-[(1R,2R)-3-Oxo-2-{(Z)-pent-2-enyl}cyclopentyl]octanoate	1.00E-06
C05122	compound	Taurocholate	1.00E-06
C05581	compound	3-Methoxy-4-hydroxyphenylacetaldehyde	1.00E-06
C05607	compound	Phenyllactate	1.00E-06
C05629	compound	Phenylpropanoate	1.90E-06
C05635	compound	5-Hydroxyindoleacetate	1.00E-06
C05832	compound	5-Hydroxyindoleacetylglycine	1.00E-06
C06051	compound	Isopyridoxal	1.00E-06
C06102	compound	Adipate semialdehyde	1.00E-06
C11135	compound	Androsterone glucuronide	1.00E-06
C11136	compound	Etiocholan-3alpha-ol-17-one 3-glucuronide	1.00E-06
C11457	compound	3-(3-Hydroxyphenyl)propanoic acid	1.00E-06
C14784	compound	1,2-Dihydroxy-3,4-epoxy-1,2,3,4-tetrahydronaphthalene	1.00E-06
C16614	compound	6-Methylmercaptopurine	1.00E-06
C16649	compound	4-Hydroxyvalproic acid	3.37E-06
C16651	compound	3-Hydroxyvalproic acid	1.00E-06
C16652	compound	3-Oxovalproic acid	1.00E-06
C16655	compound	2-n-Propyl-4-oxopentanoic acid	1.00E-06
C16657	compound	2-Propylsuccinic acid	3.62E-05
C17335	compound	3beta,7alpha-Dihydroxy-5-cholestenoate	1.00E-06

Supplementary Table 5 – Enriched KEGG pathways, modules, enzymes, reactions and metabolites in pup serum.

KEGG ID	Type	KEGG name	p-value
mmu00260	pathway	Glycine, serine and threonine metabolism	1.00E-06
mmu04614	pathway	Renin-angiotensin system	1.00E-06
mmu04974	pathway	Protein digestion and absorption	1.00E-06
mmu04978	pathway	Mineral absorption	1.00E-06
mmu05230	pathway	Central carbon metabolism in cancer	1.00E-06
M00134	module	Polyamine biosynthesis, arginine => ornithine => putrescine	1.00E-06
M00135	module	GABA biosynthesis, eukaryotes, putrescine => GABA	1.00E-06
1.1.1.103	enzyme	L-threonine 3-dehydrogenase	1.00E-06
1.2.1.31	enzyme	L-amino adipate-semialdehyde dehydrogenase	1.00E-06
1.5.3.1	enzyme	sarcosine oxidase	1.00E-06
2.1.1.20	enzyme	glycine N-methyltransferase	1.00E-06
2.1.3.3	enzyme	ornithine carbamoyltransferase	1.00E-06
2.3.1.1	enzyme	amino-acid N-acetyltransferase	1.00E-06
2.4.2.30	enzyme	NAD+ ADP-ribosyltransferase	1.00E-06
2.6.1.64	enzyme	glutamine---phenylpyruvate transaminase	1.00E-06
3.1.3.3	enzyme	phosphoserine phosphatase	1.00E-06
3.2.1.51	enzyme	alpha-L-fucosidase	1.00E-06
3.4.11.3	enzyme	cystinyl aminopeptidase	1.00E-06
3.4.11.7	enzyme	glutamyl aminopeptidase	1.00E-06
3.4.11.9	enzyme	Xaa-Pro aminopeptidase	1.00E-06
3.4.14.5	enzyme	dipeptidyl-peptidase IV	1.00E-06
3.4.16.2	enzyme	lysosomal Pro-Xaa carboxypeptidase	1.00E-06
3.4.17.1	enzyme	carboxypeptidase A	1.00E-06
3.4.17.15	enzyme	carboxypeptidase A2	1.00E-06
3.4.17.2	enzyme	carboxypeptidase B	1.00E-06
3.4.17.20	enzyme	carboxypeptidase U	1.00E-06

Continued

Supplementary Table 5 – Enriched KEGG pathways, modules, enzymes, reactions and metabolites in pup serum. - Continued

KEGG ID	Type	KEGG name	p-value
3.4.17.23	enzyme	angiotensin-converting enzyme 2	1.00E-06
3.4.21.1	enzyme	chymotrypsin	1.00E-06
3.4.21.26	enzyme	prolyl oligopeptidase	1.00E-06
3.4.21.39	enzyme	chymase	1.00E-06
3.4.21.4	enzyme	trypsin	1.00E-06
3.4.21.70	enzyme	pancreatic endopeptidase E	1.00E-06
3.4.21.71	enzyme	pancreatic elastase II	1.00E-06
3.4.23.1	enzyme	pepsin A	1.00E-06
3.4.23.15	enzyme	renin	1.00E-06
3.4.24.11	enzyme	nephrilysin	1.00E-06
3.4.24.16	enzyme	neurolysin	1.00E-06
3.4.24.18	enzyme	meprin A	1.00E-06
3.4.24.63	enzyme	meprin B	1.00E-06
3.5.3.1	enzyme	arginase	1.00E-06
3.5.4.16	enzyme	GTP cyclohydrolase I	1.00E-06
4.1.1.17	enzyme	ornithine decarboxylase	1.00E-06
4.1.2.48	enzyme	low-specificity L-threonine aldolase	1.00E-06
4.3.1.19	enzyme	threonine ammonia-lyase	1.00E-06
5.1.1.18	enzyme	serine racemase	1.00E-06
6.3.5.4	enzyme	asparagine synthase (glutamine-hydrolysing)	1.00E-06
R00220	reaction	L-serine ammonia-lyase	1.00E-06
R00221	reaction	D-serine ammonia-lyase	1.00E-06
R00259	reaction	acetyl-CoA:L-glutamate N-acetyltransferase	1.00E-06
R00269	reaction	2-oxoglutarate amidohydrolase	1.00E-06
R00401	reaction	alanine racemase	1.00E-06
R00447	reaction	L-lysine:oxygen 2-oxidoreductase (deaminating)	1.00E-06
R00483	reaction	L-aspartate:ammonia ligase (AMP-forming)	1.00E-06

Continued

Supplementary Table 5 – Enriched KEGG pathways, modules, enzymes, reactions and metabolites in pup serum. - Continued

KEGG ID	Type	KEGG name	p-value
R00485	reaction	L-asparagine amidohydrolase	1.00E-06
R00486	reaction	3-Cyano-L-alanine aminohydrolase	1.00E-06
R00489	reaction	L-aspartate 1-carboxy-lyase (beta-alanine-forming)	1.00E-06
R00551	reaction	L-Arginine amidinohydrolase	1.00E-06
R00552	reaction	L-Arginine iminohydrolase	1.00E-06
R00557	reaction	L-arginine,NADPH:oxygen oxidoreductase (nitric-oxide-forming)	1.00E-06
R00567	reaction	arginine racemase	1.00E-06
R00576	reaction	L-Glutamine:pyruvate aminotransferase	1.00E-06
R00578	reaction	L-aspartate:L-glutamine amido-ligase (AMP-forming)	1.00E-06
R00589	reaction	serine racemase	1.00E-06
R00610	reaction	sarcosine:oxygen oxidoreductase (demethylating)	1.00E-06
R00670	reaction	L-ornithine carboxy-lyase (putrescine-forming)	1.00E-06
R00671	reaction	L-ornithine ammonia-lyase (cyclizing; L-proline-forming)	1.00E-06
R00672	reaction	ornithine racemase	1.00E-06
R00688	reaction	L-phenylalanine:NAD ⁺ oxidoreductase (deaminat...)	1.00E-06
R00689	reaction	L-Phenylalanine:oxygen oxidoreductase (deaminating)	1.00E-06
R00690	reaction	L-phenylalanine:oxygen 2-oxidoreductase (decarboxylating)	1.00E-06
R00692	reaction	L-phenylalanine:pyruvate aminotransferase	1.00E-06
R00697	reaction	L-phenylalanine ammonia-lyase (trans-cinnamate-forming)	1.00E-06

Continued

Supplementary Table 5 – Enriched KEGG pathways, modules, enzymes, reactions and metabolites in pup serum. - Continued

KEGG ID	Type	KEGG name	p-value
R00698	reaction	L-phenylalanine:oxygen oxidoreductase (decarboxylating)	1.00E-06
R00729	reaction	L-Tyrosine:oxygen oxidoreductase (deaminating)	1.00E-06
R00734	reaction	L-tyrosine:2-oxoglutarate aminotransferase	1.00E-06
R00736	reaction	L-tyrosine carboxy-lyase (tyramine-forming)	1.00E-06
R00739	reaction	L-Tyrosine 2,3-aminomutase	1.00E-06
R00751	reaction	L-threonine acetaldehyde-lyase (glycine-forming)	1.00E-06
R00904	reaction	3-aminopropanal:NAD ⁺ oxidoreductase	1.00E-06
R00905	reaction	3-ureidopropionate amidohydrolase	1.00E-06
R00907	reaction	L-Alanine:3-oxopropanoate aminotransferase	1.00E-06
R00908	reaction	beta-alanine:2-oxoglutarate aminotransferase	1.00E-06
R00977	reaction	5,6-dihydrouracil:NAD ⁺ oxidoreductase	1.00E-06
R00978	reaction	5,6-Dihydrouracil:NADP ⁺ oxidoreductase	1.00E-06
R00996	reaction	L-threonine ammonia-lyase (2-oxobutanoate-forming)	1.00E-06
R00998	reaction	acetyl-CoA:2-oxobutanoate C-acetyltransferase (thioester-hydrolysing, carboxymethyl-forming)	1.00E-06
R01213	reaction	acetyl-CoA:3-methyl-2-oxobutanoate C-acetyltransferase (thioester-hydrolysing, carboxymethyl-forming)	1.00E-06
R01215	reaction	L-Valine:pyruvate aminotransferase	1.00E-06
R01255	reaction	proline racemase	1.00E-06
R01267	reaction	L-asparagine hydro-lyase (3-cyanoalanine-forming)	1.00E-06

Continued

Supplementary Table 5 – Enriched KEGG pathways, modules, enzymes, reactions and metabolites in pup serum. - Continued

KEGG ID	Type	KEGG name	p-value
R01270	reaction	Nicotinamide D-ribonucleotide phosphoribohydrolase	1.00E-06
R01271	reaction	nicotinamide-D-ribonucleotide:diphosphate phospho-alpha-D-ribosyltransferase	1.00E-06
R01370	reaction	Phenyllactate:NAD ⁺ oxidoreductase	1.00E-06
R01371	reaction	phenyllactate:NADP ⁺ oxidoreductase	1.00E-06
R01377	reaction	phenylpyruvate carboxy-lyase (phenylacetaldehyde-forming)	1.00E-06
R01398	reaction	Carbamoyl-phosphate:L-ornithine carbamoyltransferase	1.00E-06
R01426	reaction	Benzoate + Acetate + NADH + H ⁺ <=> trans-Cinnamate + 2 H ₂ O + NAD ⁺	1.00E-06
R01432	reaction	D-xylose aldose-ketose-isomerase	1.00E-06
R01466	reaction	O-phospho-L-homoserine phosphate-lyase (adding water;L-threonine-forming)	1.00E-06
R01563	reaction	N-Carbamoylsarcosine amidohydrolase	1.00E-06
R01771	reaction	ATP:L-homoserine O-phosphotransferase	1.00E-06
R01773	reaction	L-Homoserine:NAD ⁺ oxidoreductase	1.00E-06
R01775	reaction	L-homoserine:NADP ⁺ oxidoreductase	1.00E-06
R01987	reaction	4-acetamidobutanoate amidohydrolase	1.00E-06
R02269	reaction	5,6-Dihydrouracil amidohydrolase	1.00E-06
R02282	reaction	N2-Acetyl-L-ornithine:L-glutamate N-acetyltransferase	1.00E-06
R02382	reaction	Tyramine:oxygen oxidoreductase(deaminating) (flavin-containing)	1.00E-06
R02437	reaction	L-rhamnose ketol-isomerase	1.00E-06
R02458	reaction	D-Arginine amidinohydrolase	1.00E-06
R02509	reaction	N,N-Dimethylformamide amidohydrolase	1.00E-06

Continued

Supplementary Table 5 – Enriched KEGG pathways, modules, enzymes, reactions and metabolites in pup serum. - Continued

KEGG ID	Type	KEGG name	p-value
R02529	reaction	aminoacetone:oxygen oxidoreductase(deaminating)	1.00E-06
R02540	reaction	2-phenylacetamide amidohydrolase	1.00E-06
R02825	reaction	5-Aminopentanoate <=> D-Proline	1.00E-06
R02854	reaction	D-Serine + Amino acid(Arg-) <=> D-Lombricine + Ornithine	1.00E-06
R02923	reaction	D-Arginine:oxygen oxidoreductase (deaminating)	1.00E-06
R03102	reaction	L-2-amino adipate-6-semialdehyde:NAD+ 6-oxidoreductase	1.00E-06
R03103	reaction	L-2-amino adipate-6-semialdehyde:NADP+ 6-oxidoreductase	1.00E-06
R03163	reaction	L-fucose aldose-ketose-isomerase	1.00E-06
R03187	reaction	N-Methylimidazolidine-2,4-dione amidohydrolase (ATP-hydrolysing)	1.00E-06
R03342	reaction	3-(4-Hydroxyphenyl)pyruvate keto-enol-isomerase	1.00E-06
R04639	reaction	2-amino-4-hydroxy-6-(erythro-1,2,3-trihydroxypropyl) dihydropteridine triphosphate hydrolase	1.00E-06
R04899	reaction	3-(2-Hydroxyphenyl)propanoate <=> Phenylpropanoate	1.00E-06
R05046	reaction	formamidopyrimidine nucleoside triphosphate amidohydrolase	1.00E-06
R05048	reaction	2,5-diaminopyrimidine nucleoside triphosphate mutase	1.00E-06
R05050	reaction	N4-Acetylaminobutanal:NAD+ oxidoreductase	1.00E-06

Continued

Supplementary Table 5 – Enriched KEGG pathways, modules, enzymes, reactions and metabolites in pup serum. - Continued

KEGG ID	Type	KEGG name	p-value
R05070	reaction	(R)-2,3-Dihydroxy-3-methylpentanoate hydrolyase	1.00E-06
R05347	reaction	3-Methylbenzyl alcohol + NAD+ <=> 3-Methylbenzaldehyde + NADH + H+	1.00E-06
R05348	reaction	2-Methylbenzyl alcohol + NAD+ <=> 2-Methylbenzaldehyde + NADH + H+	1.00E-06
R06171	reaction	L-allo-threonine acetaldehyde-lyase (glycine-forming)	1.00E-06
R06531	reaction	ATP:L-threonine O-phosphotransferase	1.00E-06
R06780	reaction	Phenylpropanoate <=> 3-(3-Hydroxyphenyl)propanoic acid	1.00E-06
R06786	reaction	3-(3-hydroxyphenyl)propanoate,NADH:oxygen oxidoreductase (2-hydroxylating)	1.00E-06
R07419	reaction	4-(gamma-L-glutamylamino)butanoate amidohydrolase	1.00E-06
R07942	reaction	1-methylxanthine:oxygen oxidoreductase	1.00E-06
R07979	reaction	7-methylxanthine:oxygen oxidoreductase	1.00E-06
R08197	reaction	L-arginine:pyruvate aminotransferase	1.00E-06
R08296	reaction	Monoethylglycinexylidide <=> Glycinexylidide	1.00E-06
R08298	reaction	Monoethylglycinexylidide <=> 3-Hydroxymonoethylglycinexylidide	1.00E-06
R08299	reaction	Glycinexylidide <=> 2,6-Dimethylaniline	1.00E-06
R08301	reaction	2,6-Dimethylaniline <=> 4-Hydroxy-2,6-dimethylaniline	1.00E-06
R09088	reaction	Benzoate + Pyruvate <=> Pyruvophenone + CO2	1.00E-06

Continued

Supplementary Table 5 – Enriched KEGG pathways, modules, enzymes, reactions and metabolites in pup serum. - Continued

KEGG ID	Type	KEGG name	p-value
R09254	reaction	L-tyrosine:pyruvate aminotransferase	1.00E-06
R09830	reaction	L-Tyrosine:NAD ⁺ oxidoreductase (deaminating)	1.00E-06
R10052	reaction	(2R,3S)-3-isopropylmalate:NAD ⁺ oxidoreductase	1.00E-06
R10061	reaction	S-adenosyl-L-methionine:sarcosine N-methyltransferase [betaine forming]	1.00E-06
R10170	reaction	(2R,3S)-3-isopropylmalate hydro-lyase (2-isopropylmaleate-forming)	1.00E-06
R10851	reaction	L-allo-threonine:NADP ⁺ 3-oxidoreductase	1.00E-06
R11018	reaction	D-arginine:acceptor oxidoreductase (deaminating)	1.00E-06
R11679	reaction	(S)-2-amino-6-oxohexanoate:NADP ⁺ oxidoreductase	1.00E-06
R11918	reaction	L-phenylalanine carboxy-lyase (oxidative-deaminating)	1.00E-06
R12304	reaction	D-ornithine carboxy-lyase	1.00E-06
C00062	compound	L-Arginine	1.00E-06
C00077	compound	L-Ornithine	1.00E-06
C00079	compound	L-Phenylalanine	1.00E-06
C00082	compound	L-Tyrosine	1.00E-06
C00099	compound	beta-Alanine	1.00E-06
C00133	compound	D-Alanine	1.00E-06
C00148	compound	L-Proline	1.00E-06
C00152	compound	L-Asparagine	1.00E-06
C00153	compound	Nicotinamide	1.00E-06
C00181	compound	D-Xylose	1.00E-06
C00183	compound	L-Valine	1.00E-06
C00188	compound	L-Threonine	1.00E-06

Continued

Supplementary Table 5 – Enriched KEGG pathways, modules, enzymes, reactions and metabolites in pup serum. - Continued

KEGG ID	Type	KEGG name	p-value
C00213	compound	Sarcosine	1.00E-06
C00263	compound	L-Homoserine	1.00E-06
C00309	compound	D-Ribulose	1.00E-06
C00327	compound	L-Citrulline	1.00E-06
C00361	compound	dGDP	1.00E-06
C00418	compound	(R)-Mevalonate	1.00E-06
C00423	compound	trans-Cinnamate	1.00E-06
C00429	compound	5,6-Dihydrouracil	1.00E-06
C00431	compound	5-Aminopentanoate	1.00E-06
C00455	compound	Nicotinamide D-ribonucleotide	1.00E-06
C00483	compound	Tyramine	1.00E-06
C00507	compound	L-Rhamnose	1.00E-06
C00515	compound	D-Ornithine	1.00E-06
C00624	compound	N-Acetyl-L-glutamate	1.00E-06
C00628	compound	2,5-Dihydroxybenzoate	1.00E-06
C00637	compound	Indole-3-acetaldehyde	1.00E-06
C00719	compound	Betaine	1.00E-06
C00740	compound	D-Serine	1.00E-06
C00763	compound	D-Proline	1.00E-06
C00788	compound	L-Adrenaline	1.00E-06
C00792	compound	D-Arginine	1.00E-06
C00861	compound	L-Rhamnulose	1.00E-06
C00940	compound	2-Oxoglutaramate	1.00E-06
C00956	compound	L-2-Aminoadipate	1.00E-06
C01019	compound	6-Deoxy-L-galactose	1.00E-06
C01043	compound	N-Carbamoylsarcosine	1.00E-06
C01102	compound	O-Phospho-L-homoserine	1.00E-06
C01179	compound	3-(4-Hydroxyphenyl)pyruvate	1.00E-06

Continued

Supplementary Table 5 – Enriched KEGG pathways, modules, enzymes, reactions and metabolites in pup serum. - Continued

KEGG ID	Type	KEGG name	p-value
C01197	compound	Caffeate	1.00E-06
C01198	compound	3-(2-Hydroxyphenyl)propanoate	1.00E-06
C01416	compound	Cocaine	1.00E-06
C01602	compound	Ornithine	1.00E-06
C01721	compound	L-Fuculose	1.00E-06
C01851	compound	Scopolamine	1.00E-06
C01888	compound	Aminoacetone	1.00E-06
C02488	compound	(R)-2-Ethylmalate	1.00E-06
C02504	compound	alpha-Isopropylmalate	1.00E-06
C02505	compound	2-Phenylacetamide	1.00E-06
C02512	compound	3-Cyano-L-alanine	1.00E-06
C02565	compound	N-Methylhydantoin	1.00E-06
C02632	compound	2-Methylpropanoate	1.00E-06
C02642	compound	3-Ureidopropionate	1.00E-06
C02946	compound	4-Acetamidobutanoate	1.00E-06
C02949	compound	4-Hydroxybenzoyl-CoA	1.00E-06
C03134	compound	N,N-Dimethylformamide	1.00E-06
C03239	compound	6-Amino-2-oxohexanoate	1.00E-06
C03415	compound	N2-Succinyl-L-ornithine	1.00E-06
C03656	compound	(S)-5-Amino-3-oxohexanoic acid	1.00E-06
C03740	compound	(5-L-Glutamyl)-L-amino acid	1.00E-06
C04076	compound	L-2-Aminoadipate 6-semialdehyde	1.00E-06
C04368	compound	3-Amino-3-(4-hydroxyphenyl)propanoate	1.00E-06
C04409	compound	2-Amino-3-carboxymuconate semialdehyde	1.00E-06
C04411	compound	(2R,3S)-3-Isopropylmalate	1.00E-06
C04640	compound	2-(Formamido)-N1-(5'-phosphoribosyl)acetamidine	1.00E-06
C05350	compound	2-Hydroxy-3-(4-hydroxyphenyl)propenoate	1.00E-06

Continued

Supplementary Table 5 – Enriched KEGG pathways, modules, enzymes, reactions and metabolites in pup serum. - Continued

KEGG ID	Type	KEGG name	p-value
C05519	compound	L-Allothreonine	1.00E-06
C05581	compound	3-Methoxy-4-hydroxyphenylacetaldehyde	1.00E-06
C05589	compound	L-Normetanephrine	1.00E-06
C05607	compound	Phenyllactate	1.00E-06
C05608	compound	4-Hydroxycinnamyl aldehyde	1.00E-06
C05660	compound	5-Methoxyindoleacetate	1.00E-06
C05665	compound	3-Aminopropanal	1.00E-06
C05923	compound	2,5-Diaminopyrimidine nucleoside triphosphate	1.00E-06
C05936	compound	N4-Acetylaminobutanal	1.00E-06
C05981	compound	Phosphatidylinositol-3,4,5-trisphosphate	1.00E-06
C06007	compound	(R)-2,3-Dihydroxy-3-methylpentanoate	1.00E-06
C06125	compound	Sulfatide	1.00E-06
C06148	compound	2,5-Diamino-6-(5'-triphosphoryl-3',4'-trihydroxy-2'-oxopentyl)-amino-4-oxopyrimidine	1.00E-06
C06186	compound	Arbutin	1.00E-06
C06423	compound	Octanoic acid	1.00E-06
C06578	compound	p-Cumate	1.00E-06
C06758	compound	p-Tolualdehyde	1.00E-06
C07209	compound	3-Methylbenzaldehyde	1.00E-06
C07213	compound	2-Methylbenzyl alcohol	1.00E-06
C07214	compound	2-Methylbenzaldehyde	1.00E-06
C07216	compound	3-Methylbenzyl alcohol	1.00E-06
C08281	compound	Docosanoic acid	1.00E-06
C09704	compound	Nerolidol	1.00E-06
C11457	compound	3-(3-Hydroxyphenyl)propanoic acid	1.00E-06
C12147	compound	L-Threonine O-3-phosphate	1.00E-06
C12623	compound	trans-2,3-Dihydroxycinnamate	1.00E-06

Continued

Supplementary Table 5 – Enriched KEGG pathways, modules, enzymes, reactions and metabolites in pup serum. - Continued

KEGG ID	Type	KEGG name	p-value
C15767	compound	4-(L-gamma-Glutamylamino)butanoate	1.00E-06
C16355	compound	7-Methyluric acid	1.00E-06
C16359	compound	1-Methyluric acid	1.00E-06
C16569	compound	Glycinexylidide	1.00E-06
C16570	compound	4-Hydroxy-2,6-dimethylaniline	1.00E-06
C16572	compound	3-Hydroxymonoethylglycinexylidide	1.00E-06

Supplementary Table 6 – Targeted amino acid analysis of pup serum. (n = 5 per group)

Amino Acid	Control average concentration [μM]	CPS average concentration [μM]
Phospho-serine	0	27.2994
Hydroxyproline	65.5958	57.8426
Histidine	88.2938	85.4086
Palmitoylethanolamide	15.9652	11.4908
Asparagin	103.5692	105.2938
3-Methyl-L-histidine	53.564	64.4162
Taurine	1291.2258	1331.1234
1-Methyl-L-histidine	5.5098	4.8192
Serine	218.8436	235.9208
Glutamine	644.8596	617.0306
Acylcarnitine	5.5724	8.4894
Arginine	86.2118	121.6566
Glycine	567.4228	545.32
Asparagine	29.502	18.6436
EA	22.486	18.736
Aspartic acid	23.685	20.9746
Sarcosine	0	3.8042
Glutamic acid	96.1866	80.5752
Citrulline	63.7116	65.4648
Beta-Alanine	25.3536	9.3014
Threonin	207.0026	226.6268
Alanine	779.8384	698.8354
Gamma-aminobutyric acid (abbrev. GABA)	0	0.8738
((all-S,all-E)-3-Amino-9-methoxy-2,6,8-trimethyl-10-phenyldeca-4,6-dienoic acid) (abbrev. ADDA)	11.776	10.3352
Proline	236.4238	212.2428

Continued

Supplementary Table 6 – Targeted amino acid analysis of pup serum. (n = 5 per group) - continued

Amino Acid	Control average concentration [μ M]	CPS average concentration [μ M]
Hyl2	1.7888	2.5394
L-alpha-aminobutyric acid (abbrev. AABA)	6.6902	9.6316
Cystathionine	1.006	1.386
Ornithine	84.9762	92.6034
Cysteine	6.5676	7.9896
Lysine	209.2512	228.4896
Tyrosine	118.4634	108.76
Methionine	92.0502	97.948
Valine	287.4228	294.3194
Isoleucine	113.8116	117.3174
Leucine	195.3124	199.9224
Homocysteine	0	0
Phenylalanine	118.604	98.8738
Tryptophan	99.4166	75.5292

abbrev. = Abbreviated

Article

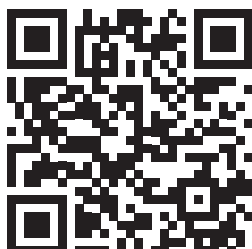
5. Effects of Early Life Stress on Bone Homeostasis in Mice and Humans

Karin Wuertz-Kozak^{1,2,3,†}, Martin Roszkowski^{3,4,†}, Elena Cambria³, Andrea Block⁵, Gisela A. Kuhn³, Thea Abele⁶, Wolfgang Hitzl^{7,8,9}, David Drießlein¹⁰, Ralph Müller³, Michael A. Rapp¹¹, Isabelle M. Mansuy^{3,4,*}, Eva M. J. Peters^{6,13,*} and Pia M. Wippert^{3,5,12,*}

† Shared first authorship: Martin Roszkowski conducted the animal experiments, participated in tissue collection and drafted the article.

* Shared last authorship

This article has been published in the journal: *International Journal of Molecular Sciences*



Publication date: 10.9.2020

DOI: 10.3390/ijms21186634

¹ Department of Biomedical Engineering, Rochester Institute of Technology (RIT), Rochester, NY 14623, USA

² Schön Clinic Munich Harlaching, Spine Center, Academic Teaching Hospital and Spine Research Institute of the Paracelsus Medical University Salzburg (AU), 81547 Munich, Germany

³ Department of Health Sciences and Technology, ETH Zurich, 8093 Zurich, Switzerland

⁴ Laboratory of Neuroepigenetics, University of Zurich and Swiss Federal Institute of Technology, Brain Research Institute, Neuroscience Center Zurich, 8057 Zurich, Switzerland

⁵ Sociology of Health and Physical Activity, University of Potsdam, 14469 Potsdam, Germany

⁶ Psychoneuroimmunology Laboratory, Department of Psychosomatics and Psychotherapy, 35390 Giessen, Germany

⁷ Research Office (Biostatistics), Paracelsus Medical University, 5020 Salzburg, Austria

⁸ Research Program Experimental Ophthalmology and Glaucoma Research, Paracelsus Medical University, 5020 Salzburg, Austria

⁹ Paracelsus Medical University Salzburg, Department of Ophthalmology and Optometry, 5020 Salzburg, Austria

¹⁰ Statistical Consulting Unit StaBLab, Ludwig-Maximilians-University Munich, 80333 Munich, Germany

¹¹ Faculty of Health Brandenburg, University of Potsdam, 14469 Potsdam, Germany

¹² Department of Health, University of Potsdam, 14469 Potsdam, German

¹³ Charité Center 12 Internal Medicine and Dermatology, Division for General Internal Medicine, Psychosomatics and Psychotherapy, Universitätsmedizin Berlin, 10117 Berlin, Germany

Correspondence: kwbme@rit.edu; Tel.: +1-585-475-7355

5.1. Abstract

Bone pathology is frequent in stressed individuals. A comprehensive examination of mechanisms linking life stress, depression and disturbed bone homeostasis is missing. In this translational study, mice exposed to early life stress (MSUS) were examined for bone microarchitecture (μ CT), metabolism (qPCR/ELISA), and neuronal stress mediator expression (qPCR) and compared with a sample of depressive patients with or without early life stress by analyzing bone mineral density (BMD) (DXA) and metabolic changes in serum (osteocalcin, PINP, CTX-I). MSUS mice showed a significant decrease in NGF, NPYR1, VIPR1 and TACR1 expression, higher innervation density in bone, and increased serum levels of CTX-I, suggesting a milieu in favor of catabolic bone turnover. MSUS mice had a significantly lower body weight compared to control mice, and this caused minor effects on bone microarchitecture. Depressive patients with experiences of childhood neglect also showed a catabolic pattern. A significant reduction in BMD was observed in depressive patients with childhood abuse and stressful life events during childhood. Therefore, future studies on prevention and treatment strategies for both mental and bone disease should consider early life stress as a risk factor for bone pathologies.

5.2. Introduction

Bones are essential components of the musculoskeletal system and subjected to continuous remodeling as an adaptation mechanism to environmental changes. Disturbances in bone development and remodeling by formation/resorption of the extracellular matrix (ECM) or differentiation of osteoblasts into osteocytes and apoptosis of osteocytes could result in reduced bone mass and increased fracture risk.

Beside well-documented mechanisms like menopause-associated hormonal changes, aging-related factors, changes in physical activity, as well as drugs and diseases, recent research suggested that psychosocial stress and stress-linked neuronal processes are associated with an increased risk for bone pathologies [1–5]. Autonomic and sensory nerve fibers densely innervate bone, predominantly in the periosteum and in areas with high metabolic activity and bone turnover. Neuronal structures can make direct contact with osteoblasts and osteoclasts, which in turn express receptors for neuronal markers on their surface, and can produce neuronal mediators in an auto- and paracrine fashion [6–10]. Importantly, sympathetic and peptidergic neuronal factors can act as stress mediators and appear to play a key role in bone turnover [11–13]. Of specific relevance are tyrosine hydroxylase (TH), a rate-limiting enzyme for noradrenaline synthesis, neuropeptide Y (NPY), often co-expressed with noradrenaline, vasoactive intestinal peptide (VIP), often co-expressed with acetylcholine, and the neuropeptides calcitonin gene related peptide (CGRP) and substance P (SP) that are expressed in sensory nerve fibers. In addition, neurotrophic growth factors such as nerve growth factor (NGF) and brain derived neurotrophic factor (BDNF) that guide outgrowing nerve fibers to bony areas requiring innervation are of interest. Stress alters their expression, and they can also act as direct and indirect growth factors for osteoblasts [14–26]. Latest studies indicate that psychosocial stress can lead to structural and functional changes in neuronal plasticity, neuronal marker expression, mitochondria and inflammation [4,27,28], possibly resulting in downstream alterations of bone homeostasis [29–33].

In humans, major early life stress like childhood maltreatment strongly affects the stress response, as well as behavioral and cognitive functions throughout life [34,35]. Strong associations were shown between childhood maltreatment and higher risk for psychological and physiological disorders including depression, hypersensitivity of the neuroendocrine, autonomic and peptidergic stress response leading to altered dynamics of the hypothalamic

pituitary adrenal (HPA) axis, and changes in the neuronal mediators that can influence bone health [36]. Childhood maltreatment is one of the best-documented risk factors for depression [37–40] and depression, in turn, has been associated with a higher risk for reduced bone mineral density (BMD), osteoporosis and bone fractures [41–45].

However, existing knowledge about the underlying mechanisms between early life stress, neurogenic stress response elements, and detrimental changes in bone metabolism and microstructure/BMD has been limited by several reasons. First, although early life stress like childhood maltreatment is a frequent phenomenon, it is hardly accessible to retrospective and longitudinal studies due to its rare diagnosis and ethical requirements for case-control studies. Second, access to biological material and strict control of confounding factors, such as physical activity and eating habits, are challenging in human studies [46,47]. Animal models offer an obvious way to investigate major stress experiences early in life despite these obstacles. Animal models are helpful counterparts of human studies to investigate underlying mechanisms in a highly controlled environment that allows extensive tissue sampling, strict definition of adverse events and confounding factors, and lower subject variability.

Unpredictable maternal separation and maternal stress during early life (mice exposed to early life stress (MSUS) paradigm [48]) is an experimental stress paradigm in rodents that can mimic aspects of childhood maltreatment and induce long-lasting health effects, such as increased depression-like behavior (anhedonia) and altered brain activity in adulthood [49]. The MSUS paradigm severely impacts physiology and behavior in the exposed animals, but also in their descendants across several generations via mechanisms involving epigenetic factors in the germline [48,50–52].

To address the knowledge gap between early life stress, stress-dependent neurogenic markers that mark neuronal plasticity and detrimental changes in bone metabolism and bone microstructure/BMD, we first examined the impact of early life stress on neuronal mediator expression (qPCR) and bone microarchitecture (μ CT), metabolism (qPCR on bone, ELISA on serum for osteocalcin OC, PINP, CTX-I), and in mice using the MSUS paradigm (Aim 1). Then, we translated the findings to humans by analyzing metabolic changes in serum (OC, PINP, CTX-I) and microarchitecture (DXA) in a sample of depressive patients, with or without retrospectively reported experiences of early life stress, like childhood maltreatment and stressful life events during childhood (Aim 2).

5.3. Results

5.3.1. Mouse Study – Bone Innervation and Neuronal Mediators

We first assessed the effects of early life stress on neuronal signaling and neurogenic factors in bone metabolism by measuring neuronal density and expression patterns of neurogenic markers in the bone of MSUS and control mice ($n = 6\text{--}8$ each).

To study changes in neuronal marker gene expression, qPCR was performed. Gene expression analysis revealed that key receptors for nerve growth factors, neurotransmitters and neuropeptides (Figure 1) and selected receptors' ligands (Figure 2) were changed in MSUS mice in a pattern that may promote higher bone turnover and lower bone density. In detail, mRNA expression of the receptors NPYR1 ($p < 0.05$, Figure 1B), VIPR1 ($p < 0.001$, Figure 1C) and TACR1 ($p < 0.01$, Figure 1D) were significantly reduced in MSUS mice whole bone homogenates (after the removal of bone marrow), suggesting their presence on osteocytes. These three receptors are involved in the regulation of proliferation and differentiation in bone, and their concomitant downregulation may lead to higher remodeling activity with less proliferation and more differentiation of bone cells. Furthermore, a significant reduction of the neurotrophin NGF ($p < 0.001$, Figure 2A) was revealed, while NPY showed a downtrend in MSUS ($p = 0.068$, Figure 2B). This would hamper both neuronal plasticity and bone remodeling when facing challenge such as a wound or aging leading to osteoporosis. Other markers of bone innervation and metabolism such as NGFR, ADRB2, CHRNA7, RAMP1, and TAC1 were similar in control and MSUS mice, whereas TRKA, TRKB, TH, ChAT and VIP were below the detection limit.

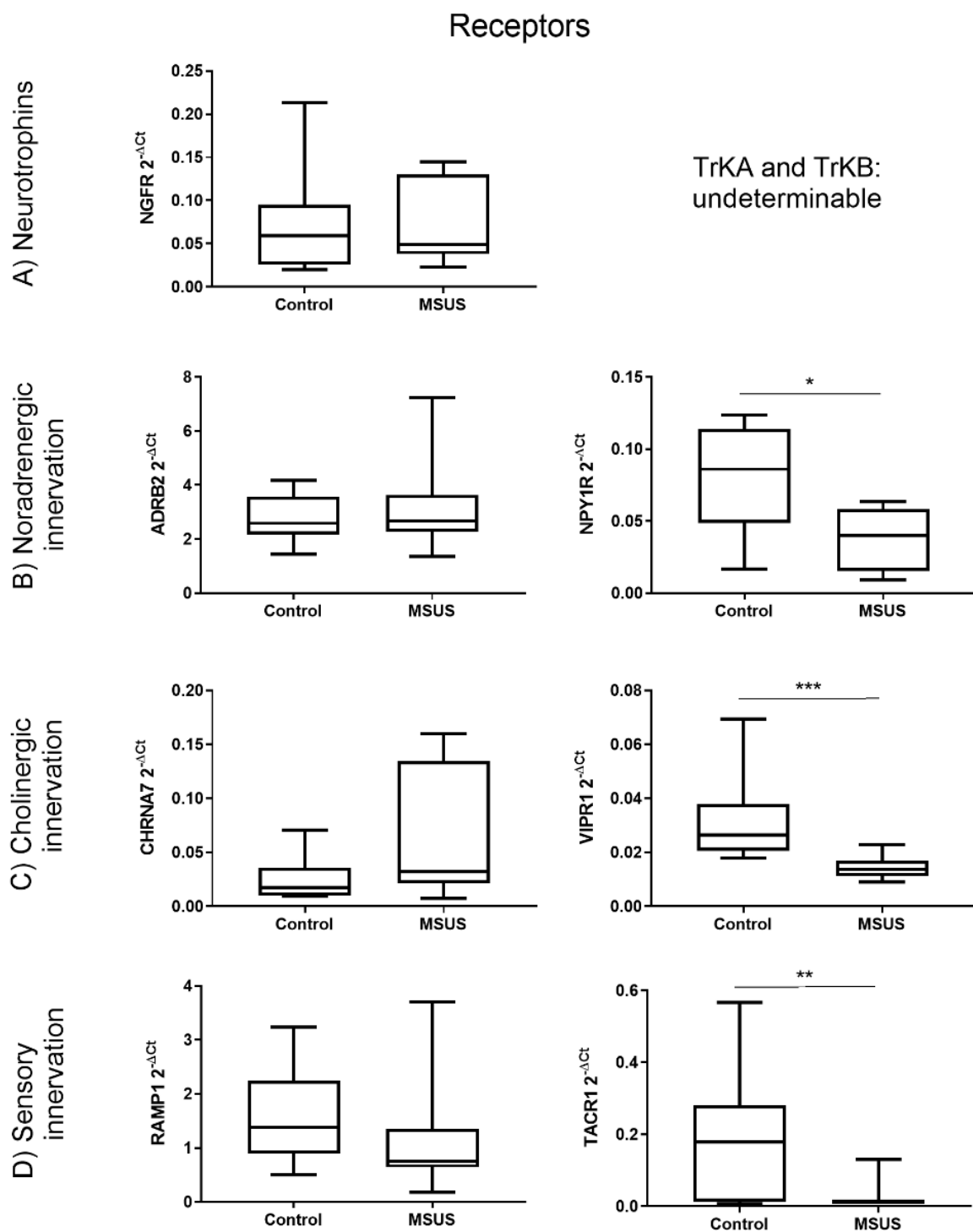


Figure 1: Differential gene expression of neuronal receptors in bone between control and mice exposed to early life stress (MSUS) mice. Shown are the gene expression of neurotrophin receptors (**A**), noradrenergic receptors (**B**), cholinergic receptors (**C**) and receptors involved in sensory innervation (**D**). Data ($n = 8$ per group) are expressed as Min to Max of $2^{-\Delta Ct}$. Significance level: *** $p < 0.001$, ** $p < 0.01$ and * $p < 0.05$ between indicated groups.

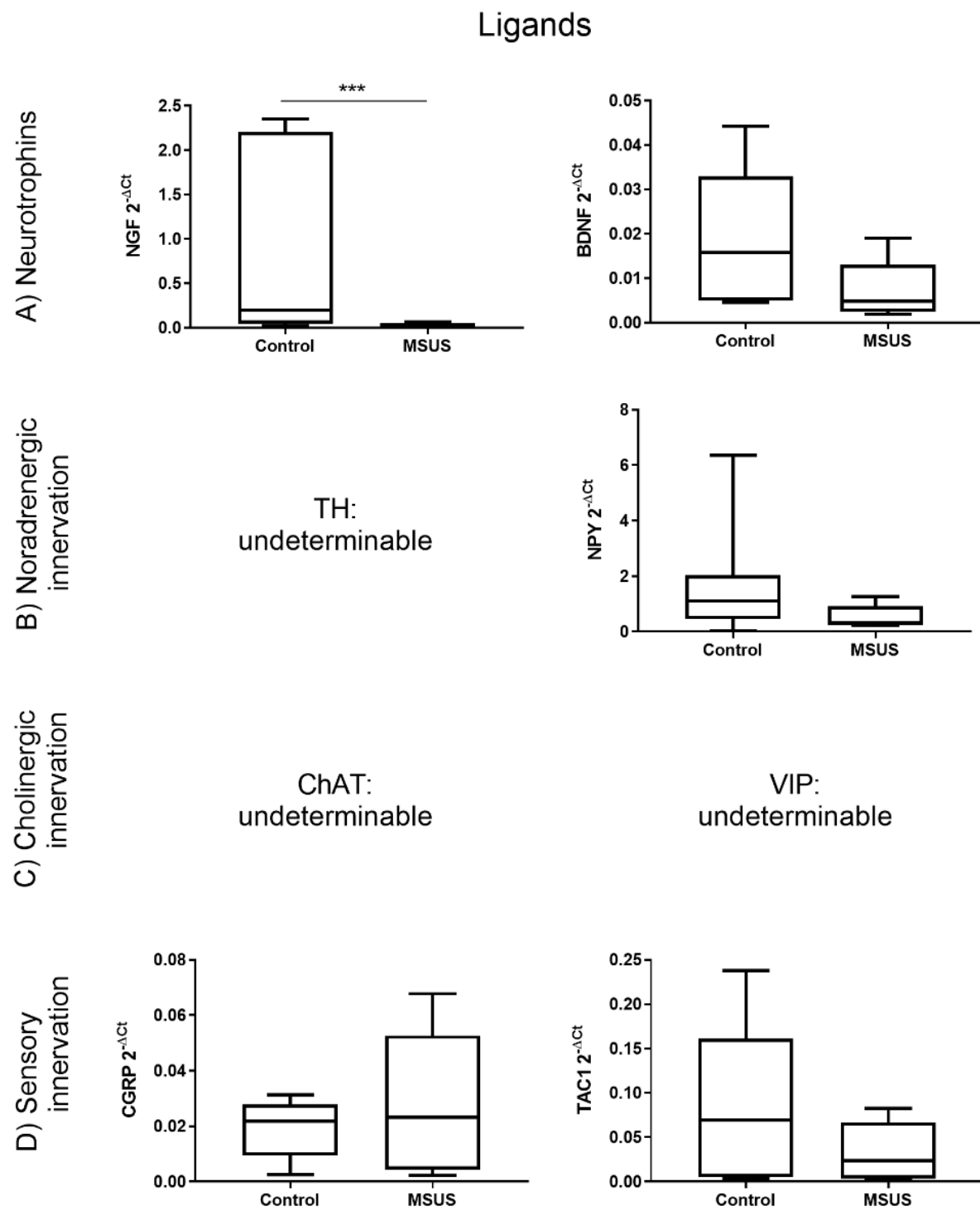


Figure 2: Differential gene expression of neuronal ligands in bone between control and MSUS mice. Shown are the gene expression of neurotrophins (A), noradrenergic ligands (B), cholinergic ligands (C) and ligands involved in sensory innervation (D). Data ($n = 8$ per group) are expressed as Min to Max of $2^{-\Delta CT}$. Significance level: *** $p < 0.001$ between indicated groups.

We subsequently investigated bone innervation by immunohistomorphometry. The density of nerve fibers labeled with the pan-neuronal marker protein gene product 9.5 (PGP 9.5) was significantly increased in the bone of MSUS mice (Figure 3), whereas nerve fibers labeled with the neuronal plasticity marker GAP 43 were unaffected (not shown), indicating that higher innervation was not due to increased neuronal plasticity, but was likely a stable feature. Higher innervation density potentially leads to higher sensitivity of bone neurons to stimuli like injury. Notably, the neuropeptides NPY, VIP and SP were undetectable by immunohistochemistry, most likely due to insufficient bone preservation. This likely results from the post-mortem fixation method used for ethical requirements, which does not preserve small peptides (the eleven amino-acid sequences of SP, for example, are rapidly digested by endogenous enzymes after termination of circulation) [53–55].

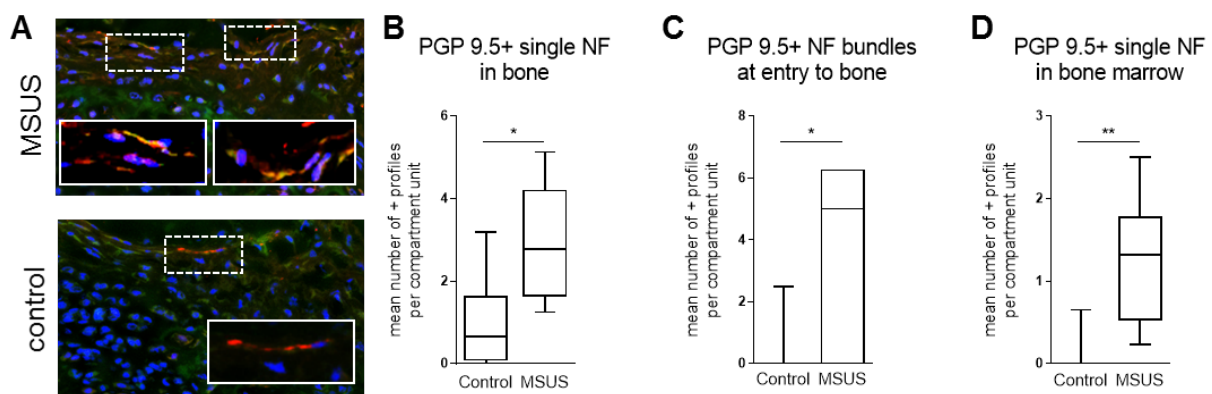


Figure 3: Increased bone innervation in MSUS mice. Representative images of the third tail bone from control and MSUS mice labeled with protein gene product 9.5 (PGP 9.5) pan-neuronal marker for immunofluorescence histomorphometry of nerve fibers (nerve fibers (NF)-red) in bone. Nuclei are counterstained with 4',6-diamidino-2-phenylindole (DAPI) (blue), mast cells with fluorescein isothiocyanate (FITC)-avidin (green) (A). Shown are the increased mean numbers of immune-positive profiles per compartment unit of single NF in bone (B), NF bundles at entry to bone (C) and single NF in bone marrow (D). Data ($n = 8$ Control, $n = 6\text{--}7$ MSUS) are expressed as Min to Max of number of positive profiles per compartment unit. Significance level: ** $p < 0.01$ and * $p < 0.05$ between indicated groups.

5.3.2. Mouse Study – Bone Metabolic Parameters

We then examined if changes in neuronal markers were associated with bone metabolic changes by measuring markers in serum and bone. Serum levels of osteocalcin and PINP, two markers associated with bone formation, did not change after MSUS (Figure 4A,B). In contrast, the level of CTX-I, which is associated with bone resorption, was significantly increased in MSUS mice compared to control mice ($p < 0.01$, $n = 14$ each; Figure 4C).

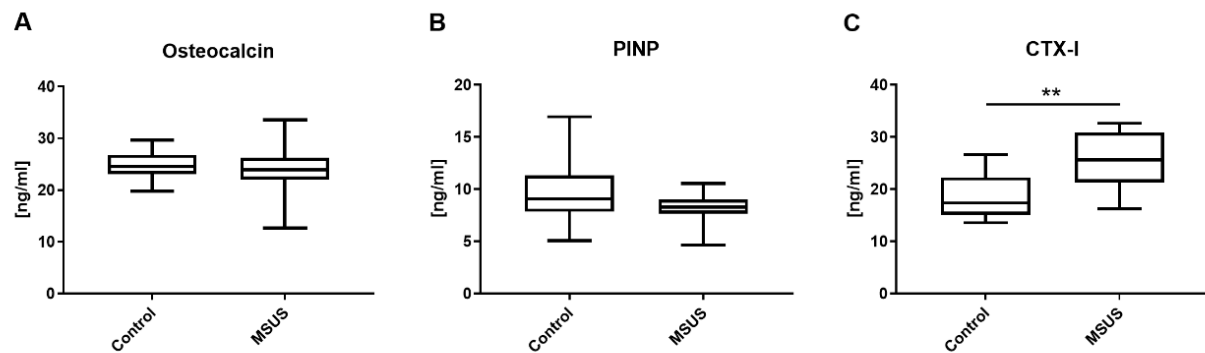


Figure 4: Bone formation and resorption markers in serum of mice. Shown are serum concentration measurements of osteocalcin (A), procollagen type 1 N-terminal propeptide (PINP) (B) and c-terminal telopeptide of type I collagen (CTX-I) (C) in mice. Data ($n = 14$ per group) are expressed as Min to Max of concentration in serum [ng/mL]. Significance level: ** $p < 0.01$ between indicated groups.

However, this catabolic shift was not reflected by altered gene expression of tissue-specific extracellular matrix markers (osteocalcin, osteoprotegerin, osteopontin, sclerostin) in bone samples of MSUS (Figure 5A–D) ($n = 8$ each).

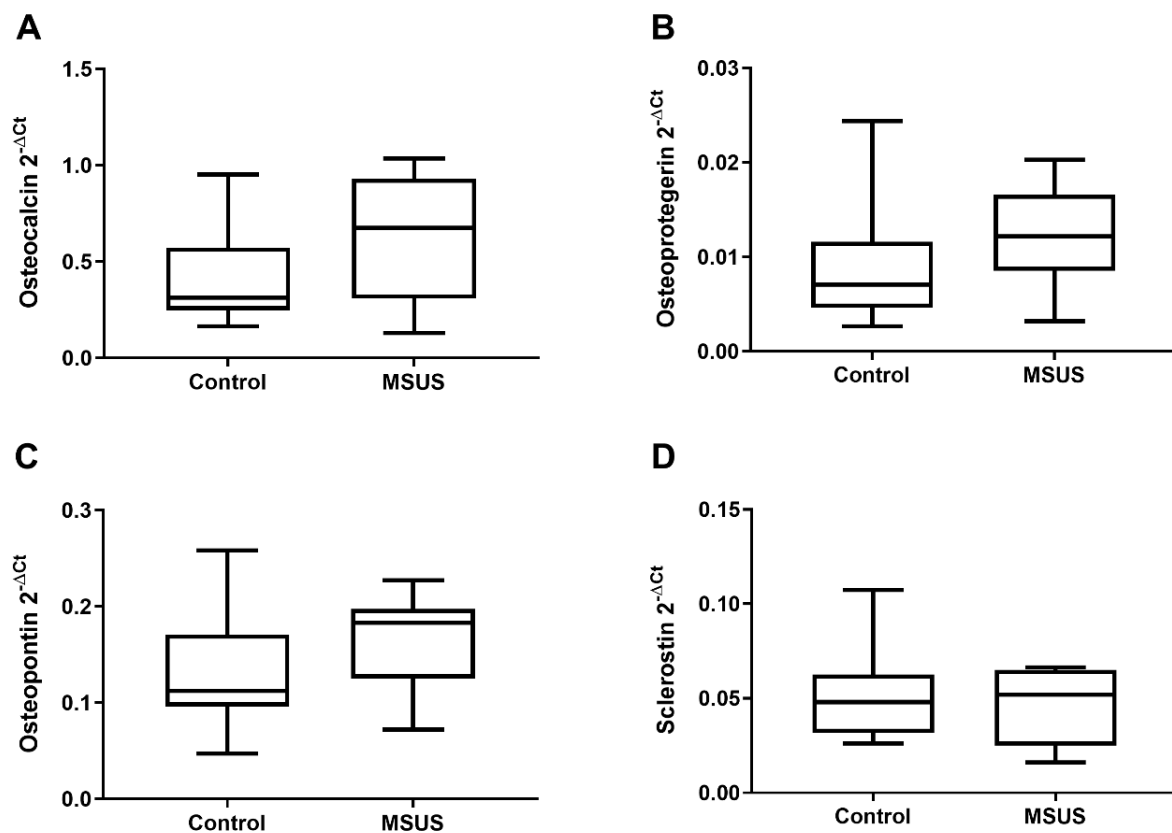


Figure 5. Gene expression of extracellular matrix in bone of mice. Shown are the gene expressions of tissue-specific extracellular matrix markers in bone of controls and MSUS. Genes include osteocalcin (A), osteoprotegerin (B), osteopontin (C) and sclerostin (D). Data ($n = 8$ per group) are expressed as Min to Max of $2^{-\Delta Ct}$. Significance level: all $p > 0.05$.

5.3.3. Mouse Study – Bone Microarchitecture

Next, it was examined if MSUS affects bone microarchitecture in mice using μ CT ($n = 14$ MSUS, $n = 13$ Control). As bone microarchitecture is sensitive to mechanical loading, we also measured the body weight of experimental animals over time. Body weight was significantly lower in MSUS mice compared to control mice starting at postnatal day 7 (PND7), and remained lower in adulthood ($p < 0.001$ for PND 7–28 and $p < 0.05$ for 10 months, Supplementary Figure S1), and this caused minor effects on bone microarchitecture.

After adjusting μ CT data for body weight, a comparison of means between control and MSUS mice did not reveal any difference in full, cortical or trabecular microarchitecture (all values $p > 0.05$) (Supplementary Table S1). We also used blocking in tertiles for body weight and conducted a two-factorial multivariate analysis of variance, which revealed that, indeed, the effects of MSUS versus controls were driven by body weight. To specify this effect, we

conducted sets of linear regression analyses to test for simple mediation effects and found that body weight mediated the effect of MSUS on full length, TV, BV, MV and BS (all p's for direct effects > 0.05).

5.3.4. Human Study - Descriptive Results

N = 193 out of n = 208 patients under study suffered from depression with minimal (35 %) up to moderate/severe (65 %) severity (BDI-II: M = 23.8, SD = 10.7) and were included in further analysis. For the analysis of bone metabolic parameters, blood samples from n = 145 patients were available, of whom n = 145 filled in the Inventory of Stressful Life Events (ILE) and n = 54 the Childhood Trauma Screener (CTS). For the BMD analysis, n = 17 patients took part in DXA bone densitometry measurements. Out of these participants, n = 15 patients filled in the Inventory of Stressful Life Events (ILE) and n = 17 the Childhood Trauma Screener (CTS). Missing data are due to incomplete questionnaires or drop out. Table 1 provides descriptive data on age, gender, antidepressant use, weight and early life stress for the subsamples. Average bone mineral density (BMD) in the sample was M = 0.942 g/cm² (SD = 0.186 g/cm²) in the trochanter region of the proximal femur.

5.3.5. Human Study - Bone Metabolic Parameters

Regarding changes in human bone metabolism following early life stress, bone serum markers OC, PINP, CTX-I were analyzed. It was shown that depressed patients with childhood trauma (CTS, CTS abuse) had an increased anabolic bone metabolism in comparison to depressed patients without early life stress (CTS: *p = 0.05 for CTX; CTS abuse: *p = 0.03 for P1PN, Table 2). This anabolic bone metabolism was likewise found for depressed patients with stressful life events during childhood (ILE child) in comparison to depressed patients without early life stress (*p = 0.04 for P1PN, Table 2). Depressed patients with experiences of childhood neglect (CTS neglect) lacked such an anabolic reaction (Table 2).

5.3.6. Human Study - Bone Mineral Density

An explorative analysis on bone mineral density in a subsample of DXA measurements suggests that depressive patients with stressful life events during childhood (ILE child) had reduced BMD in the trochanter major (*p = 0.03 for BMD_T) and as a tendency a reduction in general BMD (#p = 0.08 for BMD_G, Table 2). There are indications that depressed patients with a history of childhood abuse showed specifically a BMD reduction in the trochanter major

(* $p = 0.05$ for BMD_T), and a tendency in reduced BMD in general (# $p = 0.07$ for BMD_G). This gives notice of long-term health consequences of people with maltreatment and stressful life events during childhood in comparison to people with depression lacking experiences of early life stress (Table 2, Figure 6).

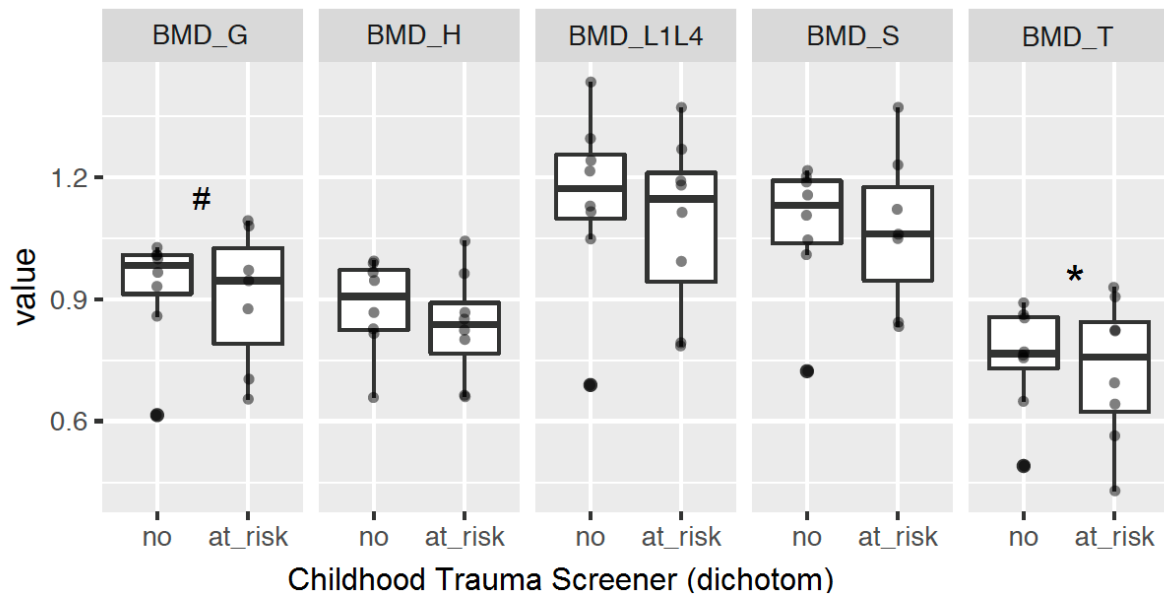


Figure 6. Bone mineral density measurements in human patients. Shown is the bone mineral density (BMD) in G (total), H (collum femoris), S (corpus femoris), and T (trochanter major) as mean of the right and left site and L1-L4 (lumbar vertebralis bodies) stratified for at risk and not at risk for childhood maltreatment (not controlled for gender, age, body weight). Data ($n = 18$) are expressed as mean and standard deviation of BMD, stratified for Childhood Trauma Screener (CTS) (at risk for abuse or neglect). Significance level: * $p < 0.05$, and # $p < 0.1$ between indicated groups.

Table 1: Descriptive Data on Sociodemographic and Clinical Characteristics of the Human Sample.

	N	Age		Depression (BDI-II Score)		Weight		Sex		Antidepressant Use		Early Life Stress			
		M	(SD)	M	(SD)	M	(SD)	N (Female)	(%)	N (Yes)	(%)	N (Yes)	(%)	N (Yes)	(%)
Sample of bone metabolic parameters ^a	145	47.9	(10.1)	24.0	(10.1)	78.1	(17.4)	118	(81.4)	100	(69.0)	128	(88.3)	47	(32.4)
↳ life events during childhood (ILE child)	128	48.1	(10.1)	24.0	(10.0)	78.2	(17.3)	104	(81.3)	86	(67.2)				
↳ childhood maltreatment (CTS)	47	47.9	(10.4)	24.6	(10.7)	75.8	(17.3)	35	(74.5)	32	(68.1)				
DXA sample ^b	17	51.9	(6.6)	23.7	(11.7)	74.3	(17.5)	12	(70.6)	13	(76.5)	15	(88.2)	17	(100.0)
↳ life events during childhood (ILE child)	15	52.2	(7.0)	24.9	(12.2)	71.2	(16.3)	11	(73.3)	11	(73.3)				
↳ childhood maltreatment (CTS)	17	51.9	(6.6)	23.7	(11.7)	74.3	(17.5)	12	(70.6)	13	(76.5)				

^a Bone serum markers OC, PINP, CTX-I^b bone mineral density (BMD) measured by Dual Energy X-ray Absorptiometry (DXA)^c Inventory of Stressful Life Events; stressful life events during childhood (≤ 12 years)^d Childhood Trauma Screener (CTS) at least at risk for one type of neglect or abuse (sexual, physical, emotional abuse, physical, emotional neglect).

Table 2: Main Effects (Regression Coefficient b) of Childhood Maltreatment (Abuse or Neglect) and Stressful Life Events During Childhood (\leq 12 years; ILE child) on Bone Serum Marker (Osteocalcin (OC), Procollagen type 1 N-terminal propeptide (PINP), and C-terminal telopeptide of Type I Collagen (CTX-I)) and Bone Mineral Density (BMD).

	P1NP			OC			CTX-I		
	b	95%CI	p	b	95%CI	p	b	95%CI	p
CTS ^a	9.27	-1.43; 19.97	0.10 [#]	2.87	-0.56; 6.30	0.11	0.10	0.01; 0.18	0.05*
CTS abuse	11.42	1.86; 20.99	0.03*	2.51	-0.65; 5.67	0.13	0.06	0.02; 0.14	0.16
CTS neglect	-6.26	-16.45; 3.93	0.24	0.32	-3.63; 2.98	0.85	0.03	-0.06; 0.12	0.50
ILE child ^b	8.37	0.71; 16.03	0.04*	2.28	-0.10; 4.65	0.06 [#]	0.06	-0.01; 0.11	0.06 [#]

	BMD L1L4 ^c				BMD T				BMD S				BMD G				BMD H	
	b	95%CI	p	b	95%CI	p	b	95%CI	p	b	95%CI	p	b	95%CI	p	b	95%CI	p
CTS	-0.07	-0.23; 0.08	0.40	-0.09	-0.22; 0.04	0.20	-0.09	-0.25; 0.08	0.33	-0.10	-0.23; 0.03	0.17	-0.10	-0.22; 0.02	0.12			
CTS abuse	-0.07	-0.26, 0.12	0.48	-0.15	-0.28; -0.02	0.05*	-0.13	-0.32, 0.06	0.22	-0.15	-0.29, -0.01	0.07 [#]	-0.12	-0.26, 0.01	0.10			
CTS neglect	-0.06	-0.21, 0.10	0.51	-0.06	-0.20, 0.07	0.39	-0.07	-0.24, 0.10	0.45	-0.07	-0.21, 0.07	0.38	-0.03	-0.16, 0.10	0.68			
ILE child	-0.18	-0.46, 0.10	0.25	-0.26	-0.44, -0.07	0.03*	-0.18	-0.48, 0.11	0.26	-0.22	-0.43, -0.01	0.08 [#]	-0.17	-0.36, 0.03	0.14			

Multiple regression models, adjusted for age, gender, and study sides. Significant Regression coefficients b are bold. Significance level: * p < 0.05, and # p < 0.1.

^a Childhood Trauma Screener (CTS) at least at risk for one type of neglect or abuse (sexual, physical, emotional abuse, physical, emotional neglect)

^b Inventory of Stressful Life Events; stressful life events during childhood (≤ 12 years)

^c Bone mineral density (BMD) was measured as mean value (M) in the lumbar spine L1-L4 (lumbar vertebral bodies), T (trochanter major), S (corpus femoris), G (total), and H (collum femoris)

5.4. Discussion

The first aim of this study was to investigate the effects of early life stress on bone health and associated biological factors in a mouse model of early life stress (MSUS). The second study aim was the translation of the gained knowledge in a human model using a sample of depressive patients with and without early life stress.

Aim 1: In summary, we found that early life stress in the MSUS model altered bone innervation and neuronal mediator expression as well as bone metabolism, as evidenced by increased CTX-I serum concentrations, but did not affect the expression of bone markers within the bone or bone microarchitecture. In detail, we found significantly decreased expression of NGF, NPYR1, VIPR1 and TACR1 in MSUS bones. This response pattern is suggestive for a higher rate of bone turnover and lower bone healing capacities as a consequence of early life stress, suggesting a concurrent joint downregulation, reduced bone remodeling and long-term destabilization. The neurotrophin NGF is important for the expression of cholinergic and sensory neuronal factors, and hence for the development and the repair of bone, as demonstrated by reduced bone length when absent [14–26]. The neuropeptide NPY promotes osteoblast differentiation and balances the effects of stress-induced bone loss through beta-adrenergic stimulation, both with consequences for bone remodeling during healing [10,53,56–63]. The neuropeptide VIPR1, finally, promotes bone mineralization [64–68], while TACR1 regulates the osteoblasts, osteoclasts and mesenchymal stem cell functionality associated with protection from osteoporosis [2,62,69–85].

While MSUS mice showed a clear neuroendocrine response pattern, the gene expression of typical bone markers (in bone) was unaffected. Similarly, we did not observe increased osteocalcin in the serum of MSUS mice. However, CTX-I serum levels were significantly increased in MSUS mice. CTX-I is an increasingly promoted and robust biochemical factor for bone resorption in clinical settings and further giving notice about correlations to bone mineral density [86–89]. Additional analyses, such as bone histomorphometry to determine whether MSUS leads to alterations in the numbers of osteoblasts (type 1 procollagen staining) and/or osteoclasts (TRAP staining) [90] could provide useful insights into bone adaptation processes.

Regarding bone microarchitecture, no significant changes were observed after normalization to body weight. Body weight itself, which was affected by MSUS, did cause minor changes in bone microarchitecture, likely due to differences in mechanical loading of the skeleton. It is unclear if altered body weight might be a post stress consequence for MSUS or an incidental finding. This should be considered in future studies, as it can be a confounding factor in μ CT analyses. We considered whether the observed lack of differences in bone microarchitecture (despite an increase in serum CTX-I) might be due to divergent timelines of these events [91] or might be sex-dependent (different susceptibility to bone alterations and/or sensitivity to stress) [92,93]. Therefore, we additionally conducted μ CT scans of the femurs of female mice over a more extended time range (up to 16 months). We did not find any differences in bone microarchitecture in the female mice, even not at later time points (data not shown). It is important to keep in mind that changes in bone microarchitecture may be site-specific, and may hence have been overlooked by restricting the μ CT analysis to the femur only. Perhaps, the use of models of aging (e.g., the senescence-accelerated mouse = SAM) [94], models that include bone injury requiring repair (such as osteotomy) [95], or a comparison of stress-resilient and stress-prone subpopulations [96] might potentially have led to observable changes in bone structure within a reasonable time frame [97], but further investigations will be needed to allow for more definite statements.

Aim 2: In summary, we found that people who experienced childhood maltreatment or stressful life events during childhood showed an overshooting anabolic bone metabolism during a depressive episode, rather than the expected minor, short-term metabolic adaptation. For example, people in our study showed a threefold higher metabolic reaction in PINP during the depressive episode, in comparison to depressed adults without childhood maltreatment [5]. This was evidenced by increased serum levels in bone metabolism markers (distinctly in PINP and CTX-I, less in OC). Furthermore, our data suggest that depressive adults with experiences of childhood maltreatment (childhood abuse) and stressful life events during childhood showed a significantly decreased BMD in the long term. In contrast, for depressive adults with no experiences of childhood neglect, these patterns were not observed. In other words, and regarding latest studies, an overshooting or lacking metabolic adaptation during a depressive episode may serve as a link for the often-observed reduction of BMD in depressed patients in the long term [5]. These mechanisms fit the hypotheses of the destructive effects of a hypersensitive central stress response (overshooting) or a blunted response (lacking adaptation) on organs and bodily tissues.

Other human studies have linked childhood maltreatment to neuroendocrinological and neuroanatomic alterations that overlap with depressive symptoms and result in a vulnerable phenotype that is affected by a hypersensitive central stress response, blunted stress reactivity and lower stress resilience [98–100]. It was suggested that further severe distress, such as additional traumatization, or the development of depression, may promote an over-adaptive reaction. The response pattern in our data seems to confirm this assumption, which can result from various aspects, such as an altered mitochondrial function, gene dysregulation, the accumulation of oxidative stress, inflammation and senescence or changes in neuronal plasticity [27,28]. The associations between stressful events early in life and an early decrease of noradrenergic, cholinergic and sensory neuronal factors were also observed in our animal model. It is also comprehensible that no such pattern could be found for childhood neglect, as it represents acts of omissions that are typically temporary, such as lack of nutrition, medical or emotional care. Hence, this might have a lower impact on a person's psychological integrity, identity and health than childhood abuse. Furthermore, the data match well with further results within this study sample: patients that suffer from chronic stress (measured by the allostatic load index) showed a catabolic shift in bone metabolism during a depression episode [5]. This can be explained by the fact that other mechanisms are expected for allostatic load as an accumulating damage over time with the consequence of neuroendocrinological and neuroanatomic alterations [36,99,101]. The observed reduced BMD can be expected in both response patterns: within a hypersensitive stress response and within an increased allostatic load. Both mechanisms were demonstrated in data of people of the presented DEPREHA-study.

In summary, we found that early life stress affects bone metabolism in mice and humans. In MSUS mice, this was evidenced by a significant shift towards a neurogenic and osteogenic catabolic milieu (decreased NGF, NPYR1, VIPR1, TACR1; higher innervation density in bone; increased serum CTX-I), but no alterations in bone microarchitecture in relatively young mice not exposed to additional life stresses. In humans however, for those who suffered both from early life stress and depression, a significant reduction in BMD was observed. Taking the age range and morbidity (depression) of the human sample under consideration, the differences between mice and human could be interpreted as patterns of vulnerability and acute consequences (mouse model) compared to long-term burden of early life stress (human). Otherwise, species-related differences in bone metabolism between mice

and humans have been described [102]. Our data support the notion that the mechanisms of bone loss seem different between mice and humans, as mice did not show any decrease in trabecular thickness, which is considered as typical for ageing humans [103]. However, this contrasts with Halloran et al. [103], who showed that cancellous bone volume fraction is reduced in 24 months old male C57BL/6J mice and is hence comparable to humans. Furthermore, the observed differences in the response of mice and humans are likely caused by differences in types of stress early in life. In fact, we were able to demonstrate clear differences between different types of early life stress in the human sample, further supporting this theory. Although the results obtained in the mouse study do not overlap entirely with the human results, they provide relevant and promising potential for translation. Furthermore, the animal model can be used to identify probable mechanisms underlying osteoporosis development, following early life stress (i.e., related to innervation patterns) that could not be investigated easily in humans, thereby allowing one to develop ideas for future studies or even intervention and prevention strategies.

In conclusion, this study demonstrates that stressful life events early in life lead to (mal-) adaptive responses in bone metabolism in both mice and humans. However, the major conclusion to be drawn from the presented data is that different types of early life stress lead to different response patterns concerning bone health. Thus, they have to be considered separately and possibly consecutively: MSUS mice responded with enhanced bone resorption, which however did not cause changes in bone microarchitecture 8–10 months after the stress exposure when later kept under stress-free conditions. In humans, a reduction in BMD was evident only in depressive patients with severe stress exposure in early life like childhood abuse and stressful life events during childhood. Similarly, the changes in bone serum markers were also dependent on the severity of stress experiences early in life. People with childhood abuse and stressful life events during childhood showed an increased bone metabolism, while people with childhood neglect showed a counter regulated reaction. Hence, the consequences of the observed changes in the context of challenges to bone health (fractures, aging etc.) should be studied in a more personalized manner. Future prevention strategies should respect the severity of the stress exposure to be treated (e.g., specific types of stress experiences during childhood, double hit paradigms), to achieve the optimal benefit for patients with increased risk for bone pathologies (such as people with depressive disorders).

5.5. Materials and Methods

5.5.1. Mouse Study – Animal Model

Animal experiments were conducted in strict adherence to the Swiss Law for Animal Protection and were approved by the local authority (Veterinäramt des Kantons Zürich, Zürich, Switzerland) under license number 57/2015. C57Bl/6J mice were obtained from Janvier Labs (Le Genest-Saint-Isle, France) and bred in-house to generate the male mice ($n = 47$ MSUS, $n = 46$ Control) used for experiments.

MSUS - Unpredictable Maternal Separation and Unpredictable Maternal Stress

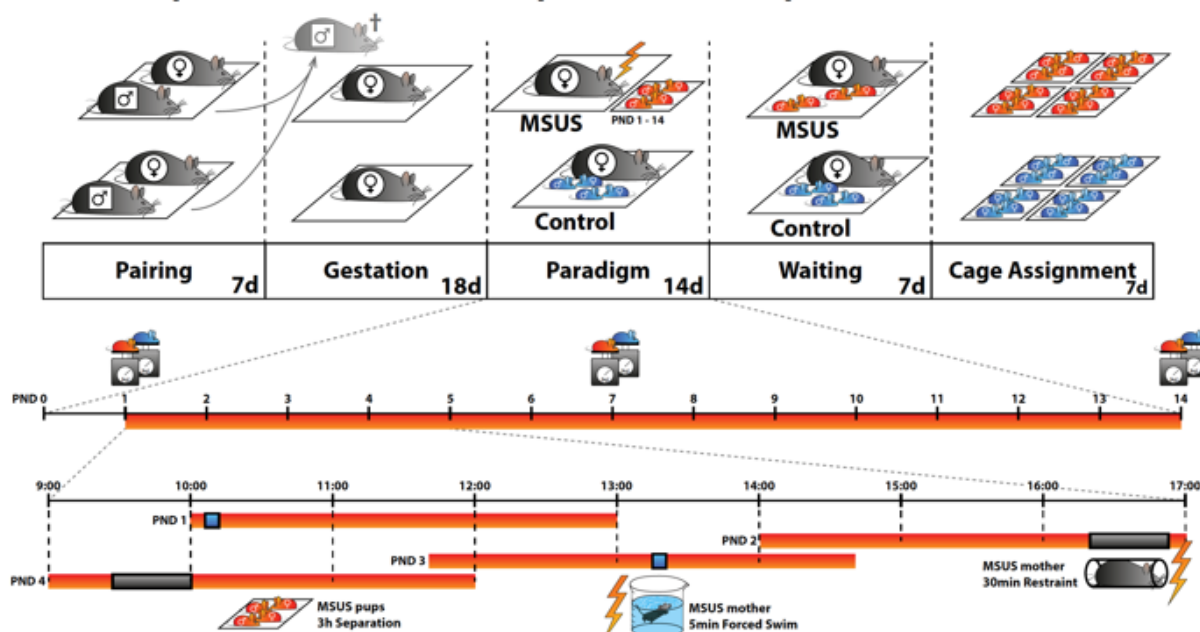


Figure 7: MSUS (unpredictable maternal separation and unpredictable maternal stress) is a mouse model of early life stress. Naïve males are mated with naïve females for 1–7 days, then males are removed. Dams gestate for about 21 days in normal conditions until delivery. The MSUS paradigm (red bar in the timeline) starts at postnatal day 1 (PND1) and lasts until PND14. During MSUS, pups are unpredictably separated from their mothers for 3 h each day at different times of the dark cycle (lights off from 8 am to 8 pm). During separation, the mother is stressed unpredictably by forced swim or restraint as shown in the timeline at the bottom. Pups and dam are left undisturbed from PND15 until weaning at PND21. Gray mice are naïve without any previous stress exposure. Blue pups are controls without any stress exposure. Red pups are exposed to MSUS.

The MSUS paradigm was conducted as previously described [48]. As shown in Figure 7, 2–3 months old C57Bl/6J naïve females were mated with naïve males for 1 week. Mothers were assigned to control or MSUS group based on the number of male pups born on that day to balance the groups. The MSUS paradigm started on postnatal day 1 (PND1): Pups were separated unpredictably from their mother for 3 h per day from PND1 until PND14. Separation occurred at any time during the dark cycle. In addition, mothers were subjected to forced swim in cold water (18 °C for 5 min) or restraint in a plastic tube (20 min) at unpredictable times during the 3 h of separation. Control mice were left undisturbed except for weekly cage changes and weight measurements. Pups were weaned at PND21 and assigned to sex and treatment matched cages (4 to 5 mice) between PND22 and PND28. The co-assignment of siblings was avoided to exclude litter effects. At the age of 8–10 months, control ($n = 24$) and MSUS ($n = 24$) males were deeply anesthetized by Isoflurane (Attane, Piramal Enterprises Limited), followed by decapitation. Males were single-housed the day before sacrifice to reduce potential acute stress effects [104]. Body weight was monitored throughout the experiment and on the day of single housing. Adult mice were housed in groups of 3 to 5 animals in individually ventilated cages (SealSafe PLUS, Tecniplast). Animals were kept in a temperature- and humidity-controlled facility on a 12 h reversed light/dark cycle (light on at 20:00), with food (M/R Haltung Extrudat, Provimi Kliba SA) and water ad libitum. Cages were changed weekly.

5.5.2. Mouse Study - Collection of Serum Samples

Trunk blood was collected in 2 mL tubes immediately after decapitation and incubated at 4 °C. Clotted blood was centrifuged at 2000 rcf at 4 °C for 10 min. The collected serum was stored at –80 °C.

5.5.3. Mouse Study - Collection of Bone Samples

After euthanasia and blood collection, the left femur was dissected on ice under aseptic conditions and cleaned from muscle tissue. The ends were cut off to allow for removal of bone marrow (flushed out with sterile phosphate buffered saline, PBS), and the entire flushed femur (including the ends) was subsequently shock-frozen in liquid nitrogen and stored at –80 °C until further processing for qPCR. Right femurs were dissected, cleaned and stored in 70% ethanol at 4 °C until μCT analysis. The third tail bone was dissected and immersed in a mixture

of 4% paraformaldehyde and 14% saturated picric acid overnight at 4 °C, cryoembedded and stored at –80 °C until further processing for histomorphometry was done.

5.5.4. Mouse Study - Histomorphometry of Neuronal Markers

For bone innervation morphometry, the immunohistochemistry of pan-neuronal marker and exemplary markers for adrenergic, cholinergic and peptidergic nerve fiber subsets were performed with decalcified 14 µm thick transverse mouse tail cryostat sections, analog to previous descriptions [55]. The sections were done through the center of the third tail bone and contained the bone with the adherent muscle, tendons and skin for internal positive control. The primary antibodies used in this study were: anti-PGP 9.5 (Biotrend, Cologne, Germany), anti-GAP 43 (Millipore, Darmstadt, Germany), anti-ChAT (Serotec, Kidlington, UK), anti-TH (Abcam, Cambridge, MA, USA) and anti-SP (BMA Biomedicals, Augst, Switzerland). Only PGP 9.5 and GAP 43 gave satisfactory staining results, most likely due to insufficient fixation of more digestion prone markers in bone compared to the skin (positive controls were all positive), which commonly require transcardial fixation [105]. Standard controls were performed by omission of the primary antibodies and by incubation with mouse IgG1 instead of primary antibodies. No labeling was observed in negative controls. Nerve fiber profiles were counted per area with the help of a grid equipped ocular at x200 magnification using a Leica inverted automated fluorescence-microscope (Leica, Wetzlar, Germany). Briefly, numbers of positively stained fibers were counted per grid field in at least 30 consecutive fields per experimental mouse and in at least n = 8 mice per experimental group by two blinded independent researchers.

5.5.5. Mouse Study - qPCR for Gene Expression in Bone Samples

Mouse femurs were pulverized using a metal ball mill (Retsch, Haan, Germany), and total RNA was isolated with Trizol/chloroform extraction, followed by column-based purification using RNeasy Mini Kit (Qiagen, Hilden, Germany) according to the manufacturer's protocol, but including proteinase K incubation (55 °C, 15 min). Contaminating DNA was removed by using the RNase-free DNase kit (Qiagen, Hilden, Germany), and 32 µL of RNA with an average yield of 48 ng/µL were reverse transcribed with Superscript II reverse transcriptase (Thermo Fisher Scientific, Dreieich, Germany) to obtain 80 µL of cDNA. qPCR analysis was performed in duplicate, using the TaqMan Fast PCR Master Mix with Taqman assays for bone markers (Life Technologies, Germany) (Supplementary Table S2) or

the QuantiTect PCR Kit with self-designed primers for neuronal factors (Qiagen, Hilden, Germany) (Supplementary Table S3). The amount of cDNA per reaction depended on the respective target gene and its expression level and was 1–18 ng. Gene expression was normalized to the housekeeping gene (dCt) and $2^{-\Delta Ct}$ were computed.

5.5.6. Mouse Study - ELISA of Serum Samples

Commercially available ELISA kits were used to determine the serum levels of OC (60-1305, Immunotopics/Teca, Switzerland), PINP (AC-33F1, Immunodiagnosticssystem, Frankfurt, Germany) and CTX-I (AC-06F1, Immunodiagnosticssystem, Frankfurt, Germany), according to the manufacturers' instructions. Serum was used either undiluted (CTX-I) or at a 1/11 (osteocalcin) or 1/10 (PINP) dilution.

5.5.7. Mouse Study - μ CT of Bone Samples

Analysis of bone microarchitecture by μ CT was conducted as previously described [106]. Briefly, bones were measured on a μ CT40 (Scanco Medical AG, Brüttisellen, Switzerland), operated at 55 kVp and 145 μ A with an integration time of 200 ms and 2-fold frame averaging. Images were reconstructed at an isotropic nominal resolution of 10 μ M and filtered using a constrained 3D Gaussian filter (sigma 0.8, support 1) to suppress noise. Masks of the full bone, cortical (shaft at 56% bone length, 1 mm long) and trabecular region of interest (from 66% to 88% of bone length) were created automatically. Morphometric parameters were calculated according to standard guidelines such as total volume (TV), bone volume (BV), marrow volume (MV), apparent volume density (AVD), femur length, cortical area fraction (Ct.Ar/Tt.Ar), cortical thickness (Ct.Th), trabecular bone volume fraction (BV/TV), specific bone surface (BS/BV), trabecular thickness (Tb.Th), trabecular spacing (Tb.Sp) and trabecular number (Tb.N) [107]. Due to differences in body weight between the control mice and the MSUS mice, data was normalized for body weight, and body weight adjusted means were compared.

5.5.8. Human Study – Participants

n = 240 patients with depressive disorder (ICD-10 F32.x, F33.x, F34.1, F43.21) were recruited, of which n = 208 completed the initial examination (baseline (t0)), for more details see [5]. A subsample of n = 54 patients took part at the fourth follow up measurement (t4) including DXA imaging. Patients who fulfilled the following criteria were included: 18 to 65

years of age, depressive episode (ICD-10 F32.x or F33.x), dysthymia (F34.1), or an adjustment disorder with prolonged depressive reaction (F43.21), ≥ 21 days absenteeism within the last year. Exclusion criteria were: pregnancy, hormonotherapy (except contraceptive and thyroid hormone therapy), inability to fill in a questionnaire, intellectual disabilities (ICD-10 F70-79), or one of the following diseases: acute infection, endocrine and metabolic disorders, neurological diseases, dementia (ICD-10 F00-F03), schizophrenia (ICD-10 F20), emotional-unstable personality disorders (ICD-10 F60.3x), disease of the immune system, substance abuse and dependency (except nicotine).

All participants were fully informed in verbal and written form about the intent and content of the study, and gave their written informed consent. The clinical investigations were conducted according to the principles of the Declaration of Helsinki. Final ethical approval was provided on 11/12/2017 from the Ethics Review Board of the University of Potsdam, Germany (number 15/2017).

5.5.9. Human Study – Study Procedure

Study objectives were investigated at two assessments (t_0 and t_4) of an 8-month observational multicenter study with four measurement points: baseline (t_0), after 5 weeks (t_1), 5 months (t_2), 8 months (t_3) and an additional follow-up measurement (t_4 : $M = 15.4$ month, $SD = 4.5$ month after baseline). At each measurement point, study participants answered a comprehensive questionnaire (t_0-t_4) under the supervision of trained study nurses. The questionnaire comprised demographic characteristics, psychological symptoms (e.g., depression) and constructs (e.g., stress, early life events, affect, coping), physical ailments, and information regarding alcohol consumption and medication intake. Blood samples were collected at baseline (t_0) and 5 months follow-up (t_2) and DXA bone densitometry measurements took place at the last follow up (t_4).

5.5.10. Human Study – Psychometric Measures

Early life stress was measured retrospectively, comprising experiences of childhood maltreatment and stressful life events during childhood. The Childhood Trauma Screener (CTS) [108], a 5-item screening tool of the 28-item Childhood Trauma Questionnaire (CTQ) [109,110], assesses five types of childhood maltreatment, such as emotional, physical, and sexual abuse, plus emotional and physical neglect. Each item is scored on a five-point rating

scale from “never true” (1) to “very often true” (5). In accordance with Glaesmer et al. [111], we classified participants at risk if they rated at least mild forms of childhood abuse or neglect. We additionally controlled for response bias by the 3-item Minimization-Denial subscale from the CTQ, and excluded participants when indicated. Cronbach’s Alpha was previously specified with 0.76 [112].

Stressful life events were assessed by a modified version of the Inventory of Stressful Life Events (ILE; [113]). Participants rated 34 adverse life events regarding occurrence, frequency and year of occurrence. The accumulation of stressful, life-changing events at different stages of development was counted for every participant, in this analysis focusing on childhood ($ILE_{child} \leq 12$ years). The scores ranged between 0 (no strain) and 4 (high strain). Cronbach’s Alpha for ILE was 0.83.

Depressive symptoms and severity were assessed using the Beck Depression Inventory-II (BDI-II) [114,115]. Internal consistency in the sample was Cronbach’s Alpha 0.89. Furthermore, confounding factors like sociodemographic and biometric characteristics and study site were assessed.

5.5.11. Human Study – Serum Bone Marker Measurement

Blood samples were drawn from the arm in the morning (7–9 am), collected in plain blood collection tubes, allowed to clot at room temperature for 30 min, followed by centrifugation, isolation of serum and freeze-storage until further analysis. Bone-related blood markers (OC, PINP, CTX-I) were analyzed in serum samples by electrochemiluminescence immunoassays “ECLIA” (12149133 122 for Osteocalcin, 03141071 190 for PINP, 11972308 122 for CTX-I, all from F. Hoffmann-La Roche, Ltd., Basel, Switzerland).

5.5.12. Human Study – DXA Measurement

Bone mineral density (BMD) was measured by DXA bone densitometry measurement (Lunar, Prodigy Advance, GE Healthcare, Madison, WI, USA) in the lumbar spine (lumbar vertebral bodies L1-L4) and both hips. Parameters are given as mean values (M) of the left and right site: G (total), H (collum femoris), S (corpus femoris), T (trochanter major), and L1L4 (lumbar vertebral bodies L1-L4).

5.5.13. Statistical Analysis

Data consistency was checked, screened for outliers and analyzed descriptively. Continuous variables were also tested for normality by using skewness, kurtosis, omnibus test; variance homogeneity was proven by variance ratio and Levene test.

For the examination of Aim 1 (mouse model), Student t-test for equal or Aspin–Welch unequal variance test were performed, using multiple t-test and adjusted for multiple comparison by Holm–Sidak method ($\alpha = 0.05$). Since body weight was found to be significantly different, ANCOVA models with body weight as covariate were applied for μ CT data to compute corresponding means at their covariate means (i.e., least square means at covariate mean for body weight of 16.41). In addition, blocking on total body weight was used as a means of accounting for collinearity in analyses of variance, and mediation analyses were conducted using linear regression models to identify mediation effects between body weight and bone microstructure. All reported tests are two-sided, and p -values < 0.05 are considered as statistically significant.

Regarding Aim 2 (human model), multiple regression models were applied. Statistical models were cross-sectional and controlled for age, gender, study sites and additionally body weight for DXA measurements.

Statistical analyses were conducted using NCSS (NCSS 10, NCSS, LLC. Kaysville, UT, USA), STATISTICA 13 (TIBCO, Palo Alto, CA, USA), IBM SPSS 25 (IBM, Armonk, NY, USA) and the statistical software R [116,117].

5.6. Author Contributions

K.W.-K. planned and coordinated the project, participated in tissue collection, supervised experiments and drafted the manuscript; M.R. conducted the animal experiments, participated in tissue collection and drafted the manuscript; E.C. participated in tissue collection, analyzed samples and drafted the manuscript; A.B. helped to coordinate the human study, analyzed sample and proof-read the manuscript; G.A.K. participated in tissue collection, analyzed samples and drafted the manuscript; T.A. analyzed samples and proof-read the manuscript; W.H. conducted statistical analysis of all animal experiments and proof-read the manuscript; D.D. conducted statistical analysis of all human experiments and proof-read the

manuscript; R.M. provided input in µCT analysis and proof-read the manuscript; M.A.R. helped in the coordination of the human study and proof-read the manuscript; I.M.M. planned and coordinated the animal study, supervised experiments, acquired funding and proof-read the manuscript; E.M.J.P. helped to coordinate the mouse study, analyzed samples and drafted the manuscript; P.M.W. planned and coordinated the project, conducted human study as PI, supervised experiments, acquired funding and drafted the manuscript. All authors have read and agreed to the published version of the manuscript.

5.7. Funding

This study was supported by the Deutsche Forschungsgemeinschaft (DFG), the Central Research Grant for Innovative Ideas from the University of Potsdam, the German Pension Fund Association (10-R-40.07.05.07.008), the Swiss National Science Foundation (31003A_153147/1) and the ETHZ grant (ETH-10 15-2).

5.8. Abbreviations

ADRB2	adrenoceptor beta 2
ANCOVA	analysis of covariance
AVD	apparent volume density
BDI-II	Beck Depression Inventory Revision
BDNF	brain derived neurotrophic factor
BMD	bone mineral density
BMD_G	bone mineral density general
BMD_H	bone mineral density collum femoris
BMD_L1L4	bone mineral density lumbar vertebralis bodies 1–4
BMD_S	bone mineral density corpus femoris
BMD_T	bone mineral density trochanter major
BV	bone volume
BS	specific bone surface
CGRP	calcitonin gene related peptide
ChAT	choline acetyltransferase
CHRNA7	cholinergic receptor nicotinic alpha 7 subunit
CTQ	Childhood Trauma Questionnaire
CTS	Childhood Trauma Screener
CTX-I	c-terminal telopeptide of type I collagen
Ct.Ar	cortical area fraction
Ct.Th	cortical thickness
DAPI	4',6-diamidino-2-phenylindole
dCt	delta Ct
DEPREHA	[Der Einfluss unterschiedlicher Behandlungs-settings auf den Therapieerfolg bei Patienten mit depressiven Erkrankungen in der Rehabilitation]
DXA	dual energy X-ray absorptiometry

ECLIA	electrochemiluminescence immunoassays
ECM	extracellular matrix
ELISA	enzyme-linked immunosorbent assay
FITC	fluorescein isothiocyanate
GAP 43	growth associated protein 43
HPA	hypothalamic pituitary adrenal
ICD-10	International Classification of Diseases Version 10
IgG1	immunoglobulin G
ILE	Inventory of Stressful Life Events
ILE child	Inventory of Stressful Life Events; life events during childhood ≤ 12 years
μ CT	micro-computed tomography
M	mean
MV	marrow volume
MSUS	maternal separation and unpredictable stress
mRNA	messenger ribonucleic acid
NF	nerve fibers
NGF	nerve growth factor
NPY	neuropeptide Y
NPYR1	neuropeptide Y receptor 1
OC	osteocalcin
qPCR	quantitative polymerase chain reaction
PBS	phosphate buffered saline
PGP 9.5	protein gene product 9.5
PINP	procollagen type 1 N-terminal propeptide
PND	postnatal day
RAMP1	receptor activity modifying protein 1
SAM	senescence-accelerated mouse
SD	standard deviation
SP	substance P
TAC1	tachykinin 1
TACR1	tachykinin receptor 1
Tb.N	trabecular number
Tb.Sp	trabecular spacing
Tb.Th	trabecular thickness
TH	tyrosine hydroxylase
TRKA	tropomyosin receptor kinase A
Tt.Ar	total area
TRKB	tropomyosin receptor kinase B
TV	total volume
VIP	vasoactive intestinal peptide
VIPR1	vasoactive intestinal peptide receptor 1

5.9. References

1. Wippert, P.M.; Rector, M.; Kuhn, G.; Wuertz-Kozak, K. Stress and Alterations in Bones: An interdisciplinary Perspective. *Front. Endocrinol.* 2017, 8, 96, doi:10.3389/fendo.2017.00096.
2. Grassel, S. The role of peripheral nerve fibers and their neurotransmitters in cartilage and bone physiology and pathophysiology. *Arthritis Res. Ther.* 2014, 16, 485, doi:10.1186/s13075-014-0485-1.
3. Mattia, C.; Coluzzi, F.; Celidonio, L.; Vellucci, R. Bone pain mechanism in osteoporosis: A narrative review. *Clin. Cases Miner. Bone Metab.* 2016, 13, 97–100, doi:10.11138/ccmbm/2016.13.2.097.
4. McEwen, B.S.; Nasca, C.; Gray, J.D. Stress effects on neuronal structure: hippocampus, amygdala, and prefrontal cortex. *Neuropsychopharmacology* 2016, 41, 3–23, doi:10.1038/npp.2015.171.
5. Wippert, P.M.; Block, A.; Mansuy, I.M.; Peters, E.M.J.; Rose, M.; Rapp, M.A.; Huppertz, A.; Wuertz-Kozak, K. Alterations in bone homeostasis and microstructure related to depression and allostatic load. *Psychother. Psychosom.* 2019, 88, 383–385, doi:10.1159/000503640.
6. Asada, K.; Obata, K.; Horiguchi, K.; Takaki, M. Age-related changes in afferent responses in sensory neurons to mechanical stimulation of osteoblasts in coculture system. *Am. J. Physiol. Cell Physiol.* 2012, 302, C757–C765, doi:10.1152/ajpcell.00362.2011.
7. Takahashi, N.; Matsuda, Y.; Sato, K.; de Jong, P.R.; Bertin, S.; Tabeta, K.; Yamazaki, K. Neuronal TRPV1 activation regulates alveolar bone resorption by suppressing osteoclastogenesis via CGRP. *Sci. Rep.* 2016, 6, 29294, doi:10.1038/srep29294.
8. Mach, D.B.; Rogers, S.D.; Sabino, M.C.; Luger, N.M.; Schwei, M.J.; Pomonis, J.D.; Keyser, C.P.; Clohisy, D.R.; Adams, D.J.; O’Leary, P.; et al. Origins of skeletal pain: Sensory and sympathetic innervation of the mouse femur. *Neuroscience* 2002, 113, 155–166.
9. Chartier, S.R.; Mitchell, S.A.T.; Majuta, L.A.; Mantyh, P.W. The changing sensory and sympathetic innervation of the young, adult and aging mouse femur. *Neuroscience* 2018, 387, 178–190, doi:10.1016/j.neuroscience.2018.01.047.
10. Alves, C.J.; Alencastre, I.S.; Neto, E.; Ribas, J.; Ferreira, S.; Vasconcelos, D.M.; Sousa, D.M.; Summavieille, T.; Lamghari, M. Bone injury and repair trigger central and peripheral NPY neuronal pathways. *PLoS ONE* 2016, 11, e0165465, doi:10.1371/journal.pone.0165465.
11. Jiao, K.; Niu, L.; Xu, X.; Liu, Y.; Li, X.; Tay, F.R.; Wang, M. Norepinephrine Regulates Condylar Bone Loss via Comorbid Factors. *J. Dent Res.* 2015, 94, 813–820, doi:10.1177/0022034515577677.
12. Yirmiya, R.; Goshen, I.; Bajayo, A.; Kreisel, T.; Feldman, S.; Tam, J.; Trembovier, V.; Csernus, V.; Shohami, E.; Bab, I. Depression induces bone loss through stimulation of the sympathetic nervous system. *Proc. Natl. Acad. Sci. USA* 2006, 103, 16876–16881, doi:10.1073/pnas.0604234103.
13. Furuzawa, M.; Chen, H.Y.; Fujiwara, S.; Yamada, K.; Kubo, K. Chewing ameliorates chronic mild stress-induced bone loss in senescence-accelerated mouse (SAMP8), a murine model of senile osteoporosis. *Exp. Gerontol.* 2014, 55, 12–18, doi:10.1016/j.exger.2014.03.003.
14. Tomlinson, R.E.; Li, Z.; Zhang, Q.; Goh, B.C.; Li, Z.; Thorek, D.L.J.; Rajbhandari, L.; Brushart, T.M.; Minichiello, L.; Zhou, F.; et al. NGF-TrkB signaling by sensory nerves coordinates the vascularization and ossification of developing endochondral bone. *Cell Rep.* 2016, 16, 2723–2735, doi:10.1016/j.celrep.2016.08.002.

15. Chen, W.H.; Mao, C.Q.; Zhuo, L.L.; Ong, J.L. Beta-nerve growth factor promotes neurogenesis and angiogenesis during the repair of bone defects. *Neural Regen. Res.* 2015, 10, 1159–1165, doi:10.4103/1673-5374.160114.
16. Zhuang, Y.F.; Li, J. Serum EGF and NGF levels of patients with brain injury and limb fracture. *Asian Pac. J. Trop. Med.* 2013, 6, 383–386, doi:10.1016/S1995-7645(13)60043-7.
17. Sabsovich, I.; Wei, T.; Guo, T.Z.; Zhao, R.; Shi, X.; Li, X.; Yeomans, D.C.; Klyukinov, M.; Kingery, W.S.; Clark, J.D. Effect of anti-NGF antibodies in a rat tibia fracture model of complex regional pain syndrome type I. *Pain* 2008, 138, 47–60, doi:10.1016/j.pain.2007.11.004.
18. Guo, T.Z.; Wei, T.P.; Shi, X.Y.; Li, W.W.; Hou, S.Y.; Wang, L.P.; Tsujikawa, K.; Rice, K.C.; Cheng, K.J.; Clark, D.J.; et al. Neuropeptide deficient mice have attenuated nociceptive, vascular, and inflammatory changes in a tibia fracture model of complex regional pain syndrome. *Mol. Pain* 2012, 8, 85, doi:10.1186/1744-8069-8-85.
19. Sang, X.G.; Wang, Z.Y.; Cheng, L.; Liu, Y.H.; Li, Y.G.; Qin, T.; Di, K. Analysis of the mechanism by which nerve growth factor promotes callus formation in mice with tibial fracture. *Exp. Ther. Med.* 2017, 13, 1376–1380, doi:10.3892/etm.2017.4108.
20. Grills, B.L.; Schuijers, J.A.; Ward, A.R. Topical application of nerve growth factor improves fracture healing in rats. *J. Orthop. Res.* 1997, 15, 235–242, doi:10.1002/jor.1100150212.
21. Hemingway, F.; Taylor, R.; Knowles, H.J.; Athanasou, N.A. RANKL-independent human osteoclast formation with APRIL, BAFF, NGF, IGF I and IGF II. *Bone* 2011, 48, 938–944, doi:10.1016/j.bone.2010.12.023.
22. Camerino, C.; Conte, E.; Caloiero, R.; Fonzino, A.; Carratu, M.; Lograno, M.D.; Tricarico, D. Evaluation of Short and Long Term Cold Stress Challenge of Nerve Grow Factor, Brain-Derived Neurotrophic Factor, Osteocalcin and Oxytocin mRNA Expression in BAT, Brain, Bone and Reproductive Tissue of Male Mice Using Real-Time PCR and Linear Correlation Analysis. *Front. Physiol.* 2017, 8, 1101, doi:10.3389/fphys.2017.01101.
23. Liu, Q.; Lei, L.; Yu, T.; Jiang, T.; Kang, Y. Effect of Brain-Derived Neurotrophic Factor on the Neurogenesis and Osteogenesis in Bone Engineering. *Tissue Eng. Part A* 2018, 24, 1283–1292, doi:10.1089/ten.TEA.2017.0462.
24. Yang, M.; Lu, B.J.; Duan, Y.Y.; Chen, X.F.; Ma, J.G.; Guo, Y. Genetics association study and functional analysis on osteoporosis susceptibility gene BDNF. *Yi Chuan* 2017, 39, 726–736, doi:10.16288/j.yczz.17-145.
25. Kauschke, V.; Gebert, A.; Calin, M.; Eckert, J.; Scheich, S.; Heiss, C.; Lips, K.S. Effects of new beta-type Ti-40Nb implant materials, brain-derived neurotrophic factor, acetylcholine and nicotine on human mesenchymal stem cells of osteoporotic and non osteoporotic donors. *PLoS ONE* 2018, 13, e0193468, doi:10.1371/journal.pone.0193468.
26. Camerino, C.; Conte, E.; Cannone, M.; Caloiero, R.; Fonzino, A.; Tricarico, D. Nerve Growth Factor, Brain-Derived Neurotrophic Factor and Osteocalcin Gene Relationship in Energy Regulation, Bone Homeostasis and Reproductive Organs Analyzed by mRNA Quantitative Evaluation and Linear Correlation Analysis. *Front. Physiol.* 2016, 7, 456, doi:10.3389/fphys.2016.00456.

27. Picard, M.; Juster, R.P.; McEwen, B.S. Mitochondrial allostatic load puts the 'gluc' back in glucocorticoids. *Nat. Rev. Endocrinol.* 2014, 10, 303–310, doi:10.1038/nrendo.2014.22.
28. Picard, M.; McEwen, B.S. Psychological Stress and Mitochondria: A Conceptual Framework. *Psychosom. Med.* 2018, 80, 126–140, doi:10.1097/PSY.0000000000000544.
29. Kelly, R.R.; McDonald, L.T.; Jensen, N.R.; Sidles, S.J.; LaRue, A.C. Impacts of Psychological Stress on Osteoporosis: Clinical Implications and Treatment Interactions. *Front. Psychiatry* 2019, 10, 200, doi:10.3389/fpsyg.2019.00200.
30. Lee, S.H.; Mastronardi, C.A.; Li, R.W.; Paz-Filho, G.; Dutcher, E.G.; Lewis, M.D.; Vincent, A.D.; Smith, P.N.; Bornstein, S.R.; Licinio, J.; et al. Short-term antidepressant treatment has long-lasting effects, and reverses stress-induced decreases in bone features in rats. *Transl. Psychiatry* 2019, 9, 10, doi:10.1038/s41398-018-0351-z.
31. He, J.-Y.; Zheng, X.-F.; Jiang, L.-S. Autonomic control of bone formation: Its clinical relevance. *Handb. Clin. Neurol.* 2013, 117, 161–171, doi:10.1016/B978-0-444-53491-0.00014-6.
32. Schiavone, S.; Morgese, M.G.; Mhillaj, E.; Bove, M.; De Giorgi, A.; Cantatore, F.P.; Camerino, C.; Tucci, P.; Maffulli, N.; Cuomo, V.; et al. Chronic Psychosocial Stress Impairs Bone Homeostasis: A Study in the Social Isolation Reared Rat. *Front. Pharmacol.* 2016, 7, 152, doi:10.3389/fphar.2016.00152.
33. Huang, W.S.; Hsu, J.W.; Huang, K.L.; Bai, Y.M.; Su, T.P.; Li, C.T.; Lin, W.C.; Chen, T.J.; Tsai, S.J.; Liou, Y.J.; et al. Post-traumatic stress disorder and risk of osteoporosis: A nationwide longitudinal study. *Stress Health* 2018, 34, 440–445, doi:10.1002/smj.2806.
34. Gershon, A.; Sudheimer, K.; Tirouvanziam, R.; Williams, L.M.; O'Hara, R. The long-term impact of early adversity on late-life psychiatric disorders. *Curr. Psychiatry Rep.* 2013, 15, 352, doi:10.1007/s11920-013-0352-9.
35. Raymond, C.; Marin, M.F.; Majeur, D.; Lupien, S. Early child adversity and psychopathology in adulthood: HPA axis and cognitive dysregulations as potential mechanisms. *Prog. Neuropsychopharmacol. Biol. Psychiatry* 2018, 85, 152–160, doi:10.1016/j.pnpbp.2017.07.015.
36. Shonkoff, J.P.; Boyce, W.T.; McEwen, B.S. Neuroscience, molecular biology, and the childhood roots of health disparities: Building a new framework for health promotion and disease prevention. *JAMA* 2009, 301, 2252–2259, doi:10.1001/jama.2009.754.
37. Falgares, G.; Marchetti, D.; Manna, G.; Musso, P.; Oasi, O.; Kopala-Sibley, D.C.; De Santis, S.; Verrocchio, M.C. Childhood Maltreatment, Pathological Personality Dimensions, and Suicide Risk in Young Adults. *Front. Psychol.* 2018, 9, 806, doi:10.3389/fpsyg.2018.00806.
38. Lindert, J.; von Ehrenstein, O.S.; Grashow, R.; Gal, G.; Braehler, E.; Weisskopf, M.G. Sexual and physical abuse in childhood is associated with depression and anxiety over the life course: Systematic review and meta-analysis. *Int. J. Public Health* 2014, 59, 359–372, doi:10.1007/s00038-013-0519-5.
39. Infurna, M.R.; Reichl, C.; Parzer, P.; Schimmenti, A.; Bifulco, A.; Kaess, M. Associations between depression and specific childhood experiences of abuse and neglect: A meta-analysis. *J. Affect Disord.* 2016, 190, 47–55, doi:10.1016/j.jad.2015.09.006.
40. Nanni, V.; Uher, R.; Danese, A. Childhood Maltreatment Predicts Unfavorable Course of Illness and Treatment Outcome in Depression: A Meta-Analysis. *Am. J. Psychiat.* 2012, 169, 141–151, doi:10.1176/appi.ajp.2011.11020335.

41. Mezuk, B.; Eaton, W.W.; Golden, S.H. Depression and osteoporosis: Epidemiology and potential mediating pathways. *Osteoporos. Int.* 2008, 19, 1–12, doi:10.1007/s00198-007-0449-2.
42. Cizza, G.; Primma, S.; Coyle, M.; Gourgiotis, L.; Csako, G. Depression and Osteoporosis: A Research Synthesis with Meta-Analysis. *Horm. Metab. Res.* 2010, 42, 467–482, doi:10.1055/s-0030-1252020.
43. Azuma, K.; Adachi, Y.; Hayashi, H.; Kubo, K.Y. Chronic Psychological Stress as a Risk Factor of Osteoporosis. *J. UOEH* 2015, 37, 245–253.
44. Williams, L.J.; Pasco, J.A.; Jackson, H.; Kiropoulos, L.; Stuart, A.L.; Jacka, F.N.; Berk, M. Depression as a risk factor for fracture in women: A 10 year longitudinal study. *J. Affect Disord.* 2016, 192, 34–40, doi:10.1016/j.jad.2015.11.048.
45. Furlan, P.M.; Ten Have, T.; Cary, M.; Zemel, B.; Wehrli, F.; Katz, I.R.; Gettes, D.R.; Evans, D.L. The role of stress-induced cortisol in the relationship between depression and decreased bone mineral density. *Biol. Psychiatry* 2005, 57, 911–917, doi:10.1016/j.biopsych.2004.12.033.
46. Stults-Kolehmainen, M.A.; Sinha, R. The effects of stress on physical activity and exercise. *Sports Med.* 2014, 44, 81–121, doi:10.1007/s40279-013-0090-5.
47. Yau, Y.H.; Potenza, M.N. Stress and eating behaviors. *Miner. Endocrinol.* 2013, 38, 255–267.
48. Franklin, T.B.; Russig, H.; Weiss, I.C.; Graff, J.; Linder, N.; Michalon, A.; Vizi, S.; Mansuy, I.M. Epigenetic Transmission of the Impact of Early Stress Across Generations. *Biol. Psychiatry* 2010, 68, 408–415, doi:10.1016/j.biopsych.2010.05.036.
49. Schmidt, M.V. Molecular mechanisms of early life stress--lessons from mouse models. *Neurosci. Biobehav. Rev.* 2010, 34, 845–852, doi:10.1016/j.neubiorev.2009.05.002.
50. McGowan, P.O.; Szyf, M. The epigenetics of social adversity in early life: Implications for mental health outcomes. *Neurobiol. Dis.* 2010, 39, 66–72, doi:10.1016/j.nbd.2009.12.026.
51. Bohacek, J.; Mansuy, I.M. Epigenetic inheritance of disease and disease risk. *Neuropsychopharmacology* 2013, 38, 220–236, doi:10.1038/npp.2012.110.
52. Gapp, K.; Jawaid, A.; Sarkies, P.; Bohacek, J.; Pelczar, P.; Prados, J.; Farinelli, L.; Miska, E.; Mansuy, I.M. Implication of sperm RNAs in transgenerational inheritance of the effects of early trauma in mice. *Nat. Neurosci.* 2014, 17, 667–669, doi:10.1038/nn.3695.
53. Baldock, P.A.; Lin, S.; Zhang, L.; Karl, T.; Shi, Y.; Driessler, F.; Zengin, A.; Hormer, B.; Lee, N.J.; Wong, I.P.L.; et al. Neuropeptide Y Attenuates Stress-Induced Bone Loss Through Suppression of Noradrenaline Circuits. *J. Bone Miner. Res.* 2014, 29, 2238–2249, doi:10.1002/jbmr.2205.
54. Ballica, R.; Valentijn, K.; Khachatrian, A.; Guerder, S.; Kapadia, S.; Gundberg, C.; Gilligan, J.; Flavell, R.A.; Vignery, A. Targeted expression of calcitonin gene-related peptide to osteoblasts increases bone density in mice. *J. Bone Miner. Res.* 1999, 14, 1067–1074, doi:10.1359/jbm.1999.14.7.1067.
55. Rommel, F.R.; Raghavan, B.; Paddenberg, R.; Kummer, W.; Tumala, S.; Lochnit, G.; Gieler, U.; Peters, E.M. Suitability of Nicotinic Acetylcholine Receptor alpha7 and Muscarinic Acetylcholine Receptor 3 Antibodies for Immune Detection: Evaluation in Murine Skin. *J. Histochem. Cytochem.* 2015, 63, 329–339, doi:10.1369/0022155415575028.
56. Sousa, D.M.; McDonald, M.M.; Mikulec, K.; Peacock, L.; Herzog, H.; Lamghari, M.; Little, D.G.; Baldock, P.A. Neuropeptide Y modulates fracture healing through Y1 receptor signaling. *J. Orthop. Res.* 2013, 31, 1570–1508, doi:10.1002/jor.22400.

57. Teixeira, L.; Sousa, D.M.; Nunes, A.F.; Sousa, M.M.; Herzog, H.; Lamghari, M. NPY Revealed as a Critical Modulator of Osteoblast Function In Vitro: New Insights Into the Role of Y1 and Y2 Receptors. *J. Cell Biochem.* 2009, 107, 908–916, doi:10.1002/jcb.22194.
58. Tang, P.; Duan, C.G.; Wang, Z.; Wang, C.M.; Meng, G.L.; Lin, K.F.; Yang, Q.; Yuan, Z. NPY and CGRP Inhibitor Influence on ERK Pathway and Macrophage Aggregation during Fracture Healing. *Cell Physiol. Biochem.* 2017, 41, 1457–1467, doi:10.1159/000468405.
59. Igwe, J.C.; Jiag, X.; Paic, F.; Ma, L.; Adams, D.J.; Baldock, P.A.; Pilbeam, C.C.; Kalajzic, I. Neuropeptide Y Is Expressed by Osteocytes and Can Inhibit Osteoblastic Activity. *J. Cell Biochem.* 2009, 108, 621–630, doi:10.1002/jcb.22294.
60. Allison, S.J.; Baldock, P.A.; Enriquez, R.F.; Lin, E.J.; During, M.; Gardiner, E.M.; Eisman, J.A.; Sainsbury, A.; Herzog, H. Critical Interplay Between Neuropeptide Y and Sex Steroid Pathways in Bone and Adipose Tissue Homeostasis. *J. Bone Miner. Res.* 2009, 24, 294–304, doi:10.1359/Jbmr.081013.
61. Sousa, D.M.; Baldock, P.A.; Enriquez, R.F.; Zhang, L.; Sainsbury, A.; Lamghari, M.; Herzog, H. Neuropeptide Y Y1 receptor antagonism increases bone mass in mice. *Bone* 2012, 51, 8–16, doi:10.1016/j.bone.2012.03.020.
62. Ma, W.H.; Liu, Y.J.; Wang, W.; Zhang, Y.Z. Neuropeptide Y, substance P, and human bone morphogenetic protein 2 stimulate human osteoblast osteogenic activity by enhancing gap junction intercellular communication. *Braz. J. Med. Biol. Res.* 2015, 48, 299–307, doi:10.1590/1414-431x20144226.
63. Long, H.; Ahmed, M.; Ackermann, P.; Stark, A.; Li, J.A. Neuropeptide Y innervation during fracture healing and remodeling. *Acta Orthop.* 2010, 81, 639–646, doi:10.3109/17453674.2010.504609.
64. Cherruau, M.; Morvan, F.O.; Schirar, A.; Saffar, J.L. Chemical sympathectomy-induced changes in TH-, VIP-, and CGRP-immunoreactive fibers in the rat mandible periosteum: Influence on bone resorption. *J. Cell Physiol.* 2003, 194, 341–348, doi:10.1002/jcp.10209.
65. Lundberg, P.; Lundgren, I.; Mukohyama, H.; Lehenkari, P.P.; Horton, M.A.; Lerner, U.H. Vasoactive intestinal peptide (VIP)/pituitary adenylate cyclase-activating peptide receptor subtypes in mouse calvarial osteoblasts: Presence of VIP-2 receptors and differentiation-induced expression of VIP-1 receptors. *Endocrinology* 2001, 142, 339–347, doi:10.1210/en.142.1.339.
66. Ransjo, M.; Lie, A.; Mukohyama, H.; Lundberg, P.; Lerner, U.H. Microisolated mouse osteoclasts express VIP-1 and PACAP receptors. *Biochem. Biophys. Res. Commun.* 2000, 274, 400–404, doi:10.1006/bbrc.2000.3151.
67. Nagata, A.; Tanaka, T.; Minezawa, A.; Poyurovsky, M.; Mayama, T.; Suzuki, S.; Hashimoto, N.; Yoshida, T.; Suyama, K.; Miyata, A.; et al. cAMP Activation by PACAP/VIP Stimulates IL-6 Release and Inhibits Osteoblastic Differentiation Through VPAC2 Receptor in Osteoblastic MC3T3 Cells. *J. Cell Physiol.* 2009, 221, 75–83, doi:10.1002/jcp.21831.
68. Persson, E.; Lerner, U.H. The Neuropeptide VIP Regulates the Expression of Osteoclastogenic Factors in Osteoblasts. *J. Cell Biochem.* 2011, 112, 3732–3741, doi:10.1002/jcb.23304.
69. Wei, T.P.; Li, W.W.; Guo, T.Z.; Zhao, R.; Wang, L.P.; Clark, D.J.; Oaklander, A.L.; Schmelz, M.; Kingery, W.S. Post-junctional facilitation of Substance P signaling in a tibia fracture rat model of complex regional pain syndrome type I. *Pain* 2009, 144, 278–286, doi:10.1016/j.pain.2009.04.020.

70. Aoki, M.; Tamai, K.; Saotome, K. Substance P-Related and Calcitonin-Gene-Related Peptide-Immunofluorescent Nerves in the Repair of Experimental Bone Defects. *Int. Orthop.* 1994, 18, 317–324.
71. Goto, T.; Yamaza, T.; Kido, M.A.; Tanaka, T. Light- and electron-microscopic study of the distribution of axons containing substance P and the localization of neurokinin-1 receptor in bone. *Cell Tissue Res.* 1998, 293, 87–93, doi:10.1007/s004410051100.
72. Wang, L.P.; Zhao, R.; Shi, X.Y.; Wei, T.P.; Halloran, B.P.; Clark, D.J.; Jacobs, C.R.; Kingery, W.S. Substance P stimulates bone marrow stromal cell osteogenic activity, osteoclast differentiation, and resorption activity in vitro. *Bone* 2009, 45, 309–320, doi:10.1016/j.bone.2009.04.203.
73. Mori, T.; Ogata, T.; Okumura, H.; Shibata, T.; Nakamura, Y.; Kataoka, K. Substance p regulates the function of rabbit cultured osteoclast; Increase of intracellular free calcium concentration and enhancement of bone resorption. *Biochem. Biophys. Res. Commun.* 1999, 262, 418–422, doi:10.1006/bbrc.1999.1220.
74. Sohn, S.J. Substance P upregulates osteoclastogenesis by activating nuclear factor kappa B in osteoclast precursors. *Acta Oto-Laryngol.* 2005, 125, 130–133, doi:10.1080/00016480410017710.
75. Matayoshi, T.; Goto, T.; Fukuwara, E.; Takano, H.; Kobayashi, S.; Takahashi, T. Neuropeptide substance P stimulates the formation of osteoclasts via synovial fibroblastic cells. *Biochem. Biophys. Res. Commun.* 2005, 327, 756–764, doi:10.1016/j.bbrc.2004.12.055.
76. Adamus, M.A.; Dabrowski, Z.J. Effect of the neuropeptide substance P on the rat bone marrow-derived osteogenic cells in vitro. *J. Cell Biochem.* 2001, 81, 499–506.
77. Liu, H.J.; Yan, H.; Yan, J.; Li, H.; Chen, L.; Han, L.R.; Yang, X.F. Substance P Promotes the Proliferation, but Inhibits Differentiation and Mineralization of Osteoblasts from Rats with Spinal Cord Injury via RANKL/OPG System. *PLoS ONE* 2016, 11, e0165063, doi:10.1371/journal.pone.0165063.
78. Shih, C.; Bernard, G.W. Neurogenic substance P stimulates osteogenesis in vitro. *Peptides* 1997, 18, 323–326.
79. Goto, T.; Nakao, K.; Gunjigake, K.K.; Kido, M.A.; Kobayashi, S.; Tanaka, T. Substance P stimulates late-stage rat osteoblastic bone formation through neurokinin-1 receptors. *Neuropeptides* 2007, 41, 25–31, doi:10.1016/j.npep.2006.11.002.
80. Kook, Y.A.; Lee, S.K.; Son, D.H.; Kim, Y.; Kang, K.H.; Cho, J.H.; Kim, S.C.; Kim, Y.S.; Lee, H.J.; Lee, S.K.; et al. Effects of substance P on osteoblastic differentiation and heme oxygenase-1 in human periodontal ligament cells. *Cell Biol. Int.* 2009, 33, 424–428, doi:10.1016/j.cellbi.2008.12.007.
81. Azuma, H.; Kido, J.; Ikeda, D.; Kataoka, M.; Nagata, T. Substance P enhances the inhibition of osteoblastic cell differentiation induced by lipopolysaccharide from *Porphyromonas gingivalis*. *J. Periodontol.* 2004, 75, 974–981, doi:10.1902/jop.2004.75.7.974.
82. Kingery, W.S.; Offley, S.C.; Guo, T.Z.; Davies, M.F.; Clark, J.D.; Jacobs, C.R. A substance P receptor (NK1) antagonist enhances the widespread osteoporotic effects of sciatic nerve section. *Bone* 2003, 33, 927–936, doi:10.1016/j.bone.2003.07.003.
83. Zheng, X.F.; Zhao, E.D.; He, J.Y.; Zhang, Y.H.; Jiang, S.D.; Jiang, L.S. Inhibition of substance P signaling aggravates the bone loss in ovariectomy-induced osteoporosis. *Prog. Biophys. Mol. Biol.* 2016, 122, 112–121, doi:10.1016/j.pbiomolbio.2016.05.011.
84. Ding, W.G.; Zhang, Z.M.; Zhang, Y.H.; Jiang, S.D.; Jiang, L.S.; Dai, L.Y. Changes of substance P during fracture healing in ovariectomized mice. *Regul. Pept.* 2010, 159, 28–34, doi:10.1016/j.regpep.2009.11.004.

85. Lerner, U.H.; Persson, E. Osteotropic effects by the neuropeptides calcitonin gene-related peptide, substance P and vasoactive intestinal peptide. *J. Musculoskelet. Neuronal Interact.* 2008, 8, 154–165.
86. Terreni, A.; Pezzati, P. Biochemical markers in the follow-up of the osteoporotic patients. *Clin Cases Miner. Bone Metab.* 2012, 9, 80–84.
87. Vasikaran, S.; Eastell, R.; Bruyere, O.; Foldes, A.J.; Garner, P.; Griesmacher, A.; McClung, M.; Morris, H.A.; Silverman, S.; Trenti, T.; et al. Markers of bone turnover for the prediction of fracture risk and monitoring of osteoporosis treatment: A need for international reference standards. *Osteoporos. Int.* 2011, 22, 391–420, doi:10.1007/s00198-010-1501-1.
88. Yoshimura, N.; Muraki, S.; Oka, H.; Kawaguchi, H.; Nakamura, K.; Akune, T. Biochemical markers of bone turnover as predictors of osteoporosis and osteoporotic fractures in men and women: 10-year follow-up of the Taiji cohort. *Mod. Rheumatol.* 2011, 21, 608–620, doi:10.1007/s10165-011-0455-2.
89. Garner, P.; Sornay-Rendu, E.; Claustre, B.; Delmas, P.D. Biochemical markers of bone turnover, endogenous hormones and the risk of fractures in postmenopausal women: The OFELY study. *J. Bone Miner. Res.* 2000, 15, 1526–1536, doi:10.1359/jbmr.2000.15.8.1526.
90. Blue, M.E.; Boskey, A.L.; Doty, S.B.; Fedarko, N.S.; Hossain, M.A.; Shapiro, J.R. Osteoblast function and bone histomorphometry in a murine model of Rett syndrome. *Bone* 2015, 76, 23–30, doi:10.1016/j.bone.2015.01.024.
91. Eastell, R.; Barton, I.; Hannon, R.A.; Chines, A.; Garner, P.; Delmas, P.D. Relationship of early changes in bone resorption to the reduction in fracture risk with risedronate. *J. Bone Miner. Res.* 2003, 18, 1051–1056, doi:10.1359/jbmr.2003.18.6.1051.
92. Callewaert, F.; Venken, K.; Kopchick, J.J.; Torcasio, A.; van Lenthe, G.H.; Boonen, S.; Vanderschueren, D. Sexual dimorphism in cortical bone size and strength but not density is determined by independent and time-specific actions of sex steroids and IGF-1: Evidence from pubertal mouse models. *J. Bone Miner. Res.* 2010, 25, 617–626, doi:10.1359/jbmr.090828.
93. Goel, N.; Bale, T.L. Sex differences in the serotonergic influence on the hypothalamic-pituitary-adrenal stress axis. *Endocrinology* 2010, 151, 1784–1794, doi:10.1210/en.2009-1180.
94. Takeda, T.; Hosokawa, M.; Higuchi, K. Senescence-accelerated mouse (SAM): A novel murine model of accelerated senescence. *J. Am. Geriatr. Soc.* 1991, 39, 911–919.
95. Paccione, M.F.; Warren, S.M.; Spector, J.A.; Greenwald, J.A.; Bouletreau, P.J.; Longaker, M.T. A mouse model of mandibular osteotomy healing. *J. Craniofac. Surg.* 2001, 12, 444–450, doi:10.1097/00001665-200109000-00008.
96. Dang, R.; Guo, Y.Y.; Zhang, K.; Jiang, P.; Zhao, M.G. Predictable chronic mild stress promotes recovery from LPS-induced depression. *Mol. Brain* 2019, 12, 42, doi:10.1186/s13041-019-0463-2.
97. Furuzawa, M.; Chen, H.; Fujiwara, S.; Yamada, K.; Kubo, K.Y. Chewing ameliorates chronic mild stress-induced bone loss in senescence-accelerated mouse (SAMP8), a murine model of senile osteoporosis. *Exp. Gerontol.* 2014, 55, 12–18, doi:10.1016/j.exger.2014.03.003.
98. Heim, C.; Mletzko, T.; Purselle, D.; Musselman, D.L.; Nemerooff, C.B. The dexamethasone/corticotropin-releasing factor test in men with major depression: Role of childhood trauma. *Biol. Psychiatry* 2008, 63, 398–405, doi:10.1016/j.biopsych.2007.07.002.

99. Heim, C.; Shugart, M.; Craighead, W.E.; Nemeroff, C.B. Neurobiological and psychiatric consequences of child abuse and neglect. *Dev. Psychobiol.* 2010, 52, 671–690, doi:10.1002/dev.20494.
100. Saveanu, R.V.; Nemeroff, C.B. Etiology of Depression: Genetic and Environmental Factors. *Psychiatry Clin. N. Am.* 2012, 35, 51, doi:10.1016/j.psc.2011.12.001.
101. Picard, M.; McEwen, B.S.; Epel, E.S.; Sandi, C. An energetic view of stress: Focus on mitochondria. *Front. Neuroendocrinol.* 2018, 49, 72–85, doi:10.1016/j.yfrne.2018.01.001.
102. Sophocleous, A.; Idris, A.I. Rodent models of osteoporosis. *Bonekey Rep.* 2014, 3, 614, doi:10.1038/bonekey.2014.109.
103. Halloran, B.P.; Ferguson, V.L.; Simske, S.J.; Burghardt, A.; Venton, L.L.; Majumdar, S. Changes in bone structure and mass with advancing age in the male C57BL/6J mouse. *J. Bone Miner. Res.* 2002, 17, 1044–1050, doi:10.1359/jbmr.2002.17.6.1044.
104. Bohacek, J.; Manuella, F.; Roszkowski, M.; Mansuy, I.M. Hippocampal gene expression induced by cold swim stress depends on sex and handling. *Psychoneuroendocrinology* 2015, 52, 1–12, doi:10.1016/j.psyneuen.2014.10.026.
105. Hendrix, S.; Picker, B.; Liezmann, C.; Peters, E.M. Skin and hair follicle innervation in experimental models: A guide for the exact and reproducible evaluation of neuronal plasticity. *Exp. Dermatol.* 2008, 17, 214–227, doi:10.1111/j.1600-0625.2007.00653.x.
106. Kohler, T.; Beyeler, M.; Webster, D.; Muller, R. Compartmental bone morphometry in the mouse femur: Reproducibility and resolution dependence of microtomographic measurements. *Calcif. Tissue Int.* 2005, 77, 281–290, doi:10.1007/s00223-005-0039-2.
107. Bouxsein, M.L.; Boyd, S.K.; Christiansen, B.A.; Guldberg, R.E.; Jepsen, K.J.; Muller, R. Guidelines for Assessment of Bone Microstructure in Rodents Using Micro-Computed Tomography. *J. Bone Miner. Res.* 2010, 25, 1468–1486, doi:10.1002/jbmr.141.
108. Glaesmer, H.; Schulz, A.; Häuser, W.; Freyberger, H.J.; Brähler, E.; Grabe, H.-J. Der Childhood Trauma Screener (CTS)—Entwicklung und Validierung von Schwellenwerten zur Klassifikation [The Childhood Trauma Screener (CTS)—Development and Validation of Cut-Off-Scores for Classificatory Diagnostics]. *Psychiatr. Praxis* 2013, 40, 220–226, doi:10.1055/s-0033-1343116.
109. Wingenfeld, K.; Spitzer, C.; Mensebach, C.; Grabe, H.J.; Hill, A.; Gast, U.; Schlosser, N.; Höpp, H.; Beblo, T.; Driessen, M. Die deutsche Version des Childhood Trauma Questionnaire (CTQ): Erste Befunde zu den psychometrischen Kennwerten [The German version of the Childhood Trauma Questionnaire (CTQ): Preliminary psychometric properties]. *Psychother. Psychosom. Med. Psychol.* 2010, 60, 442–450.
110. Bernstein, D.; Fink, L. Childhood Trauma Questionnaire (CTQ): A Retrospective Self-Report Questionnaire and Manual; Corporation, T.P., Ed.; San Antonio, TX, USA, 1998.
111. Glaesmer, H.; Schulz, A.; Hauser, W.; Freyberger, H.J.; Brähler, E.; Grabe, H.J. The childhood trauma screener (CTS)—development and validation of cut-off-scores for classificatory diagnostics. *Psychiatr. Prax.* 2013, 40, 220–226, doi:10.1055/s-0033-1343116.
112. Grabe, H.J.; Schulz, A.; Schmidt, C.O.; Appel, K.; Driessen, M.; Wingenfeld, K.; Barnow, S.; Spitzer, C.; John, U.; Berger, K.; et al. A brief instrument for the assessment of childhood abuse and neglect: The childhood trauma screener (CTS). *Psychiatr. Prax.* 2012, 39, 109–115, doi:10.1055/s-0031-1298984.

113. Siegrist, J.; Geyer, S. ILE-Inventar zur Erfassung lebensverändernder Ereignisse. In Diagnostische Verfahren in der Psychotherapie; Hogrefe, Ed.; Göttingen: 2002, 211–213.
114. Beck, A.T.; Steer, R.A.; Brown, G.K. Manual for the Beck Depression Inventory-II.; T.P. Corporation: San Antonio, TX, USA, 1996.
115. Wintjen, L.; Petermann, F. Beck-Depressions-Inventar Revision (BDI-II). Z. Psychiatr. Psych. Psychother. 2010, 58, 243–245, doi:10.1024/1661-4747.a000033.
116. Muche, R.; Lanzinger, S.; Rau, M. Medizinische Statistik Mit R und Excel; Springer: 2011.
117. R Core Team. R Foundation for Statistical Computing; R Foundation for Statistical Computing: Vienna, Austria, 2014.

Thesis chapter

6. Discussion and outlook

Experiences and environmental conditions in childhood and adolescence shape developmental processes and determine an individual's mental and physical health across life. While positive and favorable conditions allow proper development, normal behaviors and a healthy body, detrimental experiences such as those involving trauma or chronic stress have severe and persistent negative effects. Early traumatic experiences such as maltreatment, parental neglect, physical or emotional abuse in early life can severely affect behavioral and physiological functions in individuals when adult. Although early life traumatic experiences are often associated with brain related functions, mounting evidence suggests a similar impact on other tissues as well, such as the muscoskeletal system, tissues with metabolic functions and the germ line.

Such experiences are among the strongest risk factors for disabling mental disorders and are thought to cause up to 10 % of cases of depression, personality disorders, antisocial behaviors, post-traumatic stress disorder or schizophrenia across families [1]. They are postulated to underlie the missing heritability of most psychiatric conditions and the fact that their genetic basis has remained unidentified despite numerous genome-wide association studies. In addition, further to affecting the individuals directly exposed, traumatic experiences also often affect their offspring across generations. Therefore, it is of great interest to investigate the molecular mechanisms that propagate such effects from one to the next generation.

The expression and inheritance of the effects of trauma across generations are thought to implicate non-genetic mechanisms. Initial evidence for a role for DNA methylation and non-coding RNAs in these mechanisms has been recently obtained in mice. Using an established mouse model of postnatal trauma with inherited symptoms, it was shown that several microRNAs (miRNAs) are altered by postnatal traumatic stress in sperm, brain and serum across generations. Further, sperm RNAs could be causally linked to inheritance because, when injected into naïve fertilized oocytes, they can reproduce some of the effects of traumatic stress in the resulting animals [2,3].

This unique form of heredity, known as epigenetic inheritance, is distinguished by epigenetic changes induced by specific exposures in the parental germ cells that give rise to symptoms in the offspring – even when they do not experience exposure unlike their parents. Accumulating evidence supports the existence of germline-dependent epigenetic inheritance of phenotypes after exposure in early life or adulthood in rodents and other animal models, sometimes across multiple generations [4]. Recent studies in humans from our group and others also revealed changes in sperm after early life trauma, indicating that this form of inheritance is relevant for human heredity. This concept has become important for medicine and biology, and is viewed as a promising hypothesis regarding the etiology of complex diseases and their underlying mechanisms. However, investigating such transgenerational mechanisms in humans and establishing direct relations within a family lineage remains exceptionally challenging.

New insight into the potential mechanisms of non-genetic inheritance linked to traumatic stress have recently been gained in experimental mouse models. One of the most consistent models is based on the exposure of newborn pups to daily episodes of unpredictable maternal separation combined with exposure of dams to unpredictable stress during separation, for 2 weeks (MSUS) [2]. This paradigm mimics conditions of poor and traumatic childhood in humans. When adult, MSUS mice have severe behavioral and physiological alterations such as depressive-like symptoms, antisocial behaviors, cognitive deficits, increased risk-taking behaviors and also dysregulated glucose and insulin metabolism [5–9]. But the animals also have a few positive traits in particular, they exhibit improved behavioral flexibility and goal-directed behaviors in challenging conditions [8], suggesting a form of resilience to stress consistent with observations in humans of similar resilience in some traumatized people. Most strikingly, the behavioral and physiological traits induced by MSUS not only persist across life, but are also transmitted to the progeny by both males and females across several generations [10,11]. Thus, 2nd, 3rd and even 4th generation progeny can have similar behavioral and physiological disorders as their parents even if they are themselves not exposed to any trauma or stress [12]. Such patriline and matriline transmission involves the germline because it can be reproduced by *in vitro* fertilization and persists after maternal cross-fostering excluding the contribution of social or maternal factors.

As the effects of parental exposure can be transmitted to the offspring through different routes including social/behavioral, germline and body fluids (e.g. seminal fluid, milk), studies on epigenetic inheritance require not only genomic and epigenomic analyses in germ cells including DNA methylation, transcriptomic, chromatin accessibility, histone post-translational modifications, but also confirmation of germline-dependence by assisted reproduction technologies (ART) such as artificial insemination and embryo transfer [13].

Traditionally, sperm cells have been used for these investigations for their ease of collection and higher number when compared to the oocytes from the female germ line. However, conventional methods of sperm collection only yield a limited number of spermatozoa which is insufficient for reliable genomic and epigenomic analyses and ART, and does not allow parallel analyses and ART with the sperm of the same animal, which is a critical limitation. This limitation not only prevents cross-validation of the link between molecular changes identified in sperm and phenotypic transmission, but also preclude any conclusion on the way genome and epigenome interact and control heredity. Further, it also requires a considerable number of animals because separate cohorts are needed for molecular analysis, for validation studies and for ART. This is complicated by the fact that a number of conditions associated with epigenetic transmission such as early life trauma, obesity, diabetes mellitus etc. can reduce fertility and therefore, limit litter size which makes the issue of number of animals even more problematic.

Initial analyses in the MSUS model have started to delineate some of the molecular mechanisms underlying the expression and the transmission of these behavioral and physiological traits. Epigenetic analyses revealed that DNA methylation, an epigenetic mark involved in gene regulation, is altered at multiple genes and loci, not only in the brain but also in the sperm of the exposed animals when adult. Further, DNA methylation was found to be similarly affected in the brain and sperm of the progeny, which strongly suggests transmission of aberrant DNA methylation across generations [2]. Moreover, recent analyses of ncRNAs, another form of non-genetic factors recently recognized as key genomic regulators, revealed that ncRNAs, in particular several microRNAs, are consistently altered in the brain, sperm and serum of the exposed animals when adult, but also in the brain and serum of their progeny [3,14]. The key role of sperm RNAs in the transgenerational inheritance of the symptoms was further demonstrated by the observation that injection of these RNAs extracted from the sperm

of adult MSUS males into naïve fertilized mouse eggs reproduces most behavioral and physiological symptoms in the resulting progeny but also in the progeny of this progeny [3].

To answer the various questions pertaining to the hypothesis that sperm cells act as vector of molecular transmission between generations, we improved existing methods of sperm collection and extraction of RNAs because they were the starting point for subsequent molecular analyses such as next generation sequencing. Initially, we identified them as bottlenecks in our experiments because the RNA yield was so low that pooling of sperm and extracted RNAs was necessary to obtain sufficient starting amounts for even simple RT-qPCR experiments. Through initial observations we identified two areas that were subsequently improved.

Firstly, we observed a large quantity of motile sperm cells remaining at the bottom of the tube during the “classical” swim-up method procedure. Therefore, many potentially usable sperm cells were routinely discarded. Initially, we pursued an approach to simply repeat the swim-up of sperm cells multiple times to recover any additional sperm cells leaving the bottom of the tube towards the upper collection layer. However, the direction of swimming was random owing to the fact that no chemical cues were present, greatly reducing the overall number of sperm cells escaping the bottom layer. In addition, because the tissue pieces were also still present at the bottom of the tube it seemed unlikely that a majority of sperm cells would manage to escape into the upper layer for collection. By inverting the approach, we solved these issues. We were now able to wash sperm cells out of the tissue pieces, thereby massively increasing the sperm yield from a single mouse. We could then use the same approach to recover matured but mostly immotile sperm cells from other parts of epididymis, such as the caput or corpus [15]. As sperm continues to mature during the transit in the epididymis [16], future studies may investigate if early life trauma and other environmental factors alter this environment and contribute to the transmission of epigenetic signal to the next generation. It is therefore of great benefit, that the collection of epididymosome was also improved by our OmniSperm approach. These extracellular vesicles are implicated as the main modes of transferring lipids, proteins, metabolites and RNAs from the epididymal tissue to the sperm cells passing through [17,18].

Secondly, we observed that sperm cells were not lysed during normal RNA extraction procedures. This resulted in very low RNA yields despite pooling multiple mouse sperm samples. We identified that sperm cells were resistant to commonly used lysis buffers and the yields of extracted DNAs and RNAs were poor. This limited down-stream analyses substantially and hindered the use of innovative methods like DNA and RNA sequencing, or ATAC sequencing, in sperm cells. To address this issue, we conducted a series of biological and chemical experiments on mouse sperm. We found that adding the reducing agent TCEP to commercially available lysis solutions greatly enhanced sperm cells lysis and the yield of extracted RNA. In addition to microscopic observations, we showed in an *in vitro* assay that other common pH-sensitive reducing agents had to be used with a compatible lysis solution to be effective. We identified disulfide bonds, which maintain the structural integrity of sperm cells even at very low pH, as likely responsible for the resistance of sperm cells to lysis. Future studies may investigate what components of the sperm membrane are forming such resilient disulfide bonds and if they are of relevance for andrological pathologies [19] and a potential avenue for the development of alternative contraceptives [20]. In addition, such disulfide forming elements could reinforce extracellular vesicles, which see future use in therapeutics, to increase resistance against acidic environments typically encountered in the stomach [21].

Combining these two improvements enabled us to conduct epigenetic inheritance experiments which could address multiple questions at once. Increasing the starting amount of DNA and RNA from sperm will also be crucial to investigate other types of nucleotide and ribonucleotide modifications such as 1-methyladenosine and 1-methylguanosine [4,22]. To our knowledge, the role of such modification in epigenetic transmission is unexplored. As highlighted in the OmniSperm paper, we were able to sequence the DNA methylome as well as the transcriptome from a single sperm sample. When coupled with artificial insemination, we had the opportunity to not only relate two epigenetic marks within a single sperm sample but also to relate them to gene expression changes in the resulting offspring.

This approach will have great relevance not only for the field of epigenetic inheritance, but the method can also be used by scientists working in reproductive biology, urology, teratology, and genomic heredity. Isolation of spermatozoa is a key starting point in a large number of studies relevant to these fields. Our approach will reduce the number of animals required by:

- a) yielding more spermatozoa per mouse hence reducing the commonly used practice of pooling samples from different animals to perform analysis, a practice that also is also questionable from the point of scientific rigor,
- b) allowing cross-validation molecular analyses in which confirmatory studies can be performed on the same animals, that not only gives greater credibility to the over-all results but also reduces the animals that are allowed for these confirmatory studies,
- c) reducing the need to have a separate cohort of animals for ART studies.

This approach also leads to refinement in the way animals are used in research, by establishing a method that allows cross-validation studies without compromising on animal welfare. The mice will not be exposed to any additional surgical or pharmacological manipulation in this strategy, hence there will be no increase in animal suffering. The obtained results will be from a single animal and thus will provide a better representation of human conditions where the molecular changes induced in the germ cells of an individuals can potentially be transmitted to the offspring upon conception [23].

However, many challenges still remain in understanding the transmission of epigenetic marks in sperm. The most obvious one is the fact that we are investigating a large number of sperm cells, thereby averaging out any potentially relevant, heterogeneously distributed epigenetic marks. After all, sperm cells are haploid and may carry individual genomic aberrations or particular epigenomic profiles [24,25]. A fundamental question remains therefore and may not be solved with currently used methods as highlighted in this recent review:

“The selection of this high (epi)quality sperm fraction is currently impossible due to the inexistence of methods that allow the measurement of DNA methylation levels without leading to the destruction of the analysed cells. The development of such a technique could have a major impact not only on the outcome of ART but also to its safety.” [25]

Currently, there is no approach for the selection of sperm cells based on their genetic and epigenetic information. Researchers and fertility clinics use bulk sperm samples (samples containing multiple million cells) or other samples from the male donor to assess the genetic and/or epigenetic and/or transcriptomic status. Here the limitation is that they can't provide

enough precise information about the sperm cell that will itself fertilize the egg because a sperm can be used either for fertilization or for molecular analyses but not for both. Selection of sperm cells for ART still primarily relies on sperm motility, surface characteristics and morphology [26]. Intracytoplasmic morphologically selected sperm injection (IMSI) is a refined method (higher magnification in the used microscope) to assess the sperm head integrity [27]. However, it also relies on morphology and does not provide any molecular information. Surface charge selection allows the selection of sperm cells that have differentiated normally as compared to sperm cells that did not fully differentiate [26]. Magnetic assisted cell sorting has been used to separate apoptotic (dying) sperm cells from non-apoptotic sperm [28]. Hyaluronic acid binding (e.g. physiological intracytoplasmic sperm injection) is used to enrich for sperm cells that have a better chance of reaching and fusing with the egg [29]. Finally, a few publications exist that propose methods to enrich for sperm fractions with a higher or lower percentage of sperm cells carrying either the X- or Y-chromosome [30,31]. Despite such advancements, they are unable to provide precise molecular information from a single sperm cell.

Instead, we began to pursue an approach to identify meiotically related sperm cells. During meiosis, a progenitor cell undergoes two rounds of cell division resulting in four sperm cells with copies of each paternal and maternal chromosome [32]. Therefore, each sperm cell has at least one nearly identical “twin” stemming from the meiosis II division, originating from the same predecessor cell during spermatogenesis. However, this relation is lost once the developing sperm cells are released into the seminiferous tubules and efferent ducts in the testis leading to the epididymis.

We speculated that in some rare instances this relation between the “twin” sperm cells is maintained and could be exploited to confer genetic and epigenetic information while preserving one of sperm cells for ART. Such sperm cells would have two heads and share a midpiece and/or tail. One head could be used to analyze its epigenetic signature or other molecular features while the other head would remain intact for intracytoplasmic sperm injection in order to fertilize an oocyte. These dicephalic sperm and other sperm with unusual morphologies were previously described in the literature in the context of sperm morphology in general, assessment of sperm quality and as an indicators of infertility [33]. However, conjoined sperm cells can occur randomly, likely due to cellular errors during sperm

development and maturation, and are therefore also present in otherwise healthy animals and humans.

Indeed, we were able to enrich for dicephalic sperm by fluorescence activated cell sorting (FACS) and estimate their occurrence by imaging flow cytometry. A first assessment of the morphology of the dicephalic sperm heads did not reveal any apparent differences to normal sperm cells. Various degrees of midpiece bifurcation (proximal or distal to sperm head) were observed and indicated a random process in the failure to fully separate sperm cells rather than a single-point of failure during spermatogenesis. Furthermore, we did not observe any sperm cells with three (or more heads) or heads on the opposite sides of the sperm tail. Such observations would indicate that different sperm cells entangle with their tails and would not be considered dicephalic sperm.

After the FACS enrichment, we manually transferred and manipulated dicephalic sperm cells and managed to separate the sperm heads from each other. However, these attempts were made by mouth pipetting using pulled glass capillaries which was difficult and not precise enough to conduct controlled and reproducible experiments. Initial attempts to use an ICSI setup in the group of Prof. vom Berg and Prof. Buch were promising but had to be postponed due to the restrictions imposed by the corona pandemic in 2020.

Once established, such an approach to manipulate and investigate single sperm cells would face additional hurdles to fully explore the whole single cell epigenome. Recent advances in single-cell next-generation sequencing technologies and novel barcoding strategies have increasingly allowed the integration of single-cell profiling into multiplexed assays for the interrogation of multiple molecular layers of gene regulation in the same cell. The development of multiomic approaches has allowed the simultaneous interrogation of single cell modalities and overcame the highly correlative integration of unimodal datasets obtained from separate experiments [34]. In the past decade, single-cell sequencing technologies have been increasingly applied to dissect the cellular heterogeneity of complex tissues, developing embryos and tumors. Combined, multiomic strategies and single-cell sequencing platforms provide a powerful approach for the discovery of cell-specific gene regulatory programs, and for a more comprehensive identification and characterization of novel and rare cell types in seemingly homogenous populations [35].

Among the multiomic techniques that simultaneously profile the genome and transcriptome of single cells, some separate the DNA and RNA components immediately after cell lysis, before further processing, by either taking advantage of their different physical properties (eg. centrifugation), or by specifically selecting polyA(+) RNAs from the cell lysate using oligo-dT beads [36]. Other techniques subject the whole lysate, containing both the DNA and RNAs, to reverse-transcription and pre-amplification, and only then split the reaction into two aliquots, each used for different library preparation (gDNA or RNA-seq) [36,37]. Techniques also vary in the population of RNAs they profile: while most capture polyadenylated (polyA+) RNAs, some capture only nuclear polyA+ RNAs (SNARE-seq [38]), and others additionally profile non-polyadenylated RNAs (scSIDR-seq [39]). Depending on the RNA library preparation strategy, techniques vary in the extent of the transcriptome they capture, and therefore, in their applicability. Techniques based on the Switching Mechanism At the 5'-end of RNA Transcripts (Smart-seq) [40] RNA library preparation protocol (TARGET-seq [41], sc(ATAC+RNA)-seq [42], scCAT-seq [43], scNMT-seq [44]) or the Multiple Annealing and dC-Tailing-based Quantitative (MATQ-seq) [45] protocol (scNOMeRe-seq [46]) recover the whole transcript, facilitating the identification of novel isoforms, while those that apply protocols such as Droplet Based scRNA-Seq (Drop-seq) are restricted to the 3'-end of the transcript (SNARE-seq [38]). Future studies on single sperm should therefore carefully weight the most suitable method and particularly ensure that the sperm head is fully lysed in the initial buffer.

One epigenetic layer that remains to be addressed by single-cell multiomics is the targeted profiling of DNA-binding proteins, and of histone marks across the whole genome. The current lack of such exploration is in part due to the lengthy processing and optimization required by antibody-based techniques such as single-cell ChIP-seq (itChIP-seq) [47], which have mostly precluded the compatibility between such approaches and for example RNA-seq. Two exceptions to this are scDam&T-seq [48], which is limited in throughput, and single-cell calling cards (scCC [49]), a novel assay that allows simultaneous direct assessment of transcription factor binding sites and the transcriptome in single cells. However, both of these methods require genetic manipulation of the model cell or organism, precluding their application in clinical samples, for example. Potential alternatives to ChIP-seq, such as CUT&Tag [50] or CUT&Run [51], which have been applied in single cells may soon become

combined with other omics techniques and thus adopted by single-cell multiomics, further advancing the power of this technology.

To address this epigenetic layer in single sperm cells, we worked towards a novel approach to multimodal epigenomic profiling that does not rely on antibodies or chemical fixation. Our approach was to fuse a Tn5 transposase to an engineered antibody mimetic which would promote the insertion of sequencing adapters in the target regions of the antibody mimetic. Tn5 is a DNA-cutting transposase which originally facilitated the relocation of transposomes in the genome [52]. However, it's been since then repurposed to jump into accessible chromatin regions and insert sequencing oligos, thereby providing a chromatin accessibility profile after high-throughput sequencing (ATAC-seq [53]). Engineered antibody mimetics are protein fragments that have a high affinity for a target, such as nanobodies or DARPins [54]. Therefore, a Tn5 fused to a nanobody that would recognize certain histone variants would enable a ChIP-seq-like approach to map chromatin bound molecules in a single cell. Unlike in ChIP-seq, the fragments produced by the Tn5 insertion can be amplified by PCR, thereby enabling single-cell sequencing.

In collaboration with Maria-Andreea Dimitriu, we produced a fusion between Tn5 and a GFP-binding nanobody (GBN-Tn5) and verified its functionality in transposing DNA as a proof of principle. Using GBN-Tn5 (NanoTag), we generated sequencing libraries in a stem cell model expressing various GFP-labelled chromatin readers, which can recognize specific chromatin modifications such as H3K4me3 [55]. Preliminary results suggested that NanoTag is a promising strategy for targeted epigenomic profiling with many potential applications in epigenetics. Sequenced libraries are currently being analyzed to determine if an enrichment occurs. Furthermore, other optimizations to NanoTag are being pursued and we've been generating other of Tn5-variants that can detect other fluorophores [56–58], transcription factors [59–62] and regulatory chromatin features such as G-quadruplexes [63,64].

The questions addressed in my thesis required the improvement of existing or establishment of new methods to address the various questions regarding the physiological impact of early life trauma and transmission to the next generation through the male germ line. The findings presented in my thesis identified early life trauma as an adverse environmental factor that impacts a variety of molecular mechanisms in somatic tissues and the male germ line of the mouse.

6.1. References

1. Klengel, T.; Binder, E.B. Epigenetics of Stress-Related Psychiatric Disorders and Gene × Environment Interactions. *Neuron* **2015**, *86*, 1343–1357, doi:10.1016/j.neuron.2015.05.036.
2. Franklin, T.B.; Russig, H.; Weiss, I.C.; Gräff, J.; Linder, N.; Michalon, A.; Vizi, S.; Mansuy, I.M. Epigenetic transmission of the impact of early stress across generations. *Biol. Psychiatry* **2010**, *68*, 408–15, doi:10.1016/j.biopsych.2010.05.036.
3. Gapp, K.; Jawaid, A.; Sarkies, P.; Bohacek, J.; Pelczar, P.; Prados, J.; Farinelli, L.; Miska, E.; Mansuy, I.M. Implication of sperm RNAs in transgenerational inheritance of the effects of early trauma in mice. *Nat. Neurosci.* **2014**, *17*, 667–669, doi:10.1038/nn.3695.
4. Jawaid, A.; Roszkowski, M.; Mansuy, I.M. Transgenerational Epigenetics of Traumatic Stress. In *Neuroepigenetics and Mental Illness*; Elsevier Inc., 2018; pp. 1–26.
5. Gapp, K.; Corcoba, A.; van Steenwyk, G.; Mansuy, I.M.; Duarte, J.M.N. Brain metabolic alterations in mice subjected to postnatal traumatic stress and in their offspring. *J. Cereb. Blood Flow Metab.* **2017**, *37*, 2423–2432, doi:10.1177/0271678X16667525.
6. Franklin, T.B.; Linder, N.; Russig, H.; Thöny, B.; Mansuy, I.M. Influence of Early Stress on Social Abilities and Serotonergic Functions across Generations in Mice. *PLoS One* **2011**, *6*, e21842, doi:10.1371/journal.pone.0021842.
7. Bohacek, J.; Farinelli, M.; Mirante, O.; Steiner, G.; Gapp, K.; Coiret, G.; Ebeling, M.; Durán-Pacheco, G.; Iniguez, a L.; Manuella, F.; et al. Pathological brain plasticity and cognition in the offspring of males subjected to postnatal traumatic stress. *Mol. Psychiatry* **2015**, *20*, 621–631, doi:10.1038/mp.2014.80.
8. Gapp, K.; Soldado-Magraner, S.; Alvarez-Sánchez, M.; Bohacek, J.; Vernaz, G.; Shu, H.; Franklin, T.B.; Wolfer, D.; Mansuy, I.M. Early life stress in fathers improves behavioural flexibility in their offspring. *Nat. Commun.* **2014**, *5*, 5466, doi:10.1038/ncomms6466.
9. Steenwyk, G.; Gapp, K.; Jawaid, A.; Germain, P.; Manuella, F.; Tanwar, D.K.; Zamboni, N.; Gaur, N.; Efimova, A.; Thumfart, K.M.; et al. Involvement of circulating factors in the transmission of paternal experiences through the germline. *EMBO J.* **2020**, *39*, 1–16, doi:10.15252/embj.2020104579.
10. Franklin, T.B.; Russig, H.; Weiss, I.C.; Gräff, J.; Linder, N.; Michalon, A.; Vizi, S.; Mansuy, I.M. Epigenetic transmission of the impact of early stress across generations. *Biol. Psychiatry* **2010**, *68*, 408–

- 415, doi:10.1016/j.biopsych.2010.05.036.
11. Weiss, I.C.; Franklin, T.B.; Vizi, S.; Mansuy, I.M. Inheritable effect of unpredictable maternal separation on behavioral responses in mice. *Front. Behav. Neurosci.* **2011**, *5*, 3, doi:10.3389/fnbeh.2011.00003.
 12. van Steenwyk, G.; Roszkowski, M.; Manuella, F.; Franklin, T.B.; Mansuy, I.M. Transgenerational inheritance of behavioral and metabolic effects of paternal exposure to traumatic stress in early postnatal life: evidence in the 4th generation. *Environ. Epigenetics* **2018**, *4*, 1–8, doi:10.1093/eep/dvy023.
 13. Bohacek, J.; Mansuy, I.M. A guide to designing germline-dependent epigenetic inheritance experiments in mammals. *Nat. Methods* **2017**, *14*, 243–249, doi:10.1038/nmeth.4181.
 14. Gapp, K.; van Steenwyk, G.; Germain, P.L.; Matsushima, W.; Rudolph, K.L.M.; Manuella, F.; Roszkowski, M.; Vernaz, G.; Ghosh, T.; Pelczar, P.; et al. Alterations in sperm long RNA contribute to the epigenetic inheritance of the effects of postnatal trauma. *Mol. Psychiatry* **2020**, *25*, doi:10.1038/s41380-018-0271-6.
 15. HORST, G. VAN DER; SEIER, J. V.; SPINKS, A.C.; HENDRICKS, S. The maturation of sperm motility in the epididymis and vas deferens of the vervet monkey, *Cercopithecus aethiops*. *Int. J. Androl.* **1999**, *22*, 197–207, doi:10.1046/j.1365-2605.1999.00171.x.
 16. Skerget, S.; Rosenow, M.A.; Petritis, K.; Karr, T.L. Sperm proteome maturation in the mouse Epididymis. *PLoS One* **2015**, *10*, 1–23, doi:10.1371/journal.pone.0140650.
 17. Trigg, N.A.; Eamens, A.L.; Nixon, B. The contribution of epididymosomes to the sperm small RNA profile. *Reproduction* **2019**, *157*, R209–R223, doi:10.1530/REP-18-0480.
 18. Reilly, J.N.; McLaughlin, E.A.; Stanger, S.J.; Anderson, A.L.; Hutcheon, K.; Church, K.; Mihalas, B.P.; Tyagi, S.; Holt, J.E.; Eamens, A.L.; et al. Characterisation of mouse epididymosomes reveals a complex profile of microRNAs and a potential mechanism for modification of the sperm epigenome. *Sci. Rep.* **2016**, *6*, 1–15, doi:10.1038/srep31794.
 19. Tüttelmann, F.; Nieschlag, E. Classification of Andrological Disorders. In *Andrology*; Nieschlag, E., Behre, H.M., Nieschlag, S., Eds.; Springer Berlin Heidelberg: Berlin, Heidelberg, 2010; pp. 87–92 ISBN 978-3-540-78355-8.
 20. Long, J.E.; Lee, M.S.; Blithe, D.L. Male Contraceptive Development: Update on Novel Hormonal and Nonhormonal Methods. *Clin. Chem.* **2019**, *65*, 153–160, doi:10.1373/clinchem.2018.295089.
 21. Murphy, D.E.; de Jong, O.G.; Brouwer, M.; Wood, M.J.; Lavieu, G.; Schiffelers, R.M.; Vader, P. Extracellular vesicle-based therapeutics: natural versus engineered targeting and trafficking. *Exp. Mol. Med.* **2019**, *51*, 32, doi:10.1038/s12276-019-0223-5.
 22. Lewis, C.J.T.; Pan, T.; Kalsotra, A. RNA modifications and structures cooperate to guide RNA–protein interactions. *Nat. Rev. Mol. Cell Biol.* **2017**, *18*, 202–210, doi:10.1038/nrm.2016.163.
 23. Jawaid, A.; Jehle, K.-L.; Mansuy, I.M. Impact of Parental Exposure on Offspring Health in Humans. *Trends Genet.* **2020**, 1–16, doi:10.1016/j.tig.2020.10.006.
 24. Medarde, N.; Muñoz-Muñoz, F.; López-Fuster, M.; Ventura, J. Variational modularity at the cell level: insights from the sperm head of the house mouse. *BMC Evol. Biol.* **2013**, *13*, 179, doi:10.1186/1471-2148-13-179.
 25. Laurentino, S.; Borgmann, J.; Gromoll, J. On the origin of sperm epigenetic heterogeneity. *Reproduction*

- 2016, 151, R71–R78, doi:10.1530/REP-15-0436.
26. Rappa, K.L.; Rodriguez, H.F.; Hakkarainen, G.C.; Anchan, R.M.; Mutter, G.L.; Asghar, W. Sperm processing for advanced reproductive technologies: Where are we today? *Biotechnol. Adv.* **2016**, *34*, 578–587, doi:10.1016/j.biotechadv.2016.01.007.
27. Omidi, M.; Faramarzi, A.; Agharahimi, A.; Khalili, M.A. Noninvasive imaging systems for gametes and embryo selection in IVF programs: a review. *J. Microsc.* **2017**, *267*, 253–264, doi:10.1111/jmi.12573.
28. Henkel, R. Sperm preparation: State-of-the-artphysiological aspects and application of advanced sperm preparation methods. *Asian J. Androl.* **2012**, *14*, 260–269, doi:10.1038/aja.2011.133.
29. McDowell, S.; Kroon, B.; Ford, E.; Hook, Y.; Glujsovsky, D.; Yazdani, A. Advanced sperm selection techniques for assisted reproduction. *Cochrane Database Syst. Rev.* **2014**, 1–40, doi:10.1002/14651858.CD010461.pub2.
30. Naniwa, Y.; Sakamoto, Y.; Toda, S.; Uchiyama, K. Bovine sperm sex-selection technology in Japan. *Reprod. Med. Biol.* **2019**, *18*, 17–26, doi:10.1002/rmb2.12235.
31. Maxwell, W.M.C.; Evans, G.; Hollinshead, F.K.; Bathgate, R.; De Graaf, S.P.; Eriksson, B.M.; Gillan, L.; Morton, K.M.; O'Brien, J.K. Integration of sperm sexing technology into the ART toolbox. *Anim. Reprod. Sci.* **2004**, *82–83*, 79–95, doi:10.1016/j.anireprosci.2004.04.013.
32. Griswold, M.D. Spermatogenesis: The Commitment to Meiosis. *Physiol. Rev.* **2016**, *96*, 1–17, doi:10.1152/physrev.00013.2015.
33. World Health Organization *WHO laboratory manual for the Examination and processing of human semen*; 5th ed.; World Health Organization, 2010; ISBN 978 92 4 154778 9.
34. Ma, A.; Mcdermaid, A.; Xu, J.; Chang, Y. Integrative Methods and Practical Challenges for Single-Cell Multi-omics. *Trends Biotechnol.* **2020**, 1–16, doi:10.1016/j.tibtech.2020.02.013.
35. Strzelecka, P.M.; Ranzoni, A.M.; Cvejic, A. Dissecting human disease with single-cell omics: Application in model systems and in the clinic. *DMM Dis. Model. Mech.* **2018**, *11*, doi:10.1242/dmm.036525.
36. Lee, J.; Hyeon, D.Y.; Hwang, D. Single-cell multiomics: technologies and data analysis methods. *Exp. Mol. Med.* **2020**, doi:10.1038/s12276-020-0420-2.
37. Dey, S.S.; Kester, L.; Spanjaard, B.; Bienko, M.; Oudenaarden, A. Van Integrated genome and transcriptome sequencing of the same cell. **2015**, *33*, doi:10.1038/nbt.3129.
38. Chen, S.; Lake, B.B.; Zhang, K. High-throughput sequencing of the transcriptome and chromatin accessibility in the same cell. *Nat. Biotechnol.* **2019**, *37*, 1452–1457.
39. Han, K.Y.; Kim, K.T.; Joung, J.G.; Son, D.S.; Kim, Y.J.; Jo, A.; Jeon, H.J.; Moon, H.S.; Yoo, C.E.; Chung, W.; et al. SIDR: simultaneous isolation and parallel sequencing of genomic DNA and total RNA from single cells. *Genome Res.* **2018**, *28*, 75–87, doi:10.1101/gr.223263.117.
40. Ramsköld, D.; Luo, S.; Wang, Y.C.; Li, R.; Deng, Q.; Faridani, O.R.; Daniels, G.A.; Khrebtukova, I.; Loring, J.F.; Laurent, L.C.; et al. Full-length mRNA-Seq from single-cell levels of RNA and individual circulating tumor cells. *Nat. Biotechnol.* **2012**, *30*, 777–782, doi:10.1038/nbt.2282.
41. Rodriguez-Meira, A.; Buck, G.; Clark, S.A.; Povinelli, B.J.; Alcolea, V.; Louka, E.; McGowan, S.; Hamblin, A.; Sousos, N.; Barkas, N.; et al. Unravelling Intratumoral Heterogeneity through High-Sensitivity Single-Cell Mutational Analysis and Parallel RNA Sequencing. *Mol. Cell* **2019**, *73*, 1292–

- 1305.e8, doi:10.1016/j.molcel.2019.01.009.
42. Reyes, M.; Billman, K.; Hacohen, N.; Blainey, P.C. Simultaneous Profiling of Gene Expression and Chromatin Accessibility in Single Cells. *Adv. Biosyst.* **2019**, *3*, 1–6, doi:10.1002/adbi.201900065.
43. Liu, L.; Liu, C.; Quintero, A.; Wu, L.; Yuan, Y.; Wang, M.; Cheng, M.; Leng, L.; Xu, L.; Dong, G.; et al. Deconvolution of single-cell multi-omics layers reveals regulatory heterogeneity. *Nat. Commun.* **2019**, *10*, doi:10.1038/s41467-018-08205-7.
44. Clark, S.J.; Argelaguet, R.; Kapourani, C.A.; Stubbs, T.M.; Lee, H.J.; Alda-Catalinas, C.; Krueger, F.; Sanguinetti, G.; Kelsey, G.; Marioni, J.C.; et al. ScNMT-seq enables joint profiling of chromatin accessibility DNA methylation and transcription in single cells e. *Nat. Commun.* **2018**, *9*, 1–9, doi:10.1038/s41467-018-03149-4.
45. Sheng, K.; Cao, W.; Niu, Y.; Deng, Q.; Zong, C. Effective detection of variation in single-cell transcriptomes using MATQ-seq. *Nat. Methods* **2017**, *14*, 267–270, doi:10.1038/nmeth.4145.
46. Wang, Y.; Yuan, P.; Yan, Z.; Yang, M.; Huo, Y.; Nie, Y.; Zhu, X.; Yan, L.; Qiao, J. Single-cell multiomics sequencing reveals the functional regulatory landscape of early embryos. **2019**, doi:10.1101/803890.
47. Ai, S.; Xiong, H.; Li, C.C.; Luo, Y.; Shi, Q.; Liu, Y.; Yu, X.; Li, C.; He, A. Profiling chromatin states using single-cell itChIP-seq. *Nat. Cell Biol.* **2019**, *21*, 1164–1172, doi:10.1038/s41556-019-0383-5.
48. Rooijers, K.; Markodimitraki, C.M.; Rang, F.J.; de Vries, S.S.; Chialastri, A.; de Luca, K.L.; Mooijman, D.; Dey, S.S.; Kind, J. Simultaneous quantification of protein–DNA contacts and transcriptomes in single cells. *Nat. Biotechnol.* **2019**, *37*, 766–772, doi:10.1038/s41587-019-0150-y.
49. Moudgil, A.; Wilkinson, M.N.; Chen, X.; Morris, S.A.; Dougherty, J.D.; Mitra, R.D.; Moudgil, A.; Wilkinson, M.N.; Chen, X.; He, J.; et al. Self-Reporting Transposons Enable Simultaneous Readout of Gene Expression and Transcription Factor Binding in Single Cells II II Resource Self-Reporting Transposons Enable Simultaneous Readout of Gene Expression and Transcription Factor Binding in Single . **2020**, 992–1008, doi:10.1016/j.cell.2020.06.037.
50. Kaya-Okur, H.S.; Wu, S.J.; Codomo, C.A.; Pledger, E.S.; Bryson, T.D.; Henikoff, J.G.; Ahmad, K.; Henikoff, S. CUT&tag for efficient epigenomic profiling of small samples and single cells. *Nat. Commun.* **2019**, *10*, 1930, doi:10.1038/s41467-019-09982-5.
51. Skene, P.J.; Henikoff, S. An efficient targeted nuclease strategy for high-resolution mapping of DNA binding sites. **2017**, 1–35, doi:10.7554/eLife.21856.
52. Picelli, S.; Björklund, Å.K.; Reinius, B.; Sagasser, S.; Winberg, G.; Sandberg, R. Tn5 transposase and tagmentation procedures for massively scaled sequencing projects. *Genome Res.* **2014**, *24*, 2033–2040, doi:10.1101/gr.177881.114.
53. Buenrostro, J.D.; Wu, B.; Chang, H.Y.; Greenleaf, W.J. ATAC-seq: A method for assaying chromatin accessibility genome-wide. *Curr. Protoc. Mol. Biol.* **2015**, *2015*, 21.29.1-21.29.9, doi:10.1002/0471142727.mb2129s109.
54. Binz, H.K.; Amstutz, P.; Kohl, A.; Stumpp, M.T.; Briand, C.; Forrer, P.; Grütter, M.G.; Plückthun, A. High-affinity binders selected from designed ankyrin repeat protein libraries. *Nat. Biotechnol.* **2004**, *22*, 575–582, doi:10.1038/nbt962.
55. Villaseñor, R.; Pfaendler, R.; Ambrosi, C.; Butz, S.; Giuliani, S.; Bryan, E.; Sheahan, T.W.; Gable, A.L.;

- Schmolka, N.; Manzo, M.; et al. ChromID identifies the protein interactome at chromatin marks. *Nat. Biotechnol.* **2020**, doi:10.1038/s41587-020-0434-2.
56. Brauchle, M.; Hansen, S.; Caussinus, E.; Lenard, A.; Scholz, A.O.E.O.; Sprecher, S.G.; Plückthun, A.; Affolter, M. Protein interference applications in cellular and developmental biology using DARPinS that recognize GFP and mCherry. *Biol. Open* **2014**, *3*, 1252–1261, doi:10.1242/bio.201410041.
57. Hansen, S.; Stüber, J.C.; Ernst, P.; Koch, A.; Bojar, D.; Batyuk, A.; Plückthun, A. Design and applications of a clamp for Green Fluorescent Protein with picomolar affinity. *Sci. Rep.* **2017**, *7*, 16292, doi:10.1038/s41598-017-15711-z.
58. Hansen, S.; Stüber, J.C.; Ernst, P.; Koch, A.; Bojar, D.; Batyuk, A.; Plückthun, A. Design and applications of a clamp for Green Fluorescent Protein with picomolar affinity. *Sci. Rep.* **2017**, *7*, 1–16, doi:10.1038/s41598-017-15711-z.
59. Wu, Y.; Honegger, A.; Batyuk, A.; Mittl, P.R.E.; Plückthun, A. Structural Basis for the Selective Inhibition of c-Jun N-Terminal Kinase 1 Determined by Rigid DARPin–DARPin Fusions. *J. Mol. Biol.* **2018**, *430*, 2128–2138, doi:10.1016/j.jmb.2017.10.032.
60. Kummer, L.; Parizek, P.; Rube, P.; Millgramm, B.; Prinz, A.; Mittl, P.R.E.; Kaufholz, M.; Zimmermann, B.; Herberg, F.W.; Plückthun, A. Structural and functional analysis of phosphorylation-specific binders of the kinase ERK from designed ankyrin repeat protein libraries. *Proc. Natl. Acad. Sci. U. S. A.* **2012**, *109*, doi:10.1073/pnas.1205399109.
61. Kummer, L.; Hsu, C.W.; Dagliyan, O.; MacNevin, C.; Kaufholz, M.; Zimmermann, B.; Dokholyan, N. V.; Hahn, K.M.; Plückthun, A. Knowledge-based design of a biosensor to quantify localized ERK activation in living cells. *Chem. Biol.* **2013**, *20*, 847–856, doi:10.1016/j.chembiol.2013.04.016.
62. Parizek, P.; Kummer, L.; Rube, P.; Prinz, A.; Herberg, F.W.; Plückthun, A. Designed ankyrin repeat proteins (DARPinS) as novel isoform-specific intracellular inhibitors of c-jun N-terminal kinases. *ACS Chem. Biol.* **2012**, *7*, 1356–1366, doi:10.1021/cb3001167.
63. Scholz, O.; Hansen, S.; Plückthun, A. G-quadruplexes are specifically recognized and distinguished by selected designed ankyrin repeat proteins. *Nucleic Acids Res.* **2014**, *42*, 9182–9194, doi:10.1093/nar/gku571.
64. Hänsel-Hertsch, R.; Beraldi, D.; Lensing, S. V.; Marsico, G.; Zyner, K.; Parry, A.; Di Antonio, M.; Pike, J.; Kimura, H.; Narita, M.; et al. G-quadruplex structures mark human regulatory chromatin. *Nat. Genet.* **2016**, *48*, 1267–1272, doi:10.1038/ng.3662.

7. Acknowledgments

There were many people who accompanied me in this academic journey and I probably won't be able to thank them all. Either way, it's been great to have the chance to get to know so many interesting people. They supported and challenged me which allowed me to grow across all skills and competencies, and I hope that I was able to return the favour in one way or another.

I would like to thank Isabelle Mansuy for her support in developing my scientific and academic skills. I appreciated the trust and freedom to pursue various scientific questions. Her lab provided a stimulating environment that motivated and supported me. In particular, the opportunity to volunteer in the Association of Scientific Staff at ETH was greatly appreciated.

I would like to thank Johannes Bohacek for his mentorship since I first ventured out of the lecture halls into a wet lab. He taught me all the basic and advanced skills to conduct research in molecular biology. His enthusiasm for research was a great motivator and inspiration to pursue science.

Science is a team effort and I enjoyed working with many people throughout the years.

Three colleagues were particularly supportive, and our shared experiences forged a friendship in and outside of the lab. Irina Lazar-Contes, Gretchen van Steenwyk and Maria-Andreea Dimitriu! Irina, I will miss our coffee breaks on the balcony and our discussions for new projects. Gretchen, I will miss chatting with you in the lab and on long car drives. Maria, I will miss your contagious enthusiasm for fancy transposases and ideas what to do with them. All of you were always there when I requested help and support, which encouraged me in indescribable ways.

I'd like to express my gratitude to Niharika Obrist who contributed crucial work to many experiments and who always managed to lift up our spirits. Francesca Manuela, I'm not sure if we will make it to MSUS80 ;) but thanks for supporting all our/my breedings and welcoming me so warmly to your lab space when I started! Silvia

Schelbert was a wonderful lab manager and facilitated quite a few steps. Thanks also to Alberto Corcoba who has since then taken over.

Similarly, I've been fortunate to get to know, work with and exchange ideas with new colleagues in our lab:

- Andrew McDonald
- Lola Kourouma
- Anara Alshanbayeva
- Deepak Tanwar
- Anastasiia Efimova
- Kristina Thumfart
- Dimitri Schmid
- Rodrigo Arzate
- Leonard Steg
- Hadrien Le Berre
- Kristin Koppelmaa
- Matthias Heuberger
- Arianna Arpagaus
- Bogdan Mateescu
- Alessandra Stürchler
- Diane Heiser

Throughout the years I was lucky to also enjoy many supportive colleagues. First and foremost was the old guard. Your advice helped me greatly and I will always cherish our shared experiences outside of the lab:

- Ali Jawaid
- Lukas von Ziegler
- Eloïse Kremer
- Pierre-Luc Germain

Similarly, thanks to former lab members who were inspiring colleagues:

- Amalia Floriou-Servou
- Vanessa Hoop
- Oliver Sturman
- Jennifer Brown
- Chiara Boscardin
- Bisrat Woldemichael
- Neomi Marsolo
- Katharina Gapp
- Bechara Saab
- Ry Tweedy-Cullen
- Mattia Privitera

- Melissa Lee
- Aya Ashour
- Ceren Duman
- Lubka Spassova

I had the privilege to share my enthusiasm for research with a number of students. It was always a two-way street and I gained new experiences from working with them:

- Max Frank
- Luzia Stalder
- Darren Kelly
- Emily Berry

I had the pleasure to meet some amazing students and postdocs at our institute throughout the years. Sharing labs, offices, drinks and discussions:

- Dayra Lorenzo
- Nadia Rosenberg
- Anahi Hurtado
- Sebastian König
- Marie-Angela Wulf
- Ruslan Rust
- Stine Thorhauge Bak
- Martina Hruzova
- Martina Maibach
- Maria Chernysheva
- Rahel Kästli
- Aleksejs Fomins
- Pia Sipilä
- Gwendolin Schönfeld
- Flora Vajda
- Stefano Carta
- Simon Musall
- Balasz Laurenczy
- Alexander van der Bourg
- Fabian Voigt
- Lorenzo Gesuita
- Benjamin Ineichen
- Oliver Weinmann
- Natalie Russi
- Michael Arzt
- Mea Holm
- Julia Kaiser
- Dominik Groos
- Anna-Sophie Hofer
- Baptiste Jaeger

- Gregor Pilz
- Saray Soldado Magraner
- Sara Bottes
- Christopher Lewis
- Alice Mosberger
- Andreas Schmandke
- Yaroslav Sych
- Philipp Bethge
- Kevin Meyer
- Khadeesh bin Imtiaz
- Daniel Gonzalez
- Lars Royall
- Anna-Sophia Wahl
- Michael Maurer
- Annina Denoth
- Yasir Gallero-Salas
- Thomas Wegleiter
- Jochen Winterer
- Lin Que
- Abhishek Banerjee
- Megan Bowers
- Simon Braun
- and anyone else that I've forgotten to name here!

Last but not forgotten: Stewart Berry, we started together as Masters students in the same office and spent countless hours conversing and laughing together. Unfortunately, I never got to see your defense and you didn't get the opportunity to attend mine. I will cherish our shared memories. Rest in peace buddy.

I'd like to extend my gratitude to all collaborators and colleagues that helped with my research:

- Johannes vom Berg, Dalila Korkmaz, Monika Tarnowska and Mark Ormiston for teaching me how to collect embryos, and the support to use some of their equipment.
- Karin Würtz-Kozak and Elena Cambria for the interesting collaboration on bones.
- Rodrigo Villaseñor, Jeff Bernitz, Tuncay Baubec, Timm Schroeder, Thorsten Buch, Andreas Plückthung and Birgit Dreier for ongoing collaborations.
- The flow cytometry team at Irchel, in particular Claudia Dumrese for advice on imaging and sorting sperm cells.
- The functional genomics center team at Irchel.

I'd like to thank the current and former group leaders and staff from our institute for creating and maintaining a productive environment:

- Sebastian Jessberger
- Fritjof Helmchen
- Urs Gerber
- Martin Schwab
- Csaba Földy
- Theofanis Karayannis
- Fabio Sias
- Lazar Sumanovski
- Dubravka Göckeritz
- Hansjörg Kasper
- Julia Lüdke
- Martin Wieckhorst
- Stefan Giger
- Frank David
- Pietro Morciano
- Nicole Aregger
- Taner Aydinalp
- Tanya Bülbül-Aydinalp
- Isabella De Nitti
- Cecilia Nicoletti
- Minou Nadjafpour
- Ladan Egolf

During my doctoral studies I had the amazing opportunity to work on scientific and academic topics outside of our lab, institute and even ETH. These were welcome opportunities to expand my horizon and get to know wonderful colleagues and friends.

First and foremost, all the former and current volunteers at our research think-thank *reatch!* I hope that I'll now have more time to contribute.

A special thanks goes to Servan Grüninger, Joel Lüthi, Sarah Zurmühle and Carlos Mora. Your dedication was and is truly inspiring, and was a big factor for my volunteering.

Similarly I'd like to thank for all the great events and experiences we shared together:

- Valeria Eckhardt
- Sara von Salis
- Marius Rohner
- Luisa Schäfer
- Jonas Schmid
- Akash Arasu
- Michael Lerch
- Chantal von Siebenthal
- Fabienne Odermatt
- Darienne Hunziker
- Michaela Egli
- Fabio Hasler
- Levyn Bürki
- Stefan Emmenegger
- Christina Wolf
- Nathalie Gasser
- Olivia Meier
- Sandro Christensen
- Stefan Gugler
- Jonas Wittwer
- Manuel Merki
- Elena Kuslys
- Daniel Sidler
- Bettina Heim
- Muriel Fisser
- Michael Kümin
- Monika Wehrli
- Sandrine Gehriger
- Ivan Marijanovic
- Pia Schneider
- Sandro Christensen
- Lucia Caiata
- Bettina Meyer
- Adrian Hauswirth
- Remo Müller
- and any reatchler that I might have forgotten!

I have to express my fondest gratitude towards everyone that I had the privilege and pleasure of meeting and working with during my volunteering years for the Academic Association of the Scientific Staff at ETH (AVETH)! It was a crazy time but I wouldn't want to miss it.

Nina Ripin, you always made time for me, and I greatly appreciated all the support I received from you. More awe inspiring however was to see you provide unconditional support to those who needed help. You are one of the good ones, never doubt that.

Similarly, I'd like to thank Betty Friedrich-Grube who was always willing to reach out and help others. Thanks for helping me maneuver through the presidency and I hope you'll do similar great work for our ETH.

Romain Jacob, we ruffled some feathers at ETH ;) It was a great experience to work with you!

Linda Wehner, you were the best partner in crime one could hope for but more importantly: You did amazing work for our big AVETH anniversary and topped it all off with your dedication for the counseling team. Chapeau!

Rosa Visscher, was the best successor I could have hoped for. You did and continue to do an amazing job, thank you so much!

Claire Bourquard and Iselin Medhaug, I enjoyed all our debates, banters and admired all your efforts to move things forward at ETH! You did great things.

Similarly, Sasha Cisar, Viktoria Gerken, Rea Lehner, Irena Kuzmanovska and Zoe Jonassen. You all inspired new ideas and continued the political work to improve the future framework for the scientific staff at ETH.

However, politics is not everything even though it was my main passion. Michael Ferguson, Alina Teuscher, Florentine Veenstra and Anne Jomard, thanks for taking such great care of our counseling team and your dedication to helping others at ETH!

Next, I'd like to thank everyone that contributed to our AVETH in so many ways. I could probably fill pages but I will resort to just naming you all and expressing my gratitude:

- Tanja Eberhart
- Deepak Ravi Kumar
- Fabian Brüning
- Alexander Viand
- Iris Hordijk
- Francesco Ortelli
- Mahsa Bazrafshan
- Konrad Jakubowski
- Mohammad Nouraddini
- Christos Lataniotis
- Eric Burns
- Michèle Grieder
- Rashmi Rai-Rawat
- Paolo Testa
- Andrea Testa
- Anastasia Sycheva
- Luka Isenmann
- Roelinda Jongstra
- Dehua "David" Zhu
- Chris Bolesch
- Neringa Mannerheim
- Cyprien Hoelzl
- Anca-Denice Ciuta
- Roger Stark
- Uwe Lüpke
- Flavia Timpu
- Diyora Salimova
- Anna Vagstad
- and anyone else I might have forgotten!

My fascination for AVETH didn't come from nothing. From my initial participation in a politics team meeting to colleagues who encouraged me to really get involved in AVETH and at ETH Zurich were many notable characters and supporters, but I'd like to single out a few.

The initial spark gave Isabella Schalko who organized inspiring politics team meetings! Thank you so much for everything.

Arik Jung was the person to stoke the flame. My predecessor as AVETH president and someone who I greatly admired for all the effort and courage to stand up for everyone. Thanks for supporting and believing in me!

In addition, there were many others who challenged, inspired and supported me during my first years at AVETH:

- Helge Fuchs
- Emanuela Milani
- Thomas Gersdorf
- Florian Thöle
- Florian Emaury
- Stefano Duca
- Lars Büthe
- Sascha Winterberg

Finally, there were a great many throughout our various working groups, commissions, department association and events who I got to collaborate with, and more importantly, who put in a lot of effort into making ETH Zurich and academia a better place to be:

- Eva Kummer
- Murielle Schreck
- Sandro Luh
- Giovanna Giacalone
- Tomasz Kacprzak
- Michaela Oplova
- Klaus-Ulrich Miltenberger
- Pavel Oborsky
- Joel Zeder
- Dilara Perver
- Anina Gilgen
- Janne Soetbeer
- Xiaopu Wang
- Natalia Papathanasiou
- Marie André
- Christina Müller
- Salome Adam
- Simon Bachler
- Sebastian Vogg
- Clemens Vogel
- Marieke Buffing
- Lukas Braun
- Katrin Kröger

- Nino Nikolovski
- Timo Niepel
- Marc Sinner
- Andrea Tamas
- Oriana Schällibaum
- Maximilian Mandl
- Andreas Ritter
- David Fuchs
- Stefano Danzi
- Omid Maghazei
- Daniel Spies
- Anubha Garg
- Clemens Schwingshackl
- Christian Mathis-Ullrich
- Peter Tiefenböck
- Moritz Wolf
- Szymon Hennel
- Nadia Panchaud
- Carmen Weber
- Marc Stevens
- Moritz Wolf
- Oliver Furtmaier
- Thomas Mathis
- Peter Tiefenböck
- I likely forgot to name a few, thanks to you all!

I'd like to also thank all the colleagues from VSETH, PeKo, PK, University Assembly and other working groups and commissions:

- Tierry Hörmann
- Lewin Könemann
- Lukas Reichart
- Lukas Möller
- Kay Schaller
- Micha Bigler
- Nicole Gampf
- Christina Gantner
- André Blanchard
- Christopher Sauder
- Irene Müller-Gantenbein
- Stefan Karlen
- Yvonne Ogg
- Werner Wegscheider
- Andrea Heinzelmann
- Kristin Becker van Slooten
- Adrian Gilli

- Christian Schmid
- Sven Panke
- Maddalena Velona
- Joy Stekhoven
- Medea Fux
- Aline Schori
- Minh Tran
- Edoardo Mazza
- Silvia Häfliger
- Peter Widmayer
- Felicitas Pauss
- Neil Montague de Taisne
- Jasmin Cadalbert

Thanks to the opportunity to volunteer in AVETH, I had the great privilege to meet many inspiring people working at and for ETH Zurich.

First and foremost, I need to single out our rector Sarah Springmann. To see her go above and beyond for everyone at ETH was truly inspiring. I learned a great deal from her and I hope that I'll get the opportunity in my career to pay it forward.

In another stratosphere of integrity and human kindness is Antonio Togni. As vice-rector, he exemplified what it means to be responsible for us doctoral students and he spent a great amount of energy in helping anyone that needed help. Thank you so much for everything.

Of course, there were many many more at ETH Zurich that supported, helped and challenged me, ultimately leading to new experiences that I would have never made during a normal doctorate. A sincere thank you to:

- Alfredo Picariello
- Barbara La Cara
- Erik Jentges
- Ulrich Weidmann
- Florian Meyer
- Katharina Poiger
- Susanne Schuler
- Jana Seregi
- Manfred Sigrist
- Margrit Leuthold
- Sabine Hoffmann

- Lukas Sigrist
- Philipp Bieri
- Benno Volk
- Wendy Altherr
- Andreas Reinhardt
- Robert Schikowski
- Omar Kassab
- Rainer Borer
- Barbara Hellermann
- Barbara Czarniecki
- Lukas Vonesch
- Joël Mesot
- Judith Zimmermann
- Viktoria Ivarsson
- Danier Halter
- Gerd Folkers
- Urs Brändle
- Maria Hakanson
- Regula Christen
- Phil Bertschi
- Wilfred van Gunsteren
- Eva Gottschweski
- Ulrich Schutz
- Norbert Staub
- Christoph Niedermann
- Eric Ryf
- Claudine Leysinger
- Anna Bendel
- Martin Ghisletti
- Sibylle Hodel
- Vanessa Bleich
- Robert Perich
- Anders Hagström
- Reto Knutti
- Anna Maltsev
- Roland Baumann
- Evelyne Kappel
- Giorgia Zandomeneghi
- Dieter Wüest
- Renate Schubert
- Susanne Schuler
- Martine Vernooij
- Ernestine Hildebrand
- Jürg Brunnschweiler
- Detlef Günther
- Lorenz Hurni

- Gabriela Laios-Zäch
- Marianne Mandrin
- Andreas Lerch
- Elisabeth Mitter
- Franziska Schmid
- Romana Mayer
- Gerhard Tröster
- Peter Frischknecht
- Samantha Foulger
- Pia Aeschlimann

Such lists are never complete. In case I forgot you dear reader: Thank you!

Martin Roszkowski

Personal Information

Name: Martin Roszkowski
Address: Bucheggstrasse 138
8057 Zurich
Date & Place of Birth: February 4th, 1987, Zurich
Nationality: Swiss
Email: martin.roszkowski@protonmail.ch
Scientific profiles: [0000-0002-8896-5514](#) – ORCiD
[AAF-2452-2020](#) – ResearchID



Education and Professional Experience

Education and Training

- 3/2015 – 3/2021: **Doctoral student, ETH Zurich**
Research focus: Transgenerational epigenetic inheritance
Advisor: Prof. Isabelle Mansuy
- 9/2013 – 2/2015: **Master of Science in Biology/Neurosciences, University of Zurich**
Research focus: stress, gene expression, blood-brain barrier
Advisors: Prof. Isabelle Mansuy, Prof. Johannes Bohacek
- 9/2010 – 9/2013: **Bachelor of Science in Biology, University of Zurich**
Additional minors in Bioinformatics and Neuroinformatics

Qualifications

- 1/2021 – present: **Advanced Flow Cytometry** – Independent operator of cell sorters
- 1/2014 – present: **FELASA B** – Qualification to conduct animal experiments

Professional History

- 4/2010 – 5/2011: Employee at Fresh Invest GmbH, Wohlen
1/2009 – 9/2009: Intern at Birgit Casutt Human Resources, Oberwil bei Zug

Military Service

- 8/2008 – 03/2018 Soldier and driver in ABC Abwehr Batallion 10

Peer-reviewed publications - ORCID: 0000-0002-8896-5514

Wuertz-Kozak K*, **Roszkowski M***, Cambria E, Block A, Kuhn G, Abele T, Hitzl W, Driesslein D, Müller R, Rapp MA, Mansuy IM, Peters EM, Wippert PM (*equal contribution)
Effects of early life stress on bone homeostasis in mice and humans
[International Journal of Molecular Sciences](#), 2020

Gapp K, van Steenwyk G, Germain PL, Matsushima W, Rudolph KLM, Manuella F, **Roszkowski M**, Vernaz G, Ghosh T, Pelczar M, Mansuy IM, Miska EA
Alterations of sperm long RNA contributes to the epigenetic inheritance of the effects of postnatal trauma
[Molecular Psychiatry](#), 2018

van Steenwyk G, **Roszkowski M**, Manuella F, Franklin TB, Mansuy IM
Transgenerational inheritance of behavioral and metabolic effects of traumatic experiences in early postnatal life in mice: Evidence in the 4th generation.
[Environmental Epigenetics](#), 2018

Jawaid A*, **Roszkowski M*** and Mansuy IM (*equal contribution)
Transgenerational Epigenetics of Traumatic Stress
[Progress in Molecular Biology and Translational Science](#), 2018

Roszkowski M, Bohacek J
Stress does not increase blood-brain-barrier permeability in mice
[Journal of Cerebral Blood Flow and Metabolism](#), 2016

Roszkowski M, Manuella F, von Ziegler L, Duràñ-Pacheco G, Moreau J-L, Mansuy IM, Bohacek J
Rapid stress-induced transcriptomic changes in the brain depend on beta-adrenergic signaling
[Neuropharmacology](#), 2016

Bohacek J, Manuella F, **Roszkowski M**, Mansuy IM
Hippocampal gene expression induced by cold swim stress depends on sex and handling
[Psychoneuroendocrinology](#), 2015

Other publications

Lazar-Contes I, **Roszkowski M**, Tanwar D, Mansuy IM
Epigenetic Inheritance: Impact for Biology and Society - Summary Symposium Aug 26-28, 2019, Zürich, Switzerland
[Environmental Epigenetics](#), 2020

Roszkowski M
The effects of acute stress on Apold1 gene expression and blood-brain barrier permeability
[Master thesis](#), 2014

Arasu A, Grüninger S, Mora C, Lüthi J, **Roszkowski M**, Schmid J, Serwart J
Analyse zur Ecopop-Initiative
[White paper](#) by the working group “science and migration” of the association “research and technology in Switzerland”, 2014

Manuscripts in preparation

Roszkowski M, Mansuy IM

High efficiency RNA extraction from sperm cells using guanidinium thiocyanate supplemented with tris(2-carboxyethyl)phosphine

Status: Article submitted and in revision

Roszkowski M, Lazar-Contes I, Germain PL, Tanwar D, Gaur N, Alshanbayeva A, Manuella F, Korkmaz D, Ormiston D, vom Berg J, Jörg T, Bohacek J, Mansuy IM

OmniSperm: Multiomic analyses of sperm and offspring production from a single male

Status: Article in preparation

Roszkowski M, Jawaid A, Kunzi M, Zamboni N, Mansuy IM

Chronic postnatal stress dysregulates maternal milk composition and alters offspring's early life physiology

Status: Article in preparation

Dimitriu M, **Roszkowski M**, Lazar-Contes I, Mansuy IM

Single-cell multi-omics techniques: from paper to benchside

Status: Review in preparation

Poster presentations

Dimitriu M*, **Roszkowski M***, Villasenor R, Baubec T, Mansuy IM (*equal contribution)

NanoTag: A novel combinatorial sequencing approach for multimodal epigenomic profiling applicable to the nervous system

- FENS Forum of Neuroscience 2020, Glasgow, United Kingdom
- Swiss Society for Neuroscience Annual Meeting 2020, Bern, Switzerland
- FEBS3+ LS² Annual Meeting 2020, Zurich, Switzerland – **Selected for flash talk**

Roszkowski M, Lazar-Contes I, Gaur N, Manuella F, Germain PL, Gaur N, Korkmaz D, Ormiston M, vom Berg J, Mansuy IM and Bohacek J

OmniSperm – a novel experimental strategy opens new horizons in epigenetic inheritance

- LS² Annual Meeting 2019, Zurich, Switzerland
- Latsis Symposium 2017 – Transgenerational epigenetic inheritance: Impact for Biology and Society, Zurich, Switzerland - **Best Poster Award**

Roszkowski M, Vernaz G, Gapp K, Mansuy IM

ncRNA in MSUS

- Swiss Society for Neuroscience Annual Meeting 2016, Lausanne, Switzerland.
- 1st Retreat of the NCCR “RNA and Disease” 2016, Kandersteg, Switzerland.

Roszkowski M, Manuella F, von Ziegler L, Mansuy IM, Bohacek J

Multifactorial transcriptome regulation following acute stress

- Swiss Society for Neuroscience Annual Meeting 2015, Fribourg, Switzerland.

M. Roszkowski, F. Manuella, L. von Ziegler, G. Duràñ-Pacheco, J.-L. Moreau, I.M. Mansuy, J. Bohacek

Norepinephrine plays an important role in regulating hippocampal gene expression after acute stress

- ZNZ Symposium 2015, Zurich, Switzerland

Teaching and supervision of students

Teaching in courses

- 2018 – 2021: Annual course for ETHZ and UZH students “Study of Epigenetic Mechanisms in Mental Health (376-1346-00L)” Supervision of 2-3 students during 3.5 weeks.
- 2015 – 2017: Annual course for ETHZ and UZH students “Molecular Mechanisms of Learning and Memory (376-1346-00L)” Supervision of 2-3 students during 3.5 weeks.
- 2015 – 2017: Team leader and course instructor in “[mobile gene laboratory](#)” from “Forschung für Leben”. An initiative to educate high school students in the use of biotechnology at their school.

Supervision of student research projects and internships

- 2020: Maria Dimitriu, MSc Health Sciences and Technology ETH Zurich
Use of Tn5 in epigenetic inheritance
- 2018: Emily Berry, EuroScholars internship, University of New Hampshire
Investigating Epigenetic Mechanisms of Behavior in MSUS mice
- 2017: 2 school students, internship for 3 weeks
- 2016: Luzia Stalder, MSc Health Sciences and Technology ETH Zurich
Exploratory RNA sequencing analysis in the dorsal and ventral hippocampus after acute stress
- 2016: Darren Kelly, AMGEN internship by NUI Galway
War trauma and its permanent marks – Investigating a potential mouse model
- 2015: Max Frank, MSc Health Sciences and Technology ETH Zurich
RNASeq analysis and validation of sperm lncRNA in transgenerational inheritance of early life trauma

Research related projects

- 2017 – 2020: Organization of lab-internal biobank with several thousand mouse specimens and RNA, DNA and protein extraction from over 1000 mouse tissue samples in the research group of Prof. Mansuy. Supervision of a research associate assigned to this task.
- 2016 – 2019: Implementation of openBIS together with Dr. Germain in the research group of Prof. Mansuy to enable systematic management, annotation and sharing of data that have been measured in biological experiments within the lab and external collaborators.

Memberships in associations

4/2019 – present:	Life Sciences Switzerland
4/2019 – present:	European Society of Human Reproduction and Embryology
2/2019 – present:	UZH Alumni
2/2019 – present:	Science Alumni UZH
8/2016 – present:	Swiss Laboratory Animal Science Association (SGV)
5/2014 – present:	Swiss Society for Neuroscience
3/2015 – present:	Academic Association of Scientific Staff at ETH Zurich
5/2014 – present:	reatch – research and technology in Switzerland

Volunteering

9/2017 – 3/2020:	President of the Academic Association of Scientific Staff at ETH Zurich (AVETH). >2000 members, 30 board members in 7 working groups, >100 active members in 18 departmental sub-associations and Telejob , annual budget of 350'000 Fr., 1 part-time administrative assistant. Notable personal activities and initiatives: <ul style="list-style-type: none">▪ Representation of the scientific staff towards the media. Statements, interviews and background talks with journalists.▪ Renewal of the website, newsletter and membership database.▪ Implementation of new communication (Slack), organisation (Trello) and documentation tools (e-pics, polybox) to facilitate collaboration in AVETH.▪ Organisation of the 50th anniversary celebrations of AVETH - ETH Globe article.▪ Foster and strengthen the network and collaboration with various ETH-associated organisations such as international student groups and female associations.▪ Participation in ETH project groups and workshops: Critical Thinking Initiative, academic air travel, ETH+, rETHink, communication concept.
9/2016 – 9/2017:	Elected board member and coordinator of the politics team in AVETH . <ul style="list-style-type: none">▪ Representation of the scientific staff in university politics.▪ Organization of monthly politics team meetings.▪ Preparation of statements and answers to the ETH executive board and other ETH units.▪ Regular meetings with members of the school board.▪ Participation in various workshops and ad-hoc working groups.▪ Contribution to surveys: doctoral supervision, employment conditions

- 5/2014 – present: **Board and founding member** of the think-tank “[reatch – research and technology in switzerland](#)”
- Active contribution to various project groups.
 - Recruitment of new members and building up the necessary structures and organization.
 - Co-organizer of retreats, meetings and social activities.
 - Since 2017 mostly in an advisory role and facilitator for events and collaborations with other associations at ETH Zurich.

- 5/2014 – 5/2017: **Events coordinator** of “reatch – research and technology in switzerland”
- Organization of all internal (<20 participants) and public events (15 to 300 participants).
 - Recruit and organize members and helpers of the events team.
 - Preparation of event budgets and administrative tasks.
 - On-site activities to set up the event venue, prepare apéros and clean up.
 - Logistics to and from the event venue.

Service to the Academic Community

- 6/2019 – 9/2020: **Member** of the core group “ETH Zurich accreditation”
ETH Zurich was accredited by the [Swiss Accreditation Council](#) in 2020. The core group coordinated and prepared the self-evaluation report and on-site visits.
- 10/2018 – 9/2020: **Member** of the advisory committee “[ETH Talent](#)”
A strategic project group by the rector of ETH Zurich. It aimed to foster cross-disciplinary competencies, promoting personal growth and engagement in society.
- 1/2019 – 3/2020: **Member** of the advisory committee “[#howsETHgoing](#)”?
A survey organized by the student association VSETH to analyse student satisfaction and mental well-being at ETH Zurich.
- 10/2018 – 3/2020: **Member** of the ETH Zurich “Futures Network”
The Futures Network was a growing interdisciplinary community of future thinkers engaged in participatory foresight within ETH. It was part of the Strategy commissions “ETH Long Range Radar”.
- 3/2016 – 3/2020: **Elected representative** in the “[University Assembly](#)” of ETH Zurich.
The university assembly is composed equally of elected representatives of the four university groups, representing all members of ETH Zurich. The University Assembly meets monthly and is involved in consultations and approvals: legislative enactments of the ETH Board, ETH budget and planning, creation and abolition of teaching and research units and on questions of structure and participation at ETH.
- 2/2016 – 1/2018: **Elected representative** at the department conference of D-HEST.

Organization of Events

- 6/2019 – 8/2019: Member of the organization team “[Epigenetic Inheritance: Impact for Biology and Society](#)”, Prof. Mansuy, Zurich
- 6/2018 – 2/2019: Co-organiser of the “[Career workshop for scientific staff at SEC](#)”, Singapore-ETH Centre, Singapore
- 1/2018 – 3/2019: Member of the organization committee “[Symposium on Doctoral Supervision](#)” 2019, ETH Zurich, Switzerland.
- 4/2017: Organizer panel discussion “[Energiestrategie 2050](#)”, reatch, Zurich
- 12/2016 – 3/2017: Member of the core team for the exhibition “[Insects as food – A view beyond the plate](#)”, reatch, Sustainability Week Zurich 2017
- 12/2016: Organizer panel discussion “[Trump, Merkel und postfaktische Politik](#)”, reatch, Zurich
- 9/2016 – 12/2016: Organizer interactive communication and debatting training “[reatch, don't preach](#)”, reatch, Zurich
- 11/2016: Organizer of seminar “[Was macht Wissenschaft, die sich nicht anwenden lässt?](#)”, reatch, Zurich
- 10/2016: Organizer panel discussion “[Atomkraft: Nein danke! Oder ja bitte?!](#)”, reatch, Zurich
- 10/2016: Organizer of talk “[The future of medical diagnostics – From DNA to protein to real-time Immunoassays](#)”, reatch, Zurich
- 9/2016: Organizer panel discussion “[Big Data - Is data feudalism a danger for democracy?](#)”, reatch, Zurich
- 6/2016: Organizer panel discussion “[Strom aus Atom – strahlende Zukunft oder Endstation Endlager?](#)”, reatch, Zurich
- 6/2016: Organizer panel discussion “[Mit der Freiheit zündeln - Podiumsdiskussion zum Bedingunglosen Grundeinkommen](#)”, reatch, Zurich
- 5/2016: Organizer panel discussion “[Präimplantationsdiagnostik](#)”, reatch, Zurich
- 5/2016: Organizer panel discussion “[Muss Forschung nützen? Und wenn ja, warum?](#)”, reatch, Zurich
- 4/2016: Organizer talk and discussion “[CRISPR: What can and should we \(not\) do with this powerful genetic tool?](#)”, reatch, Zurich
- 4/2016: Organizer panel discussion “[Warum wir mit Tieren forschen](#)”, reatch, Zurich
- 3/2016: Organizer panel discussion “[Wissenschaft ist Grundlagenforschung – Was sonst?](#)”, reatch, Zurich
- 12/2015: Organizer panel discussion “[Kernenergie – Relikt der Vergangenheit oder Energieträger der Zukunft?](#)”, reatch, Zurich

- 12/2015: Organizer lecture and discussion “[CRISPR – Genetic Engineering 2.0](#)”, reatch, Zurich
- 11/2015: Organizer panel discussion “[Basic Research – Just a Waste of Time and Money?](#)”, reatch, Zurich
- 9/2015: Organizer talks and discussion “[Was soll Wissenschaft \(heute\)?](#)”, reatch, Zurich
- 6/2015: Organizer talk “[reatch pitch: Quantum Computing](#)”, reatch, Zurich
- 5/2015: Organizer panel discussion “[Selektion im Reagenzglas – Was ist möglich? Was wollen wir zulassen?](#)”, reatch, Zurich
- 5/2015: Organizer talks and discussion “[Energie speichern – Lösungen für morgen](#)”, reatch, Zurich
- 4/2015: Organizer panel discussion “[Gentechnisch Modifizierte Organismen – Chance oder Risiko?](#)”, reatch, Zurich
- 3/2015: Organizer talks and discussion “[Experimente an Primaten – Die ethisch-rechtliche Sicht](#)”, reatch, Zurich
- 11/2014: Organizer talks and discussion “[Primaten in der Hirnforschung – Was wir von unseren Verwandten lernen können](#)”, reatch, Zurich
- 10/2014: Organizer panel discussion “[Ecopop-Initiative – Kann man eine globale Entwicklung lokal stoppen?](#)”, reatch, Zurich

Additional activities

- 1/2020: Representative of the scientific staff at the ETH Teaching Retreat 2020, St. Gallen, Switzerland
- 9/2019: Representative of the scientific staff at the World Academic Summit 2019 “[How talent thrives](#)”, Times Higher Education, ETH Zurich
- 7/2018: Representative of ETHZ doctoral students at the “Séance de Réflexion Lugano” of the Chamber of Universities, swissuniversities, Università della Svizzera Italiana, Lugano, Switzerland
- 6/2018: Panelist in “Career Support for the Research Careers of the Future”, Talent Development and Professional Support of Researchers’ Careers 2018, EU GrantsAccess, Zurich, Switzerland
- 6/2018: Representative of the scientific staff at the ETH Teaching Retreat 2018, Emmetten, Switzerland
- 11/2017: Representative of the scientific staff and workshop leader during the [ETH Faculty Retreat 2017](#), Luzern, Switzerland
- 7/2017 & 8/2019: Representative of the scientific staff at the Scientifica
- 2012 – 2019: IT administrator for the club “Feldschützengesellschaft Waltenschwil”